

IntechOpen

# Forest Biomass

## From Trees to Energy

*Edited by Ana Cristina Gonçalves,  
Adélia Sousa and Isabel Malico*





---

# Forest Biomass - From Trees to Energy

*Edited by Ana Cristina Gonçalves,  
Adélia Sousa and Isabel Malico*

Published in London, United Kingdom

---



## IntechOpen







*Supporting open minds since 2005*



Forest Biomass – From Trees to Energy

<http://dx.doi.org/10.5772/intechopen.90324>

Edited by Ana Cristina Gonçalves, Adélia Sousa and Isabel Malico

#### Contributors

Patricia Lourenco, Ana Cristina Gonçalves, Isabel Malico, Adélia Sousa, Isabel Marques, Ana D'espiney, Helena Pinheiro, Crismeire Isbaex, Ana Margarida Coelho, Teresa Fonseca, José Lousada, Attila Bai, Zoltán Gabnai, Augusto Brasil, A K M Mominul Islam, A K M Aminul Islam, Swapan Chakrabarty, Zahira Yaakub, M. Ahiduzzaman

© The Editor(s) and the Author(s) 2021

The rights of the editor(s) and the author(s) have been asserted in accordance with the Copyright, Designs and Patents Act 1988. All rights to the book as a whole are reserved by INTECHOPEN LIMITED. The book as a whole (compilation) cannot be reproduced, distributed or used for commercial or non-commercial purposes without INTECHOPEN LIMITED's written permission. Enquiries concerning the use of the book should be directed to INTECHOPEN LIMITED rights and permissions department ([permissions@intechopen.com](mailto:permissions@intechopen.com)).

Violations are liable to prosecution under the governing Copyright Law.



Individual chapters of this publication are distributed under the terms of the Creative Commons Attribution – NonCommercial 4.0 International which permits use, distribution and reproduction of the individual chapters for non-commercial purposes, provided the original author(s) and source publication are appropriately acknowledged. More details and guidelines concerning content reuse and adaptation can be found at <http://www.intechopen.com/copyright-policy.html>.

#### Notice

Statements and opinions expressed in the chapters are these of the individual contributors and not necessarily those of the editors or publisher. No responsibility is accepted for the accuracy of information contained in the published chapters. The publisher assumes no responsibility for any damage or injury to persons or property arising out of the use of any materials, instructions, methods or ideas contained in the book.

First published in London, United Kingdom, 2021 by IntechOpen

IntechOpen is the global imprint of INTECHOPEN LIMITED, registered in England and Wales,

registration number: 11086078, 5 Princes Gate Court, London, SW7 2QJ, United Kingdom

Printed in Croatia

British Library Cataloguing-in-Publication Data

A catalogue record for this book is available from the British Library

Additional hard and PDF copies can be obtained from [orders@intechopen.com](mailto:orders@intechopen.com)

Forest Biomass – From Trees to Energy

Edited by Ana Cristina Gonçalves, Adélia Sousa and Isabel Malico

p. cm.

Print ISBN 978-1-83962-970-9

Online ISBN 978-1-83962-971-6

eBook (PDF) ISBN 978-1-83962-972-3

An electronic version of this book is freely available, thanks to the support of libraries working with Knowledge Unlatched. KU is a collaborative initiative designed to make high quality books Open Access for the public good. More information about the initiative and links to the Open Access version can be found at [www.knowledgeunlatched.org](http://www.knowledgeunlatched.org)

# We are IntechOpen, the world's leading publisher of Open Access books Built by scientists, for scientists

5,200+

Open access books available

127,000+

International authors and editors

150M+

Downloads

156

Countries delivered to

Our authors are among the  
Top 1%

most cited scientists

12.2%

Contributors from top 500 universities



WEB OF SCIENCE™

Selection of our books indexed in the Book Citation Index  
in Web of Science™ Core Collection (BKCI)

Interested in publishing with us?  
Contact [book.department@intechopen.com](mailto:book.department@intechopen.com)

Numbers displayed above are based on latest data collected.  
For more information visit [www.intechopen.com](http://www.intechopen.com)







# Meet the editors



Ana Cristina Gonçalves is Assistant Professor of Habilitation in the Department of Rural Engineering, University of Évora, Portugal, and a researcher at the Institute for Mediterranean Agrarian Sciences (ICAAM). She holds a Ph.D. in Forest Engineering and has authored more than 100 publications and participated in fifteen research projects. Dr. Gonçalves' research focuses on silviculture and modeling in pure, mixed, even-aged and uneven-aged stands, and forest management and planning integrated into a GIS environment.



Isabel Malico is an assistant professor in the Physics Department, University of Évora, Portugal, and a researcher at the Associated Laboratory for Energy, Transport and Aeronautics (LAETA). She holds a Ph.D. in Mechanical Engineering from the University of Lisbon and has authored more than 100 publications. She has worked on around twenty research projects in both the academic and private sectors. Her research focuses on computational fluid mechanics, energy systems, and bioenergy.



Adélia Sousa is an assistant professor in the Rural Department, University of Évora, Portugal, and a researcher at the Institute for Mediterranean Agrarian Sciences (ICAAM). She holds a Ph.D. in Rural Engineering from the University of Évora and has authored more than fifty publications. She has worked on around twenty-five national and international research projects in both the academic and private sectors. Her research focuses on the application of remote sensing and GIS techniques to monitoring and management of natural resources, especially in the forest and agriculture.



# Contents

|  |             |
|--|-------------|
| <b>Preface</b>   | <b>XIII</b> |
| <b>Chapter 1</b><br>Energy Production from Forest Biomass: An Overview<br><i>by Ana Cristina Gonçalves, Isabel Malico and Adélia M.O. Sousa</i>  | <b>1</b>    |
| <b>Chapter 2</b><br>The Potential of Sentinel-2 Satellite Images for Land-Cover/Land-Use<br>and Forest Biomass Estimation: A Review<br><i>by Crismeire Isbaex and Ana Margarida Coelho</i>   | <b>25</b>   |
| <b>Chapter 3</b><br>Biomass Estimation Using Satellite-Based Data<br><i>by Patrícia Lourenço</i>   | <b>49</b>   |
| <b>Chapter 4</b><br>Management of Maritime Pine: Energetic Potential with Alternative<br>Silvicultural Guidelines<br><i>by Teresa Fonseca and José Lousada</i>   | <b>71</b>   |
| <b>Chapter 5</b><br>Evergreen Oak Biomass Residues for Firewood<br><i>by Isabel Malico, Ana Cristina Gonçalves and Adélia M.O. Sousa</i>   | <b>87</b>   |
| <b>Chapter 6</b><br>Koroch ( <i>Pongamia pinnata</i> ): A Promising Unexploited Resources<br>for the Tropics and Subtropics<br><i>by Abul Kalam Mohammad Aminul Islam, Swapan Chakrabarty,<br/>Zahira Yaakob, Mohammad Ahiduzzaman<br/>and Abul Kalam Mohammad Mominul Islam</i> | <b>105</b>  |
| <b>Chapter 7</b><br>Case Study: Pathways from Forest to Energy in a Circular Economy<br>at Lafões<br><i>by Ana d’Espiney, Isabel Paula Marques and Helena Maria Pinheiro</i>   | <b>125</b>  |
| <b>Chapter 8</b><br>Methodology for the Evaluation of the Electrical Energy Potential<br>of Residual Biomass from the Wood Industry: A Case Study in Brazil<br><i>by Augusto César de Mendonça Brasil</i>  | <b>143</b>  |

## Chapter 9

### Opportunities of Circular Economy in a Complex System of Woody Biomass and Municipal Sewage Plants

*by Attila Bai and Zoltán Gabnai*

157

# Preface

Forests are responsible for the largest net biomass carbon production. They store the most standing biomass and carbon and thus are an important source of bioenergy. Their importance is linked to their relative abundance and uniformity worldwide and the neutrality of CO<sub>2</sub> emissions from biomass conversion to energy. Yet, the use of forest biomass for energy presents risks related to the forest system's sustainability and demands for new environmentally sustainable strategies for its use.

This book provides a comprehensive overview of the current state of the art in a multitude of subjects related to forest bioenergy, ranging from trees, forest stand management, and biomass assessment to waste management, conversion technologies, and routes and energy applications. It presents a global overview so that the reader can understand the whole chain starting from the tree and ending with energy generation. Written by researchers with extensive experience in various related fields, this volume is a collection of nine chapters that present different perspectives on the topic of forest biomass for energy. The book is organized as follows:

- Chapter 1 Energy Production from Forest Biomass: An Overview
- Chapter 2 The Potential of Sentinel-2 Satellite Images for Land-Cover/Land-Use and Forest Biomass Estimation: A Review
- Chapter 3 Biomass Estimation Using Satellite-Based Data
- Chapter 4 Management of Maritime Pine: Energetic Potential with Alternative Silvicultural Guidelines
- Chapter 5 Evergreen Oak Biomass Residues for Firewood
- Chapter 6 Koroch (*Pongamia pinnata*): A Promising Unexploited Resources for the Tropics and Subtropics
- Chapter 7 Case Study: Pathways from Forest to Energy in a Circular Economy at Lafões
- Chapter 8 Methodology for the Evaluation of the Electrical Energy Potential of Residual Biomass from the Wood Industry: A Case Study in Brazil
- Chapter 9 Opportunities of Circular Economy in a Complex System of Woody Biomass and Municipal Sewage Plants

**Ana Cristina Gonçalves**  
Department of Rural Engineering,  
School of Sciences and Technology,  
MED - Mediterranean Institute for Agriculture, Environment and Development,  
Institute of Research and Advanced Information (IIFA),  
University of Évora,  
Évora, Portugal



**Isabel Malico**

Department of Mechatronics Engineering,  
School of Sciences and Technology,  
University of Évora,  
Évora, Portugal

IDMEC, Instituto Superior Técnico,  
Universidade de Lisboa,  
Lisboa, Portugal

**Adélia Sousa**

Department of Rural Engineering,  
School of Sciences and Technology,  
MED - Mediterranean Institute for Agriculture, Environment and Development,  
Institute of Advanced Studies and Research (IIFA),  
University of Évora,  
Évora, Portugal

# Energy Production from Forest Biomass: An Overview

*Ana Cristina Gonçalves, Isabel Malico and Adélia M.O. Sousa*

## Abstract

As long as care is taken regarding stand and forest sustainability, forest biomass is an interesting alternative to fossil fuels because of its historical use as an energy source, its relative abundance and availability worldwide, and the fact that it is carbon-neutral. This study encompasses the revision of the state of the sources of forest biomass for energy and their estimation, the impacts on forests of biomass removal, the current demand and use of forest biomass for energy, and the most used energy conversion technologies. Forests can provide large amounts of biomass that can be used for energy. However, as the resources are limited, the increasing demand for biomass brings about management challenges. Stand structure is determinant for the amount of residues produced. Biomass can be estimated with high accuracy using both forest inventory and remote sensing. Yet, remote sensing enables biomass estimation and monitoring in shorter time periods. Different bioenergy uses and conversion technologies are characterized by different efficiencies, which should be a factor to consider in the choice of the best suited technology. Carefully analyzing the different options in terms of available conversion technologies, end-uses, costs, environmental benefits, and alternative energy vectors is of utmost importance.

**Keywords:** forest stands, forest residues, potential, bioenergy, conversion technologies

## 1. Introduction

In 2017, the world total primary energy supply was 584.98 EJ, having increased almost 60% since 1990 [1, 2]. In this period, the share of renewable energy sources had a higher increase than that of fossil or nuclear fuels, but it was still relatively low in 2017 (13.6%). Of all the renewable energy sources, renewable waste and biomass, especially solid biofuels and charcoal, contribute the most to the world renewable energy supply (in 2017, 67.9%). At this point, it is important to distinguish between traditional and modern biomass. The former refers to noncommercial wood products, charcoal, agricultural waste, and animal dung burned in inefficient equipment [3]. The promotion of the so-called modern biomass in countries with untapped potentials and the switch from traditional uses to modern ones are of extreme importance for a sustainable development.

Forests are of primordial importance to biomass accumulation and availability as an energy source because of tree dimensions and their life spans, especially when compared to herbaceous and shrubby plants [4]. In what regards forest structures, two main classes can be identified in the context of bioenergy: energy plantations

and stands where the main production is woody products. The amount of biomass and their effects on system sustainability depend on a set of factors related to stand structure, silviculture approaches, and the effects of biomass removal on the system resilience.

The evaluation of biomass and residues in a forest area is frequently done with forest inventory and/or remote sensing and geographical information systems technologies. The accuracy of their estimation is dependent on the methods and techniques used, which in turn are area- and scale-dependent.

The goals of the chapter are the characterization and analysis of (i) the current demand for biomass for energy generation and its relation with the main biomass-consuming sectors (Section 2); (ii) the variability of the availability of biomass from different stand structures and the effect of its removal in a context of sustainable management of the forest stands (Section 3); (iii) the estimation of biomass encompassing the analysis of the methods associated to forest inventory, remote sensing, and geographical information systems (Section 4); and (iv) the conversion of biomass into energy, including the most used technologies and their efficiencies (Section 5).

## 2. Characterization of biomass demand for energy

Primary world energy supply from biofuels and waste was 55.64 EJ in 2017 [1], 9.5% of the total primary energy supply. The share of these fuels decreased in relation to the 1990 value (**Figure 1**). A contrary tendency has occurred in OECD countries, which had 3.3% of their total energy supply met by biofuels and waste in 1990 and 6.1% in 2017 [1].

Biofuels and waste include a diversity of fuels (e.g., solid biofuels, biogases, liquid biofuels, or industrial waste of nonrenewable origin). When only the renewable fraction of waste is considered, the share of biofuels and (renewable) waste decreases from 9.5 to 9.2% [2]. The global supply of primary solid biofuels was 48.15 EJ in 2017 [1]. Solid biofuels and charcoal were by far the most consumed biomass sources in the world in 2017, because of their importance in developing

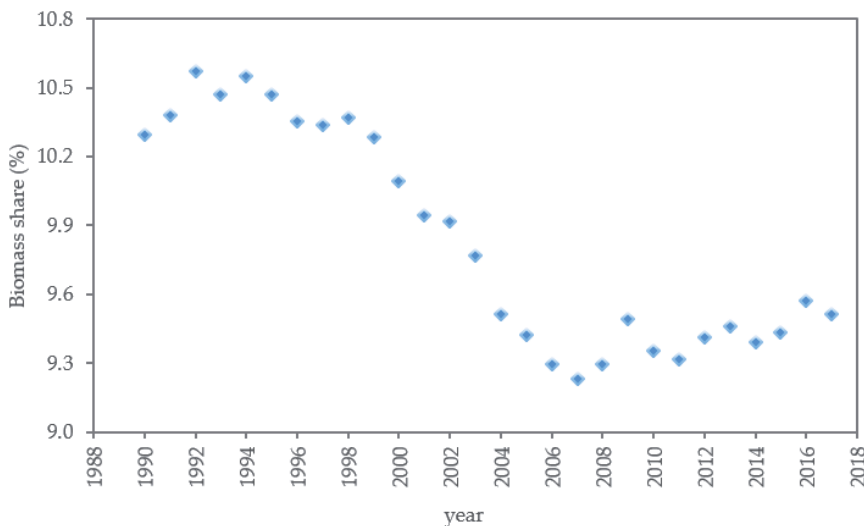


**Figure 1.** Share of biofuels and waste in the world primary energy supply from 1990 to 2017.

countries (**Figure 2**) [2]. Their share dropped to around 2/3 in OECD countries, where modern uses of biomass are the most significant.

The share of the residential sector in the world consumption of primary solid biofuels has been declining in the last decades. However, still more than half of the energy coming from primary solid biofuels was consumed worldwide in this sector in 2017 (**Figure 3**) [1]. In that year, the industrial sector was the second largest consumer of primary solid biofuels, followed by the power sector. When we look at the situation in the OECD countries, the sector that consumed most of the primary solid biofuels in 2017 was industry (35%), closely followed by the residential sector (32%).

An analysis of the world residential energy consumption (**Table 1**) shows that in 2017, biomass and waste were the most used fuels in households, followed by electricity and natural gas [1]. The biomass and waste demand in the residential sector was almost entirely supplied by primary solid biofuels (an exception was China, where biogas accounted for 9% of the biomass supply). Primary solid biofuels are

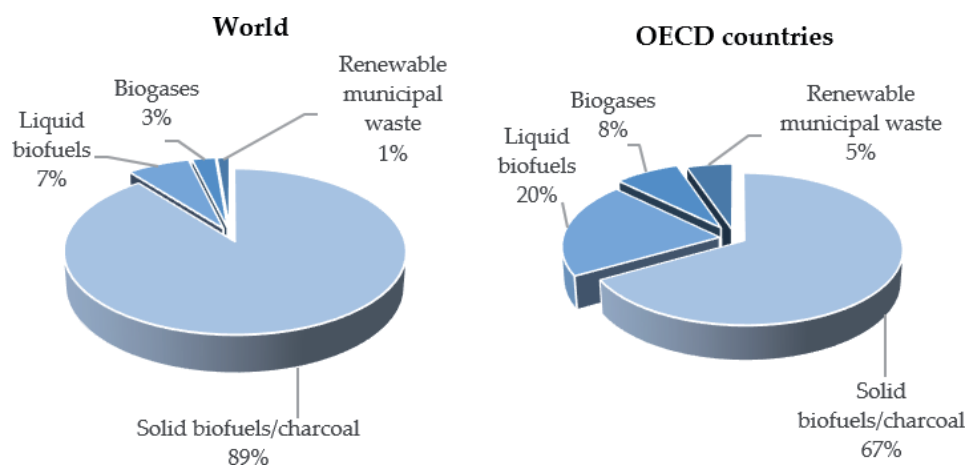


**Figure 2.** Share of the various biomass sources in the biomass primary energy supply in 2017 in the world and in the OECD countries.

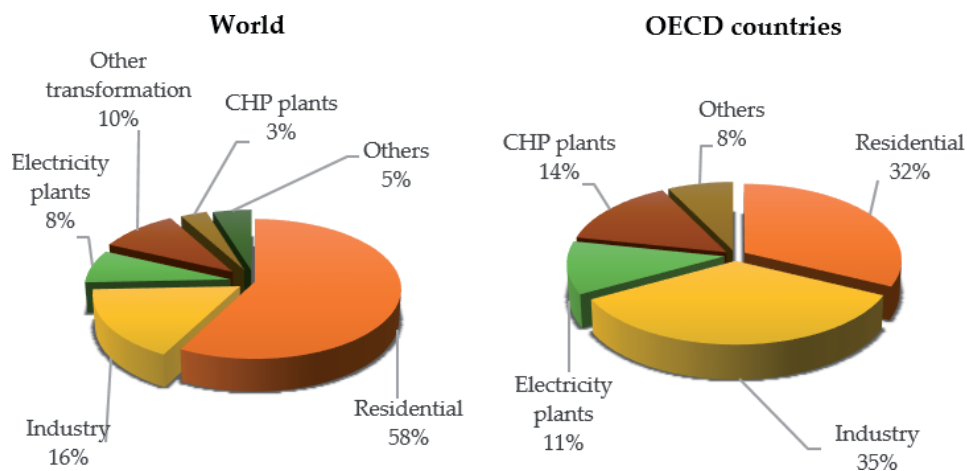


**Figure 3.** Share of the various sectors in the world consumption of primary solid biofuels in 2017 in the world and OECD countries.

|                             | Coal | Oil products | Natural gas | Biofuels and waste | Other renewables | Electricity | Heat |
|-----------------------------|------|--------------|-------------|--------------------|------------------|-------------|------|
| World                       | 3.7  | 10.4         | 21.3        | 34.0               | 1.6              | 24.1        | 4.9  |
| Africa                      | 1.6  | 4.5          | 2.9         | 85.1               | 0.0              | 5.8         | 0.0  |
| Asia excluding China        | 1.3  | 11.7         | 3.1         | 67.2               | 0.2              | 16.4        | 0.1  |
| China                       | 14.4 | 12.7         | 10.6        | 23.4               | 7.8              | 23.6        | 7.6  |
| Middle East                 | 0.0  | 15.1         | 46.1        | 0.5                | 0.2              | 38.2        | 0.0  |
| Non-OECD Americas           | 0.1  | 17.6         | 14.0        | 34.7               | 0.0              | 33.5        | 0.0  |
| Non-OECD Europe and Eurasia | 2.9  | 7.7          | 41.5        | 5.9                | 0.1              | 14.6        | 27.3 |
| OECD Americas               | 0.0  | 7.6          | 39.6        | 6.4                | 0.2              | 46.2        | 0.0  |
| OECD Asia Oceania           | 0.6  | 21.1         | 27.4        | 1.8                | 1.3              | 45.4        | 2.3  |
| OECD Europe                 | 3.7  | 11.2         | 37.4        | 14.0               | 1.3              | 25.3        | 7.2  |

**Table 1.**  
*Share of world residential energy consumption by fuel in 2017.*

|                             | Coal | Crude oil + oil products | Natural gas | Biofuels and waste | Other renewables | Electricity | Heat |
|-----------------------------|------|--------------------------|-------------|--------------------|------------------|-------------|------|
| World                       | 29.0 | 11.4                     | 20.1        | 7.3                | 0.0              | 27.3        | 4.9  |
| Africa                      | 13.1 | 21.4                     | 18.6        | 20.9               | 0.0              | 26.1        | 0.0  |
| Asia excluding China        | 35.0 | 15.7                     | 11.7        | 15.4               | 0.0              | 22.1        | 0.1  |
| China                       | 52.5 | 5.3                      | 5.7         | 0.0                | 0.0              | 30.0        | 6.5  |
| Middle East                 | 1.9  | 25.2                     | 62.7        | 0.0                | 0.0              | 10.1        | 0.0  |
| Non-OECD Americas           | 8.0  | 20.1                     | 18.1        | 0.0                | 0.0              | 31.3        | 22.5 |
| Non-OECD Europe and Eurasia | 19.4 | 11.1                     | 24.6        | 1.1                | 0.0              | 21.2        | 22.6 |
| OECD Americas               | 6.4  | 9.7                      | 43.4        | 11.2               | 0.0              | 27.8        | 1.5  |
| OECD Asia Oceania           | 19.3 | 17.2                     | 17.2        | 6.6                | 0.1              | 37.8        | 1.8  |
| OECD Europe                 | 9.8  | 10.4                     | 30.6        | 8.9                | 0.1              | 34.6        | 5.7  |

**Table 2.**  
*Share of world industrial energy consumption by fuel in 2017.*

particularly important in Africa, where they represented 85% of the fuels and energy vectors consumed in households in 2017. The reality is very different in developed countries, whose households are primarily supplied by electricity or natural gas [1].



The world relies on fossil fuels to meet its industry energy demand, with coal being the most used energy source (**Table 2**) [1]. In 2017, biomass was the only relevant renewable energy source supplying 7.3% of the world's industrial energy consumption. Primary solid biofuels and, in some regions, industrial waste were the main types of biomass consumed by the industry.

### **3. Biomass availability in different stand structures**

In general, in forest stands, biomass increases over time [5]. However, biomass accumulation is influenced by a set of factors that encompass stand structure, species traits, site quality, individual tree interactions, density, and disturbances. Stand structure is determined by the regime (high forest or coppice), composition (pure or mixed), and structure (even-aged or uneven-aged) [6]. Regime influences tree and stand growth, with coppice individuals having higher initial growth rates than high forest ones, as they use the existing root system [7]. In stands with even-aged (one cohort) structure, biomass increases from installation to old-growth stage [8]. Inversely, in the uneven-aged structure (two or more cohorts), biomass ideally remains approximately constant over time [9]. In stands with pure composition (one predominant species), biomass accumulation depends on the species traits, such as growth and shade tolerance; spatial arrangements (in regular spacing individual trees have similar growing space and growth rates); and density (the higher, the smaller the growing space and the growth rate per tree) [10, 11]. In mixed stands, biomass accumulation is determined, in addition to the aforementioned factors, by the number of species, their proportion, the interactions among species, and the spatial arrangement of the species. The biomass stock increases with species traits complementarity, and with spatial arrangements that promote facilitation, while it seems less sensitive to the number of species [12, 13]. Biomass stocks increase with site quality and complementarity among species, due to the increase of the growing space and tree growth rates. This increase is related to a higher availability of (i) light [14] or to their complementary use [14, 15]; (ii) water, which is also affected by crown cover [16]; and (iii) nutrients that can also be promoted by species with complementary traits, such as N-fixing [17]. Disturbances have two main effects on standing biomass, namely their reduction and their reallocation. In general, disturbances whether natural (e.g., storms, fires) or artificial (e.g., harvests, thinnings, prunings) reduce standing biomass, especially when woody products are exported from the stand [18]. As disturbances release growing space, they increase the tree growth rate and thus reallocate biomass stocks to the residual trees [19].

In general, the stand structures with the highest potential for biomass for energy are those that accumulate the largest biomass in the shortest time. This goal is achieved by energy plantations, which are coppice pure even-aged stands of fast-growing species, managed in high density stands in very short rotations, sometimes fertilized and/or irrigated [20, 21]. Yet, other stand structures are also of interest, such as the high forest pure or mixed even-aged stands. In these stands, only the biomass without quality for timber or without high market value is used for bioenergy, namely dead trees, trees with timber of bad quality, wood of trees species with low or very low market price and forest residues (e.g., tops, branches). The amount of biomass for energy increases from pure to mixed stands [22]. The least interesting stand structures for bioenergy are the high forest pure or mixed uneven-aged stands. This is related with the quantities of residues generated in the harvests and especially the technical difficulties for removing them without damaging the residual stand as well as the associated costs [23].

Energy plantations' yield variability seems to be related to site, species, clone, climate, density, and rotation. In the literature, a wide range of yields are referred, from 0.6 to 50 t ha<sup>-1</sup> y<sup>-1</sup> [24, 25]. Species and clones' ecological characteristics are expressed by the edaphic and climatic conditions, with yields increasing with site quality [26] and water availability [27]. Density and rotation are linked, resulting in stands of higher density and shorter rotations [26] or with lower density and longer rotations [28].

The viability of removing biomass for energy is linked to stand structure, and to environmental, legal, technical, and economic aspects. In energy plantations, all aerial biomass is removed [27], while in stands managed for woody products, residues are partially removed. The removal proportion ranges from 0 to 80% of the above ground biomass [23, 29]. The most frequently used proportions of residues removal in relation to above ground biomass range between 13 and 17%, with a mean of 15% [29–31]. In even-aged stands, the amounts of residues are larger, so it is technically and economically feasible to remove them [23]. Also, spatial distribution of residues can be scattered in the stand in which case 50% are removed or packed where 65% of the residues are removed [30, 32, 33]. In difficult topographic conditions, such as steep slopes, collecting residues is technically difficult and expensive [34].

The removal of biomass from any forest stand, regardless of their use, has always impacts on site and stand productivity and sustainability [35]. Forest ecosystems have more or less resilience [36], and management can actively promote biomass stocks in the stands [37]. This has led to an ongoing discussion about the effects of biomass removal on stand productivity, soil, hydrology, and habitat and diversity [38–40]. The impact of the removal of biomass depends on the type of biomass removed and their quantity [41]. Biomass removal implies the export, to a smaller or larger extent, of nutrients [42, 43]. The larger proportions of nutrients are found in the newest tissues, i.e., leaves, twigs, and branches, when compared to the oldest, that is, stems or large branches [44, 45]. Thus, removals of stems are more sustainable than the all tree harvest [46]. Nutrients' export is higher in coppice than in high forest [45]. Also, the poorer the site, the stronger the negative effects of biomass residue removal in the soil and stand productivity [41]. The latter can be enhanced by maintaining the residues (totally or partially) in the stands, especially those with higher nutrient content [43] or alternatively, when it is technically and economically feasible, with fertilization with inorganic or organic fertilizers [43, 47]. Soil potential productivity is influenced by soil organic matter, depending strongly on the inputs (litter) and is species and stand structure-dependent [48]. In general, high forest stands produce larger amounts of litter during more time than coppices, resulting in larger amounts of soil organic matter and nutrients, through decomposition [49].

The removal of biomass can contribute to increased runoff and, consequently, leaching and erosion [50, 51]. This risk decreases from clear-cut to selective systems and with the decrease of residues removal as they have a protection effect on the soil [23]. The minimization of the impacts of these three factors can be achieved by the maintenance of stumps, reduction of the amount of residues removed, and, when possible, compensation fertilization [51].

In general, diversity decreases from high forest mixed uneven-aged to coppice pure even-aged stands [17]. The temporal and spatial patterns of biomass removal affect differently biodiversity [52]. Biodiversity increases with the increase of rotation length [53] and with the spatial heterogeneity of the removals [7]. The increase of biodiversity can have also negative effects on biomass. One example is the populations of pest whose breeding material is the biomass residues. This increase of diversity is related to a higher risk of pest attacks to living trees. It depends on

pest density (increasing with density increase) and tree vigor (increasing with the decrease of tree vigor). In this case, if the residues are maintained in that stand, their storage in large piles is recommended as the pests colonize more the outer than the inner part of the pile, thus decreasing the pest population [54].

#### **4. Biomass estimation**

Forest biomass can be estimated at tree or area-level, and the methods can be grouped according to the data used.

At tree level biomass can be estimated with direct or indirect methods [55]. Biomass estimation with the direct method is based on destructive sampling with the determination of the dry weight of biomass, frequently evaluated per component: stem, bark, crown (or alternatively branches and leaves) and sometimes below ground biomass [56–58]. At tree level, three approaches can be used with indirect methods. In the first, biomass is determined with conversion methods, usually as function of volume, and wood apparent density [56, 59]. In the second, biomass is obtained by allometric functions which were developed with data from destructive sampling. These functions frequently have as independent variables the diameter at breast height and/or total height [56]. A wide range of allometric functions have been developed [60–63]. Yet, as they are specific to the species, regime, and site, necessity arises for new biomass functions [25, 64–66]. In the third approach, biomass is obtained by fitting functions with data from LiDAR high density 3D cloud points, where treetop, crown radii, and crown boundary are frequently used as independent variables [67, 68].

At area level, six approaches can be used with indirect methods, all of which use, as dependent variable, biomass at plot level (sum of biomass calculated with allometric functions at tree level). Forest inventory plot data are frequently used [57, 58, 69]. The first approach uses conversion factors based on absolute density measures (e.g., volume or number of trees per hectare) with more (exponential) or less (coefficient) complex formulas [66, 70]. The second approach uses expansion factors, with stand structure, topography, and edaphic and climatic variables as independent variables [66, 70, 71]. The third approach uses expansion factors with independent variables derived from thematic maps (e.g., stand structure, soil type, topographic variables) with k-nearest neighbor methods [57, 72]. In the fourth approach, biomass is modeled with independent variables derived from passive remote sensing data with several spatial resolutions. The most commonly used variables are spectral reflectance, crown diameter and crown horizontal projection [73–78], original bands, and/or vegetation indices [79–82]. Among the parametric models, the most frequently used are linear regression, both single [80, 83, 84] and multiple [80, 83]; and nonlinear regression, power [84–86] and logistic [87]. The nonparametric models include regression k-nearest neighbor [88–90], artificial neural network [91], regression tree [35, 92, 93], random forest [18, 94–96], support vector machine [94], and maximum entropy [97]. These functions have been developed with satellite imagery of low [98–100], medium [100–103], and high [73, 75–77, 104–106] spatial resolution. In the fifth approach, biomass is modeled with data from Synthetic Aperture Radar (SAR) with bagging stochastic gradient boosting algorithms, backscattering amplitudes, and multivariate linear regression [107–109]. L or P bands are better suited for forests with high level of biomass, while X and C bands for those with low biomass [109, 110]. In the sixth approach, biomass is modeled with data derived from LiDAR metrics of horizontal (crown cover) and vertical (mean, standard deviation, and percentiles of height) with linear regression, k most similar neighbors, and random forest [109, 111, 112].

The use of allometric functions at tree level is the most accurate indirect method. Yet, it has the disadvantage of being species-, regime-, and site-specific and labor-demanding [55]. The use of conversion and expansion factors is less labor-demanding, and in large areas it can be accurate enough, but accuracy decreases with the increase of stand variability [66, 70, 71]. The reduction of pixel size and area increases the accuracy of expansion factors with remote sensing data [72, 112]. This approach has the advantages of allowing automatic mapping and working at several spatial resolutions. The disadvantages are related with large pixel sizes, different dimensions of pixel and plot sizes, and poor correlation between remote sensing data and biomass [72]. The accuracy of biomass functions derived from passive sensors data increases with the increase of their spatial resolution and homogeneity of the stand structure and topographic, edaphic, and climatic conditions [109, 113]. Some shortcomings have been pointed out to the use of passive sensor data. Examples are saturation and/or the impossibility of their use under certain weather conditions, such as clouds [109, 111, 113]. These limitations are overcome by LiDAR [109, 114], but not by SAR, which also presents signal saturation for high biomass [110, 113, 115]. Biomass functions derived from LiDAR data and their raster maps are accurate, especially those from Airborne Laser Scanning data [116, 117].

The combination of data from several passive and/or active sensors has been used with several statistical methods to improve the accuracy of biomass estimates. Examples are SPOT and LiDAR data [118], LiDAR and Landsat [113, 119], RaDAR and Sentinel 1 and 2 [95], SAR and Landsat [120, 121], LiDAR and hyperspectral [122], LiDAR and RaDAR [123], Geoscience Laser Altimeter System (GLAS) and Modis [124]; LiDAR and airborne imagery of very high spatial resolution image [125], or Sentinel 1 (SAR) and Sentinel 2 [126, 127].

## **5. Conversion of forest biomass into energy**

Forest biomass is most commonly converted into energy by thermochemical processes, combustion being the most mature and widely used [128, 129]. The two other conversion routes that are commercially available are gasification and pyrolysis. They transform forest biomass into biofuels. Other primary conversion routes are possible but are still at a less developed stage. When biomass is converted into power, secondary conversion technologies are needed. Of these, conventional steam turbines are the most used [130, 131], but depending on the primary conversion technology or the end-use, other technologies commercially available may be more appropriate (e.g., organic Rankine cycles or internal combustion engines). A general description of biomass conversion technologies is outside the scope of this chapter, but readers should refer, for example, to [131–133] for more information.

Although forest biomass can be used to produce fuels for the transport sector, as referred above, currently it is mostly converted to heat and/or to electricity and it is used in the residential, industrial, and energy sectors [1]. The next sections describe the conversion technologies most frequently used in these sectors.

### **5.1 Residential sector**

As already seen in Section 2, at the world level, energy from solid biomass is mostly used in the residential sector. In developing countries, solid biomass is often used in households for heating and cooking with the use of very inefficient equipment while in developed countries, it is almost exclusively used for heating purposes [134]. The supply of bioenergy to households by district heating is also common in some countries [135] and will be described in Section 5.3.

Cooking is not the activity that consumes the most energy worldwide, but it is the most universal residential energy service, and therefore, it is of particular importance [136]. In developed countries, the use of biomass for cooking is not common and is associated with luxury [134]. In developing countries, however, cooking is the primary residential use of solid fuels (biomass and coal) [134]. Open fires and inefficient traditional cookstoves are the technologies usually used [137]. Examples of common wood-fired cookstoves are 3-stone fires, semi-open cookstoves, traditional hearths or rocket stoves [134]. Their efficiencies range from around 10% for open fires to around 40% for improved types of stoves [134, 138–140]. The traditional use of biomass results in severe negative impacts on human health [137, 141, 142], and, therefore, strategies to mitigate health risks are of utmost importance. The development, promotion, and dissemination of improved wood-fired cookstoves are important but have proved to be of limited success [137].

Globally, space and water heating are the most energy-consuming activities in the residential sector [143]. In most developing countries, however, space heating is not the main use of energy in households, because of geography and climate (typically in these countries, most energy is spent for cooking) [144]. Open fires and traditional stoves are used for heating in lower-income households in developing countries. In cold regions, the same equipment that is used for cooking is frequently used for space heating [142]. The energy efficiencies are low, and the negative impacts on human health are high. In developed countries, in general, wood is not the most used fuel for space and water heating. However, today, wood heating is still popular in many cold and temperate climate zones [134]. There is a big diversity of biomass-fired equipment used to produce heat. Open fireplaces, stoves, furnaces, and boilers are examples of frequently used equipment [132, 145]. They can produce heat locally (the case of small-size fireplaces) or centrally (the case of biomass-fired central heating systems). The conversion efficiencies is very diverse, depending on the way biomass is converted to energy. The use of inefficient fireplaces leads to efficiencies lower than 20% [146], while modern wood pellet boilers are very efficient, presenting efficiencies above 90% [147].

## **5.2 Industrial sector**

Industry is the sector that consumes most solid biomass in OECD countries, while globally, it is the second largest final use of biomass (**Figure 3**). Nonetheless, there is still an untapped potential to increase the use of solid biomass in industry, but economic viability, high investment costs, guarantee of feedstock, and security of supply are factors that often hamper the investment in bioenergy [148]. The sector is very diverse both in terms of industrial processes and energy conversion technologies used, and, consequently, developing global strategies to promote biomass use in the industry is a difficult task [148]. Solid biofuels can provide the full range of temperatures needed by the industry, which some other renewable energy sources cannot [149]. Therefore, channeling biomass into high-temperature industrial processes seems to be a good strategy in terms of greenhouse gas emission reduction (for instance, the residential sector requires low temperature heat, and, therefore, this is a sector where other renewable energy sources can easily penetrate). The share of bioenergy in the different industrial sectors and countries is very uneven, but one can say that it is essentially used to produce process heat and combined heat and power (CHP). Boilers, dryers, kilns, furnaces, and ovens are typical biomass-fired process heat generators [150–163]. The most popular technologies for heat generation in the



industrial sector are combustion boilers [131], which include fixed bed, bubbling fluidized bed, and circulating fluidized combustion [148]. The efficiencies of the former are in the range of 60–90%, while that of fluidized bed boilers are in the range of 75–92% [164]. CHP systems are also widely used in some industrial sectors, such as the pulp, food, and chemical industries [165], mostly integrating conventional steam turbines as secondary conversion technology [130, 131]. Their capacities typically range from 1 to 50 MW<sub>e</sub> [131, 166], electrical efficiencies from 15 to 35% [131], and overall efficiencies are above 80% [167, 168]. Co-firing with coal (described in the next section) is also used in some industrial sectors [169].

### **5.3 Energy sector**

Biomass use for electricity generation is well developed, biofuels often being co-fired with coal [170]. Most systems are based on fixed or fluidized bed technologies used in a steam turbine cycle, pulverized boilers also being commonly used [171]. Large biomass-fired power plants with capacities of the order of 50 MW<sub>e</sub> have efficiencies of around 40%, while smaller plants typically have efficiencies of 20–30% [132]. Generally, biomass power plants are smaller than coal ones because of local feedstock availability. Co-firing with coal in coal-fired power plants is a possibility that allows for the use of larger capacities (and efficiencies). This cost-effective strategy results in a reduction of the GHG emissions from conventional solid fuel power plants and is a low-risk option for the production of bio-power [170, 171].

In conventional power plants, the rejected heat is wasted, and the overall efficiency is low. If this heat is used (CHP) and distributed in district heating networks, the overall efficiency of the energy conversion is much higher. Market penetration of (biomass) district heating systems is quite different depending on the country. In the countries where district heating (independent of the energy carrier used) is more popular, it provides heat to around half of building stocks [135]. It is in the European Union that most CHP biomass-fired district heating plants are in operation [135, 172]. Some biomass heat-only plants also exist but are relevant for small-scale district heating systems [173]. The technologies used are similar to the ones used for indirect heating in industrial applications.

## **6. Conclusions**

Forests can provide large amounts of biomass, which can be used for energy generation. The increasing demand of forest biomass for energy brings about management challenges since biomass is a limited resource. The amount of residues produced is dependent on stand structure, with pure even-aged stands providing more biomass than mixed uneven-aged ones. Energy plantations have the highest potential for biomass for energy. Biomass can be estimated with high accuracy using both forest inventory and remote sensing. Yet, remote sensing enables biomass estimation and monitoring in shorter time periods than the forest inventories. Forest biomass can be converted into energy using distinct technologies and cover different end-uses, resulting in different overall efficiencies. Important variables to be considered when choosing the best suited biomass technology are efficiency, economic feasibility, and environmental benefits. This choice is not unique and is dependent on the region, facts that pose challenges in the management of the biomass supply chains.

## Acknowledgements

This work is funded by National Funds through FCT—Foundation for Science and Technology, under the Project UIDB/05183/2020 (MED) and Project UIDB/50022/2020 (through IDMEC, under LAETA).

## Author details

Ana Cristina Gonçalves<sup>1\*</sup>, Isabel Malico<sup>2,3</sup> and Adélia M.O. Sousa<sup>1</sup>


1 Department of Rural Engineering, School of Sciences and Technology, MED-Mediterranean Institute for Agriculture, Environment and Development, Institute of Research and Advanced Education (IIFA), University of Évora, Évora, Portugal

2 Department of Physics, School of Sciences and Technology, University of Évora, Évora, Portugal

3 IDMEC, Instituto Superior Técnico, Universidade de Lisboa, Lisboa, Portugal

\*Address all correspondence to: [acag@uevora.pt](mailto:acag@uevora.pt)

## IntechOpen

© 2020 The Author(s). Licensee IntechOpen. Distributed under the terms of the Creative Commons Attribution - NonCommercial 4.0 License (<https://creativecommons.org/licenses/by-nc/4.0/>), which permits use, distribution and reproduction for non-commercial purposes, provided the original is properly cited. 

## References

- [1] IEA. IEA Statistics [Internet]. 2020. Available from: <https://www.iea.org/data-and-statistics> [Accessed: 05 March 2020]
- [2] IEA. Renewables Information: Overview. 2019. p. 12
- [3] Goldemberg J, Coelho ST. Renewable energy—Traditional biomass vs. modern biomass. *Energy Policy*. 2004;**32**(6):711-714
- [4] Urbano AR, Keeton WS. Carbon dynamics and structural development in recovering secondary forests of the northeastern U.S. *Forest Ecology and Management*. 2017;**392**:21-35
- [5] Cardinale BJ, Wright JP, Cadotte MW, Carroll IT, Hector A, Srivastava DS, et al. Impacts of plant diversity on biomass production increase through time because of species complementarity. *Proceedings of the National Academy of Sciences*. 2007;**104**(46):18123-18128
- [6] Smith DM, Larson BC, Kelty MJ, Ashton PMS. The Practice of Silviculture. *Applied Forest Ecology*. 9th ed. New York: John Wiley & Sons, Inc; 1997. p. 560
- [7] Kirby KJ, Buckley GP, Mills J. Biodiversity implications of coppice decline, transformations to high forest and coppice restoration in British woodland. *Folia Geobotanica*. 2017 Mar;**52**(1):5-13
- [8] Zhang H, Zhou G, Wang Y, Bai S, Sun Z, Berninger F, et al. Thinning and species mixing in Chinese fir monocultures improve carbon sequestration in subtropical China. *European Journal of Forest Research*. 2019;**138**(3):433-443
- [9] Lundqvist L. Tamm review: Selection system reduces long-term volume growth in Fennoscandic uneven-aged Norway spruce forests. *Forest Ecology and Management*. 2017;**391**:362-375
- [10] Baret M, Pepin S, Ward C, Pothier D. Long-term changes in stand growth dominance as related to resource acquisition and utilization in the boreal forest. *Forest Ecology and Management*. 2017;**400**:408-416
- [11] Dye A, Ross Alexander M, Bishop D, Druckenbrod D, Pederson N, Hessler A. Size-growth asymmetry is not consistently related to productivity across an eastern US temperate forest network. *Oecologia*. 2019;**189**(2):515-528
- [12] Grossman JJ, Vanhellefont M, Barsoum N, Bauhus J, Bruelheide H, Castagneyrol B, et al. Synthesis and future research directions linking tree diversity to growth, survival, and damage in a global network of tree diversity experiments. *Environmental and Experimental Botany*. 2018;**152**:68-89
- [13] Vanhellefont M, Bijlsma R-J, De Keersmaecker L, Vandekerckhove K, Verheyen K. Species and structural diversity affect growth of oak, but not pine, in uneven-aged mature forests. *Basic and Applied Ecology*. 2018;**27**:41-50
- [14] Forrester DI, Ammer C, Annighöfer PJ, Barbeito I, Bielak K, Bravo-Oviedo A, et al. Effects of crown architecture and stand structure on light absorption in mixed and monospecific *Fagus sylvatica* and *Pinus sylvestris* forests along a productivity and climate gradient through Europe. *Journal of Ecology*. 2018;**106**(2):746-760
- [15] Fotis AT, Morin TH, Fahey RT, Hardiman BS, Bohrer G, Curtis PS. Forest structure in space and time:

Biotic and abiotic determinants of canopy complexity and their effects on net primary productivity. *Agricultural and Forest Meteorology*. 2018;**250-251**:181-191

[16] Ehbrecht M, Schall P, Ammer C, Fischer M, Seidel D. Effects of structural heterogeneity on the diurnal temperature range in temperate forest ecosystems. *Forest Ecology and Management*. 2019;**432**:860-867

[17] Liang J, Watson JV, Zhou M, Lei X. Effects of productivity on biodiversity in forest ecosystems across the United States and China: Productivity-biodiversity relationship. *Conservation Biology*. 2016;**30**(2):308-317

[18] Thom D, Keeton WS. Stand structure drives disparities in carbon storage in northern hardwood-conifer forests. *Forest Ecology and Management*. 2019;**442**:10-20

[19] Flamenco HN, Gonzalez-Benecke CA, Wightman MG. Long-term effects of vegetation management on biomass stock of four coniferous species in the Pacific Northwest United States. *Forest Ecology and Management*. 2019;**432**:276-285

[20] Pérez-Cruzado C, Sanchez-Ron D, Rodríguez-Soalleiro R, Hernández MJ, Mario Sánchez-Martín M, Cañellas I, et al. Biomass production assessment from *Populus* spp. short-rotation irrigated crops in Spain. *GCB Bioenergy*. 2014;**6**(4):312-326

[21] Stojanović M, Sánchez-Salguero R, Levanič T, Szatniewska J, Pokorný R, Linares JC. Forecasting tree growth in coppiced and high forests in the Czech Republic. The legacy of management drives the coming *Quercus petraea* climate responses. *Forest Ecology and Management*. 2017;**405**:56-68

[22] Durocher C, Thiffault E, Achim A, Auty D, Barrette J. Untapped volume

of surplus forest growth as feedstock for bioenergy. *Biomass and Bioenergy*. 2019;**120**:376-386

[23] Daioglou V, Stehfest E, Wicke B, Faaij A, van Vuuren DP. Projections of the availability and cost of residues from agriculture and forestry. *GCB Bioenergy*. 2016;**8**(2):456-470

[24] Bergante S, Manzone M, Facciotto G. Alternative planting method for short rotation coppice with poplar and willow. *Biomass and Bioenergy*. 2016;**87**:39-45

[25] Djomo SN, Ac A, Zenone T, De Groote T, Bergante S, Facciotto G, et al. Energy performances of intensive and extensive short rotation cropping systems for woody biomass production in the EU. *Renewable and Sustainable Energy Reviews*. 2015;**41**:845-854

[26] Fischer M, Kelley AM, Ward EJ, Boone JD, Ashley EM, Domec J-C, et al. A critical analysis of species selection and high vs. low-input silviculture on establishment success and early productivity of model short-rotation wood-energy cropping systems. *Biomass and Bioenergy*. 2017;**98**:214-227

[27] Dillen M, Vanhellemont M, Verdonck P, Maes WH, Steppe K, Verheyen K. Productivity, stand dynamics and the selection effect in a mixed willow clone short rotation coppice plantation. *Biomass and Bioenergy*. 2016;**87**:46-54

[28] Giannini V, Silvestri N, Dragoni F, Pistocchi C, Sabbatini T, Bonari E. Growth and nutrient uptake of perennial crops in a paludicultural approach in a drained Mediterranean peatland. *Ecological Engineering*. 2017;**103**:478-487

[29] Cintas O, Berndes G, Hansson J, Poudel BC, Bergh J, Börjesson P, et al. The potential role of forest management

in Swedish scenarios towards climate neutrality by mid century. *Forest Ecology and Management*. 2017;**383**:73-84

[30] Farine DR, O'Connell DA, John Raison R, May BM, O'Connor MH, Crawford DF, et al. An assessment of biomass for bioelectricity and biofuel, and for greenhouse gas emission reduction in Australia. *GCB Bioenergy*. 2012;**4**(2):148-175

[31] Rothe A, Moroni M, Neyland M, Wilnhammer M. Current and potential use of forest biomass for energy in Tasmania. *Biomass and Bioenergy*. 2015;**80**:162-172

[32] Martire S, Castellani V, Sala S. Carrying capacity assessment of forest resources: Enhancing environmental sustainability in energy production at local scale. *Resources, Conservation and Recycling*. 2015;**94**:11-20

[33] Pedroli B, Elbersen B, Frederiksen P, Grandin U, Heikkilä R, Krogh PH, et al. Is energy cropping in Europe compatible with biodiversity?—Opportunities and threats to biodiversity from land-based production of biomass for bioenergy purposes. *Biomass and Bioenergy*. 2013;**55**:73-86

[34] Mola-Yudego B, Arevalo J, Díaz-Yáñez O, Dimitriou I, Haapala A, Carlos Ferraz Filho A, et al. Wood biomass potentials for energy in northern Europe: Forest or plantations? *Biomass and Bioenergy*. 2017;**106**:95-103

[35] Ford SE, Keeton WS. Enhanced carbon storage through management for old-growth characteristics in northern hardwood-conifer forests. *Ecosphere*. 2017;**8**(4):e01721

[36] Powers M, Kolka R, Palik B, McDonald R, Jurgensen M. Long-term management impacts on carbon storage in Lake states forests. *Forest Ecology and Management*. 2011;**262**(3):424-431

[37] Williams NG, Powers MD. Carbon storage implications of active management in mature *Pseudotsuga menziesii* forests of western Oregon. *Forest Ecology and Management*. 2019;**432**:761-775

[38] Belleau A, Brais S, Paré D. Soil nutrient dynamics after harvesting and slash treatments in boreal Aspen stands. *Soil Science Society of America Journal*. 2006;**70**(4):1189

[39] Berndes G, Hoogwijk M, van den Broek R. The contribution of biomass in the future global energy supply: A review of 17 studies. *Biomass and Bioenergy*. 2003;**25**(1):1-28

[40] Shepard JP. Water quality protection in bioenergy production: The US system of forestry best management practices. *Biomass and Bioenergy*. 2006;**30**(4):378-384

[41] Egnell G. A review of Nordic trials studying effects of biomass harvest intensity on subsequent forest production. *Forest Ecology and Management*. 2017;**383**:27-36

[42] Guidi W, Labrecque M. Short-Rotation Coppice of Willows for the Production of Biomass in Eastern Canada. In: Matovic MD, editor. *Biomass Now—Sustainable Growth and Use*. Rijeka, Croatia: IntechOpen; 2013. Available from: <http://www.intechopen.com/books/biomass-now-sustainable-growth-and-use/short-rotation-coppice-of-willows-for-the-production-of-biomass-in-eastern-canada> [Accessed: 08 March 2018]

[43] Raulund-Rasmussen K, Stupak I, Clarke N, Callesen I, Helmisaari H-S, Karlton E, et al. Effects of very intensive forest biomass harvesting and long term site productivity. In: Röser D, Asikainen A, Raulund-Rasmussen K, Stupak I, editors. *Sustainable Use of Forest Biomass for Energy a Synthesis with Focus on the Baltic and Nordic*

Region. Dordrecht: Springer; 2008.  
pp. 29-78

[44] Achat DL, Fortin M, Landmann G, Ringeval B, Augusto L. Forest soil carbon is threatened by intensive biomass harvesting. *Scientific Reports*. 2015;5(1):15991

[45] Pyttel PL, Köhn M, Bauhus J. Effects of different harvesting intensities on the macro nutrient pools in aged oak coppice forests. *Forest Ecology and Management*. 2015;349:94-105

[46] Tamminen P, Saarsalmi A, Smolander A, Kukkola M, Helmisaari H-S. Effects of logging residue harvest in thinnings on amounts of soil carbon and nutrients in scots pine and Norway spruce stands. *Forest Ecology and Management*. 2012;263:31-38

[47] Marron N. Agronomic and environmental effects of land application of residues in short-rotation tree plantations: A literature review. *Biomass and Bioenergy*. 2015;81:378-400

[48] Jandl G, Acksel A, Baum C, Leinweber P. Indicators for soil organic matter quality in no-till soils under perennial crops in Central Sweden. *Soil and Tillage Research*. 2015;148:74-84

[49] Hölscher D, Schade E, Leuschner C. Effects of coppicing in temperate deciduous forests on ecosystem nutrient pools and soil fertility. *Basic and Applied Ecology*. 2001;2(2):155-164

[50] Fernández C, Vega JA, Fonturbel T, Pérez-Gorostiaga P, Jiménez E, Madrigal J. Effects of wildfire, salvage logging and slash treatments on soil degradation. *Land Degradation and Development*. 2007;18(6):591-607

[51] Stupak I, Asikainen A, Röser D, Pasanen K. Review of recommendations

for forest energy harvesting and wood ash recycling. In: Röser D, Asikainen A, Raulund-Rasmussen K, Stupak I, editors. *Sustainable Use of Forest Biomass for Energy a Synthesis with Focus on the Baltic and Nordic Region*. Dordrecht: Springer; 2008. pp. 155-196

[52] Jonsell M. The effects of forest biomass harvesting on biodiversity. In: Röser D, Asikainen A, Raulund-Rasmussen K, Stupak I, editors. *Sustainable Use of Forest Biomass for Energy a Synthesis with Focus on the Baltic and Nordic Region*. Dordrecht: Springer; 2008. pp. 129-154

[53] Fartmann T, Müller C, Poniatowski D. Effects of coppicing on butterfly communities of woodlands. *Biological Conservation*. 2013;159:396-404

[54] Schroeder LM. Insect pests and forest biomass for energy. In: Röser D, Asikainen A, Raulund-Rasmussen K, Stupak I, editors. *Sustainable Use of Forest Biomass for Energy a Synthesis with Focus on the Baltic and Nordic Region*. Dordrecht: Springer; 2008. pp. 109-128

[55] Gonçalves AC, Malico I, AMO S. Solid biomass from forest trees to energy: A review. In: Jacob-Lopes E, Queiroz Zepka L, editors. *Renewable Resources and Biorefineries*. Rijeka, Croatia: IntechOpen; 2019. Available from: <https://www.intechopen.com/books/renewable-resources-and-biorefineries/solid-biomass-from-forest-trees-to-energy-a-review> [Accessed: 09 August 2019]

[56] Burkhart HE, Tomé M. *Modeling Forest Trees and Stands* [Internet]. Dordrecht: Springer Netherlands; 2012. Available from: <http://link.springer.com/10.1007/978-90-481-3170-9> [Accessed: 03 July 2018]

- [57] McRoberts RE, Tomppo EO, Næsset E. Advances and emerging issues in national forest inventories. *Scandinavian Journal of Forest Research*. 2010;25(4):368-381
- [58] Tomppo E, Olsson H, Ståhl G, Nilsson M, Hagner O, Katila M. Combining national forest inventory field plots and remote sensing data for forest databases. *Remote Sensing of Environment*. 2008;112(5):1982-1999
- [59] Neumann M, Moreno A, Mues V, Härkönen S, Mura M, Bouriaud O, et al. Comparison of carbon estimation methods for European forests. *Forest Ecology and Management*. 2016;361:397-420
- [60] Eamus D, Mcguinness K, Burrows W. Review of Allometric Relationships for Estimating Woody Biomass for Queensland, the Northern Territory and Western Australia. Technical Report No. 5a2000. p. 56
- [61] Paul KI, Roxburgh SH, England JR, Ritson P, Hobbs T, Brooksbank K, et al. Development and testing of allometric equations for estimating above-ground biomass of mixed-species environmental plantings. *Forest Ecology and Management*. 2013;310:483-494
- [62] Ter-Mikaelian MT, Korzukhin MD. Biomass equations for sixty-five north American tree species. *Forest Ecology and Management*. 1997;97:1-24
- [63] Zianis D, Seura SM, Metsäntutkimuslaitos, editors. Biomass and Stem Volume Equations for Tree Species in Europe (*Silva Fennica Monographs*). Helsinki, Finland: Finnish Society of Forest Science, Finnish Forest Research Institute; 2005. p. 63
- [64] Annighöfer P, Ameztegui A, Ammer C, Balandier P, Bartsch N, Bolte A, et al. Species-specific and generic biomass equations for seedlings and saplings of European tree species. *European Journal of Forest Research*. 2016;135(2):313-329
- [65] de Jong J, Akselsson C, Egnell G, Löfgren S, Olsson BA. Realizing the energy potential of forest biomass in Sweden – How much is environmentally sustainable? *Forest Ecology and Management*. 2017;383:3-16
- [66] Jagodziński AM, Dyderski MK, Gęsikiewicz K, Horodecki P, Cysewska A, Wierczyńska S, et al. How do tree stand parameters affect young scots pine biomass? – Allometric equations and biomass conversion and expansion factors. *Forest Ecology and Management*. 2018;409:74-83
- [67] Brovkina O, Novotny J, Cienciala E, Zemek F, Russ R. Mapping forest aboveground biomass using airborne hyperspectral and LiDAR data in the mountainous conditions of Central Europe. *Ecological Engineering*. 2017;100:219-230
- [68] Chen Q. LiDAR remote sensing of vegetation biomass. In: *Remote Sensing of Natural Resources* [Internet]. CRC Press; 2013. pp. 399-420. Available from: <http://www.crcnetbase.com/doi/abs/10.1201/b15159-28> [Accessed: 21 November 2019]
- [69] Vidal C, Lanz A, Tomppo E, Schadauer K, Gschwantner T, di Cosmo L, et al. Establishing forest inventory reference definitions for forest and growing stock: A study towards common reporting. *Silva Fennica*. 2008;42(2):247-266. Available from: <http://www.silvafennica.fi/article/255> [Accessed 03 July 2018]
- [70] Jagodziński AM, Dyderski MK, Gęsikiewicz K, Horodecki P. Effects of stand features on aboveground biomass and biomass conversion and expansion factors based on a *Pinus sylvestris* L.

chronosequence in Western Poland. European Journal of Forest Research. 2019;**138**:673-683

[71] Somogyi Z, Cienciala E, Mäkipää R, Muukkonen P, Lehtonen A, Weiss P. Indirect methods of large-scale forest biomass estimation. European Journal of Forest Research. 2007;**126**(2):197-207

[72] Kangas A, Astrup R, Breidenbach J, Fridman J, Gobakken T, Korhonen KT, et al. Remote sensing and forest inventories in Nordic countries—Roadmap for the future. Scandinavian Journal of Forest Research. 2018;**33**(4):397-412

[73] Sousa AMO, Gonçalves AC, Mesquita P, Marques da Silva JR. Biomass estimation with high resolution satellite images: A case study of *Quercus rotundifolia*. ISPRS Journal of Photogrammetry and Remote Sensing. 2015;**101**:69-79

[74] Gonçalves AC, Afonso A, Pereira DG, Pinheiro A. Influence of umbrella pine (*Pinus pinea* L.) stand type and tree characteristics on cone production. Agroforestry Systems. 2017;**91**(6):1019-1030

[75] Gonçalves AC, Sousa AMO, Silva JRM. *Pinus pinea* above ground biomass estimation with very high spatial resolution satellite images 2017. p. 7

[76] Gonçalves AC, Sousa AMO, Mesquita PG. Estimation and dynamics of above ground biomass with very high resolution satellite images in *Pinus pinaster* stands. Biomass and Bioenergy. 2017;**106**:146-154

[77] AMO S, Gonçalves AC, JRM d S. Above-ground biomass estimation with high spatial resolution satellite images. In: Tumuluru JS, editor. Biomass Volume Estimation and Valorization for Energy [Internet]. IntechOpen; 2017. Available

from: <http://www.intechopen.com/books/biomass-volume-estimation-and-valorization-for-energy/above-ground-biomass-estimation-with-high-spatial-resolution-satellite-images> [Accessed: 22 December 2017]

[78] Powell SL, Cohen WB, Healey SP, Kennedy RE, Moisen GG, Pierce KB, et al. Quantification of live aboveground forest biomass dynamics with Landsat time-series and field inventory data: A comparison of empirical modeling approaches. Remote Sensing of Environment. 2010;**114**(5):1053-1068

[79] Tomppo E, Nilsson M, Rosengren M, Aalto P, Kennedy P. Simultaneous use of Landsat-TM and IRS-1C WiFS data in estimating large area tree stem volume and aboveground biomass. Remote Sensing of Environment. 2002;**82**(1):156-171

[80] Carreiras JMB, Pereira JMC, Pereira JS. Estimation of tree canopy cover in evergreen oak woodlands using remote sensing. Forest Ecology and Management. 2006;**223**(1-3):45-53

[81] Lu D. The potential and challenge of remote sensing-based biomass estimation. International Journal of Remote Sensing. 2006;**27**(7):1297-1328

[82] Muukkonen P, Heiskanen J. Biomass estimation over a large area based on standwise forest inventory data and ASTER and MODIS satellite data: A possibility to verify carbon inventories. Remote Sensing of Environment. 2007;**107**(4):617-624

[83] Salvador R, Pons X. On the applicability of Landsat TM images to Mediterranean forest inventories. Forest Ecology and Management. 1998;**104**(1-3):193-208

[84] Steininger MK. Satellite estimation of tropical secondary forest above-ground biomass: Data from Brazil and



- Bolivia. *International Journal of Remote Sensing*. 2000;**21**(6-7):1139-1157
- [85] Næsset E, Gobakken T, Solberg S, Gregoire TG, Nelson R, Ståhl G, et al. Model-assisted regional forest biomass estimation using LiDAR and InSAR as auxiliary data: A case study from a boreal forest area. *Remote Sensing of Environment*. 2011;**115**(12):3599-3614
- [86] Zheng D, Rademacher J, Chen J, Crow T, Bresee M, Le Moine J, et al. Estimating aboveground biomass using Landsat 7 ETM+ data across a managed landscape in northern Wisconsin, USA. *Remote Sensing of Environment*. 2004;**93**(3):402-411
- [87] McRoberts RE, Næsset E, Gobakken T. Inference for lidar-assisted estimation of forest growing stock volume. *Remote Sensing of Environment*. 2013;**128**:268-275
- [88] Chirici G, Mura M, McInerney D, Py N, Tomppo EO, Waser LT, et al. A meta-analysis and review of the literature on the k-nearest neighbors technique for forestry applications that use remotely sensed data. *Remote Sensing of Environment*. 2016;**176**:282-294
- [89] Chirici G, Barbati A, Corona P, Marchetti M, Travaglini D, Maselli F, et al. Non-parametric and parametric methods using satellite images for estimating growing stock volume in alpine and Mediterranean forest ecosystems. *Remote Sensing of Environment*. 2008;**112**(5):2686-2700
- [90] McRoberts RE, Gobakken T, Næsset E. Post-stratified estimation of forest area and growing stock volume using lidar-based stratifications. *Remote Sensing of Environment*. 2012;**125**:157-166
- [91] Foody GM, Cutler ME, McMorrough J, Pelz D, Tangki H, Boyd DS, et al. Mapping the biomass of Bornean tropical rain forest from remotely sensed data. *Global Ecology and Biogeography*. 2001;**10**(4):379-387
- [92] del Campo AD, González-Sanchis M, Molina AJ, García-Prats A, Ceacero CJ, Bautista I. Effectiveness of water-oriented thinning in two semiarid forests: The redistribution of increased net rainfall into soil water, drainage and runoff. *Forest Ecology and Management*. 2019;**438**:163-175
- [93] Taylor AR, Dracup E, MacLean DA, Boulanger Y, Endicott S. Forest structure more important than topography in determining windthrow during hurricane Juan in Canada's Acadian Forest. *Forest Ecology and Management*. 2019;**434**:255-263
- [94] Chen L, Wang Y, Ren C, Zhang B, Wang Z. Optimal combination of predictors and algorithms for Forest above-ground biomass mapping from sentinel and SRTM data. *Remote Sensing*. 2019;**11**(4):414
- [95] Ghosh SM, Behera MD. Aboveground biomass estimation using multi-sensor data synergy and machine learning algorithms in a dense tropical forest. *Applied Geography*. 2018;**96**:29-40
- [96] Li X, Du H, Mao F, Zhou G, Chen L, Xing L, et al. Estimating bamboo forest aboveground biomass using EnKF-assimilated MODIS LAI spatiotemporal data and machine learning algorithms. *Agricultural and Forest Meteorology*. 2018;**256-257**:445-457
- [97] Saatchi SS, Harris NL, Brown S, Lefsky M, Mitchard ET, Salas W, et al. Benchmark map of forest carbon stocks in tropical regions across three continents. *Proceedings of the National Academy of Sciences*. 2011;**108**(24):9899-9904
- [98] Barbosa P, Hines J, Kaplan I, Martinson H, Szczepanec A, Szendrei Z.

- Associational resistance and associational susceptibility: Having right or wrong neighbors. *Annual Review of Ecology, Evolution, and Systematics*. 2009; **40**(1):1-20
- [99] Propastin P. Large-scale mapping of aboveground biomass of tropical rainforest in Sulawesi, Indonesia, using Landsat ETM+ and MODIS data. *GIScience & Remote Sensing*. 2013; **50**(6):633-651
- [100] Viana H, Aranha J, Lopes D, Cohen WB. Estimation of crown biomass of *Pinus pinaster* stands and shrubland above-ground biomass using forest inventory data, remotely sensed imagery and spatial prediction models. *Ecological Modelling*. 2012; **226**:22-35
- [101] Ahmad T, Sahoo PM, Jally SK. Estimation of area under agroforestry using high resolution satellite data. *Agroforestry Systems*. 2016; **90**(2):289-303
- [102] Askar, Nuthammachot N, Phairuang W, Wicaksono P, Sayektiningsih T. Estimating above ground biomass on private Forest using Sentinel-2 imagery. *Journal of Sensors*. 2018; **2018**:1-11
- [103] Chi H, Sun G, Huang J, Li R, Ren X, Ni W, et al. Estimation of forest aboveground biomass in Changbai mountain region using ICESat/GLAS and landsat/TM data. *Remote Sensing*. 2017; **9**(7):707
- [104] Gonçalves AC, Sousa AMO, Mesquita P. Functions for aboveground biomass estimation derived from satellite images data in Mediterranean agroforestry systems. *Agroforestry Systems*. 2019; **93**(4):1485-1500
- [105] Ploton P, Barbier N, Coueron P, Antin CM, Ayyappan N, Balachandran N, et al. Toward a general tropical forest biomass prediction model from very high resolution optical satellite images. *Remote Sensing of Environment*. 2017; **200**:140-153
- [106] Schneider LC, Lerner AM, McGroddy M, Rudel T. Assessing carbon sequestration of silvopastoral tropical landscapes using optical remote sensing and field measurements. *Journal of Land Use Science*. 2018; **13**(5):455-472
- [107] Berninger A, Lohberger S, Stängel M, Siegert F. SAR-based estimation of above-ground biomass and its changes in tropical forests of Kalimantan using L- and C-band. *Remote Sensing*. 2018; **10**(6):831
- [108] Carreiras J, Melo J, Vasconcelos M. Estimating the above-ground biomass in miombo savanna woodlands (Mozambique, East Africa) using L-band synthetic aperture Radar data. *Remote Sensing*. 2013; **5**(4):1524-1548
- [109] Lu D, Chen Q, Wang G, Liu L, Li G, Moran E. A survey of remote sensing-based aboveground biomass estimation methods in forest ecosystems. *International Journal of Digital Earth*. 2016; **9**(1):63-105
- [110] Patenaude G, Milne R, Dawson TP. Synthesis of remote sensing approaches for forest carbon estimation: Reporting to the Kyoto protocol. *Environmental Science & Policy*. 2005; **8**(2):161-178
- [111] Boyd DS, Danson FM. Satellite remote sensing of forest resources: Three decades of research development. *Progress in Physical Geography-Earth and Environment*. 2005; **29**(1):1-26
- [112] Nilsson M, Nordkvist K, Jonzén J, Lindgren N, Axensten P, Wallerman J, et al. A nationwide forest attribute map of Sweden predicted using airborne laser scanning data and field data from the national forest inventory. *Remote Sensing of Environment*. 2017; **194**:447-454
- [113] Phua M-H, Johari SA, Wong OC, Ioki K, Mahali M, Nilus R, et al.

Synergistic use of Landsat 8 OLI image and airborne LiDAR data for above-ground biomass estimation in tropical lowland rainforests. *Forest Ecology and Management*. 2017;**406**:163-171

[114] Ko C, Rimmel TK. Airborne LiDAR applications in forest landscapes. In: Rimmel TK, Perera AH, editors. *Mapping Forest Landscape Patterns*. New York: Springer; 2017. pp. 105-185

[115] Nelson RF, Hyde P, Johnson P, Emessiene B, Imhoff ML, Campbell R, et al. Investigating RaDAR–LiDAR synergy in a North Carolina pine forest. *Remote Sensing of Environment*. 2007;**110**(1):98-108

[116] McRoberts RE, Chen Q, Walters BF, Kaisershot DJ. The effects of global positioning system receiver accuracy on airborne laser scanning-assisted estimates of aboveground biomass. *Remote Sensing of Environment*. 2018;**207**:42-49

[117] McRoberts RE, Chen Q, Domke GM, Ståhl G, Saarela S, Westfall JA. Hybrid estimators for mean aboveground carbon per unit area. *Forest Ecology and Management*. 2016;**378**:44-56

[118] Shendryk I, Hellström M, Klemedtsson L, Kljun N. Low-density LiDAR and optical imagery for biomass estimation over boreal forest in Sweden. *Forests*. 2014;**5**(5):992-1010

[119] Matasci G, Hermosilla T, Wulder MA, White JC, Coops NC, Hobart GW, et al. Large-area mapping of Canadian boreal forest cover, height, biomass and other structural attributes using Landsat composites and lidar plots. *Remote Sensing of Environment*. 2018;**209**:90-106

[120] Jin X, Yang G, Xu X, Yang H, Feng H, Li Z, et al. Combined multi-temporal optical and Radar parameters for estimating LAI and biomass

in winter wheat using HJ and RADARSAR-2 data. *Remote Sensing*. 2015;**7**(10):13251-13272

[121] Shao Z, Zhang L. Estimating Forest aboveground biomass by combining optical and SAR data: A case study in Genhe, Inner Mongolia, China. *Sensors*. 2016;**16**(6):834

[122] Vaglio Laurin G, Chen Q, Lindsell JA, Coomes DA, Frate FD, Guerriero L, et al. Above ground biomass estimation in an African tropical forest with lidar and hyperspectral data. *ISPRS Journal of Photogrammetry and Remote Sensing*. 2014;**89**:49-58

[123] Kaasalainen S, Holopainen M, Karjalainen M, Vastaranta M, Kankare V, Karila K, et al. Combining Lidar and synthetic aperture Radar data to estimate Forest biomass: Status and prospects. *Forests*. 2015;**6**(12):252-270

[124] Xi X, Han T, Wang C, Luo S, Xia S, Pan F. Forest above ground biomass inversion by fusing GLAS with optical remote sensing data. *ISPRS International Journal of Geo-Information*. 2016;**5**(4):45. DOI: 10.3390/ijgi5040045

[125] Reyes-Palomeque G, Dupuy JM, Johnson KD, Castillo-Santiago MA, Hernández-Stefanoni JL. Combining LiDAR data and airborne imagery of very high resolution to improve aboveground biomass estimates in tropical dry forests. *International Journal of Forestry Research*. 2019;**92**(5):599-615

[126] Laurin GV, Balling J, Corona P, Mattioli W, Papale D, Puletti N, et al. Above-ground biomass prediction by Sentinel-1 multitemporal data in Central Italy with integration of ALOS2 and Sentinel-2 data. *Journal of Applied Remote Sensing*. 2018;**12**(01):1

[127] Nuthammachot N, Askar A, Stratoulas D, Wicaksono P. Combined

use of Sentinel-1 and Sentinel-2 data for improving above-ground biomass estimation. *Geocarto International*. 2020;1-11. DOI: 10.1080/10106049.2020.1726507

[128] Pisupati SV, Tchabda AH. Thermochemical processing of biomass. In: Ravindra P, editor. *Advances in Bioprocess Technology*. Cham: Springer Science+Business Media B.V; 2015. pp. 277-314

[129] Ahmad AA, Zawawi NA, Kasim FH, Inayat A, Khasri A. Assessing the gasification performance of biomass: A review on biomass gasification process conditions, optimization and economic evaluation. *Renewable and Sustainable Energy Reviews*. 2016;53:1333-1347

[130] EPA. Biomass Combined Heat and Power Catalog of technologies. v.1.1. U. S. Environmental Protection Agency; 2007

[131] Kan T, Strezov V. Combustion of biomass. In: Strezov V, Evans TJ, editors. *Biomass Processing Technologies*. Boca Raton: CRC Press; 2014. pp. 53-80

[132] van Loo S, Koppejan J, editors. *The Handbook of Biomass Combustion and Co-Firing*. London: Earthscan; 2012. p. 464

[133] Brown RC. *Thermochemical Processing of Biomass: Conversion into Fuels, Chemicals and Powe*. John Wiley & Sons; 2019. p. 408

[134] de Carvalho RL. *Wood-Burning Stoves Worldwide: Technology, Innovation and Policy* [Internet]. Aalborg: Aalborg University; 2016. DOI: 10.5278/VBN.PHD.ENGSCI.00122

[135] Werner S. International review of district heating and cooling. *Energy*. 2017;137:617-631

[136] Malico I, Mujeebu MA. Potential of porous media combustion

technology for household applications. *International Journal of Advanced Thermofluid Research*. 2015;1:50-69

[137] Amegah AK, Jaakkola JJ. Household Air Pollution and the Sustainable Development Goals. Report No.: 94(3). World Health Organization; 2016. p. 215

[138] Chica E, Pérez JF. Development and performance evaluation of an improved biomass cookstove for isolated communities from developing countries. *Case Studies in Thermal Engineering*. 2019;14:100435

[139] Jetter J, Zhao Y, Smith KR, Khan B, Yelverton T, DeCarlo P, et al. Pollutant emissions and energy efficiency under controlled conditions for household biomass cookstoves and implications for metrics useful in setting international test standards. *Environmental Science & Technology*. 2012;46(19):10827-10834

[140] Suresh R, Singh VK, Malik JK, Datta A, Pal RC. Evaluation of the performance of improved biomass cooking stoves with different solid biomass fuel types. *Biomass and Bioenergy*. 2016;95:27-34

[141] Hanna R, Duflo E, Greenstone M. Up in smoke: The influence of household behavior on the long-run impact of improved cooking stoves. *American Economic Journal: Economic Policy*. 2016;8(1):80-114

[142] WHO. *Burning Opportunity: Clean Household Energy for Health, Sustainable Development, and Wellbeing of Women and Children*. Geneva: WHO Press; 2016. p. 113

[143] Ürge-Vorsatz D, Cabeza LF, Serrano S, Barreneche C, Petrichenko K. Heating and cooling energy trends and drivers in buildings. *Renewable and Sustainable Energy Reviews*. 2015;41:85-98

- [144] Ürge-Vorsatz D, Eyre N, Graham P, Harvey D, Hertwich E, Jiang Y, et al. Energy end-use: Buildings. In: *Global Energy Assessment: Toward a Sustainable Future*. Cambridge: Cambridge University Press; 2012. pp. 649-760
- [145] Míguez JL, Morán JC, Granada E, Porteiro J. Review of technology in small-scale biomass combustion systems in the European market. *Renewable and Sustainable Energy Reviews*. 2012;**16**(6):3867-3876
- [146] Martinopoulos G, Papakostas KT, Papadopoulos AM. A comparative review of heating systems in EU countries, based on efficiency and fuel cost. *Renewable and Sustainable Energy Reviews*. 2018;**90**:687-699
- [147] Carlon E, Schwarz M, Golicza L, Verma VK, Prada A, Baratieri M, et al. Efficiency and operational behaviour of small-scale pellet boilers installed in residential buildings. *Applied Energy*. 2015;**155**:854-865
- [148] Malico I, Nepomuceno Pereira R, Gonçalves AC, Sousa AMO. Current status and future perspectives for energy production from solid biomass in the European industry. *Renewable and Sustainable Energy Reviews*. 2019;**112**:960-977
- [149] Taibi E, Gielen D, Bazilian M. The potential for renewable energy in industrial applications. *Renewable and Sustainable Energy Reviews*. 2012;**16**(1):735-744
- [150] Barthe P, Chaugny M, Roudier S, Sancho LD. Best Available Techniques (BAT) Reference Document for the Refining of Mineral Oil and Gas. Luxembourg; 2015
- [151] Brinkmann T, Santonja CG, Schorcht F, Roudier S, Sancho LD. Best Available Techniques (BAT) Reference Document for the Production of Chlor-Alkali. Luxembourg; 2014. p. 317
- [152] Cusano G, Gonzalo MR, Farrel F, Rainer R, Roudier S, Sancho LD. Best Available Techniques (BAT) Reference Document for the Non-ferrous Metals Industries. Luxembourg; 2017
- [153] EIPPCB. Reference Document on Best Available Techniques for the Manufacture of Large Volume Inorganic Chemicals—Ammonia, Acids and Fertilisers. Seville: EIPPCB; 2007
- [154] EIPPCB. Reference Document on Best Available Techniques in the Ceramic Manufacturing Industry. Seville: EIPPCB; 2007
- [155] EIPPCB. Reference Document on Best Available Techniques in the Production of Polymers. Seville: EIPPCB; 2007
- [156] EIPPCB. Reference Document on Best Available Techniques in the Food, Drink and Milk Industries. Seville: EIPPCB; 2006
- [157] Falcke H, Holbrook S, Clenahan I, Carretero AL, Sanalan T, Brinkmann T, et al. Best Available Techniques (BAT) Reference Document for the Production of Large Volume Organic Chemicals. Luxembourg; 2017
- [158] Mikulčić H, Klemeš JJ, Vujanović M, Urbanec K, Duić N. Reducing greenhouse gasses emissions by fostering the deployment of alternative raw materials and energy sources in the cleaner cement manufacturing process. *Journal of Cleaner Production*. 2016;**136**:119-132
- [159] Mousa E, Wang C, Riesbeck J, Larsson M. Biomass applications in iron and steel industry: An overview of challenges and opportunities. *Renewable and Sustainable Energy Reviews*. 2016;**65**:1247-1266

- [160] Remus R, Aguado-Monsonet MA, Roudier S, Sancho LD. Best Available Techniques (BAT) Reference Document for Iron and Steel Production. Luxembourg; 2013
- [161] Scalet BM, Garcia Muñoz M, Sissa AQ, Roudier S, Sancho LD. Best Available Techniques (BAT) Reference Document for the Manufacture of Glass. Luxembourg: Publications Office of the European Union; 2012
- [162] Schorcht F, Kourti J, Scalet BM, Roudier S, Sancho LD. Best Available Techniques (BAT) Reference Document for the Production of Cement, Lime and Magnesium Oxide. Luxembourg; 2013
- [163] Suhr M, Klein G, Kourti I, Gonzalo MR, Santonja GG, Roudier S, et al. Best Available Techniques (BAT) Reference Document for the Production of Pulp, Paper and Board. Luxembourg; 2015
- [164] S2Biom. Biomass Conversion Technologies Database [Internet]. 2019. Available from: <http://s2biom.alterra.wur.nl/> [Accessed: 20 April 2018]
- [165] Vatopoulos K, Andrews D, Carlsson J, Papaioannou I, Zubi G. Study on the State of Play of Energy Efficiency of Heat and Electricity Production Technologies. Luxembourg; 2012
- [166] Castillo A, Panoutsou C, Bauen A. Report on Biomass Market Segments within the Transport, Heat & Electricity—CHP Sectors for EU27 & Member States. 2010
- [167] Ahrenfeldt J, Thomsen U, Clausen LR. Biomass gasification cogeneration—A review of state of the art technology and near future perspectives. *Applied Thermal Engineering*. 2013;**50**(2):1407-1417
- [168] BASIS. Report on Conversion Efficiency of Biomass. BASIS—Biomass Availability and Sustainability Information System. 2015. p. 20
- [169] Rahman A, Rasul MG, Khan MMK, Sharma S. Recent development on the uses of alternative fuels in cement manufacturing process. *Fuel*. 2015;**145**:84-99
- [170] Roni MS, Chowdhury S, Mamun S, Marufuzzaman M, Lein W, Johnson S. Biomass co-firing technology with policies, challenges, and opportunities: A global review. *Renewable and Sustainable Energy Reviews*. 2017;**78**:1089-1101
- [171] IRENA. Biomass for Power Generation. International Renewable Energy Agency; 2012. p. 12
- [172] Lake A, Rezaie B, Beyerlein S. Review of district heating and cooling systems for a sustainable future. *Renewable and Sustainable Energy Reviews*. 2017;**67**:417-425
- [173] Ericsson K, Werner S. The introduction and expansion of biomass use in Swedish district heating systems. *Biomass and Bioenergy*. 2016;**94**:57-65



# The Potential of Sentinel-2 Satellite Images for Land-Cover/Land-Use and Forest Biomass Estimation: A Review

*Crismeire Isbaex and Ana Margarida Coelho*

## Abstract

Mapping land-cover/land-use (LCLU) and estimating forest biomass using satellite images is a challenge given the diversity of sensors available and the heterogeneity of forests. Copernicus program served by the Sentinel satellites family and the Google Earth Engine (GEE) platform, both with free and open services accessible to its users, present a good approach for mapping vegetation and estimate forest biomass on a global, regional, or local scale, periodically and in a repeated way. The Sentinel-2 (S2) systematically acquires optical imagery and provides global monitoring data with high spatial resolution (10–60 m) images. Given the novelty of information on the use of S2 data, this chapter presents a review on LCLU maps and forest above-ground biomass (AGB) estimates, in addition to exploring the efficiency of using the GEE platform. The Sentinel data have great potential for studies on LCLU classification and forest biomass estimates. The GEE platform is a promising tool for executing complex workflows of satellite data processing.

**Keywords:** GEE, forest classifiers, accuracy, mapping

## 1. Introduction

In the last decades, remote sensing techniques have been applied in several studies of monitoring and classification of agricultural, forest, environmental, and socio-economic resources [1–5]. The information extracted by a set of sensors can offer information on growth, vigor, dynamics, and diversity of vegetation cover [6–8]. In the LCLU classification and forest biomass estimation studies, the proper selection of the sensor is crucial, given the variation of spatial, radiometric, spectral, and temporal resolutions available [9]. For these studies, the use of Sentinel-2 images and a free processing platform lack information about the advantages and disadvantages between different landscapes, classification methods, and biomass estimation models.

In this way, this chapter is organized as follows: Section 2 present the satellites image classification and the potential of the Sentinel-2 satellites; Section 3 describes forest LCLU maps and the assessment of accuracy; Section 4 presents the GEE platform, advantages, and disadvantages; Section 5 describes the estimative of biomass via remote sensing; and Section 6 concludes with a platform performance overview and an outlook for the future.



## 2. The potential of image classification and the Sentinel-2 satellite

The recognition of different LCLU by remote sensing is a key parameter in the application and assessment of socioeconomic and environmental changes at local, regional, and global scales. The accurate and reliable LCLU mapping, represented by a thematic map, can be obtained through the satellite images classification [10]. In studies with a focus on forest resources, forest classification provides useful information in various decision-making processes for forest planning and management [11]. On a map, this classification becomes essential for the implementation of monitoring studies of natural and/or artificial forests, offering support in the assessment of forest protection, ecology, and quantification of carbon and biomass at different scales. In this way, data from several sensors that operate in the optical range of the electromagnetic spectrum enabled important advances in the methods of mapping and monitoring different vegetation covers.

Since the launch of the first terrestrial resource satellite in the 1950s, the analysis of vegetation data via remote sensing has been improved with advances in technology. Currently, images obtained, for example, by Landsat, SPOT, MODIS, AVHRR, ASTER, CBERS QuickBird, IKONOS, WorldView, RapidEye, Radar, LiDAR, ALOS PALSAR, and Sentinel, can produce thematic maps. In the vegetation classification process, the selection of satellite images depends on factors such as the objective of the study, availability of images, cost, level of diversity in the types of cultures, and extension of the study area [12]. In general, radar data are used to model the vertical structure of a forest and data from the multispectral optical sensors are the most used in the literature to model the horizontal structure of vegetation [13]. Multispectral sensors are capable of capturing vegetation characteristics, such as species composition, canopy cover, growth stage, and health of some forest stands [13]. Thus, different spatial, spectral, and temporal parameters that allow the extraction of robust, consistent, and comparable long-term data series must be taken into account due to the better cost-benefit ratio [14, 15]. In summary, some of the sensors used for monitoring vegetation were listed in **Table 1**. More information about the costs for satellite imagery can be found in <http://www.landinfo.com>. The sensors with medium and high spatial resolution differ in terms of the number of bands, temporal resolution, scale, and costs. Depending on the classification objective, the scale is a factor to consider, because, when choosing a sensor with a high spatial resolution (<5 m), the cost and complexity of the classification can increase [16]. In addition, with a larger set of data with spectral variability for the same class, the training time can affect the computational cost [17]. Thus, the spatial resolution must be considered as an important factor, because it must be adequate to the size of the object to be identified [16]. With images from S2, it was observed that the fragmented elements of the landscape decreased the accuracy of the classification by using the spatial resolution of 10 m, due to increased bias resulting from the total composition of pixels at the fragment edges [11].

In multispectral images, vegetation analysis can be obtained by reflectance information resulting from different wavelength bands [visible (VIS), near-infrared (NIR), and short-wave infrared (SWIR)]. The reflectance of the light spectra emits different signals according to the biophysical variables of the vegetation [18]. Among the wavelengths, the emissivity (equivalent to the absorption capacity in the thermal wave range) most used in the analysis of vegetation is in the near and middle regions of the infrared [19]. Various combinations of bands have been studied over decades to derive the biophysical variables of vegetation, resulting in a range of vegetation indices (VIs). In the LCLU classification, VIs are used to extract quantitative information from the contrast of intrinsic characteristics of spectral reflectance of vegetation [20]. VIs are useful to characterize the vigor of vegetation, pigments, sugar content and carbohydrates, high plant temperature levels,

| Sensor group                     | Satellite/sensor | No of bands | Spatial resolution (m) | Temporal resolution (day) | Scale of application <sup>a</sup> | Data distribution policy (cost) | Data availability |
|----------------------------------|------------------|-------------|------------------------|---------------------------|-----------------------------------|---------------------------------|-------------------|
| Medium spatial resolution sensor | SPOT             | 4-5         | 2.5-20                 | 26                        | L-R                               | Yes                             | 1986              |
|                                  | Aster            | 14          | 15-90                  | 16                        | L-G                               | No                              | 1999              |
|                                  | IRS-P6-LISS III  | 4           | 23.5                   | 24                        | L-G                               | No                              | 2003              |
|                                  | CBERS-4          | 4           | 5-20                   | 52-26                     | L-R                               | No                              | 2014              |
|                                  | Landsat-8        | 11          | 15-100                 | 16                        | L-G                               | No                              | 2013              |
| High spatial resolution sensor   | Sentinel-2       | 13          | 10-60                  | 5                         | L-R                               | No                              | 2015              |
|                                  | IKONOS           | 5           | 1-4                    | 1.5-3                     | L-R                               | Yes                             | 1999              |
|                                  | QuickBird        | 5           | 0.61-2.24              | 2.7                       | L                                 | Yes                             | 2001              |
|                                  | WorldView        | 4-17        | 0.31-2.40              | 1-4                       | L                                 | Yes                             | 2007              |
|                                  | GeoEye           | 4           | 0.46-1.65              | 2.6                       | L                                 | Yes                             | 2008              |
|                                  | RapidEye         | 5           | 5                      | 1-5.5                     | L-R                               | Yes                             | 2012              |
|                                  |                  |             |                        |                           |                                   |                                 |                   |

<sup>a</sup>L-G: local to global; L-R: local to regional; L: local.

**Table 1.** Main characteristics of the remote sensors used for LCLU classification: spectral (number of bands), spatial and temporal resolution, data cost, the scale of application, and data availability.

and abiotic/biotic stress levels, among others [21]. Thus, VIs have become commonly applied because of computationally simple analysis of vegetation on global, regional, or local scales [20].

The forest classification is a complex task, and searching for information using individual bands can result in low accuracy models. The model input data can be represented by spectral bands combined with auxiliary bands (vegetation indices), the use of image transformation algorithms, such as principal component analysis (PCA), and image textures [13]. The combination between them helps to distinguish complex vegetation arrangements, improving thematic area estimates [13]. The vegetation indices are mathematical functions that combine two or more spectral bands [22]. The use of vegetation indices is widely discussed in the literature because they improve the classification accuracy. The VIs can reduce atmospheric interference and better distinguish the vegetation characteristics such as plant vigor, water content, sensitivity to lignin, and forest above-ground biomass (alive or dead) [23, 24]. The normalized difference vegetation index (NDVI) has been used for many years in classification studies, due to its high correlation with photosynthetically active vegetation and sensitivity to discriminate between vegetation, nonvegetation, wet, and dry areas [5, 21, 23–25].

The texture data are also important in classification studies, as it contains information of groups of pixels with similar intensity properties describing the distribution and spatial arrangement of repetitions of tones. It has been used in the quantification of the variability of pixels in a neighborhood [26]. The texture information explores information such as crown-internal shadows, size and crown shape, in coarser scales [18]. Several studies point out that the integration of texture measures increase the classification accuracy by improving the separability between classes through reducing the spectral confusion effects between spectrally similar classes [10, 27]. The incorporation of texture metrics can improve classification accuracy by up to 10 to 15% [18]. Textural information can be derived from various methods that use multiple functions of image bands in different window sizes [21]. The methods can be categorized into four main groups being based on structure, statistics, model, and transformation. As an example, we can mention the local statistics (that describe the moments of a neighborhood of individual pixels in a region of the image) and the measures of the gray level co-occurrence matrix (GLCM) (statistics set that characterize the distance and the angular relationships between pixels) [28]. In the LCLU classification, second-order GLCM texture measures have been the most used textural characteristics for characterizing the relative frequencies between the brightness values of two pixels connected by a spatial relationship [29]. However, studies that incorporate the combination of vegetation indices with image texture measurements may contribute more to improvements in classification accuracy than when they are used separately [18].

There are different classification approaches; a class can be represented based on classifiers pixel by pixel [30], per object [30], and per sub-pixel [31]. In the pixel-by-pixel classification, only spectral information of each pixel is used separately, to represent a certain class [30]. In object classification, the image segmentation is performed based on a group of pixels with similar properties, in which the algorithm examines the texture and the spectral response of the object as a basic unit, instead of individualized pixels [19]. The sub-pixel mode consists of identifying within a pixel the proportion of each type of LCLU, modifying a classification in a resolution with clear limits, without assigning mixed pixels to a dominant class [31].

In the LCLU mapping, the right choice of a classification method is essential to obtain good accuracy of representing the thematic map in an image [9]. Traditionally, the classification methods used can be supervised or unsupervised classification [32]. In particular, in supervised classification, it can be applied

parametric (e.g., linear and multiple) and nonparametric [e.g., the nearest neighbor K (K-NN), artificial neural network (RNA), random forest (RF), decision trees (DT), and support vector machines (SVM)] models [13, 33]. In the parametric models, the results are restricted, for example, to unimodal data, by assuming a relationship between the dependent and independent variables with an explicit model structure [13]. However, the nonparametric supervised classification has been the most used method in classification studies based on remote sensing data due to the more robust approach [33]. Thus, the supervised classification based on machine learning achieves better overall accuracy, due to the ability to deal with heterogeneous images, such as forest scenery [34–36]. Based on the training samples defined by the user, the algorithm searches for pixels belonging to each class [30]. The classifiers learn from the database and are efficient in identifying the nonlinearity of the data, noise in the samples, and can use less computation time [34].

In special, the Sentinel-2A (S2) launched in 2015, result from the Earth observation mission developed by the European Space Agency (ESA) as part of the Copernicus program, has been designed to support global monitoring for environment and security (GMES) [37]. The Sentinel-2 wide swath high-resolution Multi-Spectral Instrument system (MSI) aims to obtain information on the monitoring and management of terrestrial surface and provides continuity of the SPOT and Landsat missions [37]. With the wide coverage (swath width of 290 km) and minimum 5-day global revisit time (with twin satellites in orbit), the sensor becomes an extremely useful monitoring product for studies such as LCLU changes and environmental impacts [23]. The main level 2A output allows the use of orthoimage with corrected reflectance at the bottom-of-atmosphere (BOA) [38]. The MSI from optical sensor has 13 spectral bands, with three spatial resolutions, four bands with 10 m, including visible and near-infrared (NIR), six bands with 20 m, including four red-edge bands, two in the SWIR region, and three bands with 60 m (Figure 1) [39, 40].

The multispectral S2 data have several advantages over monitoring satellites available. In particular, Landsat and Sentinel-2 data are now frequently used in monitoring and management studies, to meet the demand for attributes scale data with easy access [16]. The S2 has red-edge spectral bands of longer wavelength range, essential in vegetation analysis [41]. In addition, the spatial resolution of this satellite can be

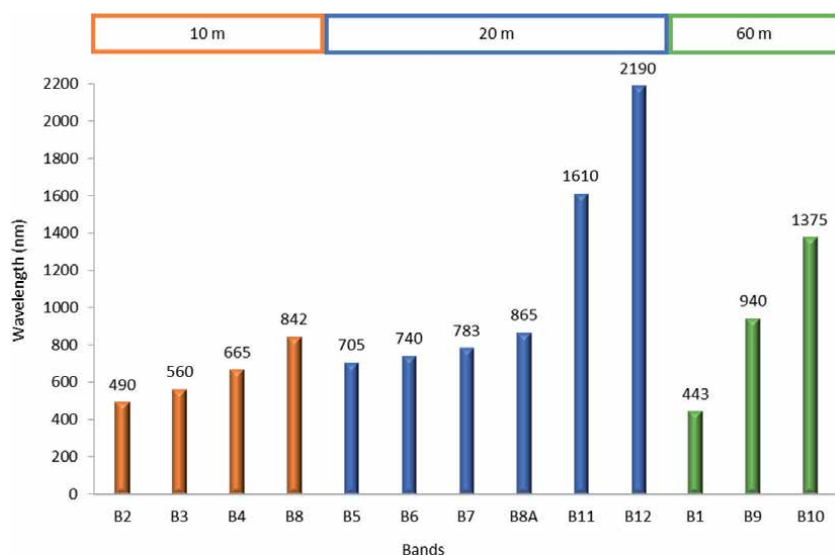


**Figure 1.** Multispectral bands of the Sentinel-2 in 10, 20, and 60 m spatial resolution and their wavenumbers.

compared to commercial SPOT or RapidEye systems, surpassing the spatial resolution of the MODIS 250 m [41]. The Sentinel-2A satellite imagery can be acquired for free at the Sentinel Hub (<https://scihub.copernicus.eu/>). For the image processing, the ESA developed the Sentinel Application Platform (SNAP) software. It is a tool available to analyze satellite information for free, specialized for the Sentinel series, has a performance comparable to that attained with other software's (e.g., QGIS or ENVI) [42], and has a discussion forum for consultations [43]. For these reasons, it seems to be justified to explore the potential of Sentinel-2 data for studies in forest monitoring [24] such as forest succession [2] and wildfire control [44], forest classification [11], forest management [45], and biomass estimation [46].

### 3. Maps of forest LCLU and accuracy assessment

In image classification, information on the spectral resolution of the sensors is also important to provide data on vegetation reflectance [25]. This is possible because each species emits an intrinsic electromagnetic wave according to chemical contents and morphology such as leaf structure, water content, pigments, carbohydrate and aromatic content, and proteins, among other factors [21]. In a light spectrum, remote vegetation detection is based on the ultraviolet, visible near, and medium infrared regions [47]. In the species, identification by remote sensing data requires attention, because there is spectral variability within and between healthy tree species, which can lead to an incorrect classification and hinder statistical assessments [48]. The spectrum can change, for example, with the differences in illumination, shadow effects, and during the seasons and growth periods of trees [48].

Generally, in the LCLU classification, the forest classes are considered more heterogeneous than the water surface, the exposed soil, urban and agricultural classes. The complexity of a forest canopy comes from a surface full of lighting and shading fluctuations [49]. The variability between forest classes can directly change the spectral response reflected in the images influenced by several parameters such as age, season, defoliation, the density (e.g., number of trees and basal area), canopy cover, and understory [49, 50]. In remote sensing, several studies show that the gain in differentiation between species increases with the wavelength, showing a greater correction with the SWIR region [11, 46, 51]. As an example, we can mention the spectral differentiation between conifer needles and broad (flat) leaves. In general, the biggest difference between them is in transmittance and reflectance in the infra-red region [51]. In relation to broad leaves, conifer needles have less transmittance at all wavelengths (greater absorption) and low reflectance in the SWIR region [11, 16, 37, 42, 43]. This effect is due to the greater sensitivity to water absorption which in conifers is deeper [51], explained by the difference in anatomical structure, biochemical composition, and thickness of the leaves, for example [11, 23, 39]. According to some studies, obtaining accurate thematic maps of the Mediterranean ecosystems multispectral bands of the Sentinel-2 in 10, 20, and 60 m spatial resolution and their wavelengths is a challenge, due to its complexity derived from the variability of tree density per unit area and similar spectral behavior [52, 53]. In the *montado* system, where there is a higher occurrence of holm oak and cork oak, in pure and mixed stands, with high spatial variability in tree densities, the effect of mixed pixels can decrease the accuracy of a classification depending on the spatial scale and resolution [54–56]. When using Landsat-8 images, the *montado* class can be classified as an agricultural class and vice versa, because some *montado* areas with 10 to 30% tree density can be masked by the high reflectance of the bare soil [57]. On the other hand, the *montado* areas with a tree density above 50% can be confused with the olive grove classes due to spectral proximity [57]. When using

Sentinel-2 images for canopy estimation of the *montado* system, it was observed that the use of red-edge bands, integrated in seven vegetation indices, was essential and sensitive in the vegetation properties evaluation during the summer, improving the tree crown coverage estimates [56]. The classification of seven forest species in Germany also achieved improvements in accuracy by including the SWIR bands (B11 and B12), one on the red border (B5) and two on the visible border (B2 and B4), using Sentinel-2 images and the RF algorithm [49]. Thus, one of the ways to capture the spectral confusion that can interfere with the results of a thematic map is through the evaluation of the classification model's accuracy.

In forest classification studies, the assessment of accuracy is necessary to validate a classified image because the estimates or forecasts can present errors and uncertainties [58]. The most common way to express the accuracy map is by comparing the final product area percentage with the reference data of an image. This statement is derived from one of the most used approaches to define the accuracy of the classified data, expressed in the form of the confusion matrix and/or contingency matrix [36]. Through this analysis, it is possible to generate information on overall accuracy, user's and producer's accuracy, and Kappa coefficient ( $k$ ) [24, 59, 60]. The confusion matrix is a cross-tabulation, which correlates the LCLU classes in rows and columns, with reference or test data (usually represented by columns) being compared with classified or training data (usually represented by lines) [58]. In the matrix, the diagonal values indicate the number of pixels in the agreement between two class sets [61].

The overall accuracy of the thematic maps is defined by the division of number of the pixels classified correctly by the total number of samples. However, with the advances in remote sensing technology, using a computational classification in the landscape complexity, the classification standardization must be analyzed with caution. The overall accuracy is not always representative of the individual class's accuracy, that is, the high overall accuracy map does not guarantee high accuracy for the individual classes [62]. When assessing the accuracy of classification, the overall accuracy assumes a minimum value and, in each class, a value with comparable precision [63]. Therefore, to obtain more detailed accuracy information, the individual class accuracy of LCLU can also be derived from the confusion matrix. Through matrix analysis, the user's and producer's accuracy points out the errors of omission and commission, respectively. In the producer's accuracy, the user has the opportunity to evaluate the number of the pixels correctly classified in the interest class. The omitted pixels that have not been classified outside the interest class are called omission errors [58]. On the other hand, the user's accuracy indicates the percentage of pixels in a classified image that really represents the class on the ground, certifying the classification, in this case measuring commission errors [58, 64, 65]. The Kappa coefficient is used to describe the possibilities of casual agreement between predicted values and field data [66]. The  $K$  values varied from 0 to 1, where the closer to 1, the better the perfect agreement between the ground truth and the classified image [66].

In the analysis of thematic mapping, it is vital that accuracy is the best possible for each particular case, avoiding interpretation errors [67]. However, there is still no record of a preestablished minimum limit in terms of accuracy, because the reliability of a map may vary depending on the study application [65, 68, 69]. Anderson et al. [70] mentioned that an accuracy of 85% in LCLU classification maps is frequently accepted. When using MODIS images with a spatial resolution of 1 km in classification studies, Thomlinson et al. [28] defined a minimum value of 85% for overall accuracy and 70% for the classes, due to the difference in errors between spatial and thematic accuracy. The United Nations Framework Convention on Climate Change (UNFCCC) does not provide any limit to the accuracy of the data for the construction of forest reference levels [65]. Despite attempts, defining

this value as a goal may be inappropriate and not represent reality in front of the challenges of the distinction of heterogeneous classes at different spatial resolutions and scales [69]. Furthermore, a classification study may be more interested in analyzing the accuracy of a particular class and disregarding others [71].

In fact, there are many studies with different classifiers that can obtain results with good accuracy [71]. Given the complexity of image classification, there are a variety of classification methods using classifying algorithms, with different approaches to achieve mapping accuracy [36]. With an emphasis on supervised classification, the machine learning algorithms exploited image data by finding hidden relationships between various input variables (parameters) with output variables (classification results) [72]. Because it is computer programming, training samples are essential to identify different spectral areas to represent a class in the image. It is based on previous samples or experiences that machine learning has the ability to generalize, that is, when trained they are able to produce solutions to an unknown data set [72]. The combination of different classification techniques has been investigated with support vector machines (SVM) [73], random forest (RF) [74], and classification and regression tree (CART) [75]. Despite the use of several methods to evaluate the performance of the algorithms, evaluating the classification accuracy is the most common one [9]. This assessment is necessary because the

| Algorithms                         | Overall accuracy (%)   | Example of use   | Reference |
|------------------------------------|------------------------|--|-----------|
| Artificial neural network (ANN)    | 65.7                   | Mapping of the forest vertical structure in Gong-ju, Korea.  | [67]      |
|                                    | 85.0 <sup>a</sup>      | Discriminating urban forest types in Xuzhou, East China.   | [60]      |
| Convolutional neural network (CNN) | 90.4                   | Forest vegetation types in Jilin Province, China.  | [77]      |
|                                    | 97.7                   | Classification forest in Semarang, Central Java, Indonesia   | [78]      |
| Random forest (RF)                 | 90.9 93.2 <sup>b</sup> | Forest classification in ecosystems in Germany and South Africa.   | [79]      |
|                                    | 88.9                   | Mapping of 11 forest classes in the Belgian Ardenne ecoregion, Ardenne, Belgium.   | [11]      |
| Support vector machine (SVM)       | 80.0                   | Mapping of the invasive species American bramble ( <i>Rubus cuneifolius</i> ) in KwaZulu-Natal province of South Africa. | [80]      |
| RF SVM                             | 84.2 81.8              | Mapping of the crop, including high and low density forest classes in the foothill of Himalaya.                          | [81]      |
| RF K-NN SVM                        | 94.44 95.29 94.13      | Classification of six types of land use, including forest cover in the Red River Delta in Vietnam.                       | [82]      |
|                                    | 80.0 74.3 80.3         | Classification land use, including forest cover in the Dak Nong province, Vietnam.                                       | [69]      |

<sup>a</sup>ANN + vegetation abundance (VA).

<sup>b</sup>Sentinel 1 and Sentinel 2.

**Table 2.**  
The overall accuracy of LCLU and forest classification with Sentinel data.

classifier's performance is affected, not only by the classifier's own limitation but also by the image quality, sample size, and computational resource [9, 76]. **Table 2** shows the overall accuracy obtained by different algorithms in some recent studies with forest classification, using Sentinel-2 images. These results aim to provide information on the current conditions of vegetation cover. In addition, it shows that the relevance of accuracy depends on the objective of the study, without being based on standard accuracy [69]. However, it was observed that classifiers have an important role in supervised classification. When using improved classification methods, such as the use of convolutional neural networks, the overall accuracy is generally higher in relation to the other methods that presented medium or fluctuating precision [36].

The studies based on forest species classification involving Sentinel-2 images are still recent [23, 33, 83–86]. The classification with S2 images of forest tree species in southwestern France obtained an overall accuracy above 90%, for plantations such as aspen (*Populus tremula*) and red oak (*Quercus rubra*). However, the species that presented more spectral confusion with an accuracy of 81 and 74% were the black pine (*Pinus nigra*) and Douglas fir (*Pseudotsuga menziesii*), respectively [87]. In tests with S2 images and the RF for forest type mapping in the Mediterranean, Italy, using four vegetation indices (NDVI, SRI, RENDVI, and AR1I) in three phenological periods (winter, spring, and summer), Puletti et al. [88] reported that the forest categories (pure coniferous forests, broadleaf forests, and mixed forests), had an overall accuracy of 86.2% and a Kappa coefficient of 0.86. The user's and producer's accuracy were above 83% for all the classes. In a study, by Duan et al. [89], they obtained overall, producer's and user's accuracy of 92.3, 92.3, and 92.2%, respectively, when mapping the distribution of urban forests in China, using eight bands and three vegetation indices (NDVI, NDWI, and NDBI) with S2 images, random forest algorithms, and the GEE platform. Thus, the spatial distribution of species and their number of trees per hectare can be understood by the classification, becoming essential in studies with different types of landscapes. When making decisions about forest resources, this information is very important, because each specific study offers support to the formulation of local and global public policies, as well as in forest planning and management up to biomass estimates.

#### **4. Google Earth Engine (GEE) platform: advantages and disadvantages in the LCLU classification**

In GEE, there is a computing platform that has a cloud infrastructure designed by Google, from the launch of the public data catalog of the Landsat 2008 series images [89]. The platform allows to manage, analyze, and store large volumes of geospatial historical data on a planetary scale, which can be applied for several scientific studies [89]. In the GEE, it is possible to have access to data catalog of the Landsat, MODIS, and Sentinel satellites [90]. In addition, the platform offers social, demographic, climatic, and digital elevation models and allowing the interaction remote sensing data with algorithms in synergy with the field data, using Java-Script or Python code [90]. Another cloud resource available in GEE is the Fusion Table, which offers support for tabular data, keyword-based mechanisms, and text data, among others [91].

Although the GEE platform is a free access tool, the LCLU mapping in large extensions and with high spatial resolution can be challenging for several reasons. The inclusion of large volumes of data from a complex and heterogeneous landscape requires a large computational load and processing time [92]. However, freely accessible data can be used in studies with limited funding. For example, the use of Sentinel-2 data is more recommended than the Landsat images, because



it provides a slightly higher spatial and spectral resolution [5]. The classification methods can also be applied on the platform according to the image type, segmentation method, classification algorithm, training sample sets, input resources, target classes, and accuracy assessment [36]. All classification procedures can be developed on the cloud computing platform, without downloading remote sensing data, processing on desktops or other software, simplifying information extraction [86]. Therefore, the GEE platform allows the use of high-performance tools for processing a large data set. Thus, GEE is an important resource for big data management and scientific development, because it lowers barriers between the global scientific community and allows the same opportunities to share and replicate geospatial analysis [89].

With millions of servers worldwide, the platform allows the combination of different algorithms and data with free availability for noncommercial use [93]. In the image processing phase, the GEE platform can synchronize all S2 data, can easily clear cloudy pixels [86], and perform a continuous workflow of complex remote sensing [94]. According to the objective of the study, it is possible to choose the specific period and create image mosaics, with the best cloudless pixel for a specific region, solve terrain effects problems, and identify any changes in LCLU in the world through classified images [95]. Also, it can use several vegetation indices at the same time when image classification is performed [96].

Although it is of easy access, users are generally not familiar with the client-server programming model. The GEE libraries offer a more familiar programming environment, but the user must have some basic knowledge of the programming language [95]. This requires much effort from the end user to be implemented [94]. Fortunately, there are learning platforms and discussion forums on GEE on the Internet, which help to solve most doubts and programming errors. However, difficulties have been encountered in studies of LCLU classification. Difficulties in validating the classification model carried out in the GEE were found by Zurqani et al. [96], as there was little availability of high-resolution aerial images in the world, to serve as a reference. The difficulties in image preprocessing were also reported, due to difficulties in the acquisition of parameters with the atmospheric correction [89], and limited availability of other algorithms, not allowing improvements in the classification accuracy [97].

The GEE memory defines a threshold limit to the size of the matrices, which constrains the training of the classification algorithms, with a large number of training samples and evaluation of the input bands [98]. The limited processing capacity can cause errors in complex computational analyses as in large spatial areas [95]. On the other hand, GEE processing can be affected by the very different preprocessing criteria, which makes analysis and comparison with other sensors difficult and makes GEE unsuitable for some types of processing [98, 99].

The approach to programming through the cloud platform is becoming increasingly common for large-scale computing and in multidisciplinary studies. In this way, the offer of high-resolution satellite images in the GEE can solve the problems of detecting global changes in LCLU, environmental monitoring, and help in the quantitative and qualitative identification of forest cover [24]. In particular, the Sentinel 1 (radar data) and Sentinel 2 data, have great potential for future studies of classification and estimates of above-ground biomass, through GEE. Until the present moment, few studies have tested the cloud platform capabilities with Sentinel data. This gap opens the opportunity to generate research and development in monitoring forest cover [100]. In future missions, the Sentinel data will be essential for studies to validate forest AGB estimates [100]. Free access to both resources can generate valuable information on forest cover, located in low-, medium-, and high-income countries.

## 5. Biomass estimation

Above-ground biomass (AGB) of forests plays a key role in the global carbon cycle, maintaining the climate and as bioenergy reservoirs [101]. In a global context, forest AGB or phytomass is generally defined by the quantification of stems, branches, and leaves. The estimation of the amount of the carbon mass or energy potential per unit area is also frequent [102]. In global discussions on climate change, the estimation of forest AGB has been one of the agenda items in public and private decision-making, integrating into sustainable development projects on a local to global scale [91].

In forest biomass estimates, data can be acquired using direct (destructive) methods based on harvesting the all tree and indirect (nondestructive) based on field inventory and synergy between remote sensing data [103]. The direct methods are considered to have the best accuracy, due to the dry weight determination of the parts of the tree [101]. However, when it is intended to estimate biomass, this method is time-consuming, costly and laborious, and inadequate for using in large geographic areas [13, 42]. In addition, the application of destructive methods causes disturbances in the fauna and flora with alterations in the microclimate and habitat [104]. Thus, one of the alternatives to reduce these impacts is through the use of remote sensing technology [105]. In addition to being a nondestructive method, it is based on forest inventory data, allowing the fitting of models in synergy with small-, medium-, and large-scale satellite images [91, 106].

The thematic mapping based on a forest classification is fundamental as input parameters for the area and biomass estimation [107]. It is through the accuracy of a thematic map that the user can assess the consistency of the overall reliability of the map data and accuracy measures for LCLU classes [107]. In biomass estimates by remote sensing, the type of sensor, different spatial and temporal resolutions, scale, field data, errors, and uncertainty are factors that hinder the statistical evaluation of the final product on the map. In the biomass estimate, several studies indicate errors that can range from 5 to 30% [13]. The forest planning and management decision scale can also influence the accuracy of forest biomass analysis. According to Lu et al. [13], it is recommended that in forest research, accuracy reaches values greater than 90% for a regional scale and 80% for a national or global scale.

Regardless of the estimation method used, it is fundamentally a thorough evaluation of the reference data and map data [108]. The agreement presented by the error matrix may not be equivalent to the product of the map and the reality, which impacts the biomass estimates [109]. Therefore, the classification validation analysis becomes essential because, depending on the classification methodology in a forest ecosystem, it is possible to observe errors and uncertainties that affected the classifier's performance [36]. In studies of the representation of the heterogeneity of a forest, the erroneous choice of spatial resolution can cause the addition of redundant data and can increase the noise of statistical models, without adding important information about the stands [110]. Even when an AGB forest map achieves high accuracy with the integration of multisource remote sensing data, some limitations and uncertainty can impact the results between LCLU and remote sensing data [42]. One of the limitations is found in the uncertainties about ground measurements with GPS, which can contain geolocation errors, difficult to eliminate in the image analysis processing [42]. In addition, some uncertainties in the prediction model can be included with the time gap between field data and remote sensing data [42, 111]. In this way, any gain in accuracy in biomass maps comes from advances in technology. The diversity of image processing software, greater processing capacity, and computer storage allowed the synergistic use of cloud platforms and machine learning use to deal with big data problems.

Revised studies for the Mediterranean region [106] found that when the estimates are based on passive sensor (optical data) are less accurate ( $R^2 \approx 0.70$ ) than

those carried by active sensors ( $R^2 \geq 0.80$ ). One of the factors can be related to the dimension of images. While the optical sensors are based mainly on two-dimensional view—2D, creating estimates with the top canopy layer, the active sensors, such as synthetic aperture radar (SAR) and LiDAR, reach the third dimension of the forest with the evaluation of the arboreal and understory, presenting a better data correlation with the biomass [106]. Among some studies, it was found that the spatial resolution has a key role in the accuracy of the biomass. The spatial resolution of Landsat can achieve a low accuracy [112], while the SPOT satellites [113], GeoEye [114], and Quickbird [55] can achieve medium to high accuracy, WorldView [115] and spatial resolution of LiDAR can achieve high accuracy [116]. Overall, the more accurate the modeling, the greater the approximation to the observed values [117]. Accurate models with optical data can be achieved using the high spatial resolution (<10 m), where the pixel size approximates the size of the study object [118]. In particular, using Sentinel-2 data, it has been reported medium accuracy in local and regional scale studies [119, 120]. Thus, the production of AGB maps, with Sentinel-2 data, has a great potential to expand to forest management and monitoring decisions on a regional scale.

In quantifying the biomass stock with Sentinel data, the cross-use of sensor data combined with forest inventory data and algorithms were fundamental for gains in

| Satellite data | Location  | Forest settings  | Model performance |                              | Reference |
|----------------|---|--|-------------------|------------------------------|-----------|
|                |   |  | $R^2$             | RMSE (Mg. ha <sup>-1</sup> ) |           |
| S2             | Evros prefecture, Rhodopes mountain range, Greece   | Mediterranean forest   | 0.63              | 63.11 <sup>a</sup>           | [122]     |
| S2             | Parsa National Park, Nepal  | Central-southern part of Nepal, subtropical climate  | 0.81              | 25.32                        | [124]     |
| S2             | Parque Nacional Yok Don, Vietnam  | Tropical monsoon climate   | 0.81              | 36.67                        | [119]     |
| S2             | Parsa National Park, Nepal  | Central-southern part of Nepal, subtropical climate  | 0.99              | 4.51                         | [125]     |
| S2             | Hunan Province, southern China  | Subtropical monsoon climate  | 0.58              | 65.03 <sup>a</sup>           | [123]     |
| S1 and S2      | Island province of Palawan, Philippines   | Southern coast of Honda Bay within the administrative jurisdiction of Puerto Princesa City, tropical climate | 0.75              | 33.81                        | [43]      |
| S1 and S2      | Ecoregion of Changbai Mountains mixed forests and eastern mountainous region of Jilin Province in northeast China | Monsoon-influenced humid continental climate   | 0.97              | 33.29                        | [76]      |

<sup>a</sup> m<sup>3</sup> ha<sup>-1</sup> (growing stock volume).

**Table 3.** Studies on forest biomass estimation using algorithms RF in different ecological settings.

the accuracy of the estimates. A study by Castillo et al. [43] showed improvements in the accuracy of biomass models with Sentinel-1 (S1) and S2, which were comparable to the image accuracy of current commercial sensors. In biomass estimates, precision can also differ depending on the order of importance of spectral bands and textures, according to the input characteristics in the model [121]. When analyzing Landsat-8 satellite images with the inclusion of S2 images, the importance of SWIR region reflectance to improve the estimation of forest parameters was observed [122]. In study using the GEE platform, it was identified that the greatest contribution of the variables in the estimates of forest AGB were those composed by the SWIR and red-edge bands [119]. In addition, Hu et al. [123] reported that the red-edge band (B5) of S2 was the best in the prediction with good performance of the RF algorithm on the GEE platform. In particular, the RF algorithm showed good accuracy in AGB estimates in subtropical deciduous forests, as it was robust with the nonlinearity of the data [124]. Due to the large reported of the random forest algorithm in biomass estimation studies, **Table 3** summarizes the results of some recent studies that used Sentinel (S1 and S2) data to estimate the forest AGB in different scenarios. It was observed that the machine learning algorithm was used in different climatic conditions and in time series with considerable accuracy.

Although advances in image resolution and use of radar data have been increasingly available, the storing of a large amount of data and with a complex data structure is one of the major challenges of research with the geospatial data [126]. With the advances in technology, cloud computing has helped researchers to solve big data problems, which reduces the costs of accessing software and maintaining hardware [93]. However, to date, studies with cloud platforms such as GEE for forest biomass estimates have been little explored. For forest AGB, cloud computing holds promise in solving problems related to big data [126]. The platform's advantages are related to the data storage and analysis process of an intensive nature and based on complex point structures, such as LIDAR data [91]. The GEE platform is being used as rasterized data management in parallel with other software such as packages in the R [125] and cloud computing applications such as Fusion Tables and Google Cloud Platform [91]. In the near future, it is hoped that it will be possible to integrate data such as high-precision LiDAR with a collection of optical images for mapping global biomass [91].

In remote sensing, the promising prospects for biomass estimates can take new directions thanks to the ESA's Earth Explorer mission Biomass. The mission scheduled for this decade aims to provide global maps of biomass and carbon stored in the world's forests [126]. As a novelty, the Biomass will have the first P-band synthetic aperture radar capable of carrying out the precise mapping of biomass estimates [126]. In addition, it will have an experimental tomograph to provide 3D views of the forests [126]. In this way, we hope that in the future, it will be possible to carry out studies with crossing Sentinel 2 data with Biomass to compose thematic maps of LCLU changes and biomass stock with greater accuracy.

## 6. Conclusions and outlook

The development of LCLU maps for biomass estimates with Sentinel images is still recent, but promising. In studies of LCLU classification, the overall accuracy and producer's and user's accuracy should be the highest possible for better support of biomass prediction models. For the refinement of the classification map, the accuracy can be improved with the combination of radar and optical data from Sentinel 1 and 2, respectively, as well as incorporating models and algorithms, vegetation indices, textures, biophysical variables, and forest inventory data, among others. However, it

is noteworthy that the accuracy of the biomass prediction models obtained by remote sensing still depends on the precision of the field-based measurements.

The GEE platform allows the use of free data, combined with the remote data and machine learning for building maps, in addition, to assess the use of land occupation on a large scale. The inclusion of samples collected in the field in the Google Fusion Table and multitemporal data, such as high-resolution images can improve the classification results.

Based on the limitations of the GEE platform, we hope that the new updates of the platform can solve problems such as memory space and the inclusion of other ranking algorithms. The improvements make the platform more accessible and attract new users to assess changes in LCLU and analysis of vegetation cover monitoring. In future works, the LCLU classification approach will be based on plots using the pixel method connected to the GEE and field validation, which facilitates the detection and understanding of the dynamics of forest areas in terms of volumetric and gravimetric production of biomass over time.

To our knowledge, studies that address the accuracy of a forest classification combined with biomass estimates, using Sentinel images on cloud platforms, have not yet been reported in the literature. Available studies make separate approaches to forest classification and biomass estimates. With Sentinel imagery, these two themes generally use field data and other thematic maps to develop the models. This limitation shows the opportunity to develop pioneering research on forest classification and biomass estimates with Sentinel images on cloud platforms.

## **Acknowledgements**


The work was supported by Programa Operativo de Cooperação Transfronteiriça Espanha-Portugal (POCTEP); project CILIFO – Centro Ibérico para la Investigación y Lucha contra Incendios Forestales and by FCT, Portugal, Fundação para a Ciência e Tecnologia, through IDMEC, under LAETA, project UIDB/05183/2020.

## **Author details**

Crismeire Isbaex\* and Ana Margarida Coelho  
Department of Rural Engineering, School of Sciences and Technology, Institute of Research and Advanced Information (IIFA), University of Évora, Évora, Portugal

\*Address all correspondence to: [cisbaex@uevora.pt](mailto:cisbaex@uevora.pt)

## **IntechOpen**

© 2020 The Author(s). Licensee IntechOpen. Distributed under the terms of the Creative Commons Attribution - NonCommercial 4.0 License (<https://creativecommons.org/licenses/by-nc/4.0/>), which permits use, distribution and reproduction for non-commercial purposes, provided the original is properly cited. 

## References

- [1] Askar, Nuthammachot N, Phairuang W, Wicaksono P, Sayektiningsih T. Estimating aboveground biomass on private forest using sentinel-2 imagery. *Journal of Sensors*. 2018;**2018**:1-11. DOI: 10.1155/2018/6745629
- [2] Szostak M, Hawryło P, Piela D. Using of Sentinel-2 images for automation of the forest succession detection. *European Journal of Remote Sensing*. 2018;**51**(1):142-149. DOI: 10.1080/22797254.2017.1412272
- [3] Caiserman A, Dumas D, Bennafla K, Faour G, Amiraslani F. Application of remotely sensed imagery and socioeconomic surveys to map crop choices in the Bekaa Valley (Lebanon). *Agriculture*. 2019;**9**(3):1-19. DOI: 10.3390/agriculture9030057
- [4] Carranza C, Benninga H, van der Velde R, van der Ploeg M. Monitoring agricultural field trafficability using Sentinel-1. *Agricultural Water Management*. 2019;**224**:1-12. DOI: 10.1016/j.agwat.2019.105698
- [5] Ganivet E, Bloomberg M. Towards rapid assessments of tree species diversity and structure in fragmented tropical forests: A review of perspectives offered by remotely-sensed and field-based data. *Forest Ecology and Management*. 2019;**432**:40-53. DOI: 10.1016/j.foreco.2018.09.003
- [6] Mulla DJ. Twenty five years of remote sensing in precision agriculture: Key advances and remaining knowledge gaps. *Biosystems Engineering*. 2013;**114**(4):358-371. DOI: 10.1016/j.biosystemseng.2012.08.009
- [7] Battude M, Al Bitar A, Morin D, Cros J, Huc M, Marais Sicre C, et al. Estimating maize biomass and yield over large areas using high spatial and temporal resolution Sentinel-2 like remote sensing data. *Remote Sensing of Environment*. 2016;**184**:668-681. DOI: 10.1016/j.rse.2016.07.030
- [8] Ali A, Ullah S, Bushra S, Ahmad N, Ali A. Quantifying forest carbon stocks by integrating satellite images and forest inventory data. *Austrian Journal of Forest Science*. 2018;**2**:93-117
- [9] Lu D, Weng Q. A survey of image classification methods and techniques for improving classification performance. *International Journal of Remote Sensing*. 2007;**28**(5):823-870. DOI: 10.1080/01431160600746456
- [10] Li M, Zang S, Zhang B, Li S, Wu C. A review of remote sensing image classification techniques: The role of spatio-contextual information. *European Journal of Remote Sensing*. 2014;**47**(1):389-411. DOI: 10.5721/EuJRS20144723
- [11] Bolyn C, Michez A, Gaucher P, Lejeune P, Bonnet S. Forest mapping and species composition using supervised per pixel classification of Sentinel-2 imagery. *Biotechnology, Agronomy, Society and Environment*. 2018;**22**(3):172-187. DOI: 10.25518/1780-4507.16524
- [12] Zheng B, Myint SW, Thenkabail PS, Aggarwal RM. A support vector machine to identify irrigated crop types using time-series Landsat NDVI data. *International Journal of Applied Earth Observation and Geoinformation*. 2015;**34**(1):103-112. DOI: 10.1016/j.jag.2014.07.002
- [13] Lu D, Chen Q, Wang G, Liu L, Li G, Moran E. A survey of remote sensing-based aboveground biomass estimation methods in forest ecosystems. *International Journal of Digital Earth*. 2016;**9**(1):63-105. DOI: 10.1080/17538947.2014.990526
- [14] Alilou H, Moghaddam Nia A, Keshtkar H, Han D, Bray M. A

cost-effective and efficient framework to determine water quality monitoring network locations. *The Science of the Total Environment*. 2018;**624**:283-293. DOI: 10.1016/j.scitotenv.2017.12.121

[15] Turner W, Rondinini C, Pettorelli N, Mora B, Leidner AK, Szantoi Z, et al. Free and open-access satellite data are key to biodiversity conservation. *Biological Conservation*. 2015;**182**:173-176. DOI: 10.1016/j.biocon.2014.11.048

[16] Chen Y, Guerschman JP, Cheng Z, Guo L. Remote sensing for vegetation monitoring in carbon capture storage regions: A review. *Applied Energy*. 2019;**240**:312-326. DOI: 10.1016/j.apenergy.2019.02.027

[17] Spiekermann R, Brandt M, Samimi C. Woody vegetation and land cover changes in the Sahel of Mali (1967-2011). *International Journal of Applied Earth Observation and Geoinformation*. 2015;**34**(1):113-121. DOI: 10.1016/j.jag.2014.08.007

[18] Fassnacht FE, Latifi H, Stereńczak K, Modzelewska A, Lefsky M, Waser LT, et al. Review of studies on tree species classification from remotely sensed data. *Remote Sensing of Environment*. 2016;**186**: 64-87. DOI: 10.1016/j.rse.2016.08.013

[19] Bernardi H, Dzedzej M, Carvalho L, Acerbi JF. Classificação digital do uso do solo comparando os métodos “pixel a pixel” e orientada ao objeto em imagem QuickBird. In: XIII Simpósio Brasileiro de Sensoriamento Remoto. Vol. 2001. 2007. pp. 5595-5602

[20] Frampton WJ, Dash J, Watmough G, Milton EJ. Evaluating the capabilities of Sentinel-2 for quantitative estimation of biophysical variables in vegetation. *ISPRS Journal of Photogrammetry and Remote Sensing*. 2013;**82**:83-92. DOI: 10.1016/j.isprsjprs.2013.04.007

[21] Xue J, Su B. Significant remote sensing vegetation indices: A review

of developments and applications. *Journal of Sensors*. 2017;**2017**:1-17. DOI: 10.1155/2017/1353691

[22] Ku NW, Popescu SC. A comparison of multiple methods for mapping local-scale mesquite tree aboveground biomass with remotely sensed data. *Biomass and Bioenergy*. 2019;**122**:270-279. DOI: 10.1016/j.biombioe.2019.01.045

[23] Haywood A, Stone C, Jones S. The potential of Sentinel satellites for large area aboveground forest biomass mapping. In: *International Geoscience and Remote Sensing Symposium (IGARSS)*. 2018. pp. 9030-9033. DOI: 10.1109/IGARSS.2018.8517597

[24] Koskinen J, Leinonen U, Vollrath A, Ortmann A, Lindquist E, D’Annunzio R, et al. Participatory mapping of forest plantations with Open Foris and Google Earth Engine. *ISPRS Journal of Photogrammetry and Remote Sensing*. 2019;**148**:63-74. DOI: 10.1016/j.isprsjprs.2018.12.011

[25] Solymosi K, Kövér G, Romvári R. The progression of vegetation indices: A short overview. *Acta Agraria Kaposváriensis*. 2019;**23**(1):75-90. DOI: 10.31914/aak.2264

[26] Jensen JR. *Remote Sensing of the Environment: An Earth Resource Perspective 2/e*. New Delhi: Pearson Education India; 2009. p. 613

[27] Chen Q, Gong P. Automatic variogram parameter extraction for textural classification of the panchromatic IKONOS imagery. *IEEE Transactions on Geoscience and Remote Sensing*. 2004;**42**(5):1106-1115. DOI: 10.1109/TGRS.2004.825591

[28] Thomlinson JR, Bolstad PV, Cohen WB. Coordinating methodologies for scaling landcover classifications from site-specific to global: Steps toward validating global

- map products. *Remote Sensing of Environment*. 1999;**70**(1):16-28. DOI: 10.1016/S0034-4257(99)00055-3
- [29] Mananze S, Pôças I, Cunha M. Mapping and assessing the dynamics of shifting agricultural landscapes using Google Earth Engine cloud computing, a case study in Mozambique. *Remote Sensing*. 2020;**12**(8):1-23. DOI: 10.3390/RS12081279
- [30] Furtado LFA, Francisco CN, Almedida CM. Análise de imagem baseada em objeto para classificação das fisionomias da vegetação em imagens de alta resolução espacial. *Geociências*. 2013;**32**(3):441-451
- [31] Wu K, Du Q, Wang Y, Yang Y. Supervised sub-pixel mapping for change detection from remotely sensed images with different resolutions. *Remote Sensing*. 2017;**9**(3):1-17. DOI: 10.3390/rs9030284
- [32] Lillesand TM, Kiefer RW. *Remote Sensing and Image Interpretation*. New York: John Wiley & Sons, inc.; 2000. p. 736
- [33] Thanh Noi P, Kappas M. Comparison of random forest, k-nearest neighbor, and support vector machine classifiers for land cover classification using Sentinel-2 imagery. *Sensors (Basel, Switzerland)*. 2018;**18**(1):1-20. DOI: 10.3390/s18010018
- [34] Belgiu M, Drăgu L. Random forest in remote sensing: A review of applications and future directions. *ISPRS Journal of Photogrammetry and Remote Sensing*. 2016;**114**:24-31. DOI: 10.1016/j.isprsjprs.2016.01.011
- [35] Fu B, Wang Y, Campbell A, Li Y, Zhang B, Yin S, et al. Comparison of object-based and pixel-based random forest algorithm for wetland vegetation mapping using high spatial resolution GF-1 and SAR data. *Ecological Indicators*. 2017;**73**:105-117. DOI: 10.1016/j.ecolind.2016.09.029
- [36] Ma L, Li M, Ma X, Cheng L, Du P, Liu Y. A review of supervised object-based land-cover image classification. *ISPRS Journal of Photogrammetry and Remote Sensing*. 2017;**130**:277-293. DOI: 10.1016/j.isprsjprs.2017.06.001
- [37] Roteta E, Bastarrrika A, Padilla M, Storm T, Chuvieco E. Development of a Sentinel-2 burned area algorithm: Generation of a small fire database for sub-Saharan Africa. *Remote Sensing of Environment*. 2019;**222**:1-17. DOI: 10.1016/j.rse.2018.12.011
- [38] ESA. *Sentinel-2 User Handbook*. Vol. 2. European Space Agency ESA Standard Document. Paris, France; 2015. p. 64. DOI: 10.1021/ie51400a018
- [39] Chang J, Shoshany M. Mediterranean shrublands biomass estimation using Sentinel-1 and Sentinel-2. In: *IEEE International Geoscience and Remote Sensing Symposium (IGARSS)*. Beijing, China; 10-15th July 2016. pp. 5300-5303. DOI: 10.1109/IGARSS.2016.7730380
- [40] ESA. *Spatial Resolution* [Internet]. 2020. Available from: <https://sentinel.esa.int/web/sentinel/user-guides/sentinel-2-msi/resolutions/spatial>
- [41] Hawryło P, Bednarz B, Wężyk P, Szostak M. Estimating defoliation of Scots pine stands using machine learning methods and vegetation indices of Sentinel-2. *European Journal of Remote Sensing*. 2018;**51**(1):194-204. DOI: 10.1080/22797254.2017.1417745
- [42] Zhang T, Su J, Liu C, Chen WH, Liu H, Liu G. Band selection in Sentinel-2 satellite for agriculture applications. In: *2017 23rd International Conference on Automation and Computing (ICAC)*. IEEE; 2017. pp. 1-6
- [43] Castillo JAA, Apan AA, Maraseni TN, Salmo SG. Estimation and mapping of above-ground biomass of mangrove forests and their replacement land uses in



- the Philippines using Sentinel imagery. *ISPRS Journal of Photogrammetry and Remote Sensing*. 2017;**134**:70-85. DOI: 10.1016/j.isprsjprs.2017.10.016
- [44] Fernandes PM, Guiomar N, Rossa CG. Analysing eucalypt expansion in Portugal as a fire-regime modifier. *The Science of the Total Environment*. 2019;**666**:79-88. DOI: 10.1016/j.scitotenv.2019.02.237
- [45] Barton I, Király G, Czimber K, Hollaus M, Pfeifer N. Treefall gap mapping using Sentinel-2 images. *Forests*. 2017;**8**(426):1-27. DOI: 10.3390/f8110426
- [46] Thomas N, Simard M, Castañeda-Moya E, Byrd K, Windham-Myers L, Bevington A, et al. High-resolution mapping of biomass and distribution of marsh and forested wetlands in southeastern coastal Louisiana. *International Journal of Applied Earth Observation and Geoinformation*. 2019;**80**:257-267. DOI: 10.1016/j.jag.2019.03.013
- [47] Randive PU, Deshmukh RR, Janse PV, Kayte JN. Study of detecting plant diseases using non-destructive methods: A review. *International Journal of Emerging Trends & Technology in Computer Science*. 2018;**7**(1):66-71
- [48] Waser LT, Küchler M, Jütte K, Stampfer T. Evaluating the potential of worldview-2 data to classify tree species and different levels of ash mortality. *Remote Sensing*. 2014;**6**:4515-4545. DOI: 10.3390/rs6054515
- [49] Immitzer M, Vuolo F, Atzberger C. First experience with Sentinel-2 data for crop and tree species classifications in Central Europe. *Remote Sensing*. 2016;**8**(3):1-27. DOI: 10.3390/rs8030166
- [50] Landry S, St-Laurent MH, Nelson PR, Pelletier G, Villard MA. Canopy cover estimation from Landsat images: Understorey impact on top-of-canopy reflectance in a northern hardwood forest. *Canadian Journal of Remote Sensing*. 2018;**44**(5):435-446. DOI: 10.1080/07038992.2018.1533399
- [51] Rautiainen M, Lukeš P, Homolová L, Hovi A, Pisek J, Möttus M. Spectral properties of coniferous forests: A review of in situ and laboratory measurements. *Remote Sensing*. 2018;**10**(2):1-28. DOI: 10.3390/rs10020207
- [52] Van Doorn AM, Pinto CT. Differences in land cover interpretation in landscapes rich in cover gradients: Reflections based on the montado of South Portugal. *Agroforestry Systems*. 2007;**70**(2):169-183. DOI: 10.1007/s10457-007-9055-8
- [53] Allen H, Simonson W, Parham E, Santos EDBE, Hotham P. Satellite remote sensing of land cover change in a mixed agro-silvo-pastoral landscape in the Alentejo, Portugal. *International Journal of Remote Sensing*. 2018;**39**(14):4663-4683. DOI: 10.1080/01431161.2018.1440095
- [54] Sousa AMO, Gonçalves AC, Mesquita P, Marques da Silva JR. Biomass estimation with high resolution satellite images: A case study of *Quercus rotundifolia*. *ISPRS Journal of Photogrammetry and Remote Sensing*. 2015;**101**:69-79. DOI: 10.1016/j.isprsjprs.2014.12.004
- [55] Macedo FL, Sousa AMO, Gonçalves AC, Marques da Silva JR, Mesquita PA, RAF R. Above-ground biomass estimation for *Quercus rotundifolia* using vegetation indices derived from high spatial resolution satellite images. *European Journal of Remote Sensing*. 2018;**51**(1):932-944. DOI: 10.1080/22797254.2018.1521250
- [56] Godinho S, Guiomar N, Gil A. Estimating tree canopy cover percentage in a Mediterranean silvopastoral systems using Sentinel-2A imagery and the stochastic gradient boosting algorithm. *International Journal of Remote Sensing*. 2018;**39**(14):4640-4662. DOI: 10.1080/01431161.2017.1399480

- [57] Godinho S, Guiomar N, Gil A. Using a stochastic gradient boosting algorithm to analyse the effectiveness of Landsat 8 data for montado land cover mapping: Application in southern Portugal. *International Journal of Applied Earth Observation and Geoinformation*. 2016;**49**:151-162. DOI: 10.1016/j.jag.2016.02.008
- [58] Nguyen HTT, Doan TM, Tomppo E, McRoberts RE. Land use/land cover mapping using multitemporal Sentinel-2 imagery and four classification methods—A case study from Dak Nong, Vietnam. *Remote Sensing*. 2020;**12**(1367):1-27. DOI: 10.3390/rs12091367
- [59] Xiong J, Thenkabail PS, Tilton JC, Gumma MK, Teluguntla P, Oliphant A, et al. Nominal 30-m cropland extent map of continental Africa by integrating pixel-based and object-based algorithms using Sentinel-2 and Landsat-8 data on Google Earth Engine. *Remote Sensing*. 2017;**9**(10):1-27. DOI: 10.3390/rs9101065
- [60] Lee YS, Lee S, Jung HS. Mapping forest vertical structure in Gong-Ju, Korea using Sentinel-2 satellite images and artificial neural networks. *Applied Sciences*. 2020;**10**(5):1-18. DOI: 10.3390/app10051666
- [61] Banko G. A review of assessing the accuracy of and of methods including remote sensing data in forest inventory. Laxenburg, Austria: International Institute for Applied Systems Analysis; 1998. IR-98-081. pp. 1-42
- [62] GFOI. Integrating Remote-Sensing and Ground-Based Observations for Estimation of Emissions and Removals of Greenhouse Gases in Forests. Geneva, Switzerland: Group on Earth; 2013. p. 164
- [63] Foody GM. Status of land cover classification accuracy assessment. *Remote Sensing of Environment*. 2002;**80**(1):185-201. DOI: 10.1016/S0034-4257(01)00295-4
- [64] Story M, Congalton RG. Remote sensing brief accuracy assessment: A user's perspective. *Photogrammetric Engineering and Remote Sensing*. 1986;**52**(3):397-399
- [65] FAO. Map accuracy assessment and area estimation: A practical guide. In: *National Forest Monitoring Assessment Working Paper No. 46/E*. Rome, Italy: Food and Agriculture Organization of the United Nations; 2016. p. 69. Available from: <http://www.fao.org/3/a-i5601e.pdf>
- [66] Liu C, Frazier P, Kumar L. Comparative assessment of the measures of thematic classification accuracy. *Remote Sensing of Environment*. 2007;**107**(4):606-616. DOI: 10.1016/j.rse.2006.10.010
- [67] Stehman SV. Selecting and interpreting measures of thematic classification accuracy. *Remote Sensing of Environment*. 1997;**62**:77-89. DOI: 10.1016/S0034-4257(97)00083-7
- [68] Foody GM. Explaining the unsuitability of the kappa coefficient in the assessment and comparison of the accuracy of thematic maps obtained by image classification. *Remote Sensing of Environment*. 2020;**239**:111630: 1-11. DOI: 10.1016/j.rse.2019.111630
- [69] Lark RM. Components of accuracy of maps with special reference to discriminant analysis on remote sensor data. *International Journal of Remote Sensing*. 1995;**16**:1461-1480. DOI: 10.1080/01431169508954488
- [70] Anderson JR, Hardy EE, Roach JT, Witmer RE. *A Land Use and Land Cover Classification System for Use with Remote Sensor Data*. Washington, DC, USA: U.S. Government Publishing Office; 1976
- [71] Sothe C, de Almeida CM, Liesenberg V, Schimalski MB. Evaluating Sentinel-2 and Landsat-8 data to map

- sucessional forest stages in a subtropical forest in southern Brazil. *Remote Sensing*. 2017;**9**(8):1-23. DOI: 10.3390/rs9080838
- [72] Farda NM. Multi-temporal land use mapping of coastal wetlands area using machine learning in Google Earth Engine. *IOP Conference Series: Earth and Environmental Science*. 2017;**98**(1):1-23. DOI: 10.1088/1755-1315/98/1/012042
- [73] Mountrakis G, Im J, Ogole C. Support vector machines in remote sensing: A review. *ISPRS Journal of Photogrammetry and Remote Sensing*. 2011;**66**(3):247-259. DOI: 10.1016/j.isprsjprs.2010.11.001
- [74] Pal M. Random forest classifier for remote sensing classification. *International Journal of Remote Sensing*. 2005;**26**(1):217-222. DOI: 10.1080/01431160412331269698
- [75] Breiman L, Friedman JH, Olshen RA, Stone CJ. *Classification and Regression Trees*. New York, USA: Chapman & Hall; 1984. p. 358. DOI: 10.1002/cyto.990080516
- [76] Chen L, Wang Y, Ren C, Zhang B, Wang Z. Assessment of multi-wavelength SAR and multispectral instrument data for forest aboveground biomass mapping using random forest kriging. *Forest Ecology and Management*. 2019;**447**:12-25. DOI: 10.1016/j.foreco.2019.05.057
- [77] Zhou X, Li L, Chen L, Liu Y, Cui Y, Zhang Y, et al. Discriminating urban forest types from Sentinel-2A image data through linear spectral mixture analysis: A case study of Xuzhou, East China. *Forests*. 2019;**10**(6):1-19. DOI: 10.3390/f10060478
- [78] Liu H, Gu L, Ren R, He F. Classification of forest vegetation types in Jilin Province, China based on deep learning and multi-temporal Sentinel-2 data. In: *Proc. SPIE 11127, Earth Observing Systems XXIV*, 1112725. pp. 1-12. DOI: 10.1117/12.2527392
- [79] Miranda E, Mutiara AB, Ernastuti, Wibowo WC. Forest classification method based on convolutional neural networks and Sentinel-2 satellite imagery. *International Journal of Fuzzy Logic and Intelligent Systems*. 2019;**19**(4):272-282. DOI: 10.5391/IJFIS.2019.19.4.272
- [80] Heckel K, Urban M, Schratz P, Mahecha MD, Schmulilius C. Predicting forest cover in distinct ecosystems: The potential of multi-source Sentinel-1 and -2 data fusion. *Remote Sensing*. 2020;**12**(2):1-22. DOI: 10.3390/rs12020302
- [81] Rajah P, Odindi J, Mutanga O, Kiala Z. The utility of Sentinel-2 vegetation indices (VIs) and Sentinel-1 synthetic aperture radar (SAR) for invasive alien species detection and mapping. *Natural Conservation*. 2019;**35**:41-61. DOI: 10.3897/natureconservation.35.29588
- [82] Saini R, Ghosh SK. Crop classification on single date Sentinel-2 imagery using random forest and support vector machine. In: *ISPRS - International Archives of the Photogrammetry, Remote Sensing and Spatial Information Sciences*. Vol. XLII-5. 2018. pp. 683-688. DOI: 10.5194/isprs-archives-xxlii-5-683-2018
- [83] Chatziantoniou A, Petropoulos GP, Psomiadis E. Co-orbital Sentinel 1 and 2 for LULC mapping with emphasis on wetlands in a Mediterranean setting based on machine learning. *Remote Sensing*. 2017;**9**(12):1-20. DOI: 10.3390/rs9121259
- [84] Fragoso-Campón L, Quirós E, Mora J, Gutiérrez JA, Durán-Barroso P. Accuracy enhancement for land cover classification using LIDAR and multitemporal Sentinel 2 images in a forested watershed. *Proceedings*. 2018;**2**(1280):1-4. DOI: 10.3390/proceedings2201280

- [85] Tieng T, Sharma S, Mackenzie RA, Venkattappa M, Sasaki NK, Collin A. Mapping mangrove forest cover using Landsat-8 imagery, Sentinel-2, very high resolution images and Google Earth Engine algorithm for entire Cambodia. IOP Conference Series: Earth and Environmental Science. 2019;**266**(1):1-12. DOI: 10.1088/1755-1315/266/1/012010
- [86] Li H, Jia M, Zhang R, Ren Y, Wen X. Incorporating the plant phenological trajectory into mangrove species mapping with dense time series Sentinel-2 imagery and the Google Earth Engine platform. Remote Sensing. 2019;**11**(21):1-16. DOI: 10.3390/rs11212479
- [87] Karasiak N, Sheeren D, Fauvel M, Willm J, Dejoux JF, Monteil C. Mapping tree species of forests in Southwest France using Sentinel-2 image time series. In: 2017 9th International Workshop on the Analysis of Multitemporal Remote Sensing Images, MultiTemp 2017. 2017. pp. 1-4. DOI: 10.1109/Multi-Temp.2017.8035215
- [88] Puletti N, Chianucci F, Castaldi C. Use of Sentinel-2 for forest classification in Mediterranean environments. Annals of Silvicultural Research. 2017;**42**(1):1-7. DOI: 10.12899/ASR-1463
- [89] Duan Q, Tan M, Guo Y, Wang X, Xin L. Understanding the spatial distribution of urban forests in China using Sentinel-2 images with Google Earth Engine. Forests. 2019;**10**(729):1-15. DOI: 10.3390/f10090729
- [90] Mutanga O, Kumar L. Google Earth Engine applications. Remote Sensing. 2019;**11**(5):1-4. DOI: 10.3390/rs11050591
- [91] Oliphant AJ, Thenkabail PS, Teluguntla P, Xiong J, Gumma MK, Congalton RG, et al. Mapping cropland extent of southeast and Northeast Asia using multi-year time-series Landsat 30-m data using a random forest classifier on the Google Earth Engine cloud. International Journal of Applied Earth Observation and Geoinformation. 2019;**81**:110-124. DOI: 10.1016/j.jag.2018.11.014
- [92] Maxwell AE, Strager MP, Warner TA, Ramezan CA, Morgan AN, Pauley CE. Large-area, high spatial resolution land cover mapping using random forests, GEOBIA, and NAIP orthophotography: Findings and recommendations. Remote Sensing. 2019;**11**(12):1-27. DOI: 10.3390/rs11121409
- [93] Dong J, Xiao X, Menarguez MA, Zhang G, Qin Y, Thau D, et al. Mapping paddy rice planting area in northeastern Asia with Landsat 8 images, phenology-based algorithm and Google Earth Engine. Remote Sensing of Environment. 2016;**185**:142-154. DOI: 10.1016/j.rse.2016.02.016
- [94] Shelestov A, Lavreniuk M, Kussul N, Novikov A, Skakun S. Exploring Google Earth Engine platform for big data processing: Classification of multi-temporal satellite imagery for crop mapping. Frontiers in Earth Science. 2017;**5**:1-10. DOI: 10.3389/feart.2017.00017
- [95] Gorelick N, Hancher M, Dixon M, Ilyushchenko S, Thau D, Moore R. Google Earth Engine: Planetary-scale geospatial analysis for everyone. Remote Sensing of Environment. 2017;**202**:18-27. DOI: 10.1016/j.rse.2017.06.031
- [96] Zurqani HA, Post CJ, Mikhailova EA, Schlautman MA, Sharp JL. Geospatial analysis of land use change in the Savannah River Basin using Google Earth Engine. International Journal of Applied Earth Observation and Geoinformation. 2018;**69**:175-185. DOI: 10.1016/j.jag.2017.12.006
- [97] Camara G, Assis LF, Ribeiro G, Ferreira KR, Llapa E, Vinhas L, et al. Big earth observation data analytics: Matching requirements to system architectures. In: Proceedings of the

- 5th ACM SIGSPATIAL International Workshop on Analytics for Big Geospatial Data, BigSpatial. Vol. 3. 2016. pp. 1-6. DOI: 10.1145/3006386.3006393
- [98] Carrasco L, O'Neil AW, Daniel Morton R, Rowland CS. Evaluating combinations of temporally aggregated Sentinel-1, Sentinel-2 and Landsat 8 for land cover mapping with Google Earth Engine. *Remote Sensing*. 2019;**11**:1-21. DOI: 10.3390/rs11030288
- [99] Coluzzi R, Imbrenda V, Lanfredi M, Simoniello T. A first assessment of the Sentinel-2 level 1-C cloud mask product to support informed surface analyses. *Remote Sensing of Environment*. 2018;**217**:426-443. DOI: 10.1016/j.rse.2018.08.009
- [100] Ghosh SM, Behera MD. Aboveground biomass estimation using multi-sensor data synergy and machine learning algorithms in a dense tropical forest. *Applied Geography*. 2018;**96**:29-40. DOI: 10.1016/j.apgeog.2018.05.011
- [101] Sun X, Li G, Wang M, Fan Z. Analyzing the uncertainty of estimating forest aboveground biomass using optical imagery and spaceborne LiDAR. *Remote Sensing*. 2019;**11**(6):1-6. DOI: 10.3390/rs11060722
- [102] Pertille CT, Nicoletti MF, Topanotti LR, Stepka TF. Biomass quantification of *Pinus taeda* L. from remote optical sensor data. *Advances in Forestry Science*. 2019;**6**(2):603-610. DOI: 10.34062/afs.v6i2.7086
- [103] Kushwaha SPS, Nandy S, Gupta M. Growing stock and woody biomass assessment in Asola-Bhatti Wildlife Sanctuary, Delhi, India. *Environmental Monitoring and Assessment*. 2014;**186**(9):5911-5920. DOI: 10.1007/s10661-014-3828-0
- [104] Vashum KT, Jayakumar J. Methods to estimate above-ground biomass and carbon stock in natural forests - A review. *Journal of Ecosystem and Ecography*. 2012;**02**(04):1-8. DOI: 10.4172/2157-7625.1000116
- [105] Timothy D, Onesimo M, Riyad I. Quantifying aboveground biomass in African environments: A review of the trade-offs between sensor estimation accuracy and costs. *Tropical Ecology*. 2016;**57**(3):393-405
- [106] Galidaki G, Zianis D, Gitas I, Radoglou K, Karathanassi V, Tsakiri-Strati M, et al. Vegetation biomass estimation with remote sensing: Focus on forest and other wooded land over the Mediterranean ecosystem. *International Journal of Remote Sensing*. 2017;**38**(7):1940-1966. DOI: 10.1080/01431161.2016.1266113
- [107] Duncanson L, Armston J, Disney M, Avitabile V, Barbier N, Calders K, et al. The importance of consistent global forest aboveground biomass product validation. *Surveys in Geophysics*. 2019;**40**(4):979-999. DOI: 10.1007/s10712-019-09538-8
- [108] Ali I, Greifeneder F, Stamenkovic J, Neumann M, Notarnicola C. Review of machine learning approaches for biomass and soil moisture retrievals from remote sensing data. *Remote Sensing*. 2015;**7**(12):16398-16421. DOI: 10.3390/rs71215841
- [109] Natarajan K, Latva-Käyrä P, Zyadin A, Pelkonen P. New methodological approach for biomass resource assessment in India using GIS application and land use/land cover (LULC) maps. *Renewable and Sustainable Energy Reviews*. 2016;**63**:256-268. DOI: 10.1016/j.rser.2016.05.070
- [110] Bajwa SG, Bajcsy P, Groves P, Tian LF. Hyperspectral image data mining for band selection in agricultural applications. *Transactions of ASAE*. 2004;**47**(3):895-908
- [111] Song C, Chen JM, Hwang T, Gonsamo A, Croft H, Zhang Q, et al.

- Ecological characterization of vegetation using multisensor remote sensing in the solar reflective spectrum. In: Thenkabail PS, editor. *Land Resources Monitoring, Modeling, and Mapping with Remote Sensing*. Remote Sensing Handbook. London, UK: Taylor and Francis; 2015;2:533-575. DOI: 10.1201/b19322
- [112] Sánchez-Ruiz S, Moreno-Martínez Á, Izquierdo-Verdiguier E, Chiesi M, Maselli F, Gilabert MA. Growing stock volume from multi-temporal landsat imagery through Google Earth Engine. *International Journal of Applied Earth Observation and Geoinformation*. 2019;83:1-10. 101913. DOI: 10.1016/j.jag.2019.101913
- [113] Wang X, Wang S, Dai L. Estimating and mapping forest biomass in Northeast China using joint forest resources inventory and remote sensing data. *Journal of Forestry Research*. 2018;29(3):797-811. DOI: 10.1007/s11676-017-0504-6
- [114] Qazi WA, Baig S, Gilani H, Waqar MM, Dhakal A, Ammar A. Comparison of forest aboveground biomass estimates from passive and active remote sensing sensors over Kayar Khola watershed, Chitwan district, Nepal. *Journal of Applied Remote Sensing*. 2017;11(2):1-17. DOI: 10.1117/1.jrs.11.026038
- [115] Rasel SMM, Chang HC, Ralph TJ, Saintilan N, Diti IJ. Application of feature selection methods and machine learning algorithms for saltmarsh biomass estimation using Worldview-2 imagery. *Geocarto International*. 2019:1-25. DOI: 10.1080/10106049.2019.1624988
- [116] Leite RV, Hummel C, Pires RDP, Silva CA, Pedro C, Soares B, et al. Estimating stem volume in eucalyptus plantations using airborne LiDAR: A comparison of area- and individual tree-based approaches. *Remote Sensing*. 2020;12(9):1-26. DOI: 10.3390/rs12091513
- [117] Sanquetta CR. Métodos de determinação de biomassa florestal. In: Sanquetta CR et al, editors. *As florestas e o carbono*. Curitiba: Universidade Federal do Paraná; 2002. pp.119-140
- [118] Roth KL, Roberts DA, Dennison PE, Peterson SH, Alonzo M. The impact of spatial resolution on the classification of plant species and functional types within imaging spectrometer data. *Remote Sensing of Environment*. 2015;171:45-57. DOI: 10.1016/j.rse.2015.10.004
- [119] Dang ATN, Nandy S, Srinet R, Luong NV, Ghosh S, Senthil KA. Forest aboveground biomass estimation using machine learning regression algorithm in Yok Don National Park, Vietnam. *Ecological Informatics*. 2019;50:24-32. DOI: 10.1016/j.ecoinf.2018.12.010
- [120] Liu Y, Gong W, Xing Y, Hu X, Gong J. Estimation of the forest stand mean height and aboveground biomass in Northeast China using SAR Sentinel-1B, multispectral Sentinel-2A, and DEM imagery. *ISPRS Journal of Photogrammetry and Remote Sensing*. 2019;151:277-289. DOI: 10.1016/j.isprsjprs.2019.03.016
- [121] Astola H, Häme T, Sirro L, Molinier M, Kilpi J. Comparison of Sentinel-2 and Landsat 8 imagery for forest variable prediction in boreal region. *Remote Sensing of Environment*. 2019;223(2018):257-273. DOI: 10.1016/j.rse.2019.01.019
- [122] Chrysafis I, Mallinis G, Siachalou S, Patias P. Assessing the relationships between growing stock volume and Sentinel-2 imagery in a Mediterranean forest ecosystem. *Remote Sensing Letters*. 2017;8(6):508-517. DOI: 10.1080/2150704X.2017.1295479
- [123] Hu Y, Xu X, Wu F, Sun Z, Xia H, Meng Q, et al. Estimating forest stock

volume in Hunan Province, China, by integrating in situ plot data, Sentinel-2 images, and linear and machine learning regression models. *Remote Sensing*. 2020;**12**(1):1-23. DOI: 10.3390/rs12010186

[124] Pandit S, Tsuyuki S, Dube T. Estimating above-ground biomass in sub-tropical buffer zone community forests, Nepal, using Sentinel 2 data. *Remote Sensing*. 2018;**10**(4):1-18. DOI: 10.3390/rs10040601

[125] Pandit S, Tsuyuki S, Dube T. Exploring the inclusion of Sentinel-2 MSI texture metrics in above-ground biomass estimation in the community forest of Nepal. *Geocarto International*. 2019;**34**:1-18. DOI: 10.1080/10106049.2019.1588390

[126] EAS. Biomass [Internet]. 2020. Available from: <https://earth.esa.int/web/guest/missions/esa-future-missions/biomass>

# Biomass Estimation Using Satellite-Based Data

*Patrícia Lourenço*

## Abstract

Comprehensive measurements of global forest aboveground biomass (AGB) are crucial information to promote the sustainable management of forests to mitigate climate change and preserve the multiple ecosystem services provided by forests. Optical and radar sensors are available at different spatial, spectral, and temporal scales. The integration of multi-sources sensor data with field measurements, using appropriated algorithms to identify the relationship between remote sensing predictors and reference measurements, is important to improve forest AGB estimation. This chapter aims to present different types of predicted variables derived from multi-sources sensors, such as original spectral bands, transformed images, vegetation indices, textural features, and different regression algorithms used (parametric and non-parametric) that contribute to a more robust, practical, and cost-effective approach for forest AGB estimation at different levels.

**Keywords:** aboveground biomass, regression algorithms, machine learning algorithms, remote sensing, satellite-derived predictor variables

## 1. Introduction

The aboveground biomass (AGB) of forests directly provides the amount of organic matter in living and dead plant materials, for example, of leaves, branches, and stem, and it is expressed in dry weight per unit area [1]. AGB is also one of the major reservoirs of carbon in forest ecosystems and a key indicator of forest health [2]. Thus, measuring and monitoring AGB changes is crucial to understanding AGB role in the global carbon cycle to reduce carbon dioxide concentrations and to mitigate climate change [3]. AGB was recognized as an Essential Climate Variable by the United Nations Framework Convention on Climate Change (UNFCCC) [4] and an essential biophysical parameter of forest ecosystems [5] for estimating carbon and water cycling, and energy fluxes between land surface and atmosphere. These are processes relevant on the background of climate change [6]. In addition, AGB resources underlie the development of a bio-based economy as part of the European Union Forest-Based Vision targets sector 2030 [7]. The key role of AGB forests leads to the need for accurate and precise estimates of AGB to assess changes in forest structure, including understanding the roles of forests in the terrestrial carbon flux and global climate change [8].

Spatial and temporal quantification and monitoring of AGB are important to assess the impacts of climate and land use changes on the global carbon cycle and understand the causing effects on ecosystem resilience [5]. Fast, accurate and



timely estimation and monitoring of AGB, at local, regional, and global scales, will significantly reduce the uncertainty in carbon stock assessments and provide valuable information to better support sustainable forest management strategies [9, 10]. The frequently used methods to estimate AGB are the indirect, which are based on mathematical relations between biomass, dependent variable and one or a few easy-to-measure tree variables, independent variables [11]. Traditionally, indirect methods use forest inventories and allometric functions at tree level to evaluate biomass at plot level and an extrapolation method to assess all area [12].

In last decade, there has been an increase of biomass mapping and estimations for global terrestrial ecosystems using remote sensing (RS) [6]. Satellite-derived predictor variables have been used to estimate AGB and assess its spatio-temporal variability through valuable RS approaches [13]. The development and implementation of RS-based AGB estimation' monitoring frameworks may provide low-cost and accurate operational geospatial tools for rapidly and effectively detecting, mapping and assessing relevant changes in AGB in any study area. On the other hand, this same type of geospatial tool might be able to support the execution, monitoring, and impact evaluation of nature conservation policies and strategies, by providing a systematic and accurate forest AGB estimation monitoring system [14]. RS provides variables indirectly related to AGB, and the spectral response (original or transformed sensor bands) of the vegetation cover, density, shade, and texture is correlated with AGB [15].

In response to the urgent need for much improved mapping of global forest biomass and the lack of current space systems capable of meeting this need, the BIOMASS mission arose from European Space Agency (ESA) as an Earth observing satellite planned to launch in October 2022 [16]. BIOMASS mission aims to provide the scientific community with accurate maps of world's forest biomass, including height, state, disturbance patterns, and how they are changing [17, 18]. Gathering BIOMASS mission information with the economic and environmental knowledge will enable to reach a better spatial planning of the forest AGB [19].

The objective of this chapter is to present the satellite images, satellite-derived predictor variables and algorithms used to estimate forest AGB with RS data. To accomplish this objective, the Section 2 presents the types of satellite sensors used in RS. The Section 3 describes the satellite-derived predictor variables. In Section 4, there is a description of the most used algorithms to predict forest AGB. Section 5 presents a discussion of the more frequently used satellite images, algorithms, and variable importance for AGB estimation with RS. Finally, in Section 6, the main conclusions are presented.

## **2. Remote sensing satellite sensors**

Currently, there is a wide variety of RS data available for forest AGB estimation, such as optical (passive) and radar (active) sensors data, at different spatial, spectral, and temporal scales resolution, from local to global scale, with or without costs [20]. The selection of the proper satellite data it will depend on the scope of the research and on the study area, considering the area size, type of forest, and available budget to obtain accurate forest AGB estimations. Optical and radar RS follow similar approaches for forest AGB analysis, modeling, mapping, and monitoring [21]. Optical RS imagery gives spectral information of the horizontal forest structure [22], while radar RS imagery gives information of the vertical forest structure due to the ability of penetrating the forest canopy to a certain depth [23].

The analyze of optical data is easier to use than radar RS data because, after calibrating and correcting the images, the data can be directly processed and

extracted and similarly interpreted as a photograph. As passive sensor, optical RS sensors need a light source (e.g., sun light), and the quality of the images is dependent of the weather and day light. These sensors record a variety of electromagnetic spectrum radiation frequency, especially at wavelengths of visible light and infra-red. Optical RS sensors record the reflectance of the electromagnetic spectrum of earth objects in the visible (Blue, Green, and Red) and infrared regions (near infrared – NIR and short wave infrared – SWIR). Visible and NIR (VNIR), and SWIR are the wavelengths more sensitive to vegetation characteristics.

Optical RS data are widely used to estimate AGB of different types of forest, such as in temperate forests [24], Mediterranean forests [25], sub-tropical forests [26], and boreal forests [27]. Different types of spatial resolution sensors (low: 100–1000 m, and medium: 10–100 m) have been used in studies of AGB estimation at global, regional, and local scale, such as MODIS [15], Landsat ETM+ [28], SPOT [29], and more recently Sentinel-2 [30]. Very high spatial resolution sensors (<1 m), such as IKONOS, Quickbird II, WorldView-2, have advantage over low and medium spatial resolution sensors, despite their cost. These sensors provide finer spatial scale with a greater thematic resolution and accuracy which can be used to complement AGB forestry measurements from the forest inventory [31, 32]. Monitoring and evaluation of AGB estimation over time can be performed by using optical RS due to existing continuous data and wide spatial coverage. However, despite the widespread usage of optical RS data in the estimation of forest AGB, these are limited to their poor penetration capacity in the forest canopies and clouds, in addition to presenting problems of data saturation in high AGB density [33].

On the contrary, interpretation of radar RS sensor data, that is, Synthetic Aperture Radar (SAR) and Light Detection and Ranging (LiDAR) sensors imagery, is not always straightforward because of the signal being responsive to surface characteristics, like structure and moisture, and consequently to have the non-intuitive and side-looking geometry. Despite that, radar provides much more information than just an image to be visually analyzed because of being characterized by two data values for each pixel, a Magnitude value (image analogous to one collected by an optical sensor) and a Phase value (it cannot be visually interpreted). As an active sensor, radar has the advantage of providing its light source and enabling it to operate 24 hours a day.

SAR sensors have been used to estimate forest AGB to complement the spectral reflectance characteristics of vegetation in the optical regions and are very useful in regions often covered by clouds [34]. These sensors are sensitive to water content in vegetation and register information independently of the weather conditions [35] through the interaction of the radar waves with tree scattering elements [17]. The techniques most used in biomass studies using SAR data are regression based on backscattering amplitudes [36] and interferometry based on backscattering amplitudes and phases [37]. The important factors in the backscattering coefficient are wavelength (e.g., K, X, C, L, P), polarization (e.g., HH, VV, HV, VH), incidence angle, land cover, and terrain properties (e.g., roughness and dielectric constant).

The short wavelength X and C bands, which interact only with tree canopy surface layer information, are more suitable for AGB estimation in areas with low biomass [38]. The long wavelength L and P bands are more suitable for AGB estimation of dense forest with relatively high biomass density for presenting greater interaction with the forest elements, such as branch, stem, and soil under the canopy [39] and by allowing canopy height to be retrieved by polarimetric interferometry [17].

The polarization information can be linear and crossed. The linear polarization is obtained through linear transmission and reception signal, horizontal (H) and

vertical (V), HH and VV, respectively [40]. In the cross-polarization, the transmission and reception signal are different, i.e., HV and VH. Cross-polarized VH backscatter has been considered the largest dynamic range and the highest correlation with biomass [17]. In the case of linear polarization, ground conditions can affect the biomass-backscatter relationship. HH backscatter comes mainly from stem-ground scattering, while VV backscatter results from both volume and ground scattering.

SAR sensors has been used in several forest AGB estimation studies, such as in Miombo Savanna Woodlands [41], deciduous broadleaved and mixed broadleaf-conifer forests [30, 42], tropical peat swamp forests [43], tropical savannas and woodlands [44], temperate deciduous forest [45], rainforest [46], coniferous temperate forest [47], and mixed and deciduous boreal forest [48]. Currently, there is a considerable number of ongoing SAR missions from various agencies, namely Sentinel-1A,B, ALOS-2, SOCOM-1a,b, Cosmo-SkyMed SG, and PAZ. For historical analysis, it can use data from sensors, such as, ERS-1,2, JERS, Envisat, Radarsat-1,2, ALOS, TerraSAR-X, and TanDEM-X. However, despite the positive correlation with the forest structure parameters, SAR data can present saturation problems. The saturation problems can be over different types of temperate, boreal, and tropical forests [49] and depend on the wavelengths, L band at around 100–150 t/ha [50] and 250 t/ha [51], polarization, characteristics of the vegetation stand structure and ground conditions [52]. Furthermore, estimating AGB with only SAR data is difficult, since these data provide information on the roughness of the land cover surfaces and do not distinguish the types of vegetation [53].

LiDAR is an active RS method sensor composed by a laser, a scanner and a specialized GPS receiver used from spacecraft satellite for Space-borne Laser Scanning (SLS), aircraft for Airborne Laser Scanning (ALS) – the most used in forestry approaches – and on the ground level, Terrestrial Laser Scanning (TLS). LiDAR uses pulsed laser light to measure ranges (variable distances) to the object Earth. Differences in return times and laser wavelengths serve to calculate distance traveled which is then converted to elevation. These measurements generate a cloud of points that allow the 3D representation of the vegetation, based on the identification of the X, Y, and Z location, and can penetrate within forest canopy [54]. The airborne LiDAR has the advantage of covering a large area, allowing its use in large areas with minimum occlusion of the terrain by vegetation. Also, it does not saturate even at very high biomass levels (>1000 Mg/ha) [55].

LiDAR provides accurate measurements of vegetation structures, such as height, crown size, basal area, stem volume, and vertical profile. These measurements to characterize the canopy or crown cover in three dimensions and consequently to estimate forest AGB in any study area [56]. The LiDAR metrics can be extracted on the basis of either individual trees [57] or areas [49]. The extraction of these metrics depends on the laser return signal (discrete-return vs. waveform), scanning pattern (scanning or profiling), and footprint size (small vs. large). LiDAR data have been used to estimate forest AGB in combination with other sensors data (optical and/or radar) [15, 58]. Moreover, LiDAR data are a good complement to forest inventory data because they capture spatial variability and can be acquired quickly and in large or difficult to access areas [58]. However, the limited availability and the cost of these data prevent its extensive application [10].

Integration of multi-source RS data, that is, optical, SAR or/and LiDAR data, is important to improve AGB estimation because more information about forest structure features is integrated than just by a sensor. The integration of multiple data sources for more accurate forest AGB estimations has been explored by several authors [44, 59, 60]. In this way, the advantages of each sensor are highlighted to the detriment of negative characteristics of the sensors [61]. Nevertheless, RS data

should be complemented with AGB field data measurements, as training and validation data, in order to improve the accuracy of the AGB estimation model [6].

### 3. Satellite-derived predictor variables

In studies of forest AGB estimation, it is important to integrate different types of independent variables derived from passive and active sensors, such as original spectral bands, transformed images, vegetation indices, and textural variables (**Table 1**), to achieve accurate predictive models [62].

Spectral bands (e.g., VNIR and SWIR) reflect the vegetation structure, texture, and shadow, related with leaf cellular structure and plant pigments, which are correlated with AGB [15]. VNIR wavelengths are more sensitive to pigments and overall canopy health, while SWIR capture many biochemical, leaf mass per area, and discriminates moisture content of soil and vegetation [15]. In Red region occurs absorption by chlorophyll, while in NIR region, there is a pronounced reflection by mesophyll cells [69]. Green band is related with the greenness of vegetation representing the absorption intensity of Blue and Red energy by plant leaves and the reflection intensity of green energy [70]. On the other hand, hyperspectral sensors allow to have many narrow contiguous spectral bands and can accurately discriminate absorption features' wavelength position and shape.

Transformed images have been used to reduce the dimension of the data, required for optimal performance, by producing new variables from optical multispectral data [21]. There are some image transformation techniques, such as Principal Component Analysis (PCA), Minimum Noise Fraction transform (MNF), and Tasseled Cap Transform (TCT). PCA is the most used transformed image to enhance the change information from stacked multisensor data and captures maximum variance generating a new reduced set of bands in which the information is concentrated and that have little correlation [71]. For  $n$  bands of multispectral data, the first PC (PC1) includes the largest percentage of the total image variance and the succeeding components (PC2, PC3, ..., PC $n$ ) each containing a decreasing percentage of the scene variance [70].

MNF transform is a linear transformation of the reflectance data of hyperspectral and high spectral resolution images to determine the inherent dimensionality of image data, to segregate noise in the data, and to reduce the computational requirements for subsequent processing [72, 73]. MNF is composed of two PCA rotations that separate the noise from the data. The first rotation consists in the call noise whitening process in which the principal components of the noise covariance matrix are used to decorrelate and rescale the noise in the data

| Sensor  | Variable          | Description  | References         |
|---------|-------------------|--|--------------------|
| Optical | Spectral features | Spectral bands, vegetation indices, and transformed images   | (e.g. [62])        |
|         | Spatial features  | Textural images  | (e.g. [63])        |
| Active  | Radar             | Backscattering coefficients, textural images, interferometry SAR, and Polarimetric SAR interferometry                      | (e.g. [38, 64–66]) |
|         | LiDAR             | Lidar metrics based on statistical measures of point clouds or estimated products (e.g. canopy height or individual trees) | (e.g. [67, 68])    |

**Table 1.**  
*Optical and active sensor derived variables used in forest AGB estimation.*

and obtain transformed data. The transformed noise data have unit variance and no band-to-band correlations. The second rotation uses the principal components derived from the noise whitening process and rescaled by the noise standard deviation. The inherent dimensionality of the second transformation data is determined by examining the final eigenvalues and the associated images. In this way, MNF transformation may reduce the dimensionality of hyperspectral image data, eliminate correlations band-to-band, and order components in terms of image quality [74].

TCT is a conversion of the original bands of an image into a new set of bands through an orthogonal transformation with defined interpretations, useful for vegetation mapping, and directly associated with important physical parameters of the vegetation [75]. TCT uses a similar concept to the PCA in which linear combinations of the original image bands are performed. The tasseled-cap bands are produced as the sum of image band 1 times a constant plus image band 2 times a constant, etc. The coefficients used to create the tasseled-cap bands are derived statistically from images and empirical observations and are specific to each imaging sensor. TCT aims to compress the spectral data in few bands associated with physical scene characteristics with minimal information loss [76]. These bands are then correlated, transforming them orthogonally into a new set of axes associated with physical features. The resulting spectral features consists in three axes defined as brightness, greenness, and wetness that are directly associated with important physical parameters [77]. Brightness – the first feature of TCT – is a weighted sum of all the bands and is related with bare or partially covered soil, natural and man-made features, and variations in topography [70]. Greenness – the second feature of TCT – is a measure of the contrast between the NIR band and the visible bands and is related with vegetation amount in the image. Wetness – the third feature of TCT – is orthogonal to the first two components and is related to canopy and soil moisture [78]. TCT was developed in 1972 for the Landsat multi-spectral scanner (MSS) to understand the growth patterns of plants, soil moisture, and other hydrological features in the spectral space formed by combinations of different bands but is adapted to current sensors.

Vegetation index is a spectral transformation of at least two bands to improve the contribution of the vegetation properties of an image. The wide variety of vegetation indices are calculated based on the ratio between two or more bands to contrast the high absorption by leaf pigments (chlorophylls, carotenoids, and xanthophylls) in the visible spectral region (400–700 nm), high reflectance by leaves in the NIR region (700–1300 nm), and moderate water absorption in the SWIR (1300–2100 nm) [79]. There is a wide range of vegetation indices that are used in the estimation of AGB (**Table 2**).

Two most common vegetation indices used in forest AGB estimation are NDVI and SR [63]. NDVI is the fraction of the difference and the sum of the NIR and Red bands where chlorophyll absorbs Red whereas the mesophyll leaf structure scatters NIR [80]. SR is the ratio between NIR and RED [81] and intends to capture the contrast between the RED and NIR bands for vegetated pixels. Both vegetation indices prove to have a good relation with the AGB estimation derived from satellite images data in several types of forests [63, 82]. Further, canopy moisture content can be quantified through vegetation water indices, namely NDWI which is related with NIR and SWIR bands [83].

Texture is a feature used to identify objects or regions of interest in an image [105], based on mathematical pattern (spatial) analysis. Texture is characterized by defining local spatial organization of spatially varying spectral values that is repeated in a region of larger spatial scale. The variations in these scales in the image values that constitute texture are generally due to an underlying physical variation

| Vegetation indices  |       | Formulation   | Reference  |
|---|-------|---|------------|
| Normalized difference vegetation index                      | NDVI  | $\frac{NIR-RED}{NIR+RED}$   | [84]       |
| Enhanced vegetation index                                   | EVI   | $G \times \frac{NIR-RED}{NIR-C1 \times RED-C2 \times BLUE+L}$<br>Note: C1 = 6; C2 = 7.5; L = 1; G = 2.5 | [85]       |
| Modified simple ratio                                       | MSR   | $\frac{\frac{NIR}{RED}-1}{\sqrt{\frac{NIR}{RED}+1}}$  | [86]       |
| Specific leaf area vegetation index                         | SLAVI | $\frac{NIR}{RED+SWIR}$  | [87]       |
| Soil-adjusted vegetation index                              | SAVI  | $(1+L) \times \frac{NIR-RED}{NIR+RED}$  | [88]       |
| Triangular vegetation index                                 | TVI   | $\sqrt{\frac{NIR-R}{NIR+RED}} + 0.5$  | [89]       |
| Corrected transformed vegetation index                      | CTVI  | $\frac{NDVI+0.5}{ABS(NDVI+0.5)} \times \sqrt{ABS(NDVI+0.5)}$  | [90]       |
| Transformed triangular vegetation index                     | TTVI  | $\sqrt{ABS\left(\frac{NIR-RED}{NIR+RED} + 0.5\right)}$  | [91]       |
| Ratio vegetation index                                      | RVI   | $\frac{RED}{NIR}$   | [92]       |
| Normalized ratio vegetation indexes                         | NRVI  | $\frac{RVI-1}{RVI+1}$   | [93]       |
| Infrared percentage vegetation index                        | IPVI  | $\frac{NIR}{NIR+RED}$   | [94]       |
| Optimized soil-adjusted vegetation index                    | OSAVI | $\frac{NIR-RED}{NIR+RED+Y}$<br>Y = 0.16   | [95]       |
| Normalized difference index using bands 4 & 5 of Sentinel-2 | NDI45 | $\frac{RE1-RED}{RE1+RED}$   | [96]       |
| Inverted red-edge chlorophyll index (Sentinel-2)            | IRECI | $\frac{RE3-RED}{RE1/RE2}$   | [97]       |
| Transformed normalized difference vegetation index          | TNDVI | $\sqrt{\frac{NIR-RED}{NIR+RED}} + 0.5$  | [98]       |
| Sentinel-2 red-edge position                                | S2REP | $705 + 35 \times \frac{\left(\frac{NIR-RED}{2}\right) - RE1}{RE2 - RE1}$                                | [97]       |
| Green normalized difference vegetation index                | GNDVI | $\frac{NIR-GREEN}{NIR+GREEN}$   | [99]       |
| Simple ratio  | SR    | $\frac{NIR}{RED}$   | [100]      |
| Green ratio vegetation index                                | GRVI  | $\frac{GREEN-RED}{GREEN+RED}$   | [101, 102] |
| Normalized difference water index                           | NDWI  | $\frac{NIR-SWIR}{NIR+SWIR}$   | [83, 103]  |
| Moisture stress index                                       | MSI   | $\frac{NIR}{SWIR}$  | [104]      |

**Table 2.**  
 Vegetation indices used to establish the AGB model.

in the landscape that changes reflectivity or emissivity [106]. Textural analysis techniques can be used to provide quantitative metrics that are highly sensitive to the underlying processes of change [107]. However, as the texture has many different dimensions, there is no single texture representation method that is suitable for a variety of textures. There are several methods of extracting textures from RS images; however, texture measurements based on the gray level co-occurrence matrix (GLCM) [105] is one of the most used in forest AGB estimation [64, 108]. The extraction of appropriate descriptions of texture involves selecting moving window sizes which in GLCM is a key parameter in texture analysis [106, 109]. Theoretically, variation and contrast should increase with increasing size and displacement of the window until the size of the textured objects is reached [108].

Overall, small windows produce noisier estimates of the texture descriptor and maintain a high spatial resolution, while larger windows amplify the estimation errors near spatial instances. Due to the variety of objects in an image, when estimating texture parameters should not be used a fixed window. The estimation of texture parameters should be done based on the directional invariant measures, which are the averages between the texture measures of four directions (0, 45, 90,° and 135°) [110]. There are also 8 statistical texture measures, from 14 suggested by Haralick [105], considered the most relevant for the analysis of RS images: angular second moment, contrast, variance, homogeneity, correlation, entropy, mean, and dissimilarity [64]. The information of each of these texture measures depends on the type of image to be analyzed in relation to the spectral domain, the spatial resolution and characteristics of detected objects (size, shape, and spatial distribution). In addition, when faced with a complex forest structure textural images have stronger relationships with biomass than the original spectral bands [64].

#### **4. Algorithms to predict forest AGB**

Forest AGB estimated from RS data is usually via an indirect relationship between the spectral response (original or transformed sensor bands) and AGB calculations based on field measurements, allowing an extrapolation of field data collected for larger scales [111, 112]. Different prediction methods can be applied to estimate forest AGB [52, 113]. The most used methods for forest AGB estimation are the linear and multiple regression models [114]. However, in recent years' machine learning methods, such as, random forest (RF), support vector machines (SVM) and artificial neural network (ANN) have become more prevalent [113].

Linear and multiple regression models are parametric algorithms which assumes that there is a linear relationship between both the dependent (i.e., AGB) and independent (derived from DR) variables [115]. Simple linear regression establishes a relationship between a dependent and one independent variable. If there is a relationship between two or more independent variables, the regression is called multiple linear regressions. Multiple regressions can be linear and nonlinear. This type of regression also allows to determine the relative contribution of each of the independent variables to the total explained variance and the explained variation of the model. Despite being an easy method to calculate the relationship between RS-derived variables and forest AGB, parametric algorithm is not simple global linear because it is affected by many factors (e.g., forest age, tree species, and tree height). Thus, a stepwise regression model might be applied to identify the appropriate RS-derived variables that present strong relations with forest AGB [114].

Among the existing non-parametric algorithms, only the most commonly applied to predict forest AGB estimation using RS data will be described, that is, RF, SVM and ANN [10, 52]. Non-parametric algorithms are more flexible than the parametric algorithms and create more complex models of non-linear AGB. These machine learning methods are a more reliable technique to estimate AGB [8] because do not have predefined model structures and the data determined the structure of the model.

RF is a machine learning classification and regression technique that creates a vast number of uncorrelated decision trees at training time, where the most accurate decision tree can be voted [116]. In addition, regression tree-based methods have a higher potential to identify non-linear relationships between dependent and independent variables [117]. This advantage is significant for RS-based studies, where data have shown low linear relation with AGB and the variables might be collinear [113]. RF has also the advantage of using multisource data in large study areas [10].

SVM is a machine learning algorithm that analyzes data used for classification and regression analysis [118]. This algorithm, from a set of category-identified training examples, build a model in which the new examples are attribute to one category or another. SVM constructs a linear separation rule between examples in a higher-dimensional space induced by a mapping function in training samples. This algorithm has the ability to use small data training samples to produce relatively high estimates of forest biophysical parameters using remote sensing data [10].

ANN is an important non-parametric model for forest parameter estimation [119] that simulates the associative memory as animal brain [120]. This algorithm learns by processing examples that have one or more inputs (independent variables from different data sources, such as RS and ancillary data) and known results, establishing associations by probability that will contribute to the “learning.” These associations are stored in their net data structure. After receiving several examples, the net is able to predict the results from inputs using the previously established associations. Thus, the greater the number of examples, the greater the accuracy of ANN’s predictions will be. However, the relationship between the dependent and the independent variable is not easily interpreted [10].

Accurate predictive models of forest AGB are of great importance for forest management and climate mitigation [121]. In general, there are three widely used methods of validation of forest AGB estimation. According to Lu et al. [10], the first method consists in selecting a set of sample plots through random, systematic, and stratified random sampling. The sample plots will be randomly divided into two subsets. One of the subsets will be used to train the model (e.g., 75% of subset data), while the other will be used to calibrate the model (e.g., 25% of subset data). In this case, both subsets are produced from the same sample plot which may lead to an overestimation of accuracy. The second method is cross-validation where a set of sample plots is selected using one of the first sampling previous methods. Here, a plot sample is removed while the remaining plots are used for the development of forest AGB estimation model. This method has a similar advantage to the first; however, it presents a more reliable precision assessment. The third method involves the use of an independent set of sample plots collected through a sampling design. However, despite being theoretically reliable, this method is more expensive.

These accuracy statistics are often expressed as the coefficient of determination ( $R^2$ ), a measure of how well model predictions explain the target variance of the validation set, and the root mean square error (RMSE), a frequently used measure that indicates the absolute fit of the model to the data (i.e., how close the observed data points are to the model’s predicted values). RMSE is a good measure of how accurately the model predicts the response, and it is the most important criterion for fit if the main purpose of the model is a prediction [122]. In general, a high  $R^2$  and a low RMSE value shows a good adjustment between the model developed and the sample plot data. Thus, obtaining an accurate predictive model of forest AGB estimation is important to provide valuable information to better support sustainable forest management strategies to mitigate climate change and preserve the multiple ecosystem services provided by forests.

## **5. Discussion of forest AGB estimation using RS data**

Over the past decades, there has been an improvement in satellite data from sparse coarse to medium and fine spatial resolutions, allowing better accuracy in estimating forest AGB at local, national, and global scale [69]. Recently with the launch of the Sentinel satellite family, more accurate predictive models of forest AGB estimation may be produced due to the existence of better spatial (bands with



10, 20, and 60 m) and spectral resolutions data, with a 5 days' revisit time of these satellite family in comparison with other free commercial satellite data, as Landsat or MODIS [59]. For instance, Landsat images with spatial resolution of 30 m contain many mixed pixels, and a pixel can contain different trees species and vegetation ages. In addition, large amount and good quality of field measurements, obtained from forest inventory plots data [123, 124] and/or from LiDAR data [125] should be used, as training and calibration data, to obtain accurate model of forest AGB estimation.

More recently, the studies of forest AGB estimation have been using the combination of optical and radar data. The integration of different remotely detected data sources showed to increase the accuracy of the predictive models of forest AGB estimation. In this way, the incorporation of forest structural parameters of SAR data overcome the problems of mixed pixels and data saturation caused by optical data [30, 126]. For instance, Townsend [127] observed that the model's performance for estimating biophysical properties of forests has improved due to the capabilities of the Landsat TM and SAR data. On the other hand, Forkuor et al. [44] when mapping forest AGB found better predictive accuracy of AGB when combining optical and SAR sensors (Sentinel-1 and 2) than individually. However, several authors corroborate that optical sensors produce better forest AGB estimation results than SAR when used individually [8, 44, 128] despite the lack of sensitivity of the optical data to AGB beyond the canopy closure and grass interference in savannas and forests [129, 130].

In the last years, predictive models to estimate forest AGB have been applying machine learning algorithms based on decision trees instead of the traditional parametric regression models [59]. Machine learning algorithm (e.g., ANN) showed advantage over regression algorithms for being versatile and flexible [131]. This advantage was observed by Ou et al. [132] when comparing with two parametric models (linear regression model and linear regression with combined variables), the two non-parametric models (RF and ANN) resulted in significantly greater estimation accuracies of forest AGB, that is, higher coefficient of determination ( $R^2$ ) and lower root mean square error (RMSE). Other authors corroborate with this statement by showing that non-parametric models have greater capacity to better capture the heterogeneity of forest AGB compared to parametric models [47, 64, 128, 133].

Among the variety of machine learning techniques, RF algorithm revealed to be one of the best methods for classification and regression by providing high accuracy in estimating forest AGB, high speed of computation, robustness and capacity to predict the important variables either using optical or SAR data [30, 59, 128, 134–137]. Also, RF showed to be suitable for analyzing a larger data set, while other non-parametric algorithms, such as support vector regression (SVR), are more suitable to be used with small data set [30, 47] and in grasslands and shrubs AGB estimations [138]. However, regardless of the algorithm applied to the model (e.g., linear regression, RF, and ANN), independent variables seem to be more important to obtain accurate forest AGB estimations [30].

The predictive models are able to explore and rank the variables importance measure in the forest AGB estimation. Textural features from optical data (spectral data) and SAR (backscattering data), spectral vegetation indices, and, more recently, biophysical variables derived from Sentinel-2 (e.g., LAI - Leaf area index, FVC - Fractional vegetation cover, and FAPAR - fraction of photosynthetically active radiation) have been considered as the most important variables for forest AGB estimation [30, 47, 141–145]. Spectral bands produce predictive models with lower accuracy than using vegetation indices, transformed images and textural features [132]. Therefore, Forkuor et al. [44] showed that SWIR bands are

important in predictive models of AGB estimation in semi-arid regions. In addition, the integration of variables (e.g., multispectral bands, transformed images, vegetation indices, and textural features) from optical and SAR sensors provide more accurate predictive models of forest AGB estimation [10, 52] than simple backscatter (SAR) and spectral (optical) bands [30, 47, 141, 142].

Vegetation indices are still important variables to estimate forest AGB as reported by several authors [59, 107, 134, 139, 140]. In last years, due to the Multi-Spectral Instrument aboard of the Sentinel-2 satellite, two relatively new vegetation indices, NDI45 and IRECI emerged (**Table 2**). Both new vegetation indices take advantage of the Sentinel-2 Red-edge bands (band 5 = 705 nm; band 6 = 740 nm; band 7 = 783 nm) to reduce the effects of saturation problem in high AGB density [44]. NDI45 is similar to NDVI but the original NIR band of 800 nm [84], is replaced by the new Red-edge band (band 5) and the Red band (band 4 of 665 nm) is kept [96]. On the other hand, IRECI uses the three available Red-edge bands of Sentinel-2 and put little emphasis in the red band to avoid saturation problem [97].

Transformed images, such as PCA, are also an important variable to face the saturation problem of optical sensor at low to intermediate biomass levels (between 60 and 150 Mg/ha) [146]. These images can also be used as input for textural images of optical and SAR sensors to prevent the saturation problem of high AGB density. For instance, textural variables showed to be more suitable to predict forest AGB estimation due to its ability to simplify complex cover structures, such as uneven-aged forests and different canopy structure than spectral bands [147, 148]. Also, textural bands from optical sensor images (e.g., sentinel-2, SPOT-6, and AVNIR) contributed to obtain accurate predictive models of forest AGB estimation than the original spectral bands [47, 132, 147, 149].

In addition, the greater interaction capacity of SAR-derived variables with the forest elements, such as branch, stem, and soil under the canopy [39, 65, 150], highlight their advantage over biophysical parameters (e.g., LAI, FVC, and FAPAR) to estimate forest AGB [44]. Hence, the importance of SAR long wavelengths (P-band), capable of providing accurate forest AGB estimations, will be harnessed in the BIOMASS mission to provide unprecedented information on the distribution of world's forest AGB and its changes [17, 18]. This mission will help to build a sustainable global system of monitoring and quantification of biomass over time to help countries in managing forest resources and mitigating the impacts of climate change and land use changes.

## 6. Conclusions

From the analysis of several forestry AGB estimation studies, the integration of optical and radar data improves the information extraction process, taking advantage of the strengths of different image data. In this way, mixed pixel problems and data saturation is reduced. Further, Sentinel satellite family showed to be promising free satellites data to reach accurate forest AGB estimation models, including in regions with few or scarce AGB information.

Non-parametric models, such as RF, SVM, and ANN, have been replacing regression models due to their greatest ability to capture the heterogeneity of forest AGB than parametric models. Among the variety of machine learning techniques, RF algorithm showed to be one of the most used with ability to obtain better accuracy in forest AGB estimation, either using optical or SAR data.

The integration of different data sources RS-derived, that is, spectral bands, transformed images, vegetation indices, textural features, showed good correlation with forest AGB. VNIR bands are the most important to calculate most of

vegetation indices. When using Sentinel-2 data, the available red-edge bands showed to reduce the effects of saturation problem in high AGB density.

PCA is a key variable to face the saturation problem of optical sensor of high AGB density and to be used as input data for textural features of optical and SAR sensors also to prevent the saturation problem of both sensors. Textural features, from both optical and SAR sensors, are among of the most suitable variables for forest AGB estimation due to their stronger relationships with AGB. SAR long wavelengths bands (L and P) showed to be very promising bands in studies of relatively high biomass density.

## **Acknowledgements**

This work is funded by the National Funds through FCT - Foundation for Science and Technology under the Project UIDB/05183/2020 and by Programa Operativo de Cooperação Transfronteiriço Espanha-Portugal (POCTEP), and Programa INTERREG V A Espanha – Project IDERCEXA – Investigación, Desarrollo y Energías Renovables para nuevos modelos empresariales en Centro, Extremadura y Alentejo, 0330\_IDERCEXA\_4\_E.

## **Author details**

Patrícia Lourenço<sup>1,2,3</sup>

1 MED - Mediterranean Institute for Agriculture, Environment and Development and Departamento de Engenharia Rural, Escola Ciências e Tecnologia, Universidade de Évora, Pólo da Mitra, Évora, Portugal


2 Research Center on Geo-Spatial Science, Faculty of Science of the University of Porto (CICGE), Vila Nova de Gaia, Portugal

3 Andalusian Center for the Evaluation and Monitoring of Global Change, University of Almeria (CAESCG), Almería, Spain

\*Address all correspondence to: pmrlourencov2@gmail.com

## **IntechOpen**

---

© 2020 The Author(s). Licensee IntechOpen. Distributed under the terms of the Creative Commons Attribution - NonCommercial 4.0 License (<https://creativecommons.org/licenses/by-nc/4.0/>), which permits use, distribution and reproduction for non-commercial purposes, provided the original is properly cited. 

## References

- [1] Brown S. Estimating Biomass and Biomass Change of Tropical Forests: A Primer. Rome: Food & Agriculture Org; 1997
- [2] Brown S, Schroeder P, Birdsey R. Aboveground biomass distribution of US eastern hardwood forests and the use of large trees as an indicator of forest development. *Forest Ecology and Management*. 1997;**96**:37-47
- [3] Qureshi A, Badola R, Hussain SA. A review of protocols used for assessment of carbon stock in forested landscapes. *Environmental Science & Policy*. 2012; **16**:81-89
- [4] Sessa R, Dolman H. Terrestrial Essential Climate Variables for Climate Change Assessment, Mitigation and Adaptation. Rome: FAO GTOS; 2008. p. 52
- [5] Wang X, Shao G, Chen H, et al. An application of remote sensing data in mapping landscape-level forest biomass for monitoring the effectiveness of forest policies in northeastern China. *Environmental Management*. 2013;**52**: 612-620
- [6] Kumar L, Mutanga O. Remote sensing of above-ground biomass. *Remote Sensing*. 2017;**9**:935
- [7] FTP. Horizons - Vision 2030 for the European Forest-Based Sector. Forest-Based Sector Technology Platform. Brussels. 2013. pp. 1-10. Available from: [www.forestplatform.org](http://www.forestplatform.org)
- [8] Vafaei S, Soosani J, Adeli K, et al. Improving accuracy estimation of Forest aboveground biomass based on incorporation of ALOS-2 PALSAR-2 and sentinel-2A imagery and machine learning: A case study of the Hyrcanian forest area (Iran). *Remote Sensing*. 2018;**10**:172
- [9] Pan Y, Birdsey RA, Fang J, et al. A large and persistent carbon sink in the world's forests. *Science*. 2011;**333**:988-993
- [10] Lu D, Chen Q, Wang G, et al. A survey of remote sensing-based aboveground biomass estimation methods in forest ecosystems. *International Journal of Digital Earth*. 2016;**9**:63-105
- [11] Sousa AM, Gonçalves AC, Marques da Silva JR. Above Ground Biomass Estimation with High Spatial Resolution Satellite Images. *Biomass Volume Estimation and Valorization for Energy*. Rijeka: InTech; 2017. pp. 47-70
- [12] Fehrmann L, Kleinn C. General considerations about the use of allometric equations for biomass estimation on the example of Norway spruce in Central Europe. *Forest Ecology and Management*. 2006;**236**: 412-421
- [13] Eisfelder C, Kuenzer C, Dech S. Derivation of biomass information for semi-arid areas using remote-sensing data. *International Journal of Remote Sensing*. 2012;**33**:2937-2984
- [14] Gil A, Fonseca C, Benedicto-Royuela J. Land cover trade-offs in small Oceanic Islands: A temporal analysis of Pico Island, Azores. *Land Degradation & Development*. 2018;**29**:349-360
- [15] Baccini A, Laporte N, Goetz SJ, et al. A first map of tropical Africa's above-ground biomass derived from satellite imagery. *Environmental Research Letters*. 2008;**3**:045011
- [16] ESA. Biomass. Report for Mission Selection. An Earth Explorer to Observe Forest Biomass. Noordwijk, The Netherlands: SP-1324/1. European Space Agency; 2012

- [17] Le Toan T, Quegan S, Davidson MWJ, et al. The BIOMASS mission: Mapping global forest biomass to better understand the terrestrial carbon cycle. *Remote Sensing of Environment*. 2011;**115**:2850-2860
- [18] Carreiras JM, Quegan S, Le Toan T, et al. Coverage of high biomass forests by the ESA BIOMASS mission under defense restrictions. *Remote Sensing of Environment*. 2017;**196**:154-162
- [19] Sani DA, Hashim M, Hossain MS. Recent advancement on estimation of blue carbon biomass using satellite-based approach. *International Journal of Remote Sensing*. 2019;**40**:7679-7715
- [20] Kumar L, Sinha P, Taylor S, et al. Review of the use of remote sensing for biomass estimation to support renewable energy generation. *Journal of Applied Remote Sensing*. 2015;**9**:097696
- [21] Cavender-Bares J, Gamon JA, Townsend PA. *Remote Sensing of Plant Biodiversity*. Switzerland: Springer; 2020
- [22] Blackard JA, Finco MV, Helmer EH, et al. Mapping US forest biomass using nationwide forest inventory data and moderate resolution information. *Remote Sensing of Environment*. 2008;**112**:1658-1677
- [23] García M, Riaño D, Chuvieco E, et al. Estimating biomass carbon stocks for a Mediterranean forest in Central Spain using LiDAR height and intensity data. *Remote Sensing of Environment*. 2010;**114**:816-830
- [24] Los Soriano-Luna MDÁ, Ángeles-Pérez G, Guevara M, et al. Determinants of above-ground biomass and its spatial variability in a temperate Forest managed for timber production. *Forests*. 2018;**9**:490
- [25] Macedo FL, Sousa AM, Gonçalves AC, et al. Above-ground biomass estimation for *Quercus rotundifolia* using vegetation indices derived from high spatial resolution satellite images. *European Journal of Remote Sensing*. 2018;**51**:932-944
- [26] Pandit S, Tsuyuki S, Dube T. Estimating above-ground biomass in sub-tropical buffer zone community forests, Nepal, using sentinel 2 data. *Remote Sensing*. 2018;**10**:601
- [27] Stelmaszczuk-Górska M, Urbazaev M, Schmillius C, et al. Estimation of above-ground biomass over boreal forests in Siberia using updated In situ, ALOS-2 PALSAR-2, and RADARSAT-2 data. *Remote Sensing*. 2018;**10**:1550
- [28] Lu D, Weng Q. Spectral mixture analysis of the urban landscape in Indianapolis with Landsat ETM+ imagery. *Photogrammetric Engineering & Remote Sensing*. 2004;**70**:1053-1062
- [29] Nichol JE, Sarker MLR. Improved biomass estimation using the texture parameters of two high-resolution optical sensors. *IEEE Transactions on Geoscience and Remote Sensing*. 2011;**49**:930-948
- [30] Chen L, Wang Y, Ren C, et al. Optimal combination of predictors and algorithms for forest above-ground biomass mapping from sentinel and SRTM data. *Remote Sensing*. 2019;**11**: 414
- [31] Gómez C, Wulder MA, Montes F, et al. Modeling forest structural parameters in the Mediterranean pines of Central Spain using QuickBird-2 imagery and classification and regression tree analysis (CART). *Remote Sensing*. 2012;**4**:135-159
- [32] Marshall M, Thenkabail P. Advantage of hyperspectral EO-1 Hyperion over multispectral IKONOS, GeoEye-1, WorldView-2, Landsat ETM+, and MODIS vegetation indices in crop

- biomass estimation. *ISPRS Journal of Photogrammetry and Remote Sensing*. 2015;**108**:205-218
- [33] Avitabile V, Baccini A, Friedl MA, et al. Capabilities and limitations of Landsat and land cover data for aboveground woody biomass estimation of Uganda. *Remote Sensing of Environment*. 2012;**117**:366-380
- [34] Sinha S, Jeganathan C, Sharma LK, et al. A review of radar remote sensing for biomass estimation. *International journal of Environmental Science and Technology*. 2015;**12**:1779-1792
- [35] Kasischke ES, Melack JM, Dobson MC. The use of imaging radars for ecological applications—A review. *Remote Sensing of Environment*. 1997;**59**:141-156
- [36] Sandberg G, Ulander LM, Fransson JE, et al. L- and P-band backscatter intensity for biomass retrieval in hemiboreal forest. *Remote Sensing of Environment*. 2011;**115**:2874-2886
- [37] Balzter H, Rowland CS, Saich P. Forest canopy height and carbon estimation at Monks Wood National Nature Reserve, UK, using dual-wavelength SAR interferometry. *Remote Sensing of Environment*. 2007;**108**:224-239
- [38] Le Toan T, Beaudoin A, Riom J, et al. Relating forest biomass to SAR data. *IEEE Transactions on Geoscience and Remote Sensing*. 1992;**30**:403-411
- [39] Carreiras JMB, Vasconcelos MJ, Lucas RM. Understanding the relationship between aboveground biomass and ALOS PALSAR data in the forests of Guinea-Bissau (West Africa). *Remote Sensing of Environment*. 2012;**121**:426-442
- [40] Zebker HA, Van Zyl JJ, Held DN. Imaging radar polarimetry from wave synthesis. *Journal of Geophysical Research - Solid Earth*. 1987;**92**:683-701
- [41] Carreiras J, Melo JB, Vasconcelos MJ. Estimating the above-ground biomass in miombo savanna woodlands (Mozambique, East Africa) using L-band synthetic aperture radar data. *Remote Sensing*. 2013;**5**:1524-1548
- [42] Liu Y, Gong W, Xing Y, et al. Estimation of the forest stand mean height and aboveground biomass in Northeast China using SAR sentinel-1B, multispectral sentinel-2A, and DEM imagery. *ISPRS Journal of Photogrammetry and Remote Sensing*. 2019;**151**:277-289
- [43] Enghart S, Franke J, Keuck V, et al. Aboveground biomass estimation of tropical peat swamp forests using SAR and optical data. In: 2012 IEEE International Geoscience and Remote Sensing Symposium. IEEE; 2012. pp. 6577-6580
- [44] Forkuor G, Zougrana J-BB, Dimobe K, et al. Above-ground biomass mapping in West African dryland forest using Sentinel-1 and 2 datasets-A case study. *Remote Sensing of Environment*. 2020;**236**:111496
- [45] Ghasemi N, Sahebi MR, Mohammadzadeh A. Biomass estimation of a temperate deciduous forest using wavelet analysis. *IEEE Transactions on Geoscience and Remote Sensing*. 2012;**51**:765-776
- [46] Hayashi M, Motohka T, Sawada Y. Aboveground biomass mapping using ALOS-2/PALSAR-2 time-series images for Borneo's Forest. *IEEE Journal of Selected Topics in Applied Earth Observations and Remote Sensing*. 2019;**12**(12):5167-5177
- [47] Morin D, Planells M, Guyon D, et al. Estimation and mapping of Forest structure parameters from open access satellite images: Development of a generic method with a study case on coniferous plantation. *Remote Sensing*. 2019;**11**:1275

- [48] Peregon A, Yamagata Y. The use of ALOS/PALSAR backscatter to estimate above-ground forest biomass: A case study in Western Siberia. *Remote Sensing of Environment*. 2013;**137**:139-146
- [49] Chen Q, Qi C. Lidar remote sensing of vegetation biomass. *Remote Sensing of Natural Resources*. 2013;**399**:399-420
- [50] Lucas R, Armston J, Fairfax R, et al. An evaluation of the ALOS PALSAR L-band backscatter—Above ground biomass relationship Queensland, Australia: Impacts of surface moisture condition and vegetation structure. *IEEE Journal of Selected Topics in Applied Earth Observations and Remote Sensing*. 2010;**3**:576-593
- [51] Enghart S, Keuck V, Siegert F. Aboveground biomass retrieval in tropical forests—The potential of combined X-and L-band SAR data use. *Remote Sensing of Environment*. 2011;**115**:1260-1271
- [52] Lu D. The potential and challenge of remote sensing-based biomass estimation. *International Journal of Remote Sensing*. 2006;**27**:1297-1328
- [53] Li G, Lu D, Moran E, et al. A comparative analysis of ALOS PALSAR L-band and RADARSAT-2 C-band data for land-cover classification in a tropical moist region. *ISPRS Journal of Photogrammetry and Remote Sensing*. 2012;**70**:26-38
- [54] Côté J-F, Fournier RA, Egli R. An architectural model of trees to estimate forest structural attributes using terrestrial LiDAR. *Environmental Modelling & Software*. 2011;**26**:761-777
- [55] Means JE, Acker SA, Harding DJ, et al. Use of large-footprint scanning airborne lidar to estimate forest stand characteristics in the Western cascades of Oregon. *Remote Sensing of Environment*. 1999;**67**:298-308
- [56] Maltamo M, Næsset E, Vauhkonen J. Forestry applications of airborne laser scanning. *Concepts, Methodologies and Case Studies*. 2014;**27**:460
- [57] Popescu SC, Wynne RH, Nelson RF. Measuring individual tree crown diameter with lidar and assessing its influence on estimating forest volume and biomass. *Canadian Journal of Remote Sensing*. 2003;**29**:564-577
- [58] Urbazaev M, Thiel C, Cremer F, et al. Estimation of forest aboveground biomass and uncertainties by integration of field measurements, airborne LiDAR, and SAR and optical satellite data in Mexico. *Carbon Balance and Management*. 2018;**13**:5
- [59] Ghosh SM, Behera MD. Aboveground biomass estimation using multi-sensor data synergy and machine learning algorithms in a dense tropical forest. *Applied Geography*. 2018;**96**: 29-40
- [60] Kattenborn T, Maack J, Snacht F, et al. Mapping forest biomass from space—fusion of hyperspectral EO1-hyperion data and Tandem-X and WorldView-2 canopy height models. *International Journal of Applied Earth Observation and Geoinformation*. 2015;**35**:359-367
- [61] Kellndorfer JM, Walker WS, LaPoint E, et al. Statistical fusion of Lidar, InSAR, and optical remote sensing data for forest stand height characterization: A regional-scale method based on LVIS, SRTM, Landsat ETM+, and ancillary data sets. *Journal of Geophysical Research – Biogeosciences*. 2010;**115**(G00E08)
- [62] Sun G, Ranson KJ, Guo Z, et al. Forest biomass mapping from lidar and radar synergies. *Remote Sensing of Environment*. 2011;**115**:2906-2916
- [63] Zheng D, Rademacher J, Chen J, et al. Estimating aboveground biomass

using Landsat 7 ETM+ data across a managed landscape in northern Wisconsin, USA. *Remote Sensing of Environment*. 2004;**93**:402-411

[64] Lu D, Batistella M. Exploring TM image texture and its relationships with biomass estimation in Rondônia, Brazilian Amazon. *Acta Amazonica*. 2005;**35**:249-257

[65] Mitchard ET, Saatchi SS, Lewis SL, et al. Measuring biomass changes due to woody encroachment and deforestation/degradation in a forest-savanna boundary region of Central Africa using multi-temporal L-band radar backscatter. *Remote Sensing of Environment*. 2011;**115**:2861-2873

[66] Saatchi S, Marlier M, Chazdon RL, et al. Impact of spatial variability of tropical forest structure on radar estimation of aboveground biomass. *Remote Sensing of Environment*. 2011;**115**:2836-2849

[67] Sarker MLR, Nichol J, Ahmad B, et al. Potential of texture measurements of two-date dual polarization PALSAR data for the improvement of forest biomass estimation. *ISPRS Journal of Photogrammetry and Remote Sensing*. 2012;**69**:146-166

[68] Popescu SC, Zhao K, Neuschwander A, et al. Satellite lidar vs. small footprint airborne lidar: Comparing the accuracy of aboveground biomass estimates and forest structure metrics at footprint level. *Remote Sensing of Environment*. 2011;**115**:2786-2797

[69] Chao Z, Liu N, Zhang P, et al. Estimation methods developing with remote sensing information for energy crop biomass: A comparative review. *Biomass and Bioenergy*. 2019;**122**:414-425

[70] Lillesand T, Kiefer RW, Chipman J. *Remote Sensing and Image Interpretation*. New York: John Wiley & Sons; 2014

[71] Deng JS, Wang K, Deng YH, et al. PCA-based land-use change detection and analysis using multitemporal and multisensor satellite data. *International Journal of Remote Sensing*. 2008;**29**: 4823-4838

[72] Boardman JW, Kruse FA. Automated spectral analysis: A geological example using AVIRIS data, north Grapevine Mountains, Nevada. In: *Proceedings, ERIM Tenth Thematic Conference on Geologic Remote Sensing*. Ann Arbor, MI: Environmental Research Institute of Michigan; 1994. pp. I-407-I-418

[73] Green AA, Berman M, Switzer P, et al. A transformation for ordering multispectral data in terms of image quality with implications for noise removal. *IEEE Transactions on Geoscience and Remote Sensing*. 1988; **26**:65-74

[74] De Jong SM, Pebesma EJ, Lacaze B. Above-ground biomass assessment of Mediterranean forests using airborne imaging spectrometry: The DAIS Payne experiment. *International Journal of Remote Sensing*. 2003;**24**:1505-1520

[75] Kauth RJ, Thomas GS. The tasseled cap—a graphic description of the spectral-temporal development of agricultural crops as seen by Landsat. In: *LARS symposia*. 1976. p. 159

[76] Baig MHA, Zhang L, Shuai T, et al. Derivation of a tasseled cap transformation based on Landsat 8 at-satellite reflectance. *Remote Sensing Letters*. 2014;**5**:423-431

[77] Zhang X, Schaaf CB, Friedl MA, et al. MODIS tasseled cap transformation and its utility. In: *IEEE International Geoscience and Remote Sensing Symposium*. IEEE; 2002. pp. 1063-1065

[78] Crist EP, Kauth RJ. The Tasseled Cap de-mystified. *Photogrammetric*



- Engineering and Remote Sensing. 1986; 52(1):81-86
- [79] Ustin SL, Roberts DA, Gamon JA, et al. Using imaging spectroscopy to study ecosystem processes and properties. *Bioscience*. 2004;54:523-534
- [80] Myneni RB, Hall FG, Sellers PJ, et al. The interpretation of spectral vegetation indexes. *IEEE Transactions on Geoscience and Remote Sensing*. 1995;33:481-486
- [81] Jordan CF. Derivation of leaf-area index from quality of light on the forest floor. *Ecology*. 1969;50:663-666
- [82] Carreiras JM, Pereira JM, Pereira JS. Estimation of tree canopy cover in evergreen oak woodlands using remote sensing. *Forest Ecology and Management*. 2006;223:45-53
- [83] Gao B-C. NDWI—A normalized difference water index for remote sensing of vegetation liquid water from space. *Remote Sensing of Environment*. 1996;58:257-266
- [84] Rouse JW, Haas RH, Schell JA, et al. Monitoring Vegetation Systems in the Great Plains with ERTS. In: *Third ERTS Symposium, NASA SP-351*. Washington DC. 1974. pp. 309-317
- [85] Huete A, Didan K, Miura T, et al. Overview of the radiometric and biophysical performance of the MODIS vegetation indices. *Remote Sensing of Environment*. 2002;83:195-213
- [86] Chen JM. Evaluation of vegetation indices and a modified simple ratio for boreal applications. *Canadian Journal of Remote Sensing*. 1996;22:229-242
- [87] Lymburner L, Beggs PJ, Jacobson CR. Estimation of canopy-average surface-specific leaf area using Landsat TM data. *Photogrammetric Engineering and Remote Sensing*. 2000;66:183-192
- [88] Huete A, Huete AR. A soil-adjusted vegetation index (SAVI). *Remote Sensing of Environment*. 1988;25: 295-309
- [89] Deering DW. Measuring “forage production” of grazing units from Landsat MSS data. In: *Proceedings of the Tenth International Symposium of Remote Sensing of the Environment*. 1975. pp. 1169-1198
- [90] Perry CR Jr, Lautenschlager LF. Functional equivalence of spectral vegetation indices. *Remote Sensing of Environment*. 1984;14:169-182
- [91] Thiam AK. *Geographic Information Systems and Remote Sensing Methods for Assessing and Monitoring Land Degradation in the Sahel Region: The Case of Southern Mauritania*. Ph.D. dissertation. Worcester, Mass: Clark University; 1998
- [92] Richardson AJ, Wiegand CL. Distinguishing vegetation from soil background information. *Photogrammetric Engineering and Remote Sensing*. 1977;43:1541-1552
- [93] Baret F, Guyot G. Potentials and limits of vegetation indices for LAI and APAR assessment. *Remote Sensing of Environment*. 1991;35:161-173
- [94] Crippen RE. Calculating the vegetation index faster. *Remote Sensing of Environment*. 1990;34:71-73
- [95] Rondeaux G, Steven M, Baret F. Optimization of soil-adjusted vegetation indices. *Remote Sensing of Environment*. 1996;55:95-107
- [96] Delegido J, Verrelst J, Alonso L, et al. Evaluation of sentinel-2 red-edge bands for empirical estimation of green LAI and chlorophyll content. *Sensors*. 2011;11:7063-7081
- [97] Frampton WJ, Dash J, Watmough G, et al. Evaluating the

capabilities of Sentinel-2 for quantitative estimation of biophysical variables in vegetation. *ISPRS Journal of Photogrammetry and Remote Sensing*. 2013;**82**:83-92

[98] Zhou X, Dandan L, Huiming Y, et al. Use of landsat TM satellite surveillance data to measure the impact of the 1998 flood on snail intermediate host dispersal in the lower Yangtze River basin. *Acta Tropica*. 2002;**82**:199-205

[99] Gitelson AA, Kaufman YJ, Merzlyak MN. Use of a green channel in remote sensing of global vegetation from EOS-MODIS. *Remote Sensing of Environment*. 1996;**58**:289-298

[100] Birth GS, McVey GR. Measuring the color of growing turf with a reflectance spectrophotometer 1. *Agronomy Journal*. 1968;**60**:640-643

[101] Falkowski MJ, Gessler PE, Morgan P, et al. Characterizing and mapping forest fire fuels using ASTER imagery and gradient modeling. *Forest Ecology and Management*. 2005;**217**: 129-146

[102] Motohka T, Nasahara KN, Oguma H, et al. Applicability of green-red vegetation index for remote sensing of vegetation phenology. *Remote Sensing*. 2010;**2**:2369-2387

[103] Hardisky MA, Klemas V, Smart M. The influence of soil salinity, growth form, and leaf moisture on the spectral radiance of *Spartina alterniflora* canopies. *Photogrammetric Engineering and Remote Sensing*. 1983;**49**(1):77-83

[104] Hunt ER Jr, Rock BN. Detection of changes in leaf water content using near-and middle-infrared reflectances. *Remote Sensing of Environment*. 1989; **30**:43-54

[105] Haralick RM, Shanmugam KS, Dinstein I. Textural features for image classification. *IEEE Transactions on*

*Systems, Man, and Cybernetics*. 1973;**3**: 610-621

[106] Lu D. Aboveground biomass estimation using Landsat TM data in the Brazilian Amazon. *International Journal of Remote Sensing*. 2005;**26**:2509-2525

[107] Dube T, Mutanga O. Evaluating the utility of the medium-spatial resolution Landsat 8 multispectral sensor in quantifying aboveground biomass in uMgeni catchment, South Africa. *ISPRS Journal of Photogrammetry and Remote Sensing*. 2015;**101**:36-46

[108] Kayitakire F, Hamel C, Defourny P. Retrieving forest structure variables based on image texture analysis and IKONOS-2 imagery. *Remote Sensing of Environment*. 2006; **102**:390-401

[109] Chen D, Stow DA, Gong P. Examining the effect of spatial resolution and texture window size on classification accuracy: An urban environment case. *International Journal of Remote Sensing*. 2004;**25**:2177-2192

[110] Nyoungui AN, Tonye E, Akono A. Evaluation of speckle filtering and texture analysis methods for land cover classification from SAR images. *International Journal of Remote Sensing*. 2002;**23**:1895-1925

[111] Baccini A, Goetz SJ, Walker WS, et al. Estimated carbon dioxide emissions from tropical deforestation improved by carbon-density maps. *Nature Climate Change*. 2012;**2**:182

[112] Saatchi SS, Harris NL, Brown S, et al. Benchmark map of forest carbon stocks in tropical regions across three continents. *Proceedings of the National Academy of Sciences*. 2011;**108**:9899-9904

[113] Fassnacht FE, Hartig F, Latifi H, et al. Importance of sample size, data type and prediction method for remote sensing-based estimations of

- aboveground forest biomass. *Remote Sensing of Environment*. 2014;**154**: 102-114
- [114] Lu D, Chen Q, Wang G, et al. Aboveground forest biomass estimation with Landsat and LiDAR data and uncertainty analysis of the estimates. *International Journal of Forestry Research*. 2012;**2012**:1-16
- [115] Liu K, Wang J, Zeng W, et al. Comparison and evaluation of three methods for estimating forest above ground biomass using TM and GLAS data. *Remote Sensing*. 2017;**9**:341
- [116] Breiman L. Random forests. *Machine Learning*. 2001;**45**:5-32
- [117] Guisan A, Edwards TC Jr, Hastie T. Generalized linear and generalized additive models in studies of species distributions: Setting the scene. *Ecological Modelling*. 2002;**157**:89-100
- [118] Vapnik VN. *The Nature of Statistical Learning Theory*. Berlin: Springer Science & Business Media; 1999
- [119] Foody GM, Cutler ME, McMorrow J, et al. Mapping the biomass of Bornean tropical rain forest from remotely sensed data. *Global Ecology and Biogeography*. 2001;**10**:379-387
- [120] Willis MJ, Di Massimo C, Montague GA, et al. Artificial neural networks in process engineering. In: *IEE Proceedings D (Control Theory and Applications)*. IET; 1991. pp. 256-266
- [121] Chen W, Chen J, Liu J, et al. Approaches for reducing uncertainties in regional forest carbon balance. *Global Biogeochemical Cycles*. 2000;**14**: 827-838
- [122] Willmott CJ, Matsuura K. Advantages of the mean absolute error (MAE) over the root mean square error (RMSE) in assessing average model performance. *Climate Research*. 2005; **30**:79-82
- [123] Deo RK, Russell MB, Domke GM, et al. Using Landsat time-series and LiDAR to inform aboveground forest biomass baselines in northern Minnesota, USA. *Canadian Journal of Remote Sensing*. 2017;**43**:28-47
- [124] Kennedy RE, Ohmann J, Gregory M, et al. An empirical, integrated forest biomass monitoring system. *Environmental Research Letters*. 2018;**13**:025004
- [125] Matasci G, Hermosilla T, Wulder MA, et al. Three decades of forest structural dynamics over Canada's forested ecosystems using Landsat time-series and lidar plots. *Remote Sensing of Environment*. 2018;**216**:697-714
- [126] Navarro JA, Algeet N, Fernández-Landa A, et al. Integration of uav, sentinel-1, and sentinel-2 data for mangrove plantation aboveground biomass monitoring in Senegal. *Remote Sensing*. 2019;**11**:77
- [127] Townsend PA. Estimating forest structure in wetlands using multitemporal SAR. *Remote Sensing of Environment*. 2002;**79**:288-304
- [128] Zhao P, Lu D, Wang G, et al. Forest aboveground biomass estimation in Zhejiang Province using the integration of Landsat TM and ALOS PALSAR data. *International Journal of Applied Earth Observation and Geoinformation*. 2016; **53**:1-15
- [129] Naidoo L, Mathieu R, Main R, et al. L-band synthetic aperture radar imagery performs better than optical datasets at retrieving woody fractional cover in deciduous, dry savannahs. *International Journal of Applied Earth Observation and Geoinformation*. 2016;**52**:54-64
- [130] Zeidler J, Wegmann M, Dech S. Spatio-temporal robustness of fractional

cover upscaling: A case study in semi-arid Savannah's of Namibia and Western Zambia. In: *Earth Resources and Environmental Remote Sensing/GIS Applications III*. International Society for Optics and Photonics; 2012. p. 85380S

[131] Ali I, Greifeneder F, Stamenkovic J, et al. Review of machine learning approaches for biomass and soil moisture retrievals from remote sensing data. *Remote Sensing*. 2015;7: 16398-16421

[132] Ou G, Li C, Lv Y, et al. Improving aboveground biomass estimation of *Pinus densata* forests in Yunnan using Landsat 8 imagery by incorporating age dummy variable and method comparison. *Remote Sensing*. 2019;11: 738

[133] Pflugmacher D, Cohen WB, Kennedy RE, et al. Using Landsat-derived disturbance and recovery history and lidar to map forest biomass dynamics. *Remote Sensing of Environment*. 2014;151:124-137

[134] Liu Y, Liu S, Li J, et al. Estimating biomass of winter oilseed rape using vegetation indices and texture metrics derived from UAV multispectral images. *Computers and Electronics in Agriculture*. 2019;166:105026

[135] Freeman EA, Moisen GG, Coulston JW, et al. Random forests and stochastic gradient boosting for predicting tree canopy cover: Comparing tuning processes and model performance. *Canadian Journal of Forest Research*. 2016;46:323-339

[136] Nguyen TH, Jones SD, Soto-Berelov M, et al. Monitoring aboveground forest biomass dynamics over three decades using Landsat time-series and single-date inventory data. *International Journal of Applied Earth Observation and Geoinformation*. 2020; 84:101952

[137] Belgiu M, Drăguț L. Random forest in remote sensing: A review of applications and future directions. *ISPRS Journal of Photogrammetry and Remote Sensing*. 2016;114:24-31

[138] Li B, Wang W, Bai L, et al. Estimation of aboveground vegetation biomass based on Landsat-8 OLI satellite images in the Guanzhong Basin, China. *International Journal of Remote Sensing*. 2019;40:3927-3947

[139] Zhu X, Liu D. Improving forest aboveground biomass estimation using seasonal Landsat NDVI time-series. *ISPRS Journal of Photogrammetry and Remote Sensing*. 2015;102:222-231

[140] Sousa AM, Gonçalves AC, Mesquita P, et al. Biomass estimation with high resolution satellite images: A case study of *Quercus rotundifolia*. *ISPRS Journal of Photogrammetry and Remote Sensing*. 2015;101:69-79

[141] Debastiani AB, Sanquetta CR, Dalla Corte AP, et al. Evaluating SAR-optical sensor fusion for aboveground biomass estimation in a Brazilian tropical forest. *Annals of Forest Research*. 2019;62: 109-122

[142] Laurin GV, Balling J, Corona P, et al. Above-ground biomass prediction by Sentinel-1 multitemporal data in Central Italy with integration of ALOS2 and Sentinel-2 data. *Journal of Applied Remote Sensing*. 2018;12:016008

[143] Godinho S, Guiomar N, Gil A. Estimating tree canopy cover percentage in a mediterranean silvopastoral systems using sentinel-2A imagery and the stochastic gradient boosting algorithm. *International Journal of Remote Sensing*. 2018;39: 4640-4662

[144] Eckert S. Improved forest biomass and carbon estimations using texture measures from WorldView-2 satellite data. *Remote Sensing*. 2012;4:810-829

[145] Rao PN, Sai MS, Sreenivas K, et al. Textural analysis of IRS-1D panchromatic data for land cover classification. *International Journal of Remote Sensing*. 2002;**23**:3327-3345

[146] Fayad I, Baghdadi N, Bailly J-S, et al. Canopy height estimation in French Guiana with LiDAR ICESat/GLAS data using principal component analysis and random forest regressions. *Remote Sensing*. 2014;**6**:11883-11914

[147] Hlatshwayo ST, Mutanga O, Lottering RT, et al. Mapping forest aboveground biomass in the reforested Buffelsdraai landfill site using texture combinations computed from SPOT-6 pan-sharpened imagery. *International Journal of Applied Earth Observation and Geoinformation*. 2019;**74**:65-77

[148] Wulder M. Optical remote-sensing techniques for the assessment of forest inventory and biophysical parameters. *Progress in Physical Geography*. 1998; **22**:449-476

[149] Sarker LR, Nichol JE. Improved forest biomass estimates using ALOS AVNIR-2 texture indices. *Remote Sensing of Environment*. 2011;**115**: 968-977

[150] Patenaude G, Milne R, Dawson TP. Synthesis of remote sensing approaches for forest carbon estimation: Reporting to the Kyoto protocol. *Environmental Science & Policy*. 2005;**8**:161-178

# Management of Maritime Pine: Energetic Potential with Alternative Silvicultural Guidelines

*Teresa Fonseca and José Lousada*

## Abstract

The interest in the use of energy of the forests has been increasing in recent decades. Biomass has the potential to provide a cost-effective and sustainable supply of renewable energy. Moreover, it could be valuable for reducing the severity of forest fires and create employment in extremely needy regions. This chapter brings to discuss the effect of forest management on the potential of energy provided by the woodlands. The authors selected as a case study the management of maritime pine (*Pinus pinaster* Ait.), an important softwood species in the southwest of Europe and, in particular, in Portugal where it represents around 22% of the forest area. A summary of traditional and new silvicultural guidelines for the species, used or proposed to be followed at the national level, is presented. The study follows with the evaluation of stand yield and the potential of energy associated with four alternative silvicultural guidelines. Two scenarios follow traditional standards (an initial density of 1100–1200 trees/ha), while the other two consider managing a high density stand (an initial density of 40,000 trees/ha). Simulations were performed with the ModisPinaster model. The results show that the new designs provide a considerable yield in terms of biomass and energy.

**Keywords:** forest management, regeneration, thinning, fire, biomass, energy, CAPSIS

## 1. Introduction

The Portuguese forest occupies an area of 3224.2 thousand hectares, which represents around 36.2% the mainland area according to the Sixth National Forest Inventory (IFN6) report [1]. The major part of the forest areas (63.7%) refers to hardwood species in pure stands (mainly *Quercus* sp. and *Eucalyptus* sp.), followed by pure stands of softwood species (23.1%). Mixtures are less common occupying around 13%. Among the softwood species, maritime pine (*Pinus pinaster* Ait.) is the most represented species, covering an area of 713.3 thousand hectares, with a growing stock of 67 Mm<sup>3</sup> [1]. The species is of great economic importance in the country. The pine sector represents 52% of the gross value added (GVA) and 46% of the turnover of forestry industries and accounts for 35% of the forest industry's exports of goods. Wood consumption amounted to 4.2 Mm<sup>3</sup> in 2018, representing

an increase in around 10% compared to 2017 [2]. Primary use ranked by descending order according to consumption level is sawmill, pellets, panels, pulp and paper, poles, and pilings [2], and since 2016, the annual production of pellets in Portugal exceeds 1.4 million tons [3].

The impact of pests (the most significant being the nematode) and fire has contributed to a severe reduction in the area occupied with maritime pine forests with time. It is worthwhile to mention a decrease in 134.7 thousand hectares just from 2015 to 2018 [1] due to the impact of severe forest fires occurring in this recent period. The same source refers that the growing volume, potentially affected by the fires between 2016 and 2018, is 15.6 Mm<sup>3</sup>.

The recurrent menace of forest fire risk in Portugal, coupled to an increase in consumption of pinewood for a diversity of uses, has been driving for a new vision of forest management for these forests.

In the past, the use of shrubs and forest residues was extremely low, being limited to small domestic uses, without any representativeness at the industrial level. However, in recent years, due to the growing awareness of the use of natural, renewable, and sustainable energy sources, there has been a high pressure for the use of forest biomass for energy purposes. It is in this context that the need arises to discuss and test new types of silvicultural management that allows exploiting not only the woody component but also the forest residues and shrubs, to increase the profitability of the forest and decrease its susceptibility to fire.

In this chapter, a summary of traditional and new silvicultural guidelines for the species used or proposed to be followed at the national level is presented. The authors proceed with the evaluation of total biomass and the potential of energy for a set of four silvicultural models through simulation. Simulation of stand development was performed with the simulator ModisPinaster [4, 5].

Two of the models (Scenarios 1 and 2) follow the traditional standards of stand establishment (plantation or direct seeding) and management. The other models (Scenarios 3 and 4) are driven by the increase of forest areas with natural regeneration regenerated post-fire and the demand for the wood of small size, with higher densities at the establishment than the traditional standards. Results will provide valuable information for forest planning and decision support to forest managers of pine forest systems.

## **2. An overall view of the silvicultural guidelines for maritime pine in Portugal**

### **2.1 Silviculture guidelines in traditional roundwood-oriented management**

In Portugal, maritime pine traditionally develops in pure stands, with mixtures (e.g., with *Eucalyptus* sp., *Castanea sativa*, or *Quercus suber*) being less frequent [1].

The traditional silvicultural guidelines for the species consider the use of artificial regeneration by seeding or by plantation. For plantations and direct seeding, initial densities differ among the silvicultural models, ranging from around 1100 to 2800 trees/ha in the stand tables by Oliveira [6] and of 2300–2500 in the models developed by the authors of Refs. [7, 8]. Oliveira [9] suggested that when the aim is wood for industry, the plantation should be the preferable method with a stem density between 1250 trees/ha (in low fertility sites) and 1670 trees/ha (in better sites), with a minimum line distance of 3 m to enable the mechanization of future interventions.

Harvest age ranges from 40 to 50 years [7, 10, 11] to ensure that the age of absolute exploitability (age at which the production of woody material per unit area

is maximum) has already been reached, and the wood harvest has adequate dimensions to be classified as sawmill wood. The age of the final cut can occur at lower ages, such as 35 years, in sites of better quality [7], or be extended up to 80 years (e.g., [6, 8]), depending on the management objectives and aiming the target of log size.

Final density varies among the silvicultural models and with the prescriptions of density regulation as both by tree release or “precommercial” thinning set at young stand ages (e.g., 5 and 10 years) and by intermediate thinning at juvenile and mature development stages. In this section, we will focus on prescriptions of the later as those prescriptions are a major differentiating element in the traditional silvicultural models for the species. Intermediate thinning (categorized as “commercial” thinning) typically begins between 15 and 20 years and may last until 5–10 years to the harvest age. The thinning frequency is defined between short and medium (5–10 years), corresponding to a top height growth of 2–3 m [12]. Wilson’s spacing factor has been dictating the density regulation. The factor is defined as:  $Fw = 100N^{-0.5}h_{dom}^{-1}$  [13], where  $h_{dom}$  refers to the dominant height defined as the average height (m) of the 100 thickest trees per hectare, and  $N$  indicates the number of trees per hectare, after thinning. Prescribed values of  $Fw$  range from 0.20 (moderate-low thinning) to 0.28–0.30 (very heavy thinning from below) [6–8, 14, 15].

Páscoa [16] suggests, in alternative to  $Fw$ , the specification of a residual area value for density regulation, while the authors of Refs. [10, 11] describe the thinning regimes in pine stands based on the removal of a specified percent range of the number of trees. The guidelines presented by the authors of Refs. [10, 11] consider a first thinning at the age of 15–20 years, with the removal of 20–40% of the trees. A second thinning should occur at the age of 25–30 years, with the removal of 20–30% of the trees and a third thinning at the age of 35–40 years, with the removal of 20–30% of the trees. The final density should be of 300–500 trees/ha.

Luis and Fonseca [17] proposed the rules based on the self-thinning theory and the stand density index [18], given as  $SDI = N(dg/25)^b$ , where  $b$  is the allometric coefficient (–1.897 for maritime pine), and  $dg$  is the quadratic mean diameter of the trees. Luis and Fonseca [17] hypothesized that 60 and 35% of  $SDI$  are appropriate values for the upper and lower limits of the optimum growth-density interval, respectively, and 25% is the reasonable value for the crown closure situation, for maritime pine in the Portuguese conditions.

Fonseca and Calçada-Duarte [12] proposed a new density regulation model under an adaptive management context, based on Wilson's spacing factor,  $Fw = 0.21$ . The model, given by  $N = 18877 \exp(-0.656dg^{0.5})$ , provides the optimal stand density, for a given mean diameter of the stand, that prevents the understory growth, thereby reducing the vulnerability to a forest fire and ensuring at the same time the highest values of stand yield.

## 2.2 Management of naturally regenerated post-fire stands

The impact of rural fire, in number and burnt area, along the recent decades, severely affected the forest cover and the age structure of the pine woodlands, leading to an increase in pinewoods in the early stages and juvenile stratum [1]. In areas naturally regenerated post-fire, density at the beginning of stand establishment can reach a far greater number than the figures of stand density registered in the traditional silvicultural models with artificial regeneration. In datasets used by Enes et al. [19] to identify the maximum attainable density trajectory at the early stages of development of the species, maximum values ranging from 7500 to 90,000 plants are reported in juvenile maritime pine stands (age less than 20 years)



in Portugal. The availability of naturally regenerated forest promotes harnessing the natural regeneration from seeds as an option that enables saving in site preparation and plantation costs. The management of these areas requires careful analysis and adaptations of traditional models to these “new” forest systems, namely for the ones growing at high density or overstocked levels. Two challenges immediately arise, one in terms of density regulation and the other about management objectives, especially concerning the size of wood produced.

Alegria [20] analyzed the alternative wood production-oriented silvicultural scenarios for maritime pine in Center of Portugal. For areas of natural regeneration, high initial stand densities of 3000 and 5000 trees/ha were selected for essay, with different density prescriptions, based on  $Fw$  spacing factor (0.25–0.28 and 0.20) and based on a crown competition factor of 100%. The alternatives analyzed consider two systematic precommercial thinnings at 5 and 10 years, three commercial thinnings from below at 15–20, 20–25, and 35–40 years, and final harvest at 45–50 years depending on the site index. According to the author, the model departing from an initial stand density of 3000 trees/ha and commercial thinning with  $Fw$  ranging from 0.25 to 0.28 was the most suitable for the existing naturally regenerated maritime pine stands of Portuguese private forest areas. Total stand volume was similar to the obtained with a traditional model ([6], with an  $Fw$  around 0.27) and showed to have a good balance between both round and pulpwood yields. However, pulpwood increased, comparatively of the traditional model.

In the essay conducted by Alegria [20], the age for the final cut was kept under the usual harvest age range (45–50 years). Due to the ongoing risk of forest fire, the managers have been discussing shortening the rotation length to 15–20 years. Exploratory essays in the field are under development, as communicated in technical meetings recently promoted by Centro Pinus (<https://centropinus.org/>) and sponsored by International Union of Forest Research Organizations (IUFRO, <https://www.iufro.org/>), but, to the best knowledge of the authors, there are no published results yet.

### 3. Materials and methods

This section is structured in two parts. In Section 3.1, the authors select and characterize a set of silvicultural models proposed for maritime pine and identify the new ones for evaluation of the potential energy purposes. In Section 3.2, the authors proceed with the introduction and general description of simulator used in the evaluation of stand growth and implementation of thinning and describe the methodology followed in the simulations.

#### 3.1 Silvicultural scenarios

The case of study selected refers to alternative management of maritime pine, differing in terms of initial stand density, density regulation, and on the rotation length.

In Section 2.1, the authors presented a summary of the silvicultural guidelines that have been proposed for the maritime pine species in Portugal for roundwood production. As shown, the management of the species traditionally considers initial densities ranging from 1100 to 2800 trees/ha, and rotations of 35–50 years, with prescription of periodic thinning – typically based on  $Fw$  spacing factors – for reducing intratree competition and providing some economic return. The model proposed by Louro et al. [10], made available by the Institute for Nature and Forest Conservation (ICNF) in supporting documents for the elaboration of forest

projects, was selected to sustain the design of Scenario 1. This scenario considers a low density at stand establishment and focuses on wood production.

To the best knowledge of the authors, the density regulation model proposed by Fonseca and Calçada-Duarte [12] is the most recent proposal within the traditional vision of wood production-oriented silviculture in Portugal. The model applies to even-aged stands managed for roundwood production but at higher densities than the model by Louro et al. [10]. As the model explicitly takes into account the risk of a forest fire was selected as a basis to define Scenario 2.

Given the representativeness in Portugal of dense pinewoods regenerated post-fire, two scenarios (Scenarios 3 and 4) were additionally considered. These scenarios were specifically designed by the authors for areas with a high density of natural regeneration after fire. Both initialize with a density of 40,000 plants per hectare at the age of 8, which are supported by Almeida et al. [21] and corroborated by Enes et al.'s [19] findings on the size-density trajectory in regenerated pine stands after a fire. Scenario 3 considers a harvest age of 45 years as typically occurs in traditional management. In this scenario, it is intended not only to maximize the high biomass production aimed at energy purposes in the initial stage of the stands but also to obtain the wood quality in the remaining mature trees. In this way, the biomass generated by mechanical thinning of 3 m width strips from natural regeneration will be used in energy purposes. In the remaining trees managed at an early stage with high stand densities followed by heavy thinning operations, the height growth will be promoted to reduce the size and influence of the crown and, in this way, the amount of juvenile wood in the stem. Scenario 4 meets the intent of managing the pine forests in short rotations, mimicking “energy crops”. The material provided by this scenario will be used basically as biomass for energy, pulp, panels, or pilings.

The characterization of the four scenarios is depicted in **Table 1**. The prescriptions of treatments scheduled for the early stage of development in Scenarios 1 and 2 follow the traditional recommendations. Pruning was not included as it is not mandatory.

### **3.2 Simulation of stand growth and assessment of potential energy in the silvicultural scenarios with ModisPinaster**

Simulators can provide valuable information to assess stand growth under different management regimes as they allow to easily essay various alternatives and provide immediate results on a set of variables that can be used to support management decision. In this study, we selected Model with Distribution of Diameters for *Pinus Pinaster* (ModisPinaster) as the appropriate simulator. ModisPinaster [4, 5] is an “easy-to-use” model, freely available for use at Computer Aided Projection of Strategies In Silviculture (CAPSIS, <http://www.inra.fr/capsis>) platform [22]. The model offers the flexibility of use in terms of input data needs (data from standard forest inventories), alternative density regulation approaches (manual or automatic prescriptions based on spacing factors and density indices, besides the usual density measures of the number of trees or basal area per hectare), and diversity of output information (volume, biomass, carbon, and energy), among other features. A comprehensive description is provided in Ref. [5]. In its general use, the model starts simulations at a minimum age of 12 years, following the restrictions of their internal modules. For specific purposes, such as in this case study, those restrictions can be punctually alleviated, providing starting points at lower ages (for further details, see [5]).

**Table 2** presents a summary of the input data used in ModisPinaster to initialize the simulations for the selected scenarios. Scenarios 1 and 2 are initialized at the age of 12 for the simulation of stand growth before the first thinning, which occurs, in

| Year  | Scenario 1   | Scenario 2  | Scenario 3   | Scenario 4   |
|-------|--|---|--|--|
| 0     | Site preparation   | Site preparation  |  |  |
| 0     | Stand establishment: artificial regeneration (plantation) 1100 plants/ha         | Artificial regeneration (seeding or plantation) 2200 plants/ha              | Natural regeneration. It is assumed a value of 40,000 plants/ha  | Natural regeneration. It is assumed a value of 40,000 plants/ha  |
| 7-8   |  |   | Release operation (8 yr). Reduction of stand density to 30,000 trees/ha through systematic (mechanical) thinning by 3 m width strips, leaving 1 m wide strips with trees | Release operation (8 yr). Reduction of stand density to 30,000 trees/ha through systematic (mechanical) thinning by 3 m width strips, leaving 1 m wide strips with trees |
| 3-10  | Control of spontaneous vegetation (3, 8 yr)                                      | Control of spontaneous vegetation (3, 8 yr)                                 | Control of spontaneous vegetation (8 yr)   | Control of spontaneous vegetation (8 yr)   |
| 8-12  |  |   | Thinning from below (12 yr). Removal of a. 60% trees/ha within the 1 m-wide strips with trees  | Thinning from below (12 yr). Removal of a. 50% trees/ha within the 1 m-wide strips with trees  |
| 15-40 | Three thinning from below (15, 25, 35 yr). Removal of a. 30% trees/ha per action | Three thinning from below (22, 29, 36 yr). <i>Fw</i> a. 0.21 after thinning | Four thinning from below (16, 20, 28, 36 yr). Removal of a. 35-40% trees/ha per action   | Thinning from below (16 yr). Removal of a. 40% trees/ha  |
| 15-45 | Final harvest at 45 yr   | Final harvest at 45 yr  | Final harvest at 45 yr   | Final harvest at 20 yr   |

**Table 1.** Characterization of the silvicultural models selected for the essay.

| Variable                               | Scenario 1  | Scenario 2  | Scenario 3 | Scenario 4 |
|--|-------------|-------------|------------|------------|
| Stand age ( $t$ , yr)                  | 12 (8)      | 12 (8)      | 8          | 8          |
| Site index ( $SI_{35}$ , m)            | 20          | 20          | 20         | 20         |
| Number of trees ( $N$ , trees/ha)      | 1100        | 2200        | 40,000     | 40,000     |
| Basal area ( $G$ , m <sup>2</sup> /ha) | 8.8 (4.0)   | 9.6 (3.0)   | 19.6       | 19.6       |
| Quadratic mean diameter ( $d_g$ , cm)  | 10.1 (6.8)  | 7.5 (4.2)   | 2.5        | 2.5        |
| Dominant diameter ( $d_{dom}$ , cm)    | 16.4 (13.0) | 13.7 (10.0) | 8.0        | 8.0        |

**Table 2.** Summary of the input data used in ModisPinaster for initializing the simulations with the selected scenarios.

the traditional models, around the age of 15 years. For Scenarios 3 and 4, the initialization point was set to a lower age, to allow for the simulation of the first intervention, scheduled for the stand age of 8 years. To enable a comparison of values, estimated values of the stand variables at the age of 8, for Scenarios 1 and 2, are shown inside the parenthesis (**Table 2**).

The simulations consider stands developing in a site of high quality for the species, with a dominant height of 20 m at the reference age of 35 years, according to Ref. [23] site index ( $SI$ ) model.

ModisPinaster allows simulating stand growth (in 1-year steps) and simulation of interventions. The prescription of thinning can be performed manually through the selection of the values of the number of trees to thin by diameter class or automatically using an algorithm of thinning. In the automatic procedure, the options include the specification of the number of trees to cut or to set the target values of the Wilson's spacing factor ( $Fw$ ) or the stand density index ( $SDI$ ) in a percentage scale. The simulator offers an extensive set of output information with detail of stand level or discriminated by diameter class. For this study, the authors selected as output, following the stand-level variables: total volume of the stem over bark, and total above-ground biomass (air-dried, assuming around 25–30% of moisture), carbon, and higher heating value ( $HHV$ ). When a thinning occurs, the simulator also provides information on volume, biomass, carbon, and energy for the removed stand and the cut wood material residuals. For the current simulations, the biomass, carbon, and  $HHV$  values were estimated using the equations from Ref. [24], integrated into ModisPinaster.

The output information was registered for the years with scheduled interventions and for the harvest age accordingly to the description made in **Table 1**. Also, the estimates about the biomass removed in shrub control for release are provided. These estimates of understory component were calculated separately based on the research on average values of shrub biomass (air-dried, t/ha) made by Enes et al. [25].

#### 4. Results and discussion

**Tables 3–6** present the results of simulations performed with ModisPinaster for the silviculture guidelines described in **Table 1**, concerning Scenarios 1–4. The information presented in **Tables 3–6** refers to the characteristics of the material removed in each intervention (release, thinning, and harvest), quantified in total stem volume ( $V_r$ , m<sup>3</sup>/ha), aboveground air-dried biomass ( $B_r$ , t/ha), carbon ( $C_r$ , t/ha), and energy ( $E_r$ , GJ/ha), calculated on the base of  $HHV_r$  and the amount of biomass per hectare. The subscript “ $r$ ” indicates “removed.” When an intervention

| $t$ (yr)                             | Interv.         | $N_b$<br>(trees/ha) | $N_r$<br>(trees/ha) | $V_r$<br>(m <sup>3</sup> /ha) | $dg_r$<br>(cm) | $B_r$<br>(t/ha)  | $C_r$<br>(t/ha) | $E_r$<br>(GJ/ha)   |
|--------------------------------------|-----------------|---------------------|---------------------|-------------------------------|----------------|------------------|-----------------|--------------------|
| 3                                    | Shrubs release  | –                   | –                   | –                             | –              | (3)              | (1)             | (53)               |
| 8                                    | Shrubs release  | –                   | –                   | –                             | –              | (7)              | (2)             | (137)              |
| 15                                   | First thinning  | 1100                | 330                 | 12                            | 10.3           | 11 (19)          | 5 (9)           | 212 (365)          |
| 25                                   | Second thinning | 770                 | 230                 | 45                            | 18.5           | 29 (36)          | 12 (17)         | 532 (635)          |
| 35                                   | Third thinning  | 540                 | 160                 | 95                            | 26.7           | 54 (45)          | 22 (21)         | 990 (769)          |
| 45                                   | Harvest         | 380                 | 380                 | 432                           | 38.5           | 238 (107)        | 97 (34)         | 4332 (1223)        |
| <b>Total</b> (total forest residues) |                 |                     |                     | <b>583</b>                    |                | <b>333</b> (217) | <b>136</b> (85) | <b>6066</b> (3181) |

**Table 3.** Characteristics of the yield from thinning and yield at harvest age, according to the simulation results obtained with Scenario 1.

| t (yr)                               | Interv.         | $N_b$<br>(trees/ha) | $N_r$<br>(trees/ha) | $V_r$<br>(m <sup>3</sup> /ha) | $dg_r$<br>(cm) | $B_r$<br>(t/ha)  | $C_r$<br>(t/ha)  | $E_r$<br>(GJ/ha)   |
|--------------------------------------|-----------------|---------------------|---------------------|-------------------------------|----------------|------------------|------------------|--------------------|
| 3                                    | Shrubs release  | –                   | –                   | –                             | –              | (3)              | (1)              | (53)               |
| 8                                    | Shrubs release  | –                   | –                   | –                             | –              | (7)              | (2)              | (137)              |
| 22                                   | First thinning  | 2200                | 787                 | 39                            | 10.1           | 30 (36)          | 12 (17)          | 537 (632)          |
| 29                                   | Second thinning | 1413                | 508                 | 67                            | 14.6           | 42 (42)          | 17 (20)          | 757 (713)          |
| 36                                   | Third thinning  | 905                 | 235                 | 66                            | 19.4           | 38 (49)          | 15 (23)          | 677 (826)          |
| 45                                   | Harvest         | 670                 | 670                 | 420                           | 28.9           | 229 (139)        | 92 (50)          | 4135 (1155)        |
| <b>Total (total forest residues)</b> |                 |                     |                     | <b>591</b>                    |                | <b>338 (276)</b> | <b>137 (113)</b> | <b>6107 (3516)</b> |

**Table 4.** Characteristics of the yield from thinning and yield at harvest age, according to the simulation results obtained with Scenario 2.

| t (yr)                               | Interv.         | $N_b$<br>(trees/ha) | $N_r$<br>(trees/ha) | $V_r$<br>(m <sup>3</sup> /ha) | $dg_r$<br>(cm) | $B_r$<br>(t/ha)   | $C_r$<br>(t/ha)  | $E_r$<br>(GJ/ha)    |
|--------------------------------------|-----------------|---------------------|---------------------|-------------------------------|----------------|-------------------|------------------|---------------------|
| 8                                    | Tree release    | 40,000              | 30,000              | –                             | –              | (890)             | (308)            | (13,527)            |
| 12                                   | Shrubs release  | –                   | –                   | –                             | –              | (3)               | (1)              | (65)                |
| 12                                   | First thinning  | 10,000              | 6000                | 45                            | 3.8            | 115 (62)          | 40 (29)          | 1744 (936)          |
| 16                                   | Second thinning | 4000                | 1600                | 27                            | 6.5            | 35 (38)           | 13 (18)          | 594 (647)           |
| 20                                   | Third thinning  | 2400                | 840                 | 35                            | 9.3            | 28 (35)           | 11 (17)          | 502 (607)           |
| 28                                   | Fourth thinning | 1560                | 470                 | 59                            | 13.9           | 36 (46)           | 15 (22)          | 657 (787)           |
| 36                                   | Fifth thinning  | 1090                | 380                 | 107                           | 18.9           | 60 (51)           | 24 (24)          | 1079 (841)          |
| 45                                   | Harvest         | 710                 | 710                 | 469                           | 28.8           | 252 (139)         | 102 (35)         | 4549 (1201)         |
| <b>Total (total forest residues)</b> |                 |                     |                     | <b>741</b>                    |                | <b>527 (1219)</b> | <b>205 (454)</b> | <b>9125 (18612)</b> |

**Table 5.** Characteristics of the yield from thinning and yield at harvest age, according to the simulation results obtained with Scenario 3.

is performed, the age of the stand (t, years) is provided along with the number of standing trees (N, trees/ha) before the intervention ( $N_b$ ) and removed ( $N_r$ ) and the quadratic mean diameter of the removed trees ( $dg_r$ , cm). Biomass, carbon, and energy of the forest residues are provided, within parenthesis, near to their counterparts of the removed material.

The distribution of trees per diameter classes, for the simulated scenarios, at harvest age is depicted in **Figure 1**. In **Figure 1**, the scale for the vertical axis in Scenarios 1 (S1) and 2 (S2) is larger than the scale used for Scenarios 3 (S3) and 4 (S4), due to the differences on the number of trees per hectare.

| t (yr)                               | Interv.         | $N_b$<br>(trees/ha) | $N_r$<br>(trees/ha) | $V_r$<br>(m <sup>3</sup> /ha) | $dg_r$<br>(cm) | $B_r$<br>(t/ha)   | $C_r$<br>(t/ha) | $E_r$<br>(GJ/ha)     |
|--------------------------------------|-----------------|---------------------|---------------------|-------------------------------|----------------|-------------------|-----------------|----------------------|
| 8                                    | Tree release    | 40,000              | 30,000              | –                             | –              | (890)             | (308)           | (13,527)             |
| 12                                   | Shrubs release  | –                   | –                   | –                             | –              | (3)               | (1)             | (65)                 |
| 12                                   | First thinning  | 10,000              | 5000                | 37                            | 3.7            | 96 (78)           | 33 (37)         | 1452 (1162)          |
| 16                                   | Second thinning | 5000                | 2000                | 27                            | 5.9            | 18 (46)           | 15 (22)         | 682 (765)            |
| 20                                   | Harvest         | 3000                | 3000                | 154                           | 11.1           | 118 (69)          | 48 (26)         | 2119 (933)           |
| <b>Total (total forest residues)</b> |                 |                     |                     | <b>218</b>                    |                | <b>232 (1086)</b> | <b>96 (394)</b> | <b>4253 (16,452)</b> |

**Table 6.** Characteristics of the yield from thinning and yield at harvest age, according to the simulation results obtained with Scenario 4.

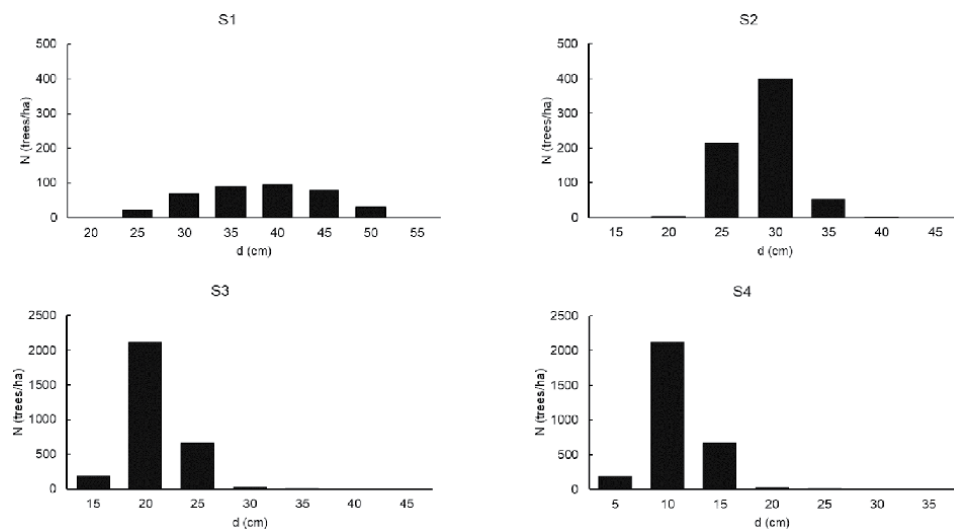


**Figure 1.** Diameter distributions per 5 cm classes at harvest age (45 years for Scenarios 1–3, and 20 years for Scenario 4).

A summary of the yield totals obtained at harvest age with the four scenarios is presented, for comparison purposes, in **Table 7**. The total yield reported as stand volume, biomass, carbon, and energy reflect the amount of yield obtained at the moment of harvest, plus the amounts obtained in silvicultural operations over stand rotation.

The percentage of differences among scenarios for the variables, mean diameter ( $dg$ ), and total yield is displayed in brackets. Differences were evaluated using the values obtained with the silvicultural guidelines proposed in Scenario 3 as the basis for comparison. This scenario corresponds to a new management design, applicable to stand with a high initial density, which is intended to know the expected management results. It allows a direct comparison with Scenarios 1 and 2 (with the same rotation length) and with the alternative model described in Scenario 4, managed at lower rotation age.

Regarding Scenarios 1 and 2 (more traditional in Portugal), there were no notable differences between them in terms of yield. Both present similar volume (583

| Scen. | t (yr) | $N_r$<br>(tree/ha) | $dg_r$ (cm)          | $V_r$ (m <sup>3</sup> /ha) | $B_r$ (t/ha) | $C_r$ (t/ha) | $E_r$ (GJ/ha)    |
|-------|--------|--------------------|----------------------|----------------------------|--------------|--------------|------------------|
| 1     | 45     | 380                | 38.5 (+25%)          | 583 (-27%)                 | 550 (-217%)  | 220 (-199%)  | 9247<br>(-200%)  |
| 2     | 45     | 670                | 28.9 ( $\approx$ 0%) | 591 (-25%)                 | 614 (-184%)  | 250 (-164%)  | 9623<br>(-188%)  |
| 3     | 45     | 710                | 28.8                 | 741                        | 1745         | 659          | 27,737           |
| 4     | 20     | 3000               | 11.1 (-159%)         | 218 (-239%)                | 1318 (-32%)  | 490 (-35%)   | 20,705<br>(-34%) |

**Table 7.**  
Total yield at harvest age obtained with the four scenarios.

and 591 m<sup>3</sup>/ha), biomass (550 and 614 t/ha), carbon (220 and 250 t/ha), and energy (9247 and 9623 GJ/ha), although with a slight superiority of Scenario 2 for these total yields. In terms of tree size, the trees in Scenario 1 span for a large interval of diameter classes (**Figure 1**). Scenario 1 provides the higher average diameter at final harvest among the three essayed with a rotation of 45 years.

Scenario 3 presents much higher yield values (volume = 741 m<sup>3</sup>/ha; biomass = 1745 t/ha; carbon = 659 t/ha; and energy = 27,737 GJ/ha), which, compared to the two previous scenarios, represent an increase in 27 and 25% in volume, 217 and 184% in biomass, 199 and 164% in carbon, and 200 and 188% in energy, respectively. Yet, trees at harvest age are distributed by smaller range of diameter classes (**Figure 1**) and present, on average, a lower diameter value in Scenario 3 than in Scenario 1 (28.8 and 38.5 cm, respectively), which is understandable since in these trees, the height growth was promoted, in detriment of diameter growth, to reduce the influence of the crown.

The forest management model of Scenario 3 is based on high stand densities followed by several heavy thinning (with 35–40% of the number of trees per ha removed in each intervention), which, in principle, reduces the amount of juvenile wood on the stem [26, 27]. It is expected that the wood from these trees presents better quality than the models with lower stand density. The forest management practices that can be used to regulate spacing between trees and act as a tool for wood quality improving are well documented in Ref. [26].

More recently, several studies with Scots pine (*Pinus sylvestris* L.), Norway spruce (*Picea abies* L.), Douglas fir (*Pseudotsuga menziesii* (Mirb.) Franco), and Sitka spruce (*Picea sitchensis* (Bong.) Carr.) concluded that higher stand density associated with high thinning intensity led to a significant change of the main wood properties for conifer species. The highest mean basic density, modulus of elasticity (MOE), and modulus of rupture (MOR) were obtained in the sites with the highest stand density followed by heavy thinning [28–32].

So, in addition to the higher productivity provided by Scenario 3, probably the trees will also have better wood quality.

In a minor extent, this feature also applies to Scenario 2. The average size of the trees, at harvest age, is lower in Scenario 2 (28.9 cm) than in Scenario 1 (38.5 cm). This difference is also expected as the average density of Scenario 2 along the rotation is higher than the one observed with Scenario 1, which is an attribute of Oliveira et al.'s [11] model to minimize the development of understory vegetation.

Regarding Scenario 4, whose management model is equal to Scenario 3 up to 12 years and the main difference is the reduction of the rotation from 45 to 20 years, it does not seem very advantageous if the objective is the production of larger pieces

of wood (and of higher economic value), even considering that in the 45-year period, it would be possible to have two rotations with Scenario 4. The anticipation of the final cut to 20 years is strongly penalized by the significant reduction in the total volume of wood obtained (741 and 218 m<sup>3</sup>/ha in Scenarios 3 and 4, respectively) aggravated by the fact that this wood comes from trees with a small diameter (only 11.1 cm) and low-economic value. However, if the main objective is the production of small material, for example, to supply the biomass units, pulp, panels, or pilings, Scenario 4 will be the most recommendable. After 20 years, this Scenario 4 provides slightly lower values of biomass (1318 t/ha), carbon (490 t/ha), and energy (20,705 GJ/ha) than the 45 years of Scenario 3 (1745 t/ha, 659 t/ha, and 27,737 GJ/ha, respectively), but after two rotations with Scenario 4, the yield will be much higher than with the other scenarios.

In this regard, it is important to emphasize that the production of pellets in Portugal is the second most important use for the pinewood in the country, whose annual production capacity is approximately 1.4 million tons [2, 3]. According to Nunes and Freitas' [33] ranking results, the Portuguese pellet productivity capacity per forest area in 2012 surpassed the total production of Central and South America, Africa, and Oceania and matched that of the entire Asian region, with Portugal representing the country with most installed capacity of pellet production plants per forest area in the world.

Thus, both Models 3 and 4 can be extremely useful to guarantee the supply of these pellet production units while alleviating the pressure to the forest roundwood in Portugal [34].

Finally, it is also worth mentioning the enormous amount of energy provided by Scenario 3 (27,737 GJ/ha) and Scenario 4 (20,705 GJ/ha), that is, the energy equivalent to 662 and 495 toe (tons of oil equivalent), respectively. Thus, if these models are adopted, they will allow approximately 890 t of biomass to be collected per hectare at the age of 8 from the natural regeneration of maritime pine, thus contributing to an additional yield from forest stands. However, in addition to this economic benefit resulting from the anticipation of an income (which definitely compensates for the costs with the operation), there is also the fact that this biomass contains around 13,500 GJ of energy equivalent to 323 toe, allowing part of the country's energy needs to be met through a natural, renewable source, with a neutral balance in CO<sub>2</sub> emissions, thus helping to comply with the commitments of Quito signed in 1998 and the Paris Agreement in 2015.

Concerning silviculture issues, managing stands in high values of density is demanding, namely to assure stability to the wind effects. A disadvantage that could be imputed to Scenarios 3 and 4 is the vulnerability to wind damages as it is expected that trees growing in dense stands present high values of height/diameter ratios, which usually denote lower stability to the wind effects [4]. As stated by Schaedel et al. [35], the long-term effect of lower stand density is to produce trees of larger size and greater stability while not sacrificing the stand yield. In stands growing at high densities, losses can occur by windthrow. In dense stands, the resistance to the wind is mostly provided by the group (block effect) [4]. Performing a thinning will interfere in the stability provided by the group. Special care with thinning practices should, therefore, be taken into account with Scenarios 3 and 4, if the stands are located in areas exposed to wind. In that situation, Scenario 4 might be a better option instead of Scenario 3 as it presents a minor interference in the stability to avoid windthrow (only two thinning, both made at early stages in contrast to the five interventions scheduled in Scenario 3) and a shorter rotation (a reduced risky period). In areas prone to forest fire, due to its minor rotation length, Scenario 4 might also be considered an option of lower risk.



## **5. Conclusion**

The results of this study corroborate the influence of management in the total yield of maritime pine species and provide new insights into the management of naturally regenerated dense stands.

The results obtained through simulation with the new design of silvicultural guidelines (Scenario 3), of managing a high dense stand, since the early stages of development proved that a considerable potential of yield, in terms of biomass and energy, can be achieved in those early interventions. Further, this new design provides multiple uses of the removed trees, as noticed by the range of mean diameter values of the removed material, and material of good quality.

Although the prescriptions of density regulation set in Scenario 3 should be interpreted as a possible recommendation, a new path on the management of maritime pine is already identified.

If the objective of forest stands is the production of small woody material, such as biomass for energy purposes, pulp, panels, or pilings, Scenario 4 will be the most recommendable since it provides the highest productivity per unit of time.

## **Acknowledgements**

This work was based on the CAPSIS platform, <http://www.inra.fr/capsis>. The authors would like to acknowledge François de Coligny for its valuable and prompt support. Acknowledgements are extended to Centro de Competências do Pinheiro Bravo, Centro Pinus, and IUFRO for promoting fruitful discussions about the silviculture and management of pine forests.

For the author integrated in the Forest Research Centre (CEF), the research was financed by the National Funds through the Portuguese funding agency, FCT (the Portuguese Foundation for Science and Technology), within the project UIDB/00239/2020. For the author integrated in the CITAB research center, it was supported by National Funds by FCT—Portuguese Foundation for Science and Technology, under the project UIDB/04033/2020.

## **Conflict of interest**

No potential conflict of interest was reported by the authors.

## Author details

Teresa Fonseca<sup>1,2,3\*</sup> and José Lousada<sup>1,4</sup>

1 Department of Forestry Sciences and Landscape Architecture (CIFAP),  
University of Trás-os-Montes and Alto Douro, Vila Real, Portugal

2 Forest Research Centre (CEF), School of Agriculture, University of Lisbon,  
Lisboa, Portugal


3 Unit Ecology and Silviculture of Pine, IUFRO, Austria

4 Centre for the Research and Technology of Agro-Environmental and Biological  
Sciences (CITAB), University of Trás-os-Montes and Alto Douro, Vila Real,  
Portugal

\*Address all correspondence to: [tfonseca@utad.pt](mailto:tfonseca@utad.pt)

## IntechOpen

---

© 2020 The Author(s). Licensee IntechOpen. Distributed under the terms of the Creative Commons Attribution - NonCommercial 4.0 License (<https://creativecommons.org/licenses/by-nc/4.0/>), which permits use, distribution and reproduction for non-commercial purposes, provided the original is properly cited. 

## References

- [1] ICNF. 6º Inventário Florestal Nacional: 2015 Relatório Final [Internet]. 2019. Available from: [http://www2.icnf.pt/portal/florestas/ifn/resource/doc/ifn/ifn6/IFN6\\_Relatorio\\_completo-2019-11-28.pdf](http://www2.icnf.pt/portal/florestas/ifn/resource/doc/ifn/ifn6/IFN6_Relatorio_completo-2019-11-28.pdf) [Accessed: 28 April 2020]
- [2] Centro PINUS. A Fileira do Pinho em 2018 [Internet]. 2019. Available from: [https://centropinus.org/files/2020/02/INDICADORES-CENTRO-PINUS-2019\\_vf.pdf](https://centropinus.org/files/2020/02/INDICADORES-CENTRO-PINUS-2019_vf.pdf) [Accessed: 28 April 2020]
- [3] Nunes LJR, Matias JCO, Catalão JPS. Wood pellets as a sustainable energy alternative in Portugal. *Renewable Energy*. 2016;**85**:1011–1016. DOI: 10.1016/j.renene.2015.07.065
- [4] Fonseca TF. Modelação do crescimento, mortalidade e distribuição diamétrica, do pinhal bravo no Vale do Tâmega [thesis]. Vila Real: University of Trás-os-Montes e Alto Douro; 2004
- [5] Fonseca TF, Parresol B, Marques C, de Coligny F. Models to implement a sustainable forest management—An overview of the ModisPinaster model. In: Martín García J, Diez Casero JJ, editors. *Sustainable Forest Management/Book 1*. London, UK: IntechOpen. 2012. p. 321-338. DOI: 10.5772/29808
- [6] Oliveira AC. Tabela de Produção Geral para o Pinheiro Bravo das Regiões Montanas e Submontanas. Lisboa: DGF, Centro de estudos Florestais (INIC); 1985. p. 38
- [7] Moreira AM, Fonseca TF. Tabela de produção para o pinhal do Vale do Tâmega. *Silva Lusitana*. 2002;**10**(1):63–71
- [8] Santos Hall A, Martins L. Tabelas de Produção para o Pinheiro Bravo. Lisboa: Projecto Florestal Português. Ministério da Agricultura, Pescas e Alimentação; 1986. p. 9
- [9] Oliveira AC. Silvicultura do Pinheiro-bravo. Manual. Porto: Centro Pinus; 1999. p. 20
- [10] Louro G, Marques H, Salinas F. Elementos de Apoio à Elaboração de Projectos Florestais. 2.ª ed. Vol. 321. Lisboa: DGF, Estudos e Informação; 2002. p. 125
- [11] Oliveira AC, Pereira JS, Correia AV. A Silvicultura do Pinheiro Bravo. Centro Pinus: Porto; 2000. p. 113
- [12] Fonseca TF, Caçada-Duarte J. An ecological stand density model to control understory in maritime pine stands. *iForest: Biogeosciences and Forestry*. 2017;**10**:829–836. DOI: 10.3832/ifor2173-010
- [13] Wilson FG. Numerical expression of stocking in terms of height. *Journal of Forestry*. 1946;**44**:758–761
- [14] Silva RFO. Gestão Dinâmica de Povoamentos Florestais. Um Modelo de Simulação para os Povoamentos de Pinheiro Bravo das Dunas do Litoral entre Mondego e Douro. Lisboa: INIA, EFN; 1989. p. 125
- [15] Peres AB. Análise de Estruturas, Crescimentos e Produções em Povoamentos de Pinheiro Bravo. Vol. 302. Lisboa: DGF, Estudos e Informação; 1990. p. 32
- [16] Páscoa F. Estrutura, crescimento e produção em povoamentos de pinheiro bravo, um modelo de simulação [thesis]. Lisboa: School of Agronomy; 1987
- [17] Luis JS, Fonseca TF. The allometric model in the stand density management of *Pinus pinaster* Ait in Portugal. *Annals of Forest Science*. 2004;**61**:1–8. DOI: 10.1051/forest:2004077
- [18] Reineke LH. Perfecting a stand-density index for even-aged forests.

Journal of Agricultural Research. 1933;  
46:627–638

[19] Enes T, Lousada JL, Aranha J, Cerveira A, Alegria C, Fonseca T. Size-density trajectory in regenerated pine stands after fire. *Forests*. 2019; **10**(12):1057–1070. DOI: 10.3390/f10121057

[20] Alegria CMM. Simulation of silvicultural scenarios and economic efficiency for maritime pine (*Pinus pinaster* Aiton) wood-oriented management in centre inland of Portugal. *Forest Systems*. 2011; **20**(3): 361–378. DOI: 10.5424/fs/20112003-11070

[21] Almeida L, Aranha J, Bento J, Fernandes P, Fonseca TF, Lopes D, et al. Regeneração natural pós-fogo em pinhal bravo no Vale do Tâmega: Respostas após 5 anos. In: Livro de Actas do 6º Congresso Florestal Nacional; 6-9 outubro 2009; Ponta Delgada: SPCF. 2009. pp. 235–243

[22] Dufour-Kowalski S, Courbaud B, Dreyfus P, Meredieu C, de Coligny F. Capsis: an open software framework and community for forest growth modelling. *Annals of Forest Science*. 2012; **69**:221–233

[23] Marques CP. Evaluating site quality of even-aged maritime pine stands in Northern Portugal using direct and indirect methods. *Forest Ecology and Management*. 1991; **41**:193–204. DOI: 10.1016/0378-1127(91)90103-3

[24] Viana H. Modelling and mapping aboveground biomass for energy usage and carbon storage assessment in Mediterranean ecosystems [thesis]. Vila Real: University of Trás-os-Montes and Alto Douro; 2012

[25] Enes T, Lousada J, Fonseca T, Viana H, Calvão A, Aranha J. Large scale shrub biomass estimates for

multiple purposes. *Life*. 2020; **10**(4):33 (article number 33). DOI: 10.3390/life10040033

[26] Zobel BJ, Buijtenen JP. *Wood Variation-its Cause and Control*. Berlin: Springer-Verlag; 1989. p. 363

[27] Zobel BJ, Sprague JR. Juvenile wood in forest trees. In: Timell TE, editor. *Springer Series in Wood Science*. Springer-Verlag; 1998. p. 300

[28] Šilinskas B, Varnagirytė-Kabašinskienė I, Aleinikovas M, Beniušienė L, Aleinikovienė J, Škėma M. Scots pine and Norway spruce mechanical wood properties in sites with different stand density. *Forests*. 2020; **11**:587. DOI: 10.3390/f11050587

[29] Peltola H, Kilpeläinen A, Sauvala K, Räsänen T, Ikonen V. Effects of early thinning regime and tree status on the radial growth and wood density of Scots pine. *Silva Fenn*. 2007; **41**:489–505. DOI: 10.14214/sf.285

[30] Jaakkola T, Mäkinen H, Saranpää P. Wood density in Norway spruce: Changes with thinning intensity and tree age. *Canadian Journal of Forest Research*. 2005; **35**:1767–1778. DOI: 10.1139/x05-118

[31] Jaakkola T, Mäkinen H, Saranpää P. Wood density of Norway spruce: Responses to timing and intensity of first commercial thinning and fertilisation. *Forest Ecology & Management*. 2006; **237**:513–521. DOI: 10.1016/j.foreco.2006.09.083

[32] Krajnc L, Farrelly N, Harte AM. The effect of thinning on mechanical properties of Douglas fir, Norway spruce, and Sitka spruce. *Annals of Forest Science*. 2019; **76**(1):25–37. DOI: 10.1007/s13595-018-0787-6

[33] Nunes J, Freitas H. An indicator to assess the pellet production per forest area. A case-study from Portugal. *Forest*

Policy and Economics. 2016;**70**:99–105.  
DOI: 10.1016/j.forpol.2016.05.022

[34] Monteiro E, Mantha V, Rouboa A.  
Portuguese pellets market: Analysis of  
the production and utilisation  
constrains. Energy Policy. 2012;**42**:  
129–135. DOI: 10.1016/j.  
enpol.2011.11.056

[35] Schaedel MS, Larson AJ,  
Affleck DLR, Belote RT, Goodburn JM,  
Wright DK, et al. Long-term  
precommercial thinning effects on *Larix*  
*occidentalis* (western larch) tree and  
stand characteristics. Canadian Journal  
of Forest Research. 2017;**47**:861–874.  
DOI: 10.1139/cjfr-2017-0074

# Evergreen Oak Biomass Residues for Firewood

*Isabel Malico, Ana Cristina Gonçalves and Adélia M.O. Sousa*

## Abstract

This chapter presents the assessment of the availability for residential heating of residual biomass from cork and holm oaks in a 12,188 ha agroforest area in Portugal. First, the above-ground biomass of evergreen oaks using very high spatial resolution satellite images was determined, followed by the definition of different scenarios for residues removal from the stands. The useful energy potential of the firewood that can be collected from the study area under the various silviculture scenarios was determined considering different energy conversion technologies: open fireplaces (still popular in Portugal) and more efficient closed burning appliances. Additionally, emissions of airborne pollutants from combusting all the available residual biomass in the study area were determined. Depending on the percentage of residues collected when the trees are pruned and on the conversion technologies used, the energy potential of evergreen oak firewood ranged from  $5.0 \times 10^6$  MJ year<sup>-1</sup> to  $7.5 \times 10^7$  MJ year<sup>-1</sup>. Heavier pruning combined with the use of open fireplaces generates less useful heat and much higher emissions of pollutants per unit useful energy produced than lighter pruning combined with a more efficient technology. This case study illustrates the need to promote the transition from inefficient to more efficient and cleaner technologies.

**Keywords:** biomass estimation, remote sensing, silviculture, energy potential, residential heating

## 1. Introduction

Forests constitute the most important stock of biomass and act as a major sink of carbon [1–3]. Among the various forest systems, the Mediterranean evergreen oak forest systems, mainly composed by cork oak (*Quercus suber*) and holm oak (*Quercus rotundifolia*), comprise two of the most abundant tree species in the Mediterranean basin [4]. They are typically managed as agroforestry systems (called *montado* in Portuguese) and are characterized by stands of low density with periodical pruning and thinning (the latter especially at the early stand development stage) and cuts of dead and diseased trees [5, 6]. Especially the wood of holm oak, but also of cork oak, was traditionally used, and still is used, for firewood and to produce charcoal [5, 6].

Using firewood for residential heating has the potential to reduce the consumption of fossil fuels and greenhouse gas emissions. Factors such as the use of fossil fuels for the production, collection and transport of firewood to households, the efficiency of the conversion systems and the energy vectors used for heating determine the level of the reductions [7]. Additionally, the source of the firewood is also a determinant

factor, and the knowledge of the availability of biomass in the vicinity of the consumption points and of the quantity of this firewood that is consumed and how it is consumed are of the utmost importance to define environmental and energy policies.

To determine the availability of firewood obtained from forest residues, it is important to quantify the amount of wood that can be collected at tree level. Several authors [8, 9] report that the average weight of holm oak pruned branches (in dry weight) divided by the diameter of the tree at breast height is in the range of 0.3 to 0.8 kg cm<sup>-1</sup> for light pruning, 1.4 to 1.5 kg cm<sup>-1</sup> for moderate pruning and 1.7 to 3.2 kg cm<sup>-1</sup> for heavy pruning.

For cork oak, a proportion of residues of 17% of the above-ground biomass is considered by Palma et al. [10]. Natividade [6] considers that 30–40% of the crown is removed in moderate prunings. This author also presents the mean weight of pruning residues (in fresh weight basis) for moderate prunings with a periodicity of 5 or 6 years as a function of the tree circumference at breast height ( $cbh$ ,  $cbh = \pi \times dbh$ , where  $dbh$  is the diameter at breast height) (Table 1).

Several studies determined the energy potential of forest residues in Portugal at country or regional level (e.g., [11–16]) and most considered the residual biomass originated from evergreen oaks. These forest species have also been considered in the assessment of the forest energy potentials of other countries (e.g., [17, 18]). Many of the studies referred above used data from field inventories and derived from remote sensing data (e.g., land use maps) in a Geographic Information Systems environment.

This work assesses the energy potential of evergreen oak residues for a region in Alentejo, South Portugal, dominated by holm and cork oaks. Through a case study, the next sections present a method that integrates the estimation of residual biomass from evergreen oaks using very high spatial resolution satellite images and the determination of its energy potential. For the evaluation of the existing forest above-ground biomass, remote sensing data was used to produce a vegetation mask with the delimitation and identification of the tree crowns by species and then calculate the crown horizontal projection. An allometric function developed by Gonçalves et al. [19] was then used to calculate the above ground biomass. Having the knowledge of the amount of above-ground biomass, different scenarios for residues removal from the stands were considered. These scenarios are based on common silvicultural practices. In the last step, the energy potential of the available firewood was calculated. Reference lower heating values for evergreen oak wood obtained from the literature were considered, as were several different conversion technologies: on the one hand, the technology most used in the country for the conversion of this type of residues, and on the other, more efficient conversion technologies. The environmental implications of using more efficient and cleaner technologies are briefly discussed.

| <i>cbh</i> (m) | Pruning residues (kg) |
|----------------|-----------------------|
| 0.8–1.0        | 30.0                  |
| 1.0–1.2        | 37.5                  |
| 1.2–1.4        | 50.0                  |
| 1.4–1.6        | 72.5                  |
| 1.6–1.8        | 100.0                 |
| 1.8–2.0        | 140.0                 |

**Table 1.** Mean mass of pruning residues (in fresh weight basis) per class of circumference at breast height.

## 2. Firewood consumption in Portugal

According to the Eurostat [20], the production of firewood (including wood for charcoal) in Portugal was 1178 thousand m<sup>3</sup> in 2018, 8.7% of the total roundwood production in the country. The reported percentage of roundwood that was used as firewood in Portugal is quite small when compared to the average of the 27 member states of the European Union (22.7%). However, the Portuguese share of firewood in the total roundwood must be read with care because its supply is largely untaxed outside urban contexts and often auto-consumption and informal markets exist [21, 22]. For instance, pruning of cork and holm oaks is not recorded as sales of industrial wood [23].

According to DGEG [24], in Portugal, the primary energy production from firewood, forest and plant residues, pellets and other agglomerates was 1575 ktoe (black liquor not included). The uses for this solid biomass are expressed in **Figure 1**, which shows that more than half of the biomass was consumed in the residential sector. The production of electricity in electricity-only power plants used 22% of the solid biomass and the industry, mostly the pulp and paper industry, had a 19% share of the consumption of this type of biomass.

The basis for the estimation of the consumption of wood in the residential sector reported in the Portuguese energy balance were the results of a national survey preformed in 2010 by INE/DGEG [24]. According to that survey [25],  $2.7 \times 10^9$  kg of firewood was consumed in Portugal between October 2009 and September 2010. This value is significantly higher than the one reported by the Eurostat for all sectors [20]. One of the reasons for this deviation is, as already referred at the beginning of this section, that firewood is often collected for auto-consumption or supplied through informal markets, so it is not recorded (only 40% of the wood consumed in households was bought; the rest was collected in the vicinity of households or had other origin [25]). The amount of pellets and other agglomerates that were consumed in the country in 2018 was  $2.25 \times 10^8$  kg [26].

National statistics show that, in 2018, electricity was the main energy vector consumed by households in Portugal, followed by primary solid biofuels [24], mainly firewood and forest and plant residues. The latter represented 26% of the energy consumed by the households. However, regional differences are important and consumption of wood in small rural cities in regions with colder weather can be much higher than the national average [27, 28]. Firewood was consumed in 40.1% of the households in 2009–2010 [25]. The various sources of wood were: pine (37.4%), *Eucalyptus* sp. (21.2%), holm oak (7.4%), cork oak (5.7%), other forest residues (4.2%) and other types of wood (24.0%). This implies that between October 2009

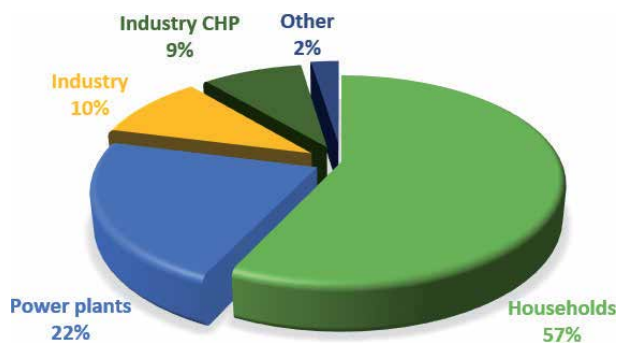


**Figure 1.** Share of the various sectors in the Portuguese consumption of firewood, forest and plant residues, pellets and other agglomerates in 2018.



and September 2010, the consumption of holm oak firewood was  $2.0 \times 10^5$  t and of cork oak firewood  $1.5 \times 10^5$  t. Oak wood is the mostly consumed as firewood in the South of the country [27], where most of its stands are situated (cork and holm oaks correspond, respectively, to 45.7% and 23.8% of the forest area in Alentejo [29]; **Figure 2** shows the location of this region).

In Portugal, between October 2009 and September 2010, firewood was mostly used in household for space heating (52.0%); other uses are cooking and water heating [25]. Indeed, firewood was the most common energy source for space heating in the country. According to the INE/DGEG survey, the most popular wood-fired equipment for household heating was the open fireplace, followed by the closed fireplace and woodstove (existent in 24%, 11.1% and 7.2% of the Portuguese households, respectively). Fireplaces were also the appliance most used for cooking with biomass. Note that regional differences in terms of technology used also exist and the technologies employed vary throughout the country [27]. For example, the study of Azevedo et al. [28] shows that in a region in the north of Portugal, the most used technologies for biomass heating are closed fireplaces and that open fireplaces only come second.

Independently of regional differences, it can be said that most biomass systems installed in the Portuguese households provide heat locally (central heating systems are not so common) and the percentage of wood that is burned inefficiently in open fireplaces is high. The efficiency of this type of technology is at best 20% [30], being typically below 10% [31]. Closed fireplaces and stoves present much higher efficiencies, which depend on the specific appliance. Efficiency values of closed fireplaces are usually above 50%, but can be as high as 80%, whereas that of batch-fed stoves characteristically range from 40–80% [32]. It is worth highlighting that compared to

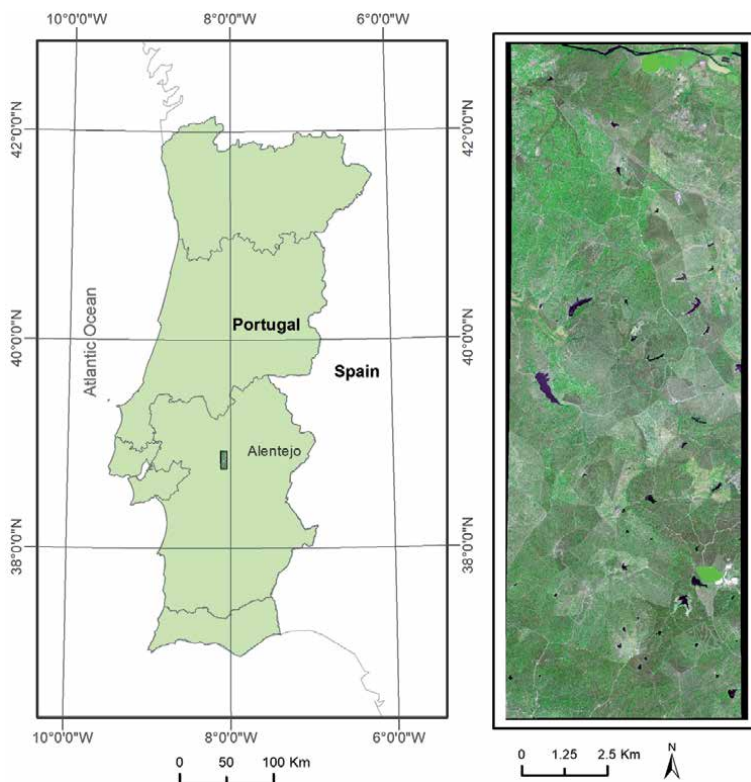


**Figure 2.** Map of the study area and the country boundaries for Portugal (left) and the QuickBird satellite image (false color composite, RGB - Red, Near-infrared (NIR), Blue).

| Wood     | Technology      | PM <sub>2.5</sub> | OC <sup>1</sup> | EC <sup>2</sup> | CO          | CO <sub>2</sub> |
|----------|-----------------|-------------------|-----------------|-----------------|-------------|-----------------|
| Holm oak | Open fireplaces | 13.1 ± 8.1        | 7.2 ± 4.0       | 0.30 ± 0.11     | 61.8 ± 24.5 | 735 ± 193       |
|          | Cast iron stove | 5.8 ± 3.9         | 3.0 ± 2.1       | 0.23 ± 0.1      | 63.7 ± 55.9 | 985 ± 570       |
| Cork oak | Open fireplaces | 17.9 ± 10         | 10.1 ± 5.2      | 0.68 ± 0.40     | 85.5 ± 22.0 | 552 ± 306       |
|          | Cast iron stove | 8.3 ± 6.1         | 4.8 ± 3.4       | 0.42 ± 0.33     | 99.2 ± 92.4 | 895 ± 693       |

<sup>1</sup>OC – Organic carbon.

<sup>2</sup>EC – Elemental carbon.

**Table 2.**

PM<sub>2.5</sub>, carbonaceous constituents, CO and CO<sub>2</sub> emission factors for closed and open burning appliances used in Portuguese households when combusting oak wood (g kg<sup>-1</sup>, dry basis).

other countries, for example to the Scandinavian countries, in Portugal the share of high efficiency biomass-fired systems is much lower [33]. However, the situation in Portugal is comparable to the one of other southern European countries (e.g., [34]).

Another important factor to have in mind when comparing different firewood burning appliances is their emissions. Traditional residential heating systems are characterized by considerable emissions of airborne pollutants, namely fine particles, volatile organic compounds and carbon monoxide. In Portugal, one of the largest sources of fine particle emissions is firewood combustion [27, 35]. **Table 2** presents the emission factors for a cast iron stove and a traditional brick open fireplace used in Portuguese households when combusting oak wood [33]. The cast iron wood stove (Portuguese stove) is representative of a closed burning appliance and the traditional open fireplace of an open burning appliance used in Portugal. It should be noted that emissions from wood combustion appliances depend not only on the fuel and appliance used, but also on operational practices and maintenance [36, 37].

### 3. Availability of evergreen oak firewood in a region in Alentejo, Portugal

Cork and holm oak stands occupy 22.3% and 10.8% of the forest area of Portugal, respectively. They are particularly important in the Alentejo region, which corresponds to about one third of mainland Portugal, and whose forest area is mainly composed by pure and mixed stands of both evergreen oaks (45.7% and 23.8%, respectively, for cork and holm oaks). This corresponds to about 85% of the area of cork oak and circa 91% of the area of holm oak in mainland Portugal [29].

This work presents a case study for the assessment of the availability of residual biomass from these two evergreen oaks in an area of 12,188 ha (**Figure 2**) located in the region of Alentejo in Portugal (central coordinates: 8.07°W, 38.85°N). The area is characterized by plain terrain (mean elevation of approximately 200 m) and Mediterranean soils and climate. The forest stands are composed of pure and mixed stands of cork and holm oaks, and are managed as agroforestry systems. Their main products are bark for cork oak and fruit for both oaks. Additionally, these systems frequently have extensive grazing and pasture as other productions. The area occupied by these agroforestry systems is 9720 ha (corresponding to about 80% of the total area).

The availability of evergreen oak firewood in the study area was assessed using published functions for the estimation of the above-ground biomass [19] and a methodology developed to estimate the amount of residues, as a function of the former, based on the literature [6, 8–10]. The study was done in a Geographical Information Systems (GIS) framework, with data derived from remote sensing techniques, which enabled the estimation for the whole area. The quantification of

the biomass residues for the evergreen oaks was done in four steps that are briefly described in the next paragraphs.

In the first step, one image from the QuickBird satellite (with four multispectral bands (Blue, Green, Red and Near-Infrared (NIR)), acquired on August 2006, was selected for the study area. It was orthorectified, georeferenced and atmospherically corrected. Object-based image analysis with contrast split segmentation was used to isolate the tree crowns from the other land uses, then the objects were classified using the nearest neighbor algorithm. More details of the methodology used can be found in [19]. This resulted in a vegetation mask, in which the two species were differentiated (**Figure 3**). The agreement between the classification and ground truth obtained by the Kappa statistic [38, 39] was 76% and the global precision was 87%, which shows a good performance of the applied methodologic procedures.

In the second step of the methodology, the study area was divided in a square grid of 2070.25 m<sup>2</sup> (45.5 × 45.5 m, corresponding to 65 × 65 image pixels) and the vegetation mask was used to identify the composition and to calculate crown cover (the share of the area occupied by the tree crown horizontal projection) per grid.

The data obtained in the previous step was used to calculate above-ground biomass (AGB, in t ha<sup>-1</sup>) per square grid with the function of Gonçalves et al. [19] (Eq. (1), where *CC* is the crown cover, *d* a dummy variable, *QR* holm oak pure stands, *PP* umbrella pine (*Pinus pinea*) pure stands and *QRPP* mixed stands of holm oak and umbrella pine). In this case, no stands of umbrella pine exist, so *dPP* and *dQSPP* are zero and the formula is reduced to the first two terms (in bold).

$$AGB = \mathbf{0.97327 \times CC} - \mathbf{7.81323 \times dQR} + 18.93157 \times dPP + 24.72573 \times dQSPP \quad (1)$$

The final step of the methodology consisted in the estimation of the forest residues as a function of above-ground biomass, considering the values referred in the

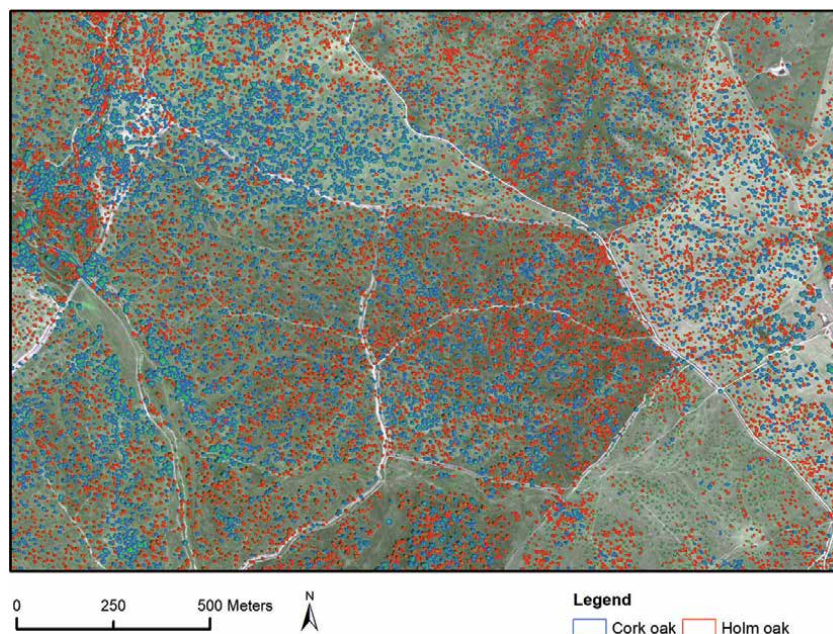


**Figure 3.** Illustration of the result of multi-resolution segmentation and object-oriented classification process over the very high spatial resolution image (false color composite, RGB – Red, NIR, Blue).

literature for the share of above-ground biomass removed in pruning. To relate the proportion of residues in relation to the above-ground biomass, a data set of 91 plots of both holm and cork oaks was used. The plots were used to convert the weight of residues at tree level to area level. For each tree the weight of pruning residues was calculated as a function of the diameter at breast height (as referred by [6, 8, 9]). Then, the amount of residues was summed per plot and converted to an area basis (per hectare). Afterwards, the share of pruning residues per plot was determined and compared with the pruning intensity referred in the literature. Five alternatives were considered: 1) 10%; 2) 15%; 3) 20%; 4) 25%; and 5) 30%. The alternatives correspond to light, light-moderate, moderate, moderate-heavy and heavy pruning, respectively.

The total weight of above-ground biomass for the study area estimated by Eq. (1) was 184,887 t. Typical of *montado*, the spatial variability of density is high, which results also in a high variability in above-ground biomass (**Figure 4**).

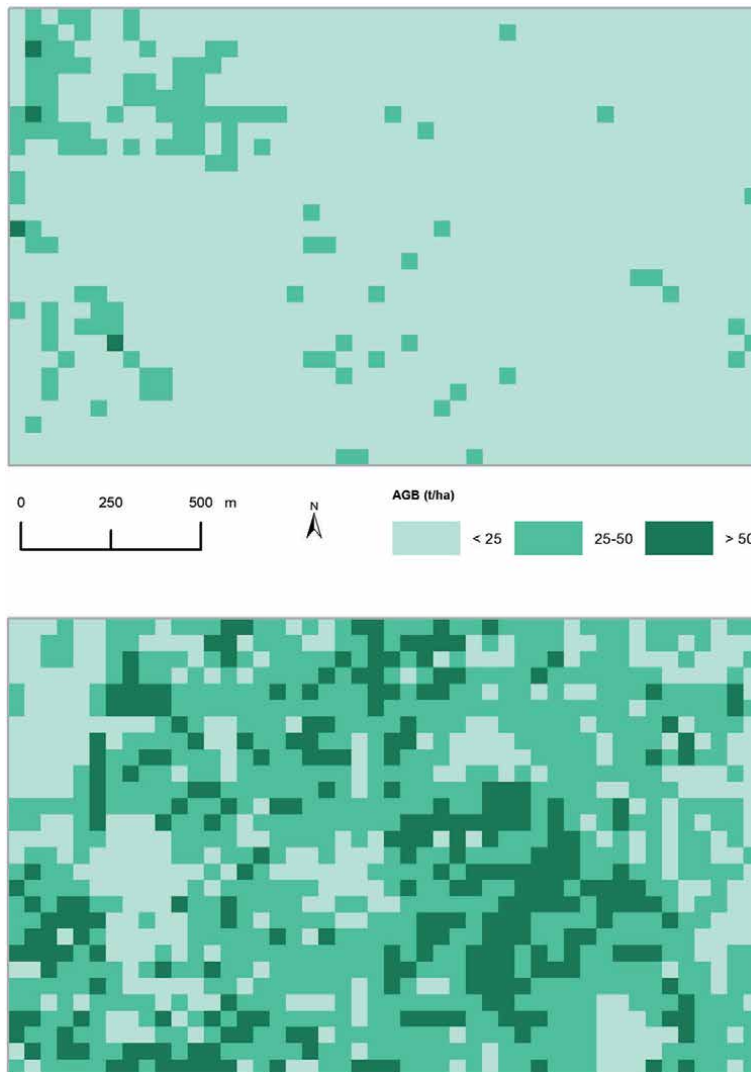


**Figure 4.** Above-ground biomass per grid (in  $t\ ha^{-1}$ ) for two areas, one with low density (top) and another with high density (bottom).

| Grids                                    | Pure |      | Mixed  |        | Pure and mixed |        | Total  |         |        |
|--|------|------|--------|--------|----------------|--------|--------|---------|--------|
|  | QR   | QS   | QR     | QS     | total          | QR     |        | QS      |        |
| AGB                                      | 8737 | 6166 | 85,158 | 84,818 | 169,976        | 93,895 | 90,984 | 184,879 |        |
| <b>Scenario/Share of AGB removed (%)</b> |      |      |        |        |                |        |        |         |        |
| A1                                       | 10   | 874  | 617    | 8516   | 8482           | 16,998 | 9390   | 9098    | 18,488 |
| A2                                       | 15   | 1311 | 925    | 12,774 | 12,723         | 25,496 | 14,084 | 13,648  | 27,732 |
| A3                                       | 20   | 1747 | 1233   | 17,032 | 16,964         | 33,995 | 18,779 | 18,197  | 36,976 |
| A4                                       | 25   | 2184 | 1542   | 21,290 | 21,205         | 42,494 | 23,474 | 22,746  | 46,220 |
| A5                                       | 30   | 2621 | 1850   | 25,547 | 25,445         | 50,993 | 28,169 | 27,295  | 55,464 |

**Table 3.**

*Above-ground biomass and weight of residues for each alternative for residues removal on a 6 year basis for the study area (in t d.b.). QR refers to holm oak and QS to cork oak.*

**Table 3** presents the above-ground biomass and the weight of residues for each alternative considered for the share of residues removed in pruning. It was assumed that the trees are pruned every 6 years and that the amount of residues per year is 1/6 of the total amount of residues for the all area in a six-year period. Also for grids with both species, it was considered that the weight of biomass of residues per species corresponded to the mean share of crown cover per species for the entire forest area (50.1% for holm oak and 49.9% for cork oak).

#### 4. Energy potential of evergreen oak firewood in the study area

The yearly amounts of oak residues estimated in the last section for the study area under different scenarios were converted to energy using Eq. (2),

$$E_{t,i} = B_i \times LHV_i, \quad (2)$$

where the subscript  $i$  refers to the forest species,  $E_{t,i}$  is the theoretical energy potential of the residual biomass,  $B_i$  the yearly quantity of biomass that can be removed from the study area and  $LHV_i$  the lower heating value (given in **Table 4**). The result of computing Eq. (2) represent the theoretical energy potentials of evergreen oak firewood that can be collected in the study area, which are the upper limits for the value of energy that can be obtained from oak biomass residues.

A moisture content of 30% was considered, resulting in LHV (a.r., as received) of 11.1 and 11.6 MJ kg<sup>-1</sup> for holm and cork oak, respectively. As a comparison, the

| Wood     | LHV <sup>1</sup> (MJ kg <sup>-1</sup> a.r.) | LHV <sup>2</sup> (MJ kg <sup>-1</sup> d.b.) |
|----------|---|---|
| Holm oak | 11.1  | 16.9  |
| Cork oak | 11.6  | 17.6  |

<sup>1</sup>Considering 30% water content.

<sup>2</sup>Taken from [17].

**Table 4.**

*Lower heating value of cork and holm oak firewood.*

Portuguese energy balance considers that the lower heating value of firewood is  $10.5 \text{ MJ kg}^{-1}$ .

Depending on the percentage of residues collected each time the trees are pruned, the amount of evergreen oak firewood that is available in the study area is in the range of  $3081$  to  $9244 \text{ t year}^{-1}$ . This corresponds to a theoretical energy potential between  $5.0 \times 10^7 \text{ MJ year}^{-1}$  and  $1.5 \times 10^8 \text{ MJ year}^{-1}$  (**Table 5**).

The values reported in **Table 5** correspond to the energy content of the residues, but, if they are used for household heating, not all this energy can be converted to heat. There is a conversion efficiency,  $\eta$ , which is dependent on the technology used, and defined by Eq. (3),

$$\eta = \frac{E_{u,i}}{E_{t,i}}, \quad (3)$$

where  $i$  refers to the forest species and  $E_{u,i}$  is the useful energy obtained from the combustion of the  $i^{\text{th}}$  firewood type, which is reported on **Table 6** for each of the scenarios considered.

Considering that all of the firewood is burned in open fireplaces, the most popular wood-fired appliance for household heating in Portugal [25], the amount of energy generated from the firewood obtained in the study area would be between  $5.0 \times 10^6 \text{ MJ year}^{-1}$  and  $1.5 \times 10^7 \text{ MJ year}^{-1}$  (**Table 6**). If instead, the firewood would be burned in more efficient appliances, the energy that could be obtained would be significantly higher (between  $2.5 \times 10^7 \text{ MJ year}^{-1}$  and  $7.5 \times 10^7 \text{ MJ year}^{-1}$ ). The use of closed burning appliances represents an increase of 400% in the energy produced.

The two alternatives for energy conversion technologies considered in **Table 6**, where only one technology is used to convert all the collected biomass into energy,

| Scenario | Amount of firewood (t d.b. year <sup>-1</sup> ) |      | Theoretical energy potential (MJ year <sup>-1</sup> ) |                   |
|----------|---|------|---|-------------------|
| A1       | Holm oak  | 1565 | Holm oak  | $2.5 \times 10^7$ |
|          | Cork oak  | 1516 | Cork oak  | $2.5 \times 10^7$ |
|          | Total   | 3081 | Total   | $5.0 \times 10^7$ |
| A2       | Holm oak  | 2347 | Holm oak  | $3.7 \times 10^7$ |
|          | Cork oak  | 2275 | Cork oak  | $3.8 \times 10^7$ |
|          | Total   | 4622 | Total   | $7.5 \times 10^7$ |
| A3       | Holm oak  | 3130 | Holm oak  | $5.0 \times 10^7$ |
|          | Cork oak  | 3033 | Cork oak  | $5.0 \times 10^7$ |
|          | Total   | 6163 | Total   | $1.0 \times 10^8$ |
| A4       | Holm oak  | 3912 | Holm oak  | $6.2 \times 10^7$ |
|          | Cork oak  | 3791 | Cork oak  | $6.3 \times 10^7$ |
|          | Total   | 7703 | Total   | $1.2 \times 10^8$ |
| A5       | Holm oak  | 4695 | Holm oak  | $7.4 \times 10^7$ |
|          | Cork oak  | 4549 | Cork oak  | $7.5 \times 10^7$ |
|          | Total   | 9244 | Total   | $1.5 \times 10^8$ |

**Table 5.** Yearly amount and theoretical energy potential of the oak firewood obtained in the study area under the different scenarios considered.

| Scenario | Available energy (MJ year <sup>-1</sup> ) |                             |          |                              |
|----------|---|-----------------------------|----------|------------------------------|
|          |   | Open fireplace <sup>1</sup> |          | Cast iron stove <sup>2</sup> |
| A1       | Holm oak                                  | 2.5 × 10 <sup>6</sup>       | Holm oak | 1.2 × 10 <sup>7</sup>        |
|          | Cork oak                                  | 2.5 × 10 <sup>6</sup>       | Cork oak | 1.3 × 10 <sup>7</sup>        |
|          | Total                                     | 5.0 × 10 <sup>6</sup>       | Total    | 2.5 × 10 <sup>7</sup>        |
| A2       | Holm oak                                  | 3.7 × 10 <sup>6</sup>       | Holm oak | 1.9 × 10 <sup>7</sup>        |
|          | Cork oak                                  | 3.8 × 10 <sup>6</sup>       | Cork oak | 1.9 × 10 <sup>7</sup>        |
|          | Total                                     | 7.5 × 10 <sup>6</sup>       | Total    | 3.7 × 10 <sup>7</sup>        |
| A3       | Holm oak                                  | 5.0 × 10 <sup>6</sup>       | Holm oak | 2.5 × 10 <sup>7</sup>        |
|          | Cork oak                                  | 5.0 × 10 <sup>6</sup>       | Cork oak | 2.5 × 10 <sup>7</sup>        |
|          | Total                                     | 1.0 × 10 <sup>7</sup>       | Total    | 5.0 × 10 <sup>7</sup>        |
| A4       | Holm oak                                  | 6.2 × 10 <sup>6</sup>       | Holm oak | 3.1 × 10 <sup>7</sup>        |
|          | Cork oak                                  | 6.3 × 10 <sup>6</sup>       | Cork oak | 3.1 × 10 <sup>7</sup>        |
|          | Total                                     | 1.2 × 10 <sup>7</sup>       | Total    | 6.2 × 10 <sup>7</sup>        |
| A5       | Holm oak                                  | 7.4 × 10 <sup>6</sup>       | Holm oak | 3.7 × 10 <sup>7</sup>        |
|          | Cork oak                                  | 7.5 × 10 <sup>6</sup>       | Cork oak | 3.8 × 10 <sup>7</sup>        |
|          | Total                                     | 1.5 × 10 <sup>7</sup>       | Total    | 7.5 × 10 <sup>7</sup>        |

<sup>1</sup>10% efficiency [31].  
<sup>2</sup>50% efficiency [28].

**Table 6.**  
*Energy potential of the oak firewood obtained in the study area under the different scenarios considered.*

do not reflect the technological split existent in the country. The biomass technologies used for residential heating are diverse and their shares change over time. The scenario that considers that only open fireplaces are used is a borderline case, which seeks to illustrate the impact of using inefficient equipment. If a technology split close to the one reported in the INE/DGEG survey [25] is considered, the amount of useful heat generated from the firewood obtained in the study area would be between  $1.4 \times 10^7$  MJ year<sup>-1</sup> and  $4.1 \times 10^7$  MJ year<sup>-1</sup>.

Knowing the amount of firewood consumed under each scenario, it is possible to estimate the emissions of airborne pollutants for each firewood species and technology considered,  $EE_{k,i,j}$ , using Eq. (4),

$$EE_{k,i,j} = EF_{k,i,j} \times B_{i,j}, \quad (4)$$

where  $k$  refers to the pollutant,  $i$  to the forest species and  $j$  to the technology.  $EF_{k,i,j}$  is the emission factor of pollutant  $k$  for the  $j^{\text{th}}$  appliance/equipment when combusting firewood of the  $i^{\text{th}}$  species and  $B_{i,j}$  the quantity of biomass  $i$  that is burned in the technology of type  $j$ .

The emissions of airborne pollutants that would be generated from the combustion of the firewood that could be collected in the study area are reported on **Table 7** for the scenario that considers heavy pruning (for the other scenarios, the emissions would be lower, but the same conclusions could be drawn). It can be seen that, in general, open fireplaces emit more pollutants than stoves. Additionally, burning cork oak is responsible for more emissions (CO<sub>2</sub> not considered, as it will be discussed in the next paragraph).

| Substance / Scenario A5 | Emissions <sup>1</sup> (t year <sup>-1</sup> ) |        |                 |        |
|-------------------------|--|--------|-----------------|--------|
|                         | Open fireplace                                 |        | Cast iron stove |        |
| PM <sub>2.5</sub>       | Holm oak                                       | 61.5   | Holm oak        | 27.2   |
|                         | Cork oak                                       | 81.4   | Cork oak        | 37.8   |
|                         | Total  | 142.9  | Total           | 65.0   |
| OC                      | Holm oak                                       | 33.8   | Holm oak        | 14.1   |
|                         | Cork oak                                       | 45.9   | Cork oak        | 21.8   |
|                         | Total  | 79.7   | Total           | 35.9   |
| EC                      | Holm oak                                       | 1.4    | Holm oak        | 1.1    |
|                         | Cork oak                                       | 3.1    | Cork oak        | 1.9    |
|                         | Total  | 4.5    | Total           | 3.0    |
| CO                      | Holm oak                                       | 290.2  | Holm oak        | 299.1  |
|                         | Cork oak                                       | 388.9  | Cork oak        | 451.3  |
|                         | Total  | 679.1  | Total           | 750.3  |
| CO <sub>2</sub>         | Holm oak                                       | 3450.8 | Holm oak        | 4624.6 |
|                         | Cork oak                                       | 2511.0 | Cork oak        | 4071.4 |
|                         | Total  | 5961.9 | Total           | 8695.9 |

<sup>1</sup>Emission factors taken from **Table 2**.

**Table 7.**  
*Emissions of the combustion of the oak firewood obtained in the study area under the scenario where more residues are obtained (A5).*

CO<sub>2</sub> emissions reported in **Table 7** are dependent on the carbon content of the biomass and inherent to biomass-fired combustion systems. A higher value of carbon dioxide emissions reflects both the carbon content of the fuel and the completeness of the combustion process (for the same fuel, when all the carbon is oxidized because combustion is complete, the CO<sub>2</sub> emissions are larger than when combustion is not so efficient). The CO<sub>2</sub> emissions are not included in the national emission inventory, though, since biomass is considered carbon neutral [23].

**Table 8** presents the amount of airborne pollutants that would be emitted when combusting the firewood that could be collected in the study area divided by the amount of thermal energy that could be usefully used for household space heating (these results are independent of the silvicultural scenario considered). As expected, the use of open fireplaces presents much higher emissions per unit energy obtained for space heating than the use of stoves.

The results presented in **Tables 6–8** show the importance of both the silvicultural practices and energy conversion technologies on the energy that can be obtained from evergreen oak firewood and on the emissions that result from burning that firewood. If the pruning is heavier, more firewood is obtained and in theory more useful energy. However, as shown in **Table 6** this does not imply that more useful energy is obtained. If this firewood is burned in a traditional fireplace, the energy efficiency is so low that more firewood is needed to reach the same useful energy as in a traditional stove. Pruning 30% of the above-ground biomass of evergreen oaks and burning all the firewood in a traditional fireplace results in less energy than pruning 10% of the above-ground biomass to fire a closed burning appliance. Additionally, the emissions of airborne pollutants per unit useful heat generated are



| Substance         | Emissions <sup>1</sup> (t MJ <sup>-1</sup> ) |        |                 |        |
|-------------------|--|--------|-----------------|--------|
|                   | Open fireplace                               |        | Cast iron stove |        |
| PM <sub>2.5</sub> | Holm oak                                     | 8.26   | Holm oak        | 0.73   |
|                   | Cork oak                                     | 10.80  | Cork oak        | 1.01   |
|                   | Total  | 19.06  | Total           | 1.75   |
| OC                | Holm oak                                     | 4.54   | Holm oak        | 0.38   |
|                   | Cork oak                                     | 6.09   | Cork oak        | 0.59   |
|                   | Total  | 10.64  | Total           | 0.96   |
| EC                | Holm oak                                     | 0.19   | Holm oak        | 0.03   |
|                   | Cork oak                                     | 0.41   | Cork oak        | 0.05   |
|                   | Total  | 0.60   | Total           | 0.08   |
| CO                | Holm oak                                     | 38.97  | Holm oak        | 8.03   |
|                   | Cork oak                                     | 51.59  | Cork oak        | 12.12  |
|                   | Total  | 90.57  | Total           | 20.16  |
| CO <sub>2</sub>   | Holm oak                                     | 463.51 | Holm oak        | 124.23 |
|                   | Cork oak                                     | 333.10 | Cork oak        | 109.37 |
|                   | Total  | 796.62 | Total           | 233.61 |

<sup>1</sup>Emission factors taken from **Table 2**.

**Table 8.**

*Emissions per unit useful energy obtained from the combustion of the oak firewood collected in the study area.*

much higher. Also important is the fact that heavier pruning practices have some undesirable environmental impacts. The higher the intensity of pruning, the higher the leaf area removed, and thus the lower the photosynthetic ability. This results in a reduction of growth and production, whether of bark (cork for cork oak) or fruit (for cork and holm oak). This is also reflected in the incomes and in the sustainability of the systems as the evergreen oaks in these type of agroforestry systems have also an important role in the conservation of habitats, soil and water.

According to the concept of “energy ladder” [40], households tend to replace inefficient and more polluting fuels and energy conversion technologies by others that are “better” as their income rises. This is what has been happening in OECD Europe, where households mainly consume natural gas, followed by electricity; biofuels and waste coming third [41]. By mid-19th century, Portuguese households mainly consumed firewood [42], but in 2018 this share was 26% and the dominant energy source in households was electricity [24]. However, the “energy ladder” does not mean that modern biomass technologies should not be used and promoted. Residential biomass is an alternative to the use of fossil fuels and presents many advantages. However, the transition from traditional appliances to more efficient and cleaner technologies should be promoted [43].

## 5. Conclusions

Cork and holm oak firewood is traditionally used for household heating in Southwest Europe. This wood, as other types of firewood, is mostly traded in informal markets in Portugal. The latter results in a lack of statistics on firewood

consumption in the country, which hinders energy and environmental planning. Additionally, the assessment of the amount of wood that can sustainably be removed from the forest is of the utmost importance for the definition of bioenergy policies. In this context, this study used a method based on very high resolution remote sensing data to determine the energy potential of evergreen oak firewood for household heating. Different silvicultural and energy utilization scenarios were considered. The method was applied to an area of 12,188 ha dominated by cork and holm oak stands. The results show that both silvicultural practices and energy conversion technology choices are of primordial importance to the sustainability of the use of firewood for household heating. The use of inefficient equipment, still popular in Portugal, leads to considerable amounts of emissions of airborne pollutants and firewood consumption. The results presented in this study show that the use of open fireplaces results in much larger biomass removals from the stands (for the same amount of useful heat obtained) with various environmental implications. When using more efficient equipment, the same amount of heat could be obtained with less biomass and airborne emissions. This fact is often forgotten in public energy policies, but is of primordial importance in a country where biomass is the most important source for household heating. Through the presentation of a case study, the authors want to put in evidence the need for the development of public policies that are directed to a transition from traditional to modern biomass uses for household heating.

## **Acknowledgements**

This work was supported by the European Fund for Regional Development (ref. 0753\_CILIFO\_5\_E) and by National Funds through FCT - Foundation for Science and Technology, under the Project UIDP/05183/2020 (MED) and Project UIDB/50022/2020 (through IDMEC, under LAETA).

## **Author details**

Isabel Malico<sup>1,2\*</sup>, Ana Cristina Gonçalves<sup>3</sup> and Adélia M.O. Sousa<sup>3</sup>


1 Department of Mechatronics Engineering, School of Sciences and Technology, University of Évora, Évora, Portugal

2 IDMEC, Instituto Superior Técnico, Universidade de Lisboa, Av. Rovisco Pais, 1049-001, Lisboa, Portugal

3 Department of Rural Engineering, School of Sciences and Technology, MED - Mediterranean Institute for Agriculture, Environment and Development, Institute of Advanced Studies and Research (IIFA), University of Évora, Évora, Portugal

\*Address all correspondence to: [imbm@uevora.pt](mailto:imbm@uevora.pt)

## **IntechOpen**

© 2020 The Author(s). Licensee IntechOpen. Distributed under the terms of the Creative Commons Attribution - NonCommercial 4.0 License (<https://creativecommons.org/licenses/by-nc/4.0/>), which permits use, distribution and reproduction for non-commercial purposes, provided the original is properly cited. 

## References

- [1] Pan Y, Birdsey RA, Fang J, Houghton R, Kauppi PE, Kurz WA, Phillips OL, Shvidenko A, Lewis SL, Canadell JG, Ciais P, Jackson RB, Pacala SW, McGuire AD, Piao S, Rautiainen A, Sitch S, Hayes D. A large and persistent carbon sink in the World's forests. *Science*. 2011;333:988-993. DOI: 10.1126/science.1201609
- [2] Skog KE, McKinley DC, Birdsey RA, Hines SJ, Woodall CW, Reinhardt ED, Vose JM. Managing carbon. In: Peterson DL, Vose JM, Patel-Weynand T, editors. *Climate Change and United States Forests*. Dordrecht: Springer Netherlands; 2014. p. 151-182. DOI: 10.1007/978-94-007-7515-2\_7
- [3] Urbano AR, Keeton WS. Carbon dynamics and structural development in recovering secondary forests of the northeastern U.S.. *Forest Ecology and Management*. 2017;392:21-35. DOI: 10.1016/j.foreco.2017.02.037
- [4] Caudullo G, Welk E, San-Miguel-Ayanz J. Chorological maps for the main European woody species. *Data in Brief*. 2017;12:662-666. DOI: 10.1016/j.dib.2017.05.007
- [5] Correia AV, Oliveira AC. *Principais Espécies Florestais com Interesse para Portugal: Zonas de Influência Mediterrânica*. Lisbon: Direção-Geral das Florestas; 1999.
- [6] Natividade JV. *Subericultura*. 2nd ed. Lisbon: Ministério da Agricultura, Pescas e Alimentação. Direção Geral das Florestas; 1950.
- [7] Paul KI, Booth TH, Elliott A, Kirschbaum MUF, Jovanovic T, Polglase PJ. Net carbon dioxide emissions from alternative firewood-production systems in Australia. *Biomass and Bioenergy*. 2006;30(7):638-647. DOI: 10.1016/j.biombioe.2006.01.004
- [8] Alejano R, Tapias R, Fernández M, Torres E, Alaejos J, Domingo J. Influence of pruning and the climatic conditions on acorn production in holm oak (*Quercus ilex* L.) dehesas in SW Spain. *Annals of Forest Science*. 2008;65:209-209. DOI: 10.1051/forest:2007092
- [9] Martín D, Vázquez-Piqué J, Alejano R. Effect of pruning and soil treatments on stem growth of holm oak in open woodland forests. *Agroforestry Systems*. 2015;89:599-609. DOI: 10.1007/s10457-015-9794-x
- [10] Palma JHN, Paulo JA, Tomé M. Carbon sequestration of modern *Quercus suber* L. silvoarable agroforestry systems in Portugal: a YieldSAFE-based estimation. *Agroforestry Systems*. 2014;88:791-801. DOI: 10.1007/s10457-014-9725-2
- [11] Fernandes U, Costa M. Potential of biomass residues for energy production and utilization in a region of Portugal. *Biomass and Bioenergy*. 2010;34(5):661-666. DOI: 10.1016/j.biombioe.2010.01.009
- [12] Viana H, Cohen WB, Lopes D, Aranha J. Assessment of forest biomass for use as energy. GIS-based analysis of geographical availability and locations of wood-fired power plants in Portugal. *Applied Energy*. 2010;87(8):2551-2560. DOI: 10.1016/j.apenergy.2010.02.007
- [13] Malico I, Carrajola J, Gomes CP, Lima JC. Biomass residues for energy production and habitat preservation. Case study in a *montado* area in Southwestern Europe. *Journal of Cleaner Production*. 2016;112:3676-3683. DOI: 10.1016/j.jclepro.2015.07.131
- [14] Lourinho G, Brito P. Assessment of biomass energy potential in a region of Portugal (Alto Alentejo). *Energy*. 2015;81:189-201. DOI: 10.1016/j.energy.2014.12.021

- [15] Mesquita P, Pereira R, Malico I, Gonçalves AC, Sousa A. GIS based analysis of potential forest residues for energy in Alentejo, Portugal. In: Proceedings of the International Sustainable Energy Conference 2018; 3-5 October 2018; Graz. Austria.
- [16] Torres Rocha J, Malico I, Gonçalves AC, Sousa AMO. Análise do potencial de biomassa residual no Algarve, Portugal, baseada em SIG. *Ciência da Madeira (Brazilian Journal of Wood Science)*. 2020;11:42-52. DOI: 10.12953/2177-6830/rcm.v11n1p42-52
- [17] López-Rodríguez F, Atanet CP, Blázquez FC, Celma AR. Spatial assessment of the bioenergy potential of forest residues in the western province of Spain, Caceres. *Biomass and Bioenergy*. 2009;33(10):1358-1366. DOI: 10.1016/j.biombioe.2009.05.026
- [18] Gómez A, Rodrigues M, Montañés C, Dopazo C, Fueyo N. The potential for electricity generation from crop and forestry residues in Spain. *Biomass and Bioenergy*. 2010;34(5):703-719. DOI: 10.1016/j.biombioe.2010.01.013
- [19] Gonçalves AC, Sousa AMO, Mesquita P. Functions for aboveground biomass estimation derived from satellite images data in Mediterranean agroforestry systems. *Agroforestry Systems*. 2019;93:1485-1500. DOI: 10.1007/s10457-018-0252-4
- [20] Eurostat. Eurostat Database. 2020. Available from: <https://ec.europa.eu/eurostat/data/database> [Accessed: 2020-04-11]
- [21] Henriques S. *Energy Consumption in Portugal 1856-2006*. Roma: Consiglio Nazionale delle Ricerche;2009. 166 p.
- [22] Warde P. Firewood consumption and energy transition: a survey of sources, methods and explanations in Europe and North America. *Historia Agraria*. 2019;77:7-32. DOI: 10.26882/histagrar.077e02w
- [23] Pereira TC, Amaro A, Borges M, Silva R, Pina A, Canaveira P. Portuguese National Inventory Report on Greenhouse Gases, 1990-2018. Amadora: Portuguese Environmental Agency; 2020. 714 p.
- [24] DGEG. DGEG Statistics. 2020. Available from: <http://www.dgeg.gov.pt/> [Accessed 2020-04-12]
- [25] INE, I. P. /DGEG. Inquérito ao Consumo de Energia no Sector Doméstico 2010. Lisbon: Instituto Nacional de Estatística, I. P. and Direcção-Geral de Energia e Geologia; 2011. 115 p.
- [26] FAO. FAO Statistics. 2020. Available from: <http://www.fao.org/faostat/en/#data/FO> [Accessed 2020-04-12]
- [27] Gonçalves C, Alves C, Pio C. Inventory of fine particulate organic compound emissions from residential wood combustion in Portugal. *Atmospheric Environment*. 2012;50:297-306. DOI: 10.1016/j.atmosenv.2011.12.013
- [28] Azevedo JC, Ferreira MC, Nunes LF, Feliciano M. What drives consumption of wood energy in the residential sector of small cities in Europe and how that can affect forest resources locally? The case of Bragança, Portugal. *International Forestry Review*. 2016;18(1):1-12. DOI: 10.1505/146554816818206177
- [29] ICNF. 6º Inventário Florestal Nacional, IFN6. Lisbon: Instituto da Conservação da Natureza e das Florestas; 2015.
- [30] Martinopoulos G, Papakostas KT, Papadopoulos AM. A comparative review of heating systems in EU countries, based on efficiency and

fuel cost. *Renewable and Sustainable Energy Reviews*. 2018;90:687-699. DOI: 10.1016/j.rser.2018.03.060

[31] van Loo S, Koppejan J. *The Handbook of Biomass Combustion and Co-firing*. London: Earthscan; 2012. p 64.

[32] EEA. *EMEP/EEA Air Pollutant Emission Inventory Guidebook 2019*. EEA Report 13/2019. Technical Guidance to Prepare National Emission Inventories. Luxembourg: Publications Office of the European Union; 2019. DOI: 10.2800/293657.

[33] Fernandes AP, Alves CA, Gonçalves C, Tarelho L, Pio C, Schmidl C, Bauer H. Emission factors from residential combustion appliances burning Portuguese biomass fuels. *Journal of Environmental Monitoring*. 2011;13(11):3196-3206. DOI: 10.1039/C1EM10500K

[34] Pastorello C, Caserini S, Galante S, Dilara P, Galletti F. Importance of activity data for improving the residential wood combustion emission inventory at regional level. *Atmospheric Environment*. 2011;45(17):2869-2876. DOI: 10.1016/j.atmosenv.2011.02.070

[35] Borrego C, Valente J, Carvalho A, Sá E, Lopes M, Miranda AI. Contribution of residential wood combustion to PM10 levels in Portugal. *Atmospheric Environment*. 2010;44(5):642-651. DOI: 10.1016/j.atmosenv.2009.11.020

[36] Schmidl C, Lüsser M, Padouvas E, Lasselsberger L, Rzáca M, Ramirez-Santa Cruz C, Handler M, Peng G, Bauer H, Puxbaum H. Particulate and gaseous emissions from manually and automatically fired small scale combustion systems. *Atmospheric Environment*. 2011;45(39):7443-7454. DOI: 10.1016/j.atmosenv.2011.05.006

[37] Kindbom K, Mawdsley I, Nielsen OK, Saarinen K, Jónsson K, Aasestad K. Emission Factors for SLCP Emissions from Residential Wood Combustion in the Nordic Countries: Improved Emission Inventories of Short Lived Climate Pollutants (SLCP). Copenhagen: Nordic Council of Ministers; 2018. 76 p. DOI: 10.6027/TN2017-570

[38] Congalton RG, Oderwald RG, Mead RA. Assessing Landsat classification accuracy using discrete multivariate statistical techniques. *Photogrammetric Engineering & Remote Sensing*. 1983;49:1671-1678.

[39] Stehman SV. Estimating the kappa coefficient and its variance under stratified random sampling. *Photogrammetric Engineering & Remote Sensing*. 1996;62:401-407.

[40] van der Kroon B, Brouwer R, van Beukering PJH. The energy ladder: Theoretical myth or empirical truth? Results from a meta-analysis. *Renewable and Sustainable Energy Reviews*. 2013;20:504-513. DOI: 10.1016/j.rser.2012.11.045

[41] IEA. *IEA Statistics*. 2020. Available from: <https://www.iea.org/data-and-statistics> [Accessed 2020-03-05]

[42] Serrenho AC, Warr B, Sousa T, Ayres R, Domingos T. Useful Work Transitions in Portugal, 1856-2009. In: Reddy B, Ulgiati S, editors. *Energy Security and Development*. New Delhi: Springer; 2015. p. 133-146. DOI: 10.1007/978-81-322-2065-7\_8

[43] Malico I, Pereira SN, Costa MJ. Black carbon trends in southwestern Iberia in the context of the financial and economic crisis. The role of bioenergy. *Environmental Science and Pollution Research*. 2017;24(1):476-488. DOI: 10.1007/s11356-016-7805-8



# Koroch (*Pongamia pinnata*): A Promising Unexploited Resources for the Tropics and Subtropics

*Abul Kalam Mohammad Aminul Islam,  
Swapan Chakrabarty, Zahira Yaakob,  
Mohammad Ahiduzzaman and  
Abul Kalam Mohammad Mominul Islam*

## Abstract

The demand of petroleum fuel is increasing day by day. To meet up the energy demand, people of developing countries like Bangladesh basically used energy from indigenous sources, which are reducing quickly. Hence, it should be emphasized to explore unconventional fuel to overwhelm the crisis of petroleum fuels. Koroch (*Pongamia pinnata* L. Pierre) is a quick-growing leguminous tree that has the ability to grow on marginal land. Higher oil yield as well as physicochemical properties increases the suitability of using *Pongamia* as a promising substitute for supplying feedstock of biofuel production. Besides biofuel production, *P. pinnata* has multi-purpose uses as traditional medicine to animal feed, bio-pesticides, and bio-fertilizers. A better understanding and knowledge on the ecological distribution, botanical characteristics, physiology, and mode of reproduction along with physicochemical properties, and biosynthesis of oil is essential for sustainable production of biofuel from *P. pinnata*. In this chapter, we discuss overall biological and physicochemical properties as well as cultivation and propagation methods that provide a fundamentals for exploiting and improving of *P. pinnata* as a promising renewable source of biofuel feedstock.

**Keywords:** *Pongamia pinnata*, biofuel crops, underutilized, agriculture, environment

## 1. Introduction

Koroch (*P. pinnata*) is the member of Leguminosae family and Papilionoideae, more specifically the Millettieae tribe [1]. It is an oil seed tree known for its versatile applications but still remain unexploited. It is medium-sized, drought resistant, fast-growing, nitrogen fixing leguminous tree or glabrous shrub (15–25 m tall). It has been delineated as briefly deciduous or evergreen with a broad canopy of drooping or spreading branching behavior [2]. *P. pinnata* has a broadly distribution across coastal and riverine areas, primarily in humid tropical and subtropical environment of Indian subcontinent, Asia, Africa, Pacific, and America. It is found that the center of origin for *Pongamia* is most likely India (Figure 1) [3]. In the USA,



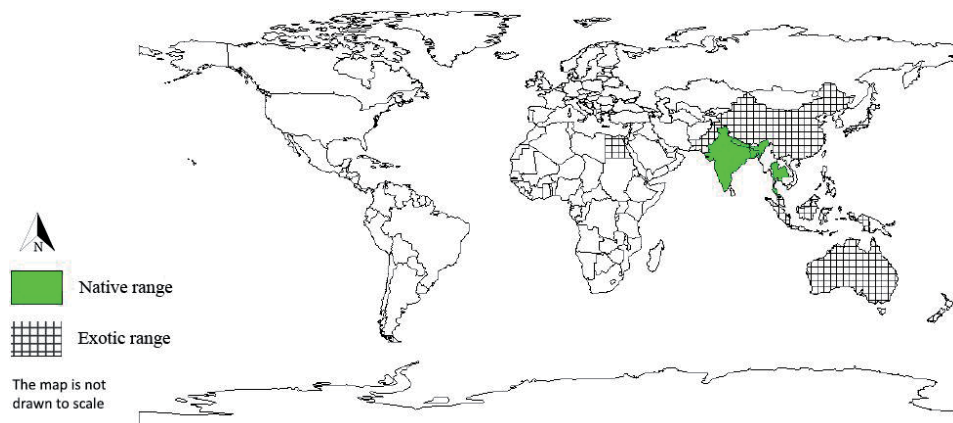


**Figure 1.**

*Distribution of P. pinnata. The species has been planted in the above shown countries on the map. It does not indicate that the species can be planted in every ecological zone within that countries or in other countries than those depicted. Source: Agroforestry database 4.0 [2].*

*P. pinnata* was introduced into Hawaii in the 1960s by Hillebrand. It is also found in the Andaman and Nicobar Islands, Bismarck, Archipelago, Northern Marianas, Djibouti, Tanzania, Zaire, Uganda, Caribbean, and Nicaragua. Traditionally, Koroch has been utilized in Indian sub-continent and neighboring countries as folk medicines, green manure, animal fodder, wood, and poison for fish and fuel [4, 5]. It is also used in agriculture and management of environment as fungicide, insecticide, nematicide [6], and soil improver as it fixes atmospheric nitrogen [1, 7]. *Pongamia* has bio-ameliorative capacity which adds nitrogen, phosphorous, potassium, and organic carbon to soil. It also improves the rural economic condition by engendering employment opportunities during different phases of cultivation and further processing.

As the reserve of non-renewable fossil fuel become declining, the society is increasingly aware of the alternate source for the production of fuels. Now it is discernible that biofuel has substantial contribution to the future energy demands both for domestic and industrial economics. For production of biofuel, USA and some European countries are looking for various vegetable oils such as soybean, rapeseed, and sunflower oil but these are edible in nature [8, 9]. Developing countries like Bangladesh, India, and some Asian countries cannot provide edible oil as fuel alternative. But some non-edible species such as Koroch (*P. pinnata*), Jatropha (*Jatropha curcas*), castor (*Ricinus communis*), neem (*Azadirachta indica*), etc. can be utilized as alternate fuel sources. Among these, *P. pinnata* has high potentiality for extraction of seed oil for manufacturing biodiesel. *Pongamia* seed comprises 30–40% oil that can be utilized as biodiesel through transesterification [10, 11]. It has the potentiality to provide a renewable energy resource and mitigate the competitive situation of the use of food crops as biofuel as it can be cultivated on marginal lands. Further research is needed into different areas of production and utilization of this species as a source of biodiesel [1, 12, 13]. Identification and evaluation of elite genotypes has been very limited for the production of seed and its oil content. To increase the biodiesel production, selection of elite genotypes for economically important traits such as high seed yield, high oil content, and desirable fatty acid composition is the pre-requirement [14]. Finally, large scale plantation of clonal stocks of elite genotypes needs to be done through encouraging afforestation programs. The overall objective of this chapter is to encourage exploiting these promising resources for sustainable biofuel production by

updating knowledge on the ecological and botanical characteristics, cultivation and propagation techniques and physicochemical properties and biosynthesis of *Pongamia* oil.

## 2. Ecological, botanical and cultural characteristics

### 2.1 Ecology of *P. pinnata*

*P. pinnata* is native to humid tropical and sub-tropical region. Areas having annual rainfall ranging from 500 to 2500 mm and maximum temperature 27–38°C and the minimum from 1 to 16°C is suitable for cultivation. Although it requires rain, trees need a dry season of 2–6 months. Probably, it ranges from Tropical Dry to Moist through Subtropical Dry to Moist Forest Life Zones [15, 16]. The trees also can cope with adverse climatic and soil moisture conditions and naturally generate in lowland forest on limestone and rocky coral outcrops on the coast, along the border of mangrove forest and along tidal streams and rivers. Mature trees can stand against water logging and slight frost, also counteract to high winds, draught, and salinity but are susceptible to freezing temperatures [17–19]. This species grows at altitude ranges from 0 to 1200 m, but in the Himalayan, foothills is not found above 600 m [2, 20]. It has been considered as a “maritime species” since it tends to grow naturally along coasts and riverbanks in India, Bangladesh, and Myanmar [16, 21]. *P. pinnata* can be grown in wider soil types ranging from stony to sandy to heavy swelling clay soils including oolitic limestone, but it exhibits best growth in deep, well-drained and sandy loam soils with certain moisture, but it does not grow well on very dry sands, although it tolerates saline conditions, alkalinity, and waterlogged soils even with its root in fresh or salt water [2]. If *Pongamia* grown on soils with a pH above 7.5, it will show nutritional deficiencies [22].

### 2.2 Botanical characteristics

The odd pinnately compound leaves with long slender leaf stalk are fixed up alternately and consist of 5–9 leaflets that are ovate elliptical or oblong (5–25 cm × 2.5–15 cm), obtuse-acuminate at the tip, rounded to cuneate at the base, not toothed at the edges and slightly thickened. The leaflets are settled in two or three pairs except largest terminal leaflet. In juvenile stage, leaves remain without hair and pinkish red in color and turn into glossy dull green above and dull green with prominent veins at maturity [2]. The raceme type inflorescence is 6–27 cm long, axillary, pendant and it has pairs of strongly balsamic flowers which are fascicled (2–4 together), short stalked and pea shaped (15–18 mm long). The calyx is campanulate, truncate (4–5 mm long), short dentate, lowermost lobe, sometimes longer and the corolla is white to pink, purple inside and brownish veins on the outside and five-toothed. The standard is sub-orbicular (1–2 cm), broad with basal auricles often with a green blotch and thin silky hair on the outside. The wings are oblong, oblique with a slightly adherent to obtuse keel. The stamens are monadelphous, vexillary stamen free at the base but jointed with others into a close tube. The ovary is sub sessile to short-stalked and pubescent and there are usually two ovules (rarely three). The style is filiform, upper half incurved and glabrous, and the stigma is small and terminal [2, 23].

Pods are short stalked, smooth, flattened but slightly swollen, oblique-oblong to ellipsoid (3–8 cm × 2–3.5 cm × 1–1.5), brown, thick-walled and leathery to sub-woody, reniform, hard, and indehiscent. It contains 1–2 seeds which are elliptical or

compressed ovoid, bean-like, with a brittle coat (1.5–2.5 cm × 1.2–2 cm × 0.8 cm), flattened, dark brown, and oily. The bark is thin gray to grayish-brown with smooth or faint vertical crevasse and yellow in the inside [24]. The branchlets are hairless with prominent pale stipule scars. The lateral roots are legionary, and the taproot is thick and long which is expanded about 10 m into the ground to uptake water from far beneath the ground surface without competing with other crops [2] (**Figure 2**).

### 2.3 Reproductive biology and propagation

In *P. pinnata*, mature buds open during 07:00–10:00 h with peak anthesis at 08:00 h and all the 10 anthers dehisce by longitudinal slits in mature bud stage. It happens approximately 3h prior to anthesis. The number of pollen grains per anther is  $2785 \pm 266$  and per flower 27,850 [25]. The prevailing environmental condition such as temperature, relative humidity, rainfall, etc. also attributed with the time of anthesis. The style is solid with central core of transmitting tissue in *P. pinnata*. Stigma receptivity may greatly caliber the rate of pollination success [26]. Raju and Rao [25] reported that in *P. pinnata*, the stigma receptivity is brought about 1 hour after anther dehiscence, but strong receptivity occurs during 09:00–16:00 h. The flowers start to concatenate gradually from 17:00 h onwards and close completely at 18:00 h. The closure of flower indicates by gradual movement of the standard petal to enclose the wing and keel petal completely. The closed flowers remain permanent which is analogous to mature buds. In pollinated flowers, the corolla drops-off on third day, staminal tube after 10 days and calyx after 20 days and unpollinated flowers fall off on the third day. The ovary consecutively enlarges and burgeons into a fruit. The flowering of *P. pinnata* generally occurs through the year in some areas in the world. In Southeast Asia falling of leaves occurs in April and burgeoning new leaves from May and flower blossom in April to June. Its pod gets mature during March–May of following year and ripening of seeds occurs during February–May (**Table 1**).

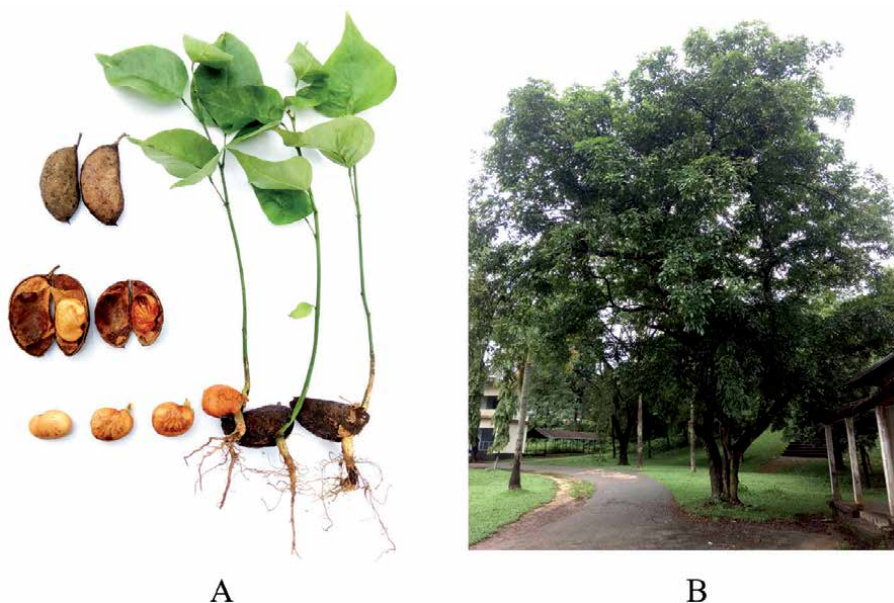


**Figure 2.** *P. pinnata* (A) pod, seed, and seedling, (B) whole *P. pinnata* tree. These photos of *P. pinnata* were taken from Murari Chand College campus, Sylhet, Bangladesh.

| Physiological stages    | Jan | Feb    | Mar   | Apr    | May         | Jun | Jul | Aug | Sep | Oct | Nov | Dec  |
|-------------------------|-----|--------|-------|--------|-------------|-----|-----|-----|-----|-----|-----|------|
| Seed ripening           |     | Yellow |       |        |             |     |     |     |     |     |     |      |
| Pod ripening            |     |        | Brown |        |             |     |     |     |     |     |     |      |
| Flowering               |     |        |       | Purple |             |     |     |     |     |     |     |      |
| Fruiting                |     |        |       |        |             |     |     |     |     |     |     | Blue |
| Falling of leaves       |     |        |       | Grey   |             |     |     |     |     |     |     |      |
| Emergence of new leaves |     |        |       |        | Light Green |     |     |     |     |     |     |      |

Source: Sangwan et al. [27].

**Table 1.**  
 Growth pattern of *P. pinnata*.

For raising of extensive plantations and successful introduction of a species, identification of plus trees with good genetic qualities and selection of most feasible methods for the multiplication of huge number of plants are essential. Propagation of *Pongamia* is needed for many purposes. The planting time of *Pongamia* cannot be band together with its reproductive phase (flowering and fruiting) in different eco-geographic zones and in such case, year-round supply of planting material can be obtained by vegetative propagation. Further, *Pongamia* can be cultivated in large areas of non-arable and wastelands for domestic and commercial purposes. *Pongamia* can be successfully propagated through seeds, cuttings [28–30] and tissue culture [3] and the viability of seeds remain up to 1 year. *P. pinnata* is a cross pollinated species, and vegetative propagation is advantageous to such type of plant in producing true to type plants with shorter juvenile period leading to early productivity [25]. It can be propagated through semi hard and hard wood cuttings consist of 3–4 nodes. The stem cutting shows better rooting in terms of percentage response, average root number, and average root length which are collected during January than those are collected during October [14]. By grafting, long juvenile period can be avoided as well as good productivity can be assured owing to elite scions. In grafting of *Pongamia*, one-year old seedlings are used as rootstock and the scions can be collected from a superior genotype with the same dimensions as that of rootstock. The most successful grafting may be Wedge grafting, and it is done by using 3months old seedling as the stocks and 12–15 cm length semi hard wood scion [31]. *P. pinnata* can be easily multiplied by grafting than that of propagation by cuttings. Tissue culture techniques have the potential to reproduce large quantities of genetically identical propagules from a small amount of source tissue within short time. Generally, explants used for regeneration through tissue culture are buds, meristems, and leaves. Regeneration of explants may occur through organogenesis or somatic embryogenesis [32, 33]. However, success of tissue culture is mostly dependent on genetic constituents of individual tree under identical tissue culture conditions [3].

### 3. *P. pinnata* seed oil as biodiesel feedstock

#### 3.1 Phytochemistry of *P. pinnata*

The chemical composition including major fatty acids of *P. pinnata* oil such as palmitic acid, stearic acid, linoleic acid, and eicosenoic acid indicate this oil could be

good source for biodiesel feedstock [34]. The fatty acid compositions of *Pongamia* seed oil are described in **Table 2**. Some alkaloids such as demethoxy, gamaty, glabin, glabro saponin, kaempferol, kanjone, kanugin, karangin, neuroglobin, pinnatin, pongamol, pongapin, quercetin, saponin, b-sitosterol, and tannin were reported to found in *P. pinnata*. 31.0% charcoal, 36.69% pyrolygneous acid, 4.3% acid, 3.4% ester, 1.9% acetone, 1.1% methanol, 9.0% tar, 4.4% pitches and losses, and 0.12m<sup>3</sup>/kg gas were found by destructive distillation of the wood (dry weight basis). The nutrient level of *Pongamia* leaf, twig, and fruit are shown in **Table 3**.

Furthermore, the comparative composition of the predominant fatty acids in *Pongamia* and other biofuel sources such as corn, soybean, canola, palm, *Jatropha*, *Algae*, and tallow indicate the suitability of *Pongamia* oil as biodiesel feedstock (**Table 4**). These chemical properties of *Pongamia* establish it as potential biofuel crop. It has also been reported that the oil yield (liter/ha per annum) from *Pongamia* seed is higher than corn, soybean, canola, and *Jatropha*. From 4th to 5th year onward of plantation of *Pongamia* starts flowering and fruiting and producing seeds in 4th–7th years and a full-grown tree may give 9–90 kg seed which indicates it has the potential of yielding 900–9000 kg seed/ha (assuming 100 trees/ha). In India, 24–27.5% oil can be extracted in mills, 18–22% can be extracted by village crushers [15]. The yield of kernel ranges 8–24 kg per tree [12, 35] and contains about 28–34% oil with high percentage of polyunsaturated fatty acids [36]. In Australia per tree produces approximately 30 kg seeds per annum and containing up to 55% oil [3].

### 3.2 Physicochemical properties

The physicochemical properties of *Pongamia* seed oil have established it as a renewable source of biodiesel production. Oleic acid is responsible for low cloud

| Fatty acids                | Molecular formula                              | Composition (%) | Structure  |
|----------------------------|--|-----------------|--|
| Saturated fat              | —  | 20.5            | —  |
| Monounsaturated fatty acid | —  | 46.0            | —  |
| Polyunsaturated fatty acid | —  | 33.4            | —  |
| Palmitic acid              | C <sub>16</sub> H <sub>32</sub> O <sub>2</sub> | 3.7–11.3        | CH <sub>3</sub> (CH <sub>2</sub> ) <sub>14</sub> COOH                      |
| Stearic acid               | C <sub>18</sub> H <sub>36</sub> O <sub>2</sub> | 2.4–9.8         | CH <sub>3</sub> (CH <sub>2</sub> ) <sub>16</sub> COOH                      |
| Oleic acid                 | C <sub>18</sub> H <sub>34</sub> O <sub>2</sub> | 44.5–71.3       | CH <sub>3</sub> (CH <sub>2</sub> ) <sub>14</sub> (CH=CH)COOH               |
| Linoleic acid              | C <sub>18</sub> H <sub>32</sub> O <sub>2</sub> | 10.8–24.75      | CH <sub>3</sub> (CH <sub>2</sub> ) <sub>12</sub> (CH=CH) <sub>2</sub> COOH |
| Linolenic acid             | C <sub>18</sub> H <sub>30</sub> O <sub>2</sub> | 2.9–6.3         | CH <sub>3</sub> (CH <sub>2</sub> ) <sub>10</sub> (CH=CH) <sub>3</sub> COOH |
| Eicosanoic acid            | C <sub>20</sub> H <sub>40</sub> O <sub>2</sub> | 9.5–12.4        | CH <sub>3</sub> (CH <sub>2</sub> ) <sub>18</sub> COOH                      |
| Behenic acid               | C <sub>22</sub> H <sub>44</sub> O <sub>2</sub> | 4.2–5.3         | CH <sub>3</sub> (CH <sub>2</sub> ) <sub>20</sub> COOH                      |
| Arachidic acid             | C <sub>20</sub> H <sub>40</sub> O <sub>2</sub> | 0.8–4.7         | CH <sub>3</sub> (CH <sub>2</sub> ) <sub>18</sub> COOH                      |
| Lignoceric acid            | C <sub>24</sub> H <sub>48</sub> O <sub>2</sub> | 1.1–3.5         | CH <sub>3</sub> (CH <sub>2</sub> ) <sub>22</sub> COOH                      |
| Myristic acid              | C <sub>14</sub> H <sub>28</sub> O <sub>2</sub> | 0.23            | CH <sub>3</sub> (CH <sub>2</sub> ) <sub>12</sub> COOH                      |
| Lauric acid                | C <sub>12</sub> H <sub>24</sub> O <sub>2</sub> | 0.1             | CH <sub>3</sub> (CH <sub>2</sub> ) <sub>10</sub> COOH                      |
| Capric acid                | C <sub>10</sub> H <sub>20</sub> O <sub>2</sub> | 0.1             | CH <sub>3</sub> (CH <sub>2</sub> ) <sub>8</sub> COOH                       |
| Unidentified               | —  | 0.1–1.05        | —  |

Source: Modified from Duke [15]; Ahmad et al. [37]; Karmee & Chadha [38]; Sarma et al. [15]; Kesari et al. [39].

**Table 2.**  
Fatty acid composition of crude oil of *Pongamia pinnata*.

| Parameter               | Leaf and twig | Fruit (pod and seed) |
|-------------------------|---------------|----------------------|
| Protein                 | —             | 17.4%                |
| Fatty oil               | —             | 27.5%                |
| Nitrogen free extract   | —             | 55.4%                |
| Crude fiber             | —             | 7.3%                 |
| Acid detergent fiber    | 40%           | 1.16%                |
| Ash                     | —             | 2.4%                 |
| Tannin                  | —             | 2.32 g/100 g         |
| Acid detergent lignin   | —             | 6.67%                |
| Trypsin                 | —             | 6.2 g/100 g          |
| P                       | 0.11, 0.14%   | 0.61%                |
| Ca                      | 1.54, 1.58%   | 0.65%                |
| K                       | 0.49, 0.62%   | 1.3%                 |
| Crude protein           | 18%           | 19.5 g/100 g         |
| Neutral detergent fiber | 62%           | 17.98%               |
| N                       | 0.71, 1.16%   | 5.1%                 |
| Moisture                | —             | 19.0%                |
| Starch                  | —             | 6.6%                 |
| Mucilage                | —             | 13.5%                |
| Na <sup>+</sup>         | —             | 0.8%                 |

Source: Duke [15] and Singh [40].

**Table 3.**  
 Level of nutrients present in *Pongamia* leaf and fruit.

| Plant              | Oil yield (liter/ha per annum) | Percent oleic acid (C18:1) | Percent palmitic acid (C16:0) | Percent stearic acid (C18:0) | Reference                                    |
|--------------------|--------------------------------|----------------------------|-------------------------------|------------------------------|--|
| Corn               | 172                            | 30.5–43                    | 7–13                          | 2.5–3                        | Dantas et al. [41]                           |
| Soybean            | 446                            | 22–30.8                    | 2.3–11                        | 2.4–6                        | Hildebrand et al. [42]                       |
| Canola             | 1196                           | 55–63                      | 4–5                           | 1–2                          | Moser [43]                                   |
| <i>Jatropha</i>    | 1892                           | 34.3–45.8                  | 13.4–15.3                     | 3.7–9.8                      | Becker and Makkar [44];<br>Islam et al. [45] |
| Palm oil           | 5950                           | 38.2–43.5                  | 41–47                         | 3.7–5.6                      | Sarin et al. [46]                            |
| Algae <sup>*</sup> | 59,000                         | 1.7–14.3                   | 3.7–40                        | 0.6–6                        | Hu et al. [47]                               |
| Tallow             | Not applicable                 | 26–50                      | 25–37                         | 14–29                        | CanakciandSanli [48]                         |
| <i>Pongamia</i>    | 3600–4800                      | 25.3–68.3                  | 5.41–9.49                     | 2.15–8                       | Biswas et al. [3]                            |

<sup>\*</sup>The yield of Algae derived from smaller volume trails of multiple species.

**Table 4.**  
 Major components of oil of several plants currently used as feedstock for biofuel production.

point so it is considered as important fatty acid in biodiesel production. Palmitic acid and stearic acid molecules have less mobility, thus increases the cloud point. As oxidation occurs in unsaturated C18 acids (linoleic acid and linolenic acid), these

are less desirable (**Table 5**). These properties of *Pongamia* biodiesel ascertained as per ASTM (American Standards for Testing and Materials) standards which consist of viscosity (4.78 mm<sup>2</sup>/s) that controls the characteristics of injection from diesel injector and for better performance the viscosity level should be minimized. The saponification number (187 mg/KOH) shows the relative length fatty acid chain; the iodine value (91I<sub>2</sub> 100/g) indicates the total number of double bonds among the respective fatty acids; and the cetane number (41.7) gives an indication of ignition quality of the fuel. The flash point (144°C) is also an important property. Flash point is the temperature at which it ignites when exposed to a flame or spark. The flash point of biodiesel is higher than that of petroleum diesel, that's why it is safe for transport purpose. The lowest temperature at which oil can flow is known as pour point (-3°C for crude oil) and the cloud point (6°C) which is the temperature that will cause the dissolution of dissolved solids from the oil and indicates the possibility of use of biodiesel in temperature and cold climates. The pour point and cloud point of *Pongamia* biodiesel indicates the suitability of its use in tropical and some temperate regions. This non-edible *Pongamia* vegetables oil is the source of greenhouse gas neutral and environmentally acceptable biofuel. As an alternate to fossil fuel, *Pongamia* biodiesel can reduce CO<sub>2</sub>, CO, HC, and NO emission by producing about 0.52 million tone of biodiesel per year from the unused lands [49].

| Property                   | <i>Pongamia</i> crude oil | <i>Pongamia</i> biodiesel | Diesel                  |
|----------------------------|---------------------------|---------------------------|-------------------------|
| Color                      | Yellowish red             | Amber yellow              | White or slightly amber |
| Odor                       | Characteristic odd odor   | —                         | —                       |
| Density                    | 0.92 g/m <sup>3</sup>     | 0.86 g/m <sup>3</sup>     | 0.84 g/m <sup>3</sup>   |
| Kinematic viscosity @ 40°C | 40.2 mm <sup>2</sup> /s   | 4.78 mm <sup>2</sup> /s   | 2.98 mm <sup>2</sup> /s |
| Acid value                 | 5.40 mg/KOH               | 0.42 mg/KOH               | 0.35 mg/KOH             |
| Iodine value               | 87(I <sub>2</sub> 100/g)  | 91(I <sub>2</sub> 100/g)  | —                       |
| Saponification value       | 184 (mg/KOH)              | 187 (mg/KOH)              | —                       |
| Calorific value            | 8742 kcal/kg              | 3700 kcal/kg              | 4285 kcal/kg            |
| Specific gravity           | 0.925                     | —                         | —                       |
| Unsaponifiable matter      | 2.9% w/w                  | —                         | —                       |
| Flash point                | 225°C                     | 144°C                     | 74°C                    |
| Fire point                 | 230°C                     | —                         | —                       |
| Cloud point                | 3.5 °C                    | 6 °C                      | -16°C                   |
| Pour point                 | -3 °C                     | —                         | —                       |
| Boiling point              | 316°C                     | —                         | —                       |
| Cetane number              | 42                        | 41.7                      | 49.0                    |
| Copper strip corrosion     | No corrosion observed     | —                         | —                       |
| Ash content                | 0.07%                     | 0.005%                    | 0.02%                   |
| Moisture                   | —                         | 0.02%                     | 0.02%                   |
| Carbon residue             | 1.51%                     | 0.005%                    | 0.01%                   |

Source: Modified from Bobade and Khyade [39, 50].

**Table 5.** Physico-chemical properties of *P. pinnata* oil with diesel.

Successful implementation of biofuels is depending on the supply of feedstock from non-food crops as well as the capacity to grow on marginal land that is not used for the cultivation of food crops [51]. From 15 years onward up to more 20 years, a *Pongamia* tree can produce 25–100 kg seed per year and after 30 years onward even up to 100 years, and each tree may produce 300–500 kg of seed per year with proper maintenance [52]. In this regard, *Pongamia* has the potentiality to supply significant amount of biofuel feedstock.

### 3.3 Biodiesel production

Biodiesel saves about 74% carbon dioxide emissions than conventional fuel [53]. Biodiesel from *P. pinnata* seed oil is the most useful product. However, *P. pinnata* seed oil could not considered to be suitable for direct use in the diesel engine due to high viscosity, free fatty acid content, and formation of gum during storage and combustion that causes thickening of lubricating oil and carbon deposits [54]. These drawbacks can be overcome by transesterification of bio-oil or straight vegetable oil that can produce biodiesel of nearly same properties as petroleum diesel. The transesterification process is the reaction of a triglyceride (with an alcohol to produce ester and glycerol). A triglyceride has a glycerine molecule as its base with three long chain fatty acids annexed. The characteristics of the fat are determined by the nature of the fatty acids subsumed to the glycerine which affects the characteristics of the biodiesel. In production of biodiesel, vegetable oil in the form of triglycerides reacts with small chain alcohol (methanol, ethanol, propanol, etc.) in the presence of homogeneous catalyst such as base (KOH, NaOH) or acid (HCl, H<sub>2</sub>SO<sub>4</sub>, H<sub>3</sub>PO<sub>4</sub>). The process is also called alcoholysis. When methanol is used, it is called methanolysis and esters that produced in methanolysis are called fatty acid methyl esters (FAMES) and in case of ethanol, the process is termed as ethanolysis and the esters produced in this process are called fatty acid ethyl esters (FAEEs) [55]. The transesterification is a reversible reaction, so alcohol must be added in excess to ensure the reaction in the right direction. 80% methyl ester and 20% glycerin can be produced as by product through transesterification at low temperature and pressure [39]. The conditions for optimal reaction such as concentration of catalyst, molar ratio of alcohol/oil, and temperature have been investigated and optimized by Meher et al. [56]. Furthermore, Azam et al. [10] have reported that the FAMES of *Pongamia* seed oil is most suitable as it meets the standard specifications of biodiesel. The reaction during transesterification can be described as below [57] (**Figure 3**).

The transesterification process for biodiesel production from *Pongamia* was described by Mahanta et al. [57]. Briefly, a known amount of oil was preheated to remove the moisture from the oil and then the oil was transferred to a reaction chamber in a hot water bath where 65–70°C temperature should be maintained. Based on the acid value of the oil, calculated amount of KOH and methanol were added and the mixture was stirred for 10–15 minutes for complete mixing. The temperature of the reaction should be maintained at 60°C. The reaction was considered to be completed when a clear separation was observed between oil and glycerol. After removing from the water bath, the mixture was kept for 7–8 hours for complete separation. After cooling, two layers were differentiated: the upper layer is methyl ester (biodiesel) with a little amount of KOH, soap, and other impurities and the lower layer is glycerol. The biodiesel was collected by drain out of the upper layer, and remaining KOH, soap, and impurities were removed by using a separating funnel. Twenty-five percent by volume of impure methyl ester with warm distilled water is taken in a separating funnel. The impurities, KOH, and soap were solubilized in water and settled at the bottom of the funnel that can be drained



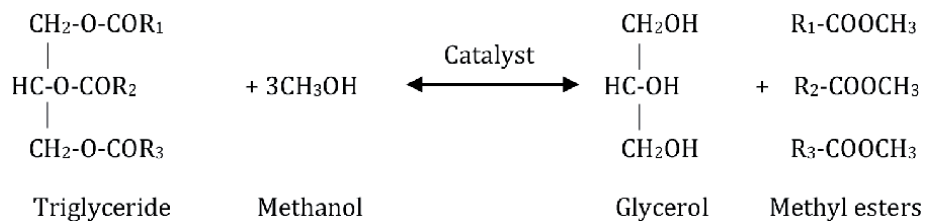


**Figure 3.**  
 Transesterification reaction for biodiesel production.

out easily. This washing was repeated until the pH of the separated water reaches at level of 7–8. Finally, amber yellow color biodiesel was obtained from *P. pinnata* seed oil [57]. Transesterification of 100 L of *P. pinnata* crude oil can produce about 85 L of biodiesel and 15 L of glycerin as byproduct [58]. The Koroch tree has long life up 100 years. Its seed contains 25–35% non-edible oil extracted by mechanical press. It is also reported that 1 L of crude oil can be produced from about 4 kg of *P. pinnata* seed which ultimately can produce about 896 mL of biodiesel [59]. After oil extraction, oil cake, a by-product could be used as fertilizer or solid fuel [52].

## 4. Other uses and benefits

### 4.1 Biogas production and bio-fertilizer

The biomass waste from biofuel crops like *Jatropha* can be utilized for the production of biogas and bio-fertilizer [60]. Gunaseelan et al. [61] studied the potential of biogas (CH<sub>4</sub>) production from NaOH treated and untreated *P. pinnata* biomass waste. The results indicated that maximum amount of CH<sub>4</sub> was produced from untreated seeds, whereas lower amount of CH<sub>4</sub> was produced from withered yellow leaves of *P. pinnata*. The yield of CH<sub>4</sub> from fiber rich leaves and pod husk was increased by 15–22% when treated with NaOH [61]. The deoiled cake of *Pongamia* cannot be used for animal feeding or agricultural farming directly due to its toxic properties. The generation of biogas by anaerobic digestion of oilseed cakes would be best solution for its efficient utilization which provides a better quality renewable gaseous fuel (biogas) than cattle dung to generate biogas. However, the co-digestion of cattle dung with *Pongamia* seed cakes accelerate the digestion process. The C-N ratio of *P. pinnata* oil seeds cake was found 8.7, and the pH value ranges between 4.8–9.4 depending on percentage of cattle dung, cake, and water dilution ratio. Total biogas generation potential from *P. pinnata* cakes has been estimated as 377 million cubic meter from 0.145 million tone of *P. pinnata* oil cakes [62]. Along with fuel, anaerobic digestion gives good manorial value effluent for organic farming. *P. pinnata* oil cake contains higher amount of N, P, K (4%, 1%, 1%) than vermicompost [63].

### 4.2 Firewood and briquette

The wood of *P. pinnata* is considered as low quality timber due to its softness, tendency to split during sowing, and vulnerability to insect attack [16]. Traditionally, *P. pinnata* wood is used as fuel in rural areas in India, Bangladesh, and other neighboring regions. It has no distinct heartwood and varies from white to yellowish gray color with a calorific value of 19.32 MJ/kg. The ash produced from burning wood is used for dyeing [64]. Briquettes can be produced from shell and deoiled cake of *Pongamia*. The harvested pods are decorticated to separate the

shells, and the shells are pulverized to prepare the materials for briquette preparation. The pulverized product is blended with other biomass to increase calorific value and compressed with a piston press to produce the *Pongamia* briquette. Briquettes that produced by following typical method result in a high heating value of 4000 kcal/kg [63].

### 4.3 Medicinal and pharmaceutical use

*P. pinnata* has been used as folk medicine or crude drug from pre-modern period. Recently, many pharmacological studies have been carried out on *P. pinnata*. Ethanolic extract of *P. pinnata* leaf was reported to have anti-inflammatory activity against various stages (acute, sub-acute, and chronic) of inflammation and also anti-pyretic function against Brewer's yeast-induced pyrexia [65]. Shing and Pandey [66] showed that petroleum ether extraction of seeds of *P. pinnata* have powerful acute anti-inflammatory activity, whereas the aqueous suspension showed pro-inflammatory activity. It shows anti-plasmodial activity against *Plasmodium falciparum* [67]. The leaf extract of Koroch shows defensive characteristics against blood ammonia and urea levels in ammonium chlorides induced hyperammonemia [68]. Shoba and Thomas [69] reported on the protective effect of *P. pinnata* in inhibiting castor oil induced diarrhea. Brijesh et al. [70] found that the crude extract of dried leaves of *P. pinnata* had a potential effect against the production of cholera toxin and enteroinvasive bacterial strains that cause diarrhea. Antihyperglycaemic and Antilipidperoxidative effects of ethanolic extract of *Pongamia* flowers in alloxan induced diabetic rats were evaluated by Punitha and Manoharan [71]. Rameshthangam and Ramasamy [72] noticed the antiviral activity of bis (2-methylheptyl) phthalate isolated from *Pongamia* leaves against White Spot Syndrome Virus of *Penaeus mondon fabricius*. Oral injection of ethanolic extract and purified compound from the leaves of *Pongamia pinnata* has increased the survival of WSSV infected *Penaeus mondon*. The fruits and leaves extract of *Pongamia pinnata* possess antifilarial potential of on cattle filarial parasite which was investigated by Uddin et al. [73].

### 4.4 Bio-pesticide

Oil extracted from seeds of *Pongamia* used in agriculture as it functions against the insect pests. The main active ingredient of *Pongamia* oil is Karanjin which used as acaricide and insecticide. Karanjin also possess nitrification inhibitory properties. Application of the insecticide based on *Pongamia* oil causes high larval mortality of *Plutella xylostella* and significantly reduces the damage caused by feeding to crops. The product formulation based on the combination of *P. pinnata* and *Thymus vulgaris* or *Foeniculum vulgare* essential oils can be recommended against *Plutella xylostella* larvae for protection of cabbage crops [74]. Mechanical extraction of *Pongamia* seeds produces oil seeds cakes as byproducts. These seed cakes are generally toxic but the toxicity can be minimized by using them as bio-pesticides. Further this oil cake can be used as low cost substrates for the growth of the fungus *Paecilomyces* playing an important role in controlling nematodes. The aqueous and methanolic extracts and the crude active components of the cake cause significant termite mortality [75].

### 4.5 Nitrogen fixation and nodulation

*P. pinnata* has the quality to fix atmospheric nitrogen. The nodulation of most legumes occurs effectively with one or few specific species of *Rhizobia*. However,

nodulation process of *Pongamia* has been found to be quite promiscuous, which make symbiosis with different species of both *Bradyrhizobium* and *Rhizobium* [76–78]. The capacity of *Pongamia* to fix nitrogen with these species of *Rhizobium* has not been reported, and the establishment of superior inoculants was not possible [78]. Nodulation in legume can either be determinate with a spherical morphology due to lack of persistent meristems or indeterminate where holding of meristems produces more cylindrical nodules. *Pongamia* nodules have been noticed to be determinate in nature [1, 79] but older *Pongamia* trees will indicate a combination of spherical and coralloid nodules. Therefore, as a tree, *Pongamia* represents both qualitatively and quantitatively major features found in other better-characterized annual legume crops, such as soybean and pea (*Pisum sativum* L.).

Besides above discussed uses different part or as whole *Pongamia* also be used for shade and shelter, controlling soil erosion, soil reclamation, fish poison, apiculture, fiber, tannin or dyestuff, and ornamentals.

## 5. Current status and future prospects and challenges

*Pongamia* is versatile plant, and it is more valued for its biodiesel properties but its production is not satisfactory level. In Bangladesh, commercial cultivation and production of biodiesel and bio-ethanol from *P. pinnata* has not started yet [16]. *Pongamia* and other fuel crops are not planted commercially, and no mass plantation program has been taken yet. *Pongamia* is planted in lower areas of Sunamganj district of Bangladesh for windbreak and to control soil erosion. In Bangladesh, Koroch was naturally grown at Ratargul Swamp Forest, Gowainghat, Sylhet. The International Crops Research Institute for the Semi-Arid Tropics (ICRISAT), Andhra Pradesh, India is supporting innovative research on the *Pongamia* “journey from Forest to Micro-enterprise” to ameliorate rural liflode and empowerment. The purpose of this organization is to exonerate the degraded lands and conserve the environments, to assess and elevate sustainable crop management practices and to assess the enhancement of income of self-helped groups by planting *Pongamia*. There is also another target to value addition of its byproducts after extraction of oil. There is about 28 institution in India, and they are working for undertaking joint research on some issues such as marking of prime planting materials, seed resource assessment, collection and storage, phonological and chemical analysis for characterization, improvement of trees to get quality and reliable seed source, multi-location trials of superior planting materials, and agro-forestry models for evolving good intercropping system of tree borne oilseeds [54]. It has been cultivated outside its native range in South-eastern Queensland, Australia.

To fulfill the future demands for biodiesel and to increase the production of *Pongamia*, mass plantation program should be taken through commercially or social afforestation by the Government, NGOs, and by Private Public Partnership. Local communities who participate in this program may not be much interested until they know the value of plant genetic resources. The involvement of the local people will be assured through a program to aware them by display of charts and posters arranged in the local language and also by field demonstration to present the economic viability and feasibility of cultivation as an alternative choice on degraded lands and community wastelands. Therefore, value addition to a plant, thereby emphasizing on the livings of the local communities, would be an efficient mode for propagation and management in *Pongamia*. Field-level laborers are engaged in extension activities of *Pongamia* cultivation should be trained on the different aspects of *Pongamia* plant cultivation such as value of superior planting elements, collection of elite germplasm, developing nursery, plantation establishment, and

post cultivation care. Clonal cuttings of the elite materials or candidate plus tree can be supplied to enhance the plantation of *Pongamia* on more marginal and waste-lands. Different improved plant breeding methods should be used to develop of early bearing *Pongamia* varieties so that it shortens the growth period and increases oil content with desirable oil properties especially monounsaturated fatty acid from the point of view of using it as biofuel. Again to produce *Pongamia* seeds all the year round, selection of day neutral varieties is necessary. So development of high yield *Pongamia* varieties produced in the “off season” could also be attempted for strategies toward development of dwarf high-yielding varieties that can minimize the management cost also be possible. Further techniques for development of location-specific genotypes that are resistant to adverse growing condition such as salinity, draught, alkalinity, and water logging can be considered as future research so as to enhance the range of growth and cultivation of *Pongamia*.

## 6. Conclusion

*Pongamia* is an underutilized species but it has great potential for use in production of biodiesel and in pharmaceuticals. Furthermore, wasteland can be effectively used for cultivation and subsequent agronomic or silvicultural practices and also helps in bucolic development and poverty alleviation through development of employment opportunities. To increase the production of *Pongamia* standardization of the vegetative propagation techniques, large-scale production of genetically superior saplings throughout the year, appropriate planting models for different agro-ecological zones and land uses and post planting care are of prime importance. Thus, the future success of *Pongamia* as a sustainable source of feedstock for the biofuel industry is dependent on an extensive knowledge of the genetics, physiology, and propagation of this legume. Moreover, research activities should be targeted to ameliorate the physic-chemical properties and plant growth as it relates to oil biosynthesis.

## Acknowledgements

The author acknowledges the support of the Ministry of Science and Technology (NST), Government of Bangladesh for providing all research inputs and cost of the project. The authors would like to thank NST authority for their support.

## Conflict of interest

There is no conflict of interest regarding the publication of this chapter.

## **Author details**

Abul Kalam Mohammad Aminul Islam<sup>1\*</sup>, Swapan Chakrabarty<sup>1</sup>, Zahira Yaakob<sup>2</sup>,  
Mohammad Ahiduzzaman<sup>3</sup> and Abul Kalam Mohammad Mominul Islam<sup>4</sup>

1 Department of Genetics and Plant Breeding, Faculty of Agriculture, Bangabandhu Sheikh Mujibur Rahman Agricultural University, Gazipur, Bangladesh

2 Department of Chemical and Process Engineering, Faculty of Engineering and Built Environment, Universiti Kebangsaan Malaysia, Selangor, Malaysia


3 Department of Agro-Processing, Faculty of Agriculture, Bangabandhu Sheikh Mujibur Rahman Agricultural University, Gazipur, Bangladesh

4 Department of Agronomy, Faculty of Agriculture, Bangladesh Agricultural University, Mymensingh, Bangladesh

\*Address all correspondence to: aminulgp@bsmrau.edu.bd

## **IntechOpen**

---

© 2020 The Author(s). Licensee IntechOpen. Distributed under the terms of the Creative Commons Attribution - NonCommercial 4.0 License (<https://creativecommons.org/licenses/by-nc/4.0/>), which permits use, distribution and reproduction for non-commercial purposes, provided the original is properly cited. 

## References

- [1] Scott PT, Pregelj L, Chen N, Hadler JS, Djordjevic MA, Gresshoff PM. *Pongamia pinnata*: An untapped resource for the biofuels industry of the future. *Bioenergy Research*. 2008;1(1):2-11
- [2] Orwa C, Mutua A, Kindt R, Jamnadass R, Simons A. *Agroforestry Database: A Tree Species Reference and Selection Guide Version 4.0*. Nairobi, KE: World Agroforestry Centre ICRAF; 2009
- [3] Biswas B, Kazakoff SH, Jiang Q, Samuel S, Gresshoff PM, Scott PT. Genetic and genomic analysis of the tree legume as a feedstock for biofuels. *Plant Genome*. 2013;6(3):1-15
- [4] Bottoms T, Lane M. Bama country - aboriginal homelands. In: McDonald GG, Lane MM, editors. *Securing the Wet Tropics*. Leichardt, NSW: Federation Press; 2000. pp. 32-47
- [5] Cribb AB, Cribb JW. *Useful Wild Plants in Australia*. Sydney: Collins; 1981
- [6] Chopade V, Tankar A, Pande V, Tekade A, Gowekar N, Bhandari S, et al. *Pongamia pinnata*: Phytochemical constituents, traditional uses and pharmacological properties: A review. *International Journal of Green Pharmacy*. 2008;2(2):72
- [7] Uddin MB, Mukul SA, Khan MASA, Hossain MK. Seedling response of three agroforestry tree species to phosphorous fertilizer application in Bangladesh: Growth and nodulation capabilities. *Journal of Forestry Research*. 2009;20(1):45-48
- [8] Shereena KM, Thangaraj T. Biodiesel: An alternative fuel produced from vegetable oils by transesterification. *Electronic Journal of Biology*. 2009;5(3):67-74
- [9] Barnwal BK, Sharma MP. Prospects of biodiesel production from vegetable oils in India. *Renewable and Sustainable Energy Reviews*. 2005;9:363-378
- [10] Azam MM, Waris A, Nahar NM. Prospects and potential of fatty acid methyl esters of some non-traditional seed oils for use as biodiesel in India. *Biomass and Bioenergy*. 2005;29(4):293-302
- [11] Nagaraj G, Mukta N. Seed composition and fatty acid profile of some tree borne oilseeds. *Journal of Oilseeds Research*. 2004;21(1): 117-120
- [12] Kesari V, Krishnamachari A, Rangan L. Systematic characterisation and seed oil analysis in candidate plus trees of biodiesel plant, *Pongamia pinnata*. *Annals of Applied Biology*. 2008;152(3):397-404
- [13] Mukta N, Sreevalli Y. Propagation techniques, evaluation and improvement of the biodiesel plant, *Pongamia pinnata* (L.) Pierre—A review. *Industrial Crops and Products*. 2010;31(1):1-12
- [14] Kesari V, Krishnamachari A, Rangan L. Effect of auxins on adventitious rooting from stem cuttings of candidate plus tree *Pongamia pinnata* (L.), a potential biodiesel plant. *Trees - Structure and Function*. 2009;23(3):597-604
- [15] Duke JA. *Handbook of Energy Crops*, unpublished. 1983. Available from: [https://www.hort.purdue.edu/newcrop/duke\\_energy/Pongamia\\_pinnata.html](https://www.hort.purdue.edu/newcrop/duke_energy/Pongamia_pinnata.html) [Accessed: 03 June 2017]
- [16] Daniel JN. *Pongamia pinnata*-a nitrogen fixing tree for oilseed. In: *NFT Highlights*. Arkansas, USA: Winrock International; 1997

- [17] Gilman EF, Watson DG. *Pongamia pinnata* Pongam. In: Fact Sheet ST-498. A series of the Environmental Horticulture Department, Florida Cooperative Extension Service, Institute of Food and Agricultural Sciences. Gainesville, FL, USA: University of Florida; 1994
- [18] Misra CM, Singh SL. Ecological evaluation of certain leguminous trees for agroforestry. Nitrogen Fixing Tree Research Reports. 1987;5:5
- [19] Tomar OS, Gupta RK. Performance of some forest tree species in saline soils under shallow and saline water-table conditions. Plant and Soil. 1985;87(3):329-335
- [20] Troup RS, Joshi HB. Troup's Silviculture of Indian Trees, Vol. IV Leguminosae. Dehra Dun, India: Forest Research Institute and Colleges; 1983. pp. 33-38
- [21] CAB International. Forestry Compendium Global Module. Wallingford, UK: CAB International; 2000
- [22] Dwivedi G, Jain S, Sharma MP. *Pongamia* as a source of biodiesel in India. Smart Grids and Renewables. 2011;2:184-189
- [23] Allen ON, Allen EK. The Leguminosae. Madison, Wisconsin, USA: The University of Wisconsin Press; 1981. p. 812
- [24] Daniel JN, Hegde NG. Tree-borne oilseeds in agroforestry. In: Proceedings of the National Seminar on Changing Global Vegetable Oils Scenario: Issues and Challenges before India. Hyderabad, India: Indian Society of Oil seeds Research Publication; 2007. pp. 263-276
- [25] Raju AS, Rao SP. Explosive pollen release and pollination as a function of nectar-feeding activity of certain bees in the biodiesel plant, *Pongamia pinnata* (L.) Pierre (Fabaceae). Current Science (Bangalore). 2006;90(7):960
- [26] Galen C, Zimmer KA, Newport ME. Pollination in floral scent morphs of *Polemonium viscosum*: A mechanism for disruptive selection on flower size. Evolution. 1987;41(3):599-606
- [27] Sangwan S, Rao DV, Sharma RA. A review on *Pongamia pinnata* (L.) Pierre: A great versatile leguminous plant. Nature and Science. 2010;8(11):130-139
- [28] Handa AK, Nandini D. An alternative source of biofuel, seed germination trials of *Pongamia pinnata*. International Journal of Forest Usufructs Management. 2005;6(2):75-80
- [29] Singh KP, Dhakre G, Chauhan SVS. Effect of mechanical and chemical treatments on seed germination in *Pongamia glabra* L. Seed Research. 2005;33(2):169
- [30] Kesari V, Das A, Rangan L. Effect of genotype and auxin treatments on rooting response in stem cuttings of CPTs of *Pongamia pinnata*, a potential biodiesel legume crop. Current Science. 2010;98(9):1234-1237
- [31] Karoshi VR, Hegde GV. Vegetative propagation of *Pongamia pinnata* (L.) Pierre: Hitherto a neglected species. Indian Forester. 2002;128(3):348-350
- [32] Biswas B, Scott PT, Gresshoff PM. Tree legumes as feedstock for sustainable biofuel production: Opportunities and challenges. Journal of Plant Physiology. 2011;168(16):1877-1884
- [33] Sujatha K, Panda BM, Hazra S. De novo organogenesis and plant regeneration in *Pongamia pinnata*, oil producing tree legume. Trees. 2008;22(5):711-716

- [34] Bobade SN, Khyade VB. Detail study on the properties of *Pongamia pinnata* (Karanja) for the production of biofuel. *Research Journal of Chemical Sciences*. 2012;2(7):16-20
- [35] Bringi NV. *Non-Traditional Oilseeds and Oils in India*. New Delhi: Oxford and IBH Pub. Co. Pvt. Ltd; 1987. pp. 143-166
- [36] Sarma AK, Konwer D, Bordoloi PK. A comprehensive analysis of fuel properties of biodiesel from Koroch seed oil. *Energy & Fuels*. 2005;19(2):656-657
- [37] Ahmad S, Ashraf SM, Naqvi F, Yadav S, Hasnat A. A polyesteramide from *Pongamia glabra* oil for biologically safe anticorrosive coating. *Progress in Organic Coatings*. 2003;47(2):95-102
- [38] Karmee SK, Chadha A. Preparation of biodiesel from crude oil of *Pongamia pinnata*. *Bioresource Technology*. 2005;96(13):1425-1429
- [39] Kesari V, Das A, Rangan L. Physico-chemical characterization and antimicrobial activity from seed oil of *Pongamia pinnata*, a potential biofuel crop. *Biomass and Bioenergy*. 2010;34(1):108-115
- [40] Singh RV. *Fodder Trees of India*. New Delhi, India: Oxford and IBH Co.; 1982
- [41] Dantas M, Conceição M, Fernandes V Jr, Santos N, Rosenhaim R, Marques A, et al. Thermal and kinetic study of corn biodiesel obtained by the methanol and ethanol routes. *Journal of Thermal Analysis and Calorimetry*. 2007;87(3):835-839
- [42] Hildebrand DF, Li R, Hatanaka T. Genomics of soybean oil traits. In: *Genetics and Genomics of Soybean*. New York: Springer; 2008. pp. 185-209
- [43] Moser BR. Biodiesel production, properties, and feedstocks. *In Vitro Cellular & Developmental Biology – Plant*. 2009;45(3):229-266
- [44] Becker K, Makkar HPS. *Jatropha curcas*: A potential source for tomorrow's oil and biodiesel. *Lipid Technology*. 2008;20(5):104-107
- [45] Islam AKMA, Primandari SRP, Anuar N, Yaakob Z, Osman M. Preparation of biodiesel from *Jatropha* hybrid seed oil through two step transesterification. *Energy Sources, Part A: Recovery, Utilization, and Environmental Effects*. 2015;37(14):1550-1559
- [46] Sarin R, Sharma M, Sinharay S, Malhotra RK. *Jatropha*-palm biodiesel blends: An optimum mix for Asia. *Fuel*. 2007;86(10):1365-1371
- [47] Hu Q, Sommerfeld M, Jarvis E, Ghirardi M, Posewitz M, Seibert M, et al. Microalgal triacylglycerols as feedstocks for biofuel production: Perspectives and advances. *The Plant Journal*. 2008;54(4):621-639
- [48] Canakci M, Sanli H. Biodiesel production from various feed stocks and their effects on the fuel properties. *Journal of Industrial Microbiology & Biotechnology*. 2008;35(5):431-441
- [49] Halder PK, Paul N, Beg MRA. Prospect of *Pongamia pinnata* (Karanja) in Bangladesh: A sustainable source of liquid fuel. *Journal of Renewable Energy*. 2014:1-12. Article ID 647324. DOI: 10.1155/2014/647324
- [50] Bobade SN, Khyade VB. Preparation of methyl ester (biodiesel) from karanja (*Pongamia pinnata*) oil. *Research Journal of Chemical Sciences*. 2012;2(8):43-50
- [51] Hill J, Nelson E, Tilman D, Polasky S, Tiffany D. Environmental, economic, and energetic costs and benefits of biodiesel and ethanol biofuels.



- Proceedings of the National Academy of Sciences. 2006;**103**(30):11206-11210
- [52] Rahman MM, Ahiduzzaman M, Islam AS, Blanchard R. Karoch (*Pongamia pinnata*)-An alternative source of biofuel in Bangladesh. In: 2014 3rd International Conference on the Developments in Renewable Energy Technology (ICDRET). IEEE; 2014. pp. 1-6
- [53] US-DOE. Alternative Fuel Data Center, Energy Efficiency and Renewable Energy. 2017. Available from: [https://www.afdc.energy.gov/fuels/biodiesel\\_benefits.html](https://www.afdc.energy.gov/fuels/biodiesel_benefits.html) [Accessed: 25 July 2017]
- [54] Kesari V, Rangan L. Development of *Pongamia pinnata* as an alternative biofuel crop-current status and scope of plantations in India. Journal of Crop Science and Biotechnology. 2010;**13**(3):127-137
- [55] Roces SA, Tan R, Da Cruz FJT, Gong SC. Methanolysis of *Jatropha* oil using conventional heating. ASEAN Journal of Chemical Engineering. 2011;**11**(1):41-46
- [56] Meher LC, Dharmagadda VS, Naik SN. Optimization of alkali-catalyzed transesterification of *Pongamia pinnata* oil for production of biodiesel. Bioresource Technology. 2006;**97**(12):1392-1397
- [57] Mahanta P, Sarmah JK, Kalita P, Shrivastava A. Parametric study on transesterification process for biodiesel production from *Pongamia pinnata* and *Jatropha curcas* oil. International Energy Journal. 2008;**9**(1):41-46
- [58] Chandrashekar LA, Mahesh NS, Gowda B, Hall W. Life cycle assessment of biodiesel production from pongamia oil in rural Karnataka. Agricultural Engineering International: CIGR Journal. 2012;**14**(3):67-77
- [59] Patil VK, Bhandare P, Kulkarni PB, Naik GR. Progeny evaluation of *Jatropha curcas* and *Pongamia pinnata* with comparison to bioproductivity and biodiesel parameters. Journal of Forestry Research. 2015;**26**(1):137-142
- [60] Primandari SRP, Islam AKMA, Yaakob Z, Chakrabarty S. *Jatropha curcas* L. biomass waste and its utilization. In: Advances in Biofuels and Bioenergy. London, UK: InTech Open; 2018. p. 273
- [61] Gunaseelan VN. Biogas production from *Pongamia* biomass wastes and a model to estimate biodegradability from their composition. Waste Management & Research. 2014;**32**(2):131-139
- [62] Chandra R, Vijay VK, Subbarao PM. A study on biogas generation from non-edible oil seed cakes: Potential and prospects in India. In: The 2nd Joint International Conference on Sustainable Energy and Environment. 2006. pp. 21-23
- [63] Venkatesan R, Dampuri K, Chaloo R, Shankar A. Green power production from Pinnata. In: World Environmental and Water Resources Congress. Sacramento, California, USA: American Society of Civil Engineers; 2017. pp. 228-240
- [64] Moniruzzaman M, Yaakob Z, Shahinuzzaman M, Khatun R, Islam AKMA. *Jatropha* Biofuel Industry: The Challenges. USA: Publish by INTECH publisher; 2016
- [65] Srinivasan K, Muruganandan S, Lal J, Chandra S, Tandan SK, Prakash VR. Evaluation of anti-inflammatory activity of *Pongamia pinnata* leaves in rats. Journal of Ethnopharmacology. 2001;**78**(2):151-157
- [66] Singh RK, Pandey BL. Anti-inflammatory potential of *Pongamia pinnata* root extracts in experimentally

- induced inflammation in rats. *Journal of Applied Biomedicine*. 1996;4:21-24
- [67] Simonsen HT, Nordskjold JB, Smitt UW, Nyman U, Palpu P, Joshi P, et al. *In vitro* screening of Indian medicinal plants for antiplasmodial activity. *Journal of Ethnopharmacology*. 2001;74(2):195-204
- [68] Essa MM, Subramanian P, Suthakar G, Manivasagam T, Dakshayani KB. Protective influence of *Pongamia pinnata* (Karanja) on blood ammonia and urea levels in ammonium chloride-induced hyperammonemia. *Journal of Applied Biomedicine*. 2005;3(3):133-138
- [69] Shoba FG, Thomas M. Study of antidiarrheal activity of four medicinal plants in castor-oil induced diarrhoea. *Journal of Ethnopharmacology*. 2001;76(1):73-76
- [70] Brijesh S, Daswani PG, Tetali P, Rojatkar SR, Antia NH, Birdi TJ. Studies on *Pongamia pinnata* (L.) Pierre leaves: Understanding the mechanism (s) of action in infectious diarrhea. *Journal of Zhejiang University. Science. B*. 2006;7(8):665-674
- [71] Punitha R, Manoharan S. Antihyperglycemic and antilipidperoxidative effects of *Pongamia pinnata* (Linn.) Pierre flowers in alloxan induced diabetic rats. *Journal of Ethnopharmacology*. 2006;105(1):39-46
- [72] Rameshthangam P, Ramasamy P. Antiviral activity of bis (2-methylheptyl) phthalate isolated from *Pongamia pinnata* leaves against white spot syndrome virus of *Penaeus mondon fabricius*. *Virus Research*. 2007;126(1):38-44
- [73] Uddin Q, Parveen N, Khan NU, Singhal KC. Antifilarial potential of the fruits and leaves extracts of *Pongamia pinnata* on cattle filarial parasite *Setaria cervi*. *Phytotherapy Research*. 2003;17(9):1104-1107
- [74] Pavela R. Efficacy of three newly developed botanical insecticides based on pongam oil against *Plutella xylostella* L. larvae. *Journal of Biopesticides*. 2012;5(1):62-70
- [75] Sharma S, Verma M, Sharma A. Utilization of non- edible oil seed cakes as substrate for growth of *Paecilomyces lilacinus* and as biopesticide against termites. *Waste and Biomass Valorization*. 2013;4(2):325-330
- [76] Arpiwi NL, Yan G, Barbour EL, Plummer JA. Genetic diversity, seed traits and salinity tolerance of *Millettia pinnata* (L.) Panigrahi, a biodiesel tree. *Genetic Resources and Crop Evolution*. 2013;60(2):677-692
- [77] Kesari V, Ramesh AM, Rangan L. *Rhizobium pongamiae* sp. nov. from root nodules of *Pongamia pinnata*. *BioMed Research International*. 2013:1-9. Article ID 165198. DOI: 10.1155/2013/165198
- [78] Rasul A, Amalraj E, Praveen Kumar G, Grover M, Venkateswarlu B. Characterization of rhizobial isolates modulating *Millettia pinnata* in India. *FEMS Microbiology Letters*. 2012;336(2):148-158
- [79] Kazakoff SH, Gresshoff PM, Scott PT. *Pongamia pinnata*, a Sustainable Feedstock for Biodiesel Production. London: Energy crops. Royal Society of Chemistry; 2011. pp. 233-254



# Case Study: Pathways from Forest to Energy in a Circular Economy at Lafões

*Ana d'Espiney, Isabel Paula Marques  
and Helena Maria Pinheiro*

## Abstract

The present case study deals with new pathways in demand for forest residues disposal in the Lafões region (Portugal), since this biomass is presently regarded as a residue and eliminated through open air burning. Different biomass-to-energy conversion systems have a high sustainability value and, thus, the energy potential of the biomass supplied by the forest of Lafões was assessed, using GIS-based methods and assumptions from the literature. The Lafões region produces large amounts of chicken manure from which energy can be recovered through anaerobic digestion. The energy potential held by the effluent of the several classes of the poultry industry of Lafões was assessed, using IPCC 2006 guidelines to estimate their biomass and methane production potential. Furthermore, integrated solutions were pursued. The present challenge is to explore complementarities between effluents for anaerobic digestion to achieve improved energy and waste management system performances. The complementarity between the residues from maritime pine forest management and from broiler production was assessed through bench-scale anaerobic co-digestion assays, leading to increased methane production when compared to those achieved with single substrate anaerobic digestion. This result highlights the interest of further research concerning complementarities between other effluents in the Lafões region.

**Keywords:** forest residues, chicken manure, anaerobic digestion, substrate complementarity, energy potential assessment

## 1. Introduction

The damage to ecosystems generated by the current consumption patterns and associated energy demand, as well as by many of the current waste management systems, has been driving the scientific community to develop research on the mitigation of this damage through integrated and more sustainable energy and waste management systems.

Alongside, decision makers, non-governmental organizations and even market agents (both from supply and demand sectors) are concerned with current consumption impacts. They demand new or improved services and products, paying attention to all their supply chain impacts, including the energy and waste management systems required to provide them.

The present case study had the collaboration of some of the entity types mentioned above, in order to pursue more sustainable energy and waste management systems for the region of Lafões, a region of the Viseu district, located in the centre of Portugal. Its area corresponds to the earlier Lafões municipality and presently comprises three municipalities, namely, Oliveira de Frades, São Pedro do Sul and Vouzela. **Figure 1** depicts the official administrative map of Portugal [1] and the region of Lafões, with the borders of the three municipalities and their location in Portugal.

The Lafões region is characterized by large forest areas. In the last decade, its forests have been severely affected by wildfires which also endanger food crops, industrial facilities and households. The promoter of the research here reported was the Lafões rural development association (ADRL), a certified forest management entity (EGF—*Entidade de Gestão Florestal*) responsible by two forest management units (UGF—*Unidade de Gestão Florestal*) in the region of Lafões, which is responsible for two main activities, namely, fire preventive forestry and surveillance during fire hazard periods.

ADRL is presently much concerned with the disposal of the forest residues generated by its fire preventive forestry management operations, which include thinning, pruning and sometimes harvesting, generating large amounts of biomass presently disposed of by open air burning. Regarding this effluent no longer as a residue and using knowledge on environmental management systems and technologies with a higher sustainability value, ADRL brought together local key actors and entities, to work on the common goal of finding new integrated energy systems to jointly deal with their effluents.

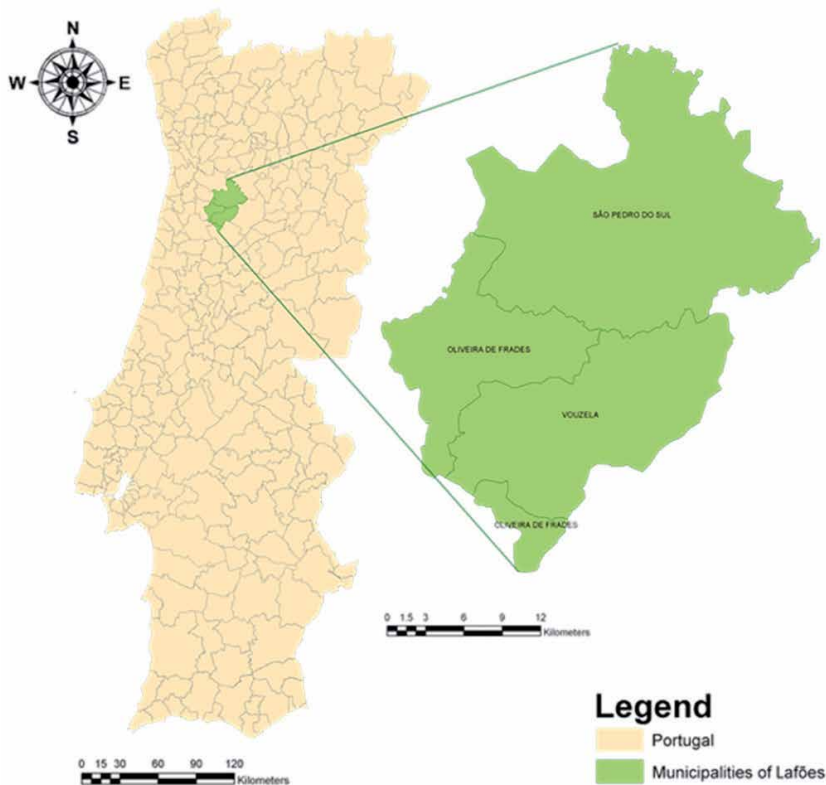


**Figure 1.** Official administrative map of Portugal with the location of the Lafões region municipalities [1].

The Lafões region is also the home of a large poultry industry sector (15.9% of the Portuguese production, according to [2] and the directorate-general of food and veterinary (DGAV) of Viseu), which produces large amounts of waste. The present case study thus aims to explore complementarities in the joint valorisation of the effluents from this activity with those of the forest management operations. The challenge is then to quantify the production of these effluents in the Lafões region and to identify promising ways to convert them into energy, in a circular economy, integrated strategy. To tackle this challenge, ADRL sought the contribution of the institutions to which the authors belong.

The decision on the most promising biomass conversion processes depends on many factors, including the type and quantity of available biomass, the desired end-uses, the relevant governmental policies, environmental standards and economic conditions, as well as project specific factors. The available biomass types is one of the most determinant factors [3]. In the present case, the ADRL challenge, involving such different biomasses (forest residues and chicken manure), is not an easy one.

Since it is hardly biodegradable and carries low moisture content, forest residues are a suitable substrate for thermochemical conversion. Within thermochemical conversion process options, namely, combustion, pyrolysis, gasification and liquefaction, the combustion of residues in small-scale decentralized facilities can be considered the most promising present option for forest residues exploitation. This is due to the fact that other options involve technological challenges that remain unsolved and somewhat uncertain investment costs [4].

Chicken manure, a more easily biodegradable substrate with higher moisture content, is adequate for biochemical conversion processes. There are different possible routes within biochemical processes, mainly through fermentation and anaerobic digestion. The first is widely implemented to produce ethanol from sugar- and cellulose-rich crops and the second is frequently used for the direct conversion of manure to biogas [5].

Anaerobic digestion can provide a “major contribution to the safeguarding of energy supplies in future” [6], as stated by the head of the “Anaerobic Processes” research focus area of the German biomass research centre (DBFZ). As he also states, “biogas plants must become more flexible in terms of their substrates and energy delivery”. This thus became a core issue of the present case study, in order to recover as much as possible of the energy potential of the two biomass types in consideration, through integrated solutions.

Many assessments of the biomass and energy potentials of forest [4, 7–10], chicken manure [11–15] and overall organic residues [2, 16–19] can be found in the literature, considering different boundaries (local, regional, national or worldwide levels) and different plant scales (small, medium and large). For forest and manure biomasses, the assessment of the energy potential starts with the assessment of the biomass potential. This done, it is possible to obtain their theoretical energy potential and, according to the conversion process specifications, the associated technical energy potential.

In addition to the mentioned assessment levels (biomass potential, theoretical and technical energy potentials), three more levels theoretically remain to be considered (economical, implementation and sustainable implementation) [19], however they are beyond the scope of this preliminary case study.

Concerning forest residues, it is common to rely on GIS-based methods for supply quantification, using geo-referenced data derived from remote sensing imagery, taking into account important constraints such as slope, accessibility, and land use conflicts. The theoretical energy potential is subsequently obtained using the lower heating value of each biomass species and the technical energy potential is obtained using the conversion efficiency of the selected process.

The chicken manure biomass potential assessment starts by the quantification of the number of birds in the covered industrial facilities, which is usually available through local or national statistics offices. For the present case study, this information was readily provided by the DGAV of Viseu, which has been struggling to promote sustainable standards in the local poultry sector, through inspections and guidance provided to the producers.

The Tier 2 methodology of the IPCC Guidelines 2006 [11] allows the calculation of the volatile solids and methane emissions per bird, which can then be used to return the Lafões biomass and methane potentials per poultry class. The theoretical and technical energy potentials can then be obtained as described for forest residues, using the lower heating value of methane and the technical specifications of the implemented system.

Up to this point, only the energy potentials for the separate conversion of the two types of biomass are obtained and an integrated solution remains to be assessed. Since the aim of the present case study is to estimate the increment in energy potential that can be obtained when an integrated solution is implemented, two bench-scale biomass-to-energy conversion systems (BTES) were assessed: chicken manure anaerobic digestion and anaerobic co-digestion of chicken manure and forest residues.

There are scarce results in the literature from computing the energy potential of the joint digestion of biomass from plant and animal origins, and those available are case specific, as, for example, in [20–24]. The values for this case study were thus measured experimentally and choices had to be made concerning the classes of the two types of biomass to be used as substrates. The details of the methodological procedures employed in this case study, the discussion of the results and some conclusions that can be drawn from the results, are presented in the following sections.

## **2. Assessment of the energy potential of the two biomass-to-energy conversion systems**

The energy potential of the two BTES was assessed in three main steps. In the first step, the available classes of both types of biomass were examined and one class from each was selected to feed the bench-scale BTES assays. This selection was based on the theoretical energy potential (ThEP) for the forest classes and on the theoretical methane production (MP) from manure for the poultry classes. The second step was conducted to experimentally assess the methane production capacity of both BTES using the selected substrates. With the third step, the energy potential of each BTES was finally estimated.

These three assessment steps are presented in the following sections and the discussion concerning the energy potential increment between the two considered BTES is presented in Section 3.

### **2.1 Selection of biomass classes**

#### *2.1.1 Selection of the forest species*

For the assessment of the ThEP of the forest residues, the analysis of geo-referenced data obtained through GIS-based methods is largely accepted and, thus, ArcGIS version 10.5 was used to map the several forest class areas. Subsequently, the annual residue productivity (RP) and the percentage of the land covered by the horizontal projection of the vegetation (HPV) were considered to assess the biomass potential of each forest class. Finally, the lower heating value (LHV) was

used to obtain the ThEP of each forest class. Between the two forest classes with higher ThEP, the one with higher C:N ratio was selected, since it favors the methane potential in anaerobic digestion. This methodology is applied as described in detail subsequently.

After defining the Lafões region area (**Figure 1**), which was obtained from the official administrative map of Portugal [1], all areas with land uses other than forest were eliminated from the land use cover map [25] of the region. When mapping the forest area, land use conflicts with nature conservation areas must be considered [7, 18], which can be located in the geocatalogue of the nature and forest conservation institute (ICNF) [26].

Nevertheless, because of the fire hazard threatening nature conservation areas (rendering fire preventive biomass removal mandatory) and since the residue fraction that needs to be left on the soil for environmental purposes is taken into account in the subsequent calculations, these areas were not subtracted from the forest area to be considered.

When quantifying the biomass supply area, accessibility must also be considered, since there are technical difficulties with the collection of forest residues from steep slope areas. Due to environmental concerns like soil erosion, but also to allow mechanization and to reduce collection costs, only areas with slopes of less than 20% [4] were selected from the terrain digital model [27] of Lafões.

To further meet accessibility criteria, technical restrictions imposed by large distances to roads or passable tracks must also be taken into account. Thus areas at distances of less than 3 km were to be selected [4] from the forest road maps of Oliveira de Frades [28], São Pedro do Sul [29] and Vouzela [30]. Dense road coverage of the entire region was observed, thus, no area was subtracted concerning this technical restriction to biomass collection, since no point in the map is at a distance to a road greater than 3 km.

With all the mentioned assumptions, the available and accessible supply area for each forest class was obtained. Those areas are illustrated in **Figure 2** and the forest class nomenclature used is in accordance with the technical specifications in [31].

The forest biomass residues potential (FBP) present in the residues was estimated, multiplying the selected areas by the RP for each forest class and the percentage of land covered by the HPV of the predominant species of each forest class, as suggested in [10]. Finally, to calculate the ThEP, the LHV of the predominant species of each forest class, taken from [4], was multiplied by the FBP. All the input data used is shown in **Table 1**, as well as the results for the FBP and the ThEP.

As observed from the results, the eucalyptus forest and the maritime pine forest are those with the highest ThEP in the region of Lafões, 601 TJ/year and 374 TJ/year, respectively. According to [32], the C:N ratio values for pine and hardwood are 73:1 and 39:1, respectively, and since high C:N ratios favor the methane potential in anaerobic digestion of chicken manure, maritime pine was the selected residue source.

### 2.1.2 Selection of the poultry class

The assessment of the ThEP of the chicken manure in the region of Lafões was implemented in three stages: (1) data collection on the number of birds in the region's industrial units; (2) calculation of the biomass potential of each poultry class using volatile solids excretion rate (VS); (3) estimation of the theoretical methane potential using the maximum methane production capacity ( $B_0$ ) of each poultry class. The methodological assumptions, procedures and results in each stage are subsequently explained in detail.



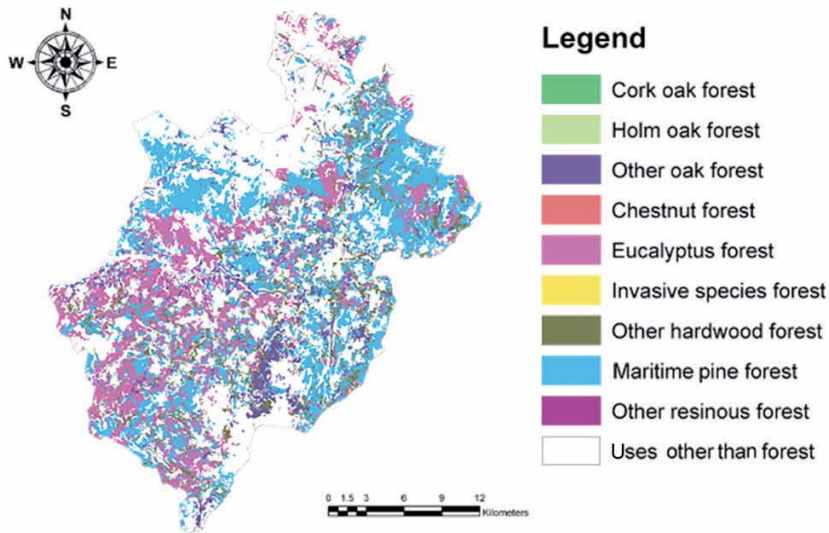


**Figure 2.**  
Map of the forest land cover of the Lafões region.

To start the computation of the chicken manure production in the region of Lafões, the first collected input data was the number of birds in the industrial sector of the region. The number of birds existing in the three municipalities of Lafões in February 2020 was registered and provided by DGAV. A total of 328 producers and 5,716,945 birds were registered, distributed among four classes of poultry industry, namely, broilers, laying hens, reproductive hens and turkeys. **Table 2** shows the number of birds of each class registered in the three municipalities of Lafões.

With the information on the number of birds, calculation of the biomass potential is usually done considering the chemical oxygen demand (COD) or volatile solids (VS) content of the chicken manure. The methodology applied in this case study is that suggested in the IPCC guidelines [11]. In this, the assessment uses the volatile solids excretion rate, calculated through Eq. (1) for each class of bird.

$$VS = \left[ GE \times \left( 1 - \frac{DE}{100} \right) + (UE \times GE) \right] \times \left[ \frac{1 - ASH}{18.45} \right] \quad (1)$$

where VS is the volatile solids excreted by an average bird [kg VS/(bird.day)]; GE is the gross energy intake in the feed for an average bird [MJ/(bird.day)]; DE is the digestibility of the feed [%]; UE is the urinary energy expressed as mass fraction of GE; ASH is the ash content of manure calculated as mass fraction of the dry matter in the feed intake; 18.45 is the conversion factor for dietary GE per kg of feed dry matter [MJ/kg].

The results of the estimation of the VS per bird class, as well as all the input data (taken from [2]) are presented in **Table 3**. The calculation of the gross energy intake (GE), which depends on the recommended metabolic energy ingestion and metabolisability, is explained in detail in [11]. The presented values are class specific, except for that of UE (no value available for poultry) for which the value given for other livestock (cattle, sheep and goats) was used.

In the third stage, the value obtained for the VS in the second stage was multiplied by the maximum methane production capacity ( $B_o$ ) from manure, specific for each bird class, all taken from [2], resulting the methane production (MP) per bird. The total MP was calculated on a basis of 365 days/year and using the number of birds in each poultry class presented in **Table 2**. The values of  $B_o$  and the results

| Forest class            | $A^r$ [ha] | RP [t residue/(ha·year)] | HPV [%] | FBP [t residue/year] | LHV [GJ/t residue] | THEP [GJ/year] |
|-------------------------|------------|--------------------------|---------|----------------------|--------------------|----------------|
| Cork oak forest         | 15         | 0.48                     | 20      | 1                    | 14                 | 20             |
| Holm oak forest         | 24         | 0.48                     | 20      | 2                    | 14                 | 33             |
| Other oak forest        | 4453       | 0.50                     | 65      | 1447                 | 15                 | 21,710         |
| Chestnut forest         | 30         | 0.50                     | 65      | 10                   | 15                 | 145            |
| Eucalyptus forest       | 70,077     | 0.88                     | 65      | 40,080               | 15                 | 601,300        |
| Invasive species forest | 85         | 20.00                    | 65      | 1106                 | 14                 | 15,480         |
| Other hardwood forest   | 4989       | 0.75                     | 65      | 2432                 | 15                 | 36,480         |
| Maritime pine forest    | 33,868     | 1.00                     | 65      | 22,010               | 17                 | 374,200        |
| Other resinous forest   | 29         | 0.85                     | 65      | 16                   | 15                 | 241            |

**Table 1.** Forest biomass residues potential (FBP), theoretical energy potential (THEP) and input data used for their estimation: total area ( $A^r$ ) of the forest class; annual residue productivity (RP) of the forest class [10]; percentage of land covered by the horizontal projection of the vegetation (HPV) of the predominant species of the forest class [10]; lower heating value (LHV) of the predominant species of the forest class [4].

| Poultry class    | Oliveira de Frades | São Pedro do Sul | Vouzela   | Total     |
|------------------|--------------------|------------------|-----------|-----------|
| Broiler          | 1,869,294          | 1,734,020        | 1,361,166 | 4,964,480 |
| Laying hen       | 102,108            | 46,607           | 27,027    | 175,742   |
| Reproductive hen | 201,149            | 0                | 209,200   | 410,349   |
| Turkey           | 75,919             | 63,055           | 27,400    | 166,374   |

**Table 2.**  
Number of birds registered by class and municipality (data from February 2020).

| Poultry class    | GE<br>[MJ/(bird.day)] | DE<br>[%] | UE<br>[kg/kg] | ASH<br>[kg/kg] | VS<br>[kg VS/(bird.day)] |
|------------------|-----------------------|-----------|---------------|----------------|--------------------------|
| Broiler          | 1.56                  | 68        | 0.04          | 0.020          | 0.03                     |
| Laying hen       | 2.2                   | 64        | 0.04          | 0.048          | 0.05                     |
| Reproductive hen | 2.15                  | 64        | 0.04          | 0.048          | 0.04                     |
| Turkey           | 4.75                  | 68        | 0.04          | 0.026          | 0.09                     |

Gross feed energy intake (GE), digestibility of the feed (DE), urinary energy expressed as mass fraction of GE (UE) and manure ash content (ASH) [2].

**Table 3.**  
Volatile solid excretion rate (VS) calculated for each poultry class in the Lafões region and its input data.

of the estimation of the MP potential of the several poultry classes of Lafões are presented in **Table 4**.

According to the calculations, the poultry class that contributes the most to the MP potential of the Lafões region is the broilers (77.3%) and was therefore selected for the experimental study.

### 2.1.3 Selection of the broiler litter type

The characterization of the litter practices in the region was provided by a company that integrates 73 producers, representing a sample of 26.8% of the total population of producers in the region of Lafões. Within this sample, 88% of the producers use straw litter for the bed of the broilers, 10% use sawdust litter and 2% use rice chaff litter. Straw litter is thus the favorite and, therefore, a poultry production facility that uses this litter type was selected to provide the sample used to feed the bench-scale BTES assays.

## 2.2 Estimation of the methane production capacity of the two BTES

After the residue class selection, samples were collected, submitted to a pre-treatment and characterized. With these, different compositions of mother suspensions were prepared to feed bench-scale digestion assays. The methane productivity results obtained from the assays were then used to compute the experimental and technical energy potentials of the two BTES being assessed.

The samples collected are identified as follows: straw litter chicken manure (CM) from the poultry breeding pavilion; maritime pine forest biomass residues (FB) containing residues of woody tissues (with diameter smaller than 6 mm) and leaves; wastewater (WW) from the cleaning of the poultry pavilion; inoculum (I) from an anaerobic digester treating wastewater sludge.

Both CM and FB were collected in triplicate, from a broiler production pavilion and from a maritime pine forest area, respectively, in the region of Lafões. The WW

was collected from a drain usually connected to a septic tank, in the facility that provided the CM sample, while the inoculum (I) was obtained at the wastewater treatment plant of Quinta do Conde (SIMARSUL, Setúbal, Portugal).

At the laboratory, all the samples were submitted to a pre-treatment and subsequently characterized. For both the CM and FB samples, the collected triplicates were hand homogenized together in a single large container. After this, the CM was slightly chopped and shifted to produce particles with an approximate diameter lower than 5 mm, while the FB was crushed in a mill to produce particles less than 0.5 mm in diameter. No pre-treatment was applied to the WW and I samples. Characterization of the four substrates was performed in duplicate using standard methods [33] for volatile solids (VS\*) and bulk density. Results are presented in **Table 5**.

To experimentally assess the methane potential of the anaerobic digestion and co-digestion options, four mother suspensions were prepared: chicken manure (CMms); chicken manure and forest biomass (CM + FBms); forest biomass (FBms); and inoculum (Ims).

The CMms was used to determine the methane production capacity from the CM substrate and the CM + FBms was used for the same purpose regarding co-digestion of the CM and FB substrates. Inoculum was added to both CMms and CM + FBms, at a concentration of 0.3 mL per mL of mother suspension. The preparation of these mother suspensions also incorporated the wastewater from cleaning of the poultry pavilion (WW). For this, a volumetric proportion between the liquid and solid substrates of 1:4.5 was considered, the average value among those provided by several poultry production facilities in the region.

The other two mother suspensions, Ims and FBms, were included in the study with the intention of measuring their individual methane production capacity

| Poultry class    | $B_o$ [ $\text{m}^3 \text{CH}_4/\text{kg VS}^*$ ] | MP [ $10^3 \text{m}^3 \text{CH}_4/\text{year}$ ] |
|------------------|---|--|
| Broiler          | 0.36  | 19,460   |
| Laying hen       | 0.39  | 1136   |
| Reproductive hen | 0.39  | 2592   |
| Turkey           | 0.36  | 1974   |

**Table 4.**  
 Methane production (MP) and maximum methane production capacity ( $B_o$ ) per poultry class [2].

| Sample   | VS* [g/g]       | Bulk Density [g/mL] |
|--|-----------------|---------------------|
| Straw litter chicken manure (CM)                   | 0.519 ± 0.001   | 0.3 ± 0.01          |
| Maritime pine forest biomass residues (FB)         | 0.767 ± 0.001   | 0.21 ± 0.02         |
| Wastewater from the poultry pavilion cleaning (WW) | 0.0016 ± 0.0001 | 0.97 ± 0.02         |
| Inoculum (I)                                       | 0.0133 ± 0.0003 | n.d.                |

*The values presented are average ± standard deviation from duplicate measurements using standard methods [33].*

**Table 5.**  
 Values for the characterization parameters of the substrates used in the anaerobic digestion experiments, volatile solids (VS\*) and bulk density.

(in the absence of CM). The same inoculum concentration was used in these two (0.3 mL I/mL mother suspension) and distilled water was added to complete the assay volume, instead of poultry wastewater. The composition of the four mother suspensions is summarized in **Table 6**.

From each 400 mL of mother suspensions, 40 mL were taken to feed each of three 70-mL reactors, leaving a headspace of 30 mL. The reactors were operated in batch mode under temperature control at  $37 \pm 1^\circ\text{C}$ , thus in mesophilic conditions.

The assay had a duration of 48 days and during this period biogas production was monitored every day with a pressure transducer and the methane content in the biogas was monitored every week by gas chromatography (Varian 430-GC). The cumulative methane production results after the incubation period are presented in **Table 7** and their evolution along time is illustrated in **Figure 3**. The step increase episodes that can be observed correspond to gas sampling for chromatographic analysis.

Considering the methane production achieved from each mother suspension (**Table 7**), the value from the inoculum alone (Ims) was subtracted from the CMms and the CM + FBms values. The resulting methane volume was then used in Eq. (2), together with the volatile solids content and the density of the CM (**Table 5**) and the volume of CM added to mother suspensions CMms and CM + FBms (**Table 6**), to compute their average maximum methane production capacity achieved from the added CM, resulting in values of 0.01 and 0.2  $\text{m}^3 \text{CH}_4/\text{kg VS}^*$ , respectively (@STP).

$$B_{o\_ms} = \frac{Vol_{CH_4\_CM}}{VS^*_{CM} \times Vol_{CM} \times \rho_{CM}} \quad (2)$$

where  $B_{o\_ms}$  is the average methane production capacity from the  $VS^*$  in the CM residue [ $\text{m}^3 \text{CH}_4/\text{kg VS}^*$ ];  $Vol_{CH_4\_CM}$  is the average accumulated methane production from the reactors carrying the CM [ $\text{m}^3 \text{CH}_4$ ];  $VS^*_{CM}$  is the volatile solids content of the CM [ $\text{kg VS}^*/\text{g CM}$ ];  $Vol_{CM}$  is the volume of CM added to the reactors [ $\text{mL}$ ];  $\rho_{CM}$  is the CM density [ $\text{g/mL}$ ]. All methane volume values are expressed at STP.

### 2.3 Estimation of the theoretical and technical energy potential of the two BTES

The estimation of the energy potential of the two BTES starts with the estimation of their average methane production (MP), using the biomass supply of the broiler production of Lafões, considering the average  $B_o$  calculated in the previous section and using Eq. (3) presented below. This equation was adapted from the one suggested in [11] to estimate methane emissions from chicken manure. The methane density value was expressed at STP, corresponding to the experimental methane volume values.

| Mother suspension | CM<br>[mL] | FB<br>[mL] | WW<br>[mL] | I<br>[mL] | Water<br>[mL] | Total<br>[mL] |
|-------------------|------------|------------|------------|-----------|---------------|---------------|
| CMms              | 228.8      | 0.0        | 51.2       | 120       | 0             | 400           |
| FBms              | 0.0        | 228.8      | 0.0        | 120       | 51.2          | 400           |
| CM + FBms         | 114.4      | 114.4      | 51.2       | 120       | 0             | 400           |
| Ims               | 0.0        | 0.0        | 0.0        | 120       | 280           | 400           |

*Substrates were straw litter chicken manure (CM), maritime pine forest biomass (FB), wastewater from poultry pavilion cleaning (WW), and inoculum (I).*

**Table 6.**  
Composition of the mother suspensions.

| Mother suspension | Methane production [mL CH <sub>4</sub> @STP] |
|-------------------|--|
| CMms              | 36.5 ± 4.5                                   |
| FBms              | 0.10 ± 0.03                                  |
| CM + FBms         | 356.8 ± 25.0                                 |
| Ims               | 2.6 ± 0.03                                   |

*The values presented are average ± standard deviation from triplicate digestion runs.*

**Table 7.**  
 Total methane production in the anaerobic digestion reactors using the mother suspensions chicken manure (CMms), chicken manure and forest biomass (CM + FBms), forest biomass (FBms) and inoculum (Ims).

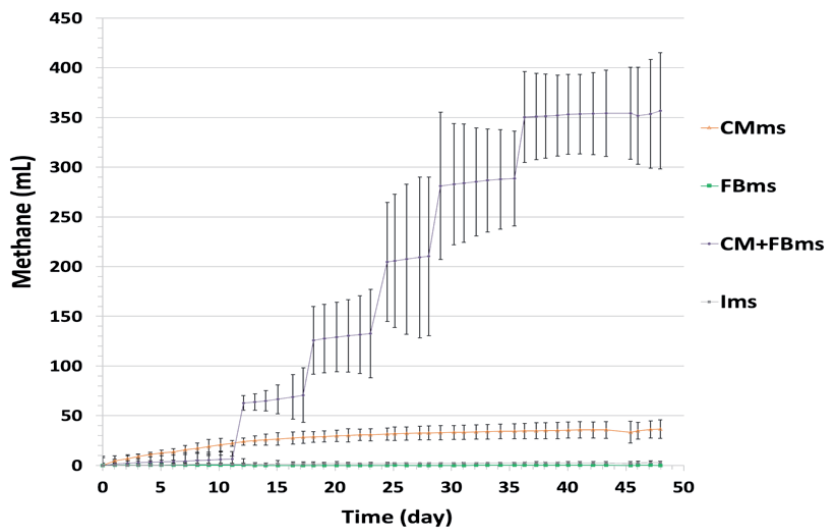


**Figure 3.**  
 Time course of cumulative methane production (in mL@STP) in the anaerobic digestion reactors using the mother suspensions chicken manure (CMms), chicken manure and forest biomass (CM + FBms), forest biomass (FBms) and inoculum (Ims). Average values are given, with standard deviation (error bars) from triplicate runs.

$$MP_i = VS \times B_{o_i} \times 0.71 \quad (3)$$

where  $MP_i$  is the methane production achieved by the BTES  $i$  [kgCH<sub>4</sub>/(bird.day)];  $VS$  is the volatile solids excretion rate obtained with Eq. (1) [kgVS/(bird.day)];  $B_{o_i}$  is the maximum methane production capacity of the BTES  $i$  [m<sup>3</sup> CH<sub>4</sub>/kg VS excreted]; 0.71 is the conversion factor of m<sup>3</sup> CH<sub>4</sub> to kg CH<sub>4</sub> at STP;  $i$  stands for the anaerobic digestion or anaerobic co-digestion BTES.

The total MP for each BTES was calculated on a basis of 365 days/year and using the number of birds in the broiler poultry class presented in **Table 2**. The obtained values of MP were 369 t CH<sub>4</sub>/year and 7719 t CH<sub>4</sub>/year, for anaerobic digestion and co-digestion BTES, respectively. Multiplying the MP of each BTES by the methane LHV of 50 MJ/kg [34], the theoretical energy potential (ThEP) values of 18,450 TJ/year and 386,000 TJ/year for anaerobic digestion and co-digestion, respectively, were obtained.

Finally, the technical energy potential (TeEP) of the two BTES was estimated. The methane losses that occur in different unit operations of the anaerobic digestion process, namely, pre-storage, digestion and digestate storage, as well as the conversion yield of methane into energy, were taken into consideration.

The methodology proposed in [35] accounts for the methane conversion (emissions to the atmosphere) during manure pre-storage and the gastight storage of the digestate, as well as methane losses in its recovery from the digester. Using Eq. (4) and the input data presented in **Table 8**, the value of  $0.011 \text{ m}^3/\text{m}^3$  was obtained for the overall effective methane conversion factor (*MCF*) that represents the total losses during the digestion process of both BTES. The value is then used, multiplying by the TeEP value previously calculated, to compute methane energy losses in the three mentioned system components, resulting in 212 TJ/year and 4433 TJ/year for the anaerobic digestion and co-digestion BTES, respectively.

$$MCF = MCF_{ps} + (1 - MCF_{ps}) \times [(1 - \mu_{rg}) \times L_{prod} + \mu_{rg} \times MCF_{digestate}] \quad (4)$$

where *MCF* is the effective methane conversion factor for the combination “pre-storage + digester + storage” [ $\text{m}^3/\text{m}^3$ ];  $MCF_{ps}$  is the methane conversion factor for pre-storage [ $\text{m}^3/\text{m}^3$ ];  $\mu_{rg}$  is the relative potential of residual gas, in relation to  $B_o$  (with  $0 \leq \mu_{rg} \leq 1 \text{ [m}^3/\text{m}^3]$ );  $L_{prod}$  is the leakage rate of the digester (with  $0 \leq L_{prod} \leq 1 \text{ [m}^3/\text{m}^3]$ );  $MCF_{digestate}$  is the methane conversion factor for the gastight storage of the digested manure [ $\text{m}^3/\text{m}^3$ ].

It is assumed, according to [36], that the biogas recovered from the digester of both BTES is conveyed to a combined heat and power (CHP) plant with electrical and thermal yield values of 35% and 43%, respectively, and the remaining 22% are taken as overall losses in the co-generation process. Still according to [36], some

| Parameter  | Value  |
|--|--------|
| $\mu_{rg} \text{ [m}^3/\text{m}^3]$                    | 0.046  |
| MCF of the pre-storage [ $\text{m}^3/\text{m}^3$ ]     | 0.0015 |
| $L_{prod} \text{ [m}^3/\text{m}^3]$                    | 0.01   |
| MCF of the digestate [ $\text{m}^3/\text{m}^3$ ]       | 0.01   |
| MCF of the overall process [ $\text{m}^3/\text{m}^3$ ] | 0.011  |

**Table 8.**

*Process specific methane conversion factors (MCF), relative potential of residual gas ( $\mu_{rg}$ ) and leakage rate of the digester ( $L_{prod}$ ) values [35] used for the calculation of the overall MCF for methane losses in the anaerobic digestion process.*

| Parameter                                   | Anaerobic digestion energy<br>[ $10^3 \text{ Tj/year}$ ] | Anaerobic co-digestion energy<br>[ $10^3 \text{ Tj/year}$ ] |
|---|--|---|
| Methane losses in the digestion process     | 0.2  | 4.4   |
| Electricity produced                        | 6.3  | 135.0   |
| Heat produced                               | 7.8  | 165.9   |
| Electricity for internal use                | 0.6  | 27.0  |
| Heat for internal use                       | 1.6  | 33.2  |
| Overall losses in the co-generation process | 4.0  | 83.9  |
| <b>TeEP</b>                                 | <b>12.0</b>  | <b>241</b>  |

*Digestion processes losses, co-generation balance and energy diverted for internal use are also given.*

**Table 9.**

*Technical energy potential (TeEP) of the anaerobic digestion and co-digestion BTES.*

internal use of the produced energy is assumed, namely, 10% of the generated electricity is used for digester agitation and material conveying operations and 10% of the produced heat is used for temperature control in the digester.

The first value concerning internal electricity use was adopted for the anaerobic digestion BTES, but for the anaerobic co-digestion BTES the value was increased to 20%, since there are energy requirements associated to the pre-treatment of the maritime pine biomass. The second value, heat used internally, was increased to 20% for both BTES, anticipating less efficient heat conservation systems in Portugal.

The technical energy potential of both BTES,  $TeEP$ , is given by Eq. (5). **Table 9** presents the results of the above assumptions and the total  $TeEP$  values, 12 PJ/year and 241 PJ/year (presented in bold in the table) for the anaerobic digestion and co-digestion BTES, respectively.

$$TeEP = ThEP \times (1 - MCF) \times [\eta_{el}(1 - int.eluse) + \eta_{th}(1 - int.thuse)] \quad (5)$$

where  $TeEP$  is the technical energy potential of the BTES [TJ/year];  $ThEP$  is the theoretical energy potential of the BTES [TJ/year];  $MCF$  is the methane conversion factor for losses in anaerobic digestion systems [ $m^3/m^3$ ];  $\eta_{el}$  is the electrical yield of the CHP [%/100];  $int.eluse$  is the electricity fraction used internally [%/100];  $\eta_{th}$  is the thermal yield of the CHP [%/100];  $int.thuse$  is the heat fraction used internally [%/100].

### 3. Energy potential increment due to the exploitation of substrate complementarities

The results obtained experimentally allow an optimistic perspective on the performance of the BTES handling forest residues and chicken manure together. With the BTES running on complementary substrates it is possible to achieve an increment of 229 PJ/year, one order of magnitude from the value for the BTES running only on chicken manure.

It can however be argued that the overall efficiency values considered for the two BTES are unrealistic since much higher internal use fractions for electricity and heat should be considered to account for the pre-treatment. Dividing the  $TeEP$  by the  $ThEP$  of each BTES, overall yield values of 65% and 62% are obtained for the anaerobic digestion and co-digestion BTES, respectively. A more realistic comparison would require further knowledge on energy demand for these pre-treatment options.

Nevertheless, the obtained results allow the conclusion that, even considering further technical differences, the anaerobic co-digestion BTES is likely to achieve better performance levels than the single substrate chicken manure BTES, since a clearly improved methane production capacity can be obtained through its complementarity with the maritime pine biomass.

### 4. Conclusions

The main conclusion that can be drawn from this case study is that integrated solutions, such as anaerobic co-digestion of complementary substrates, can be appealing from the point of view of their theoretical and technical energy potentials.

The large production of chicken manure in the Lafões region is presently handled through solid storage or pasture solutions, therefore emitting methane



into the atmosphere. This is a waste of its energy content and contributes to climate change. Thus, this residue class presents itself as a strong candidate to create synergies in the implementation of integrated systems, in a circular economy concept, whereby complementary effluents are managed together to produce value gains in the region.

It is advisable to perform assessments on further levels, namely in terms of the economical, implementation and sustainable implementation energy potentials. Even within the scope of the assessment levels addressed in the present case study (theoretical and technical), the total energy potential is yet to be determined, since the classes from both biomass types that were left out in this preliminary study must also be tested in terms of their complementarity.

More research has also yet to be carried out concerning the forest residues supply needed to run the anaerobic co-digestion, since only the small size fraction was used in the BTES assay. The total amount of available residues was estimated, but the amounts corresponding to this fraction remain unknown.

Finally, another aspect needing further research concerns the biochemical mechanisms responsible for the increment in methane production when substrate complementarities in co-digestion are exploited. The physicochemical composition of the different effluents generated by the industrial activities of Lafões must be analyzed in more detail and their possible combinations must be experimentally assessed, in order to develop new pathways from forest to energy.

## **Acknowledgements**

The authors would like to acknowledge Associação de Desenvolvimento Rural de Lafões (ADRL) for introducing this challenging topic of research, and Fundação para a Ciência e a Tecnologia for PhD studentship SFRH/BD/146002/2019.

For their extensive support, the authors would also like to acknowledge the poultry sector integrating company and the DGAV of Viseu, who provided the data and intermediated the contacts with poultry producers. The producers who provided the samples are also gratefully acknowledged.

The three municipalities of Lafões (Oliveira de Frades, São Pedro do Sul and Vouzela) must also be acknowledged for providing the data necessary for the forest residues assessment. Acknowledgments are also due to the forest sappers for sharing their knowledge concerning the Lafões forest.

## **Nomenclature**

|           |   |
|-----------|---|
| AD        | anaerobic digestion                                 |
| ADRL      | Lafões rural development association                |
| $B_o$     | maximum methane production capacity                 |
| BTES      | biomass-to-energy conversion systems                |
| CHP       | combined heat and power                             |
| CM        | straw litter chicken manure                         |
| CM + FBms | chicken manure and forest biomass mother suspension |
| CMms      | chicken manure mother suspension                    |
| DBFZ      | German Biomass Research Centre                      |
| DGAV      | Directorate-General for Food and Veterinary         |
| EGF       | forest management entity                            |
| FB        | maritime pine forest biomass residues               |
| FBms      | forest biomass residues mother suspension           |

|      |  |
|------|--|
| FBP  | forest biomass residues potential                    |
| GIS  | Geographical Information Systems                     |
| HPV  | horizontal projection of the vegetation              |
| I    | inoculum   |
| ICNF | Instituto da Conservação da Natureza e das Florestas |
| Ims  | inoculum mother suspension                           |
| IPCC | Intergovernmental Panel on Climate Change            |
| LHV  | lower heating value                                  |
| MCF  | methane conversion factor                            |
| MP   | methane production                                   |
| RNAP | national network of protected areas                  |
| RP   | residues productivity                                |
| TeEP | technical energy potential                           |
| ThEP | theoretical energy potential                         |
| VS   | volatile solids excretion rate                       |
| VS*  | volatile solids                                      |
| UGF  | forest management units                              |
| WW   | wastewater from poultry pavilion cleaning            |

## Author details

Ana d’Espiney<sup>1,2</sup>, Isabel Paula Marques<sup>1\*</sup> and Helena Maria Pinheiro<sup>3</sup>


1 Bioenergy and Biorefineries Unit, LNEG – National Laboratory of Energy and Geology, Lisbon, Portugal

2 Instituto Superior Técnico, Universidade de Lisboa, Lisbon, Portugal

3 iBB - Institute for Bioengineering and Biosciences, Instituto Superior Técnico, Universidade de Lisboa, Lisbon, Portugal

\*Address all correspondence to: [isabel.paula@lneg.pt](mailto:isabel.paula@lneg.pt)

## IntechOpen

© 2020 The Author(s). Licensee IntechOpen. Distributed under the terms of the Creative Commons Attribution - NonCommercial 4.0 License (<https://creativecommons.org/licenses/by-nc/4.0/>), which permits use, distribution and reproduction for non-commercial purposes, provided the original is properly cited. 

## References

- [1] Direção-Geral do Território. In: Carta Administrativa Oficial de Portugal (CAOP 2019); 2019. Available from: [http://www.dgterritorio.pt/cartografia\\_e\\_geodesia/cartografia/carta\\_administrativa\\_oficial\\_de\\_portugal\\_caop/caop\\_download/carta\\_administrativa\\_oficial\\_de\\_portugal\\_\\_versao\\_2019\\_em\\_vigor/](http://www.dgterritorio.pt/cartografia_e_geodesia/cartografia/carta_administrativa_oficial_de_portugal_caop/caop_download/carta_administrativa_oficial_de_portugal__versao_2019_em_vigor/) [Accessed: 27 June 2020]
- [2] Pereira T, Amaro A, Borges M, Silva R, Pina A, Canaveira P. Portuguese National Inventory Report on Greenhouse Gases, 1990-2017. Submitted under the United Nations Framework Convention on Climate Change. Amadora: Portuguese Environmental Agency; 2020. p. 751
- [3] McKendry P. Energy production from biomass (Part 2): Conversion technologies. *Bioresource Technology*. 2002;**83**(July):47-54. DOI: 10.1016/S0960-8524(01)00119-5
- [4] Lourinho G, Brito P. Assessment of biomass energy potential in a region of Portugal (AltoAlentejo). *Energy*. 2015;**81**:189-201. DOI: 10.1016/j.energy.2014.12.021
- [5] Ferreira S, Moreira NA, Monteiro E. Bioenergy overview for Portugal. *Biomass and Bioenergy*. 2009;**33**(11):1567-1576. DOI: 10.1016/j.biombioe.2009.07.020
- [6] Kornatz P. Introduction Statement of the Anaerobic Processes Research Focus Area [Internet]. 2020. Available from: <https://www.dbfz.de/en/research/researchfocusareas/anaerobicprocesses/> [Accessed: 20 April 2020]
- [7] Quinta-Nova L, Fernandez P, Pedro N. GIS-based suitability model for assessment of Forest biomass energy potential in a region of Portugal. *IOP Conference Series: Earth and Environmental Science*. 2017;**95**(4):1-7. DOI: 10.1088/1755-1315/95/4/042059
- [8] Viana H, Cohen WB, Lopes D, Aranha J. Assessment of forest biomass for use as energy. GIS-based analysis of geographical availability and locations of wood-fired power plants in Portugal. *Applied Energy*. 2010;**87**(8):2551-2560. DOI: 10.1016/j.apenergy.2010.02.007
- [9] Mateos E, Garrido F, Ormaetxea L. Assessment of biomass energy potential and forest carbon stocks in Biscay (Spain). *Forest*. 2016;**7**:75. DOI: 10.3390/f7040075
- [10] Rocha JT, Malico I, Gonçalves AC, Sousa AMO. Análise do potencial de biomassa residual no Algarve, Portugal, baseada em SIG. *Ciência da Madeira (Brazilian Journal of Wood Science)*. 2020;**11**(1):42-52. DOI: 10.12953/2177-6830/rcm.v11n1p42-52
- [11] Dong H, Mangino J, McAllister T. Chapter 10: Emissions from livestock and manure management. In: 2006 IPCC Guidelines for National Greenhouse Gas Inventories. Volume 4: Agriculture, Forestry and Other Land Use. 2006. p. 87
- [12] Bao W, Yang Y, Fu T, Xie GH. Estimation of livestock excrement and its biogas production potential in China. *Journal of Cleaner Production*. 2019;**229**:1158-1166. DOI: 10.1016/j.jclepro.2019.05.059
- [13] Bhattacharya SC, Thomas JM, Salam PA. Greenhouse gas emissions and the mitigation potential of using animal wastes in Asia. *Energy*. 1997;**22**(11):1079-1085. DOI: 10.1016/S0360-5442(97)00039-X
- [14] Tańczuk M, Junga R, Kolasa-Więceć A, Niemiec P. Assessment of the energy potential of chicken manure in Poland. *Energies*. 2019;**12**(7):1-18. DOI: 10.3390/en12071244

- [15] Amon BJW, Hutchings N, Dämmgen U, Sommer S. EMEP/EEA Air Pollutant Emission Inventory Guidebook 2019. Technical Guidance to Prepare National Emission Inventories 2019. p. 26. ISSN: 1977-8449
- [16] Roberts JJ, Cassula AM, Osvaldo P, Dias R, Balestieri JAP. Assessment of dry residual biomass potential for use as alternative energy source in the party of General Pueyrredón, Argentina. *Renewable and Sustainable Energy Reviews*. 2015;**41**:568-583. DOI: 10.1016/j.rser.2014.08.066
- [17] Mosaddek M, Sazedur AHM, Kabir AS, Faruque MM, Ahmed S. Systematic assessment of the availability and utilization potential of biomass in Bangladesh. *Renewable and Sustainable Energy Reviews*. 2017;**67**:94-105. DOI: 10.1016/j.rser.2016.09.008
- [18] Vieira A, Franco C, Marques F, Rosa F, Monsanto M. Avaliação do Potencial de Biomassa da Região do Algarve. Lisboa: INETI; 2006. p. 114
- [19] Papilo P, Kusumanto I, Kunaifi K. Assessment of agricultural biomass potential to electricity generation in Riau Province. In: IOP Conference Series: Earth and Environmental Science, Volume 65, International Conference on Biomass: Technology, Application, and Sustainable Development; 10-11 October, 2016; Bogor, Indonesia; 2017. DOI: 10.1088/1755-1315/65/1/012006
- [20] Marques IP. Anaerobic digestion treatment of olive mill wastewater for effluent re-use in irrigation. *Desalination*. 2001;**137**(1-3):233-239. DOI: 10.1016/S0011-9164(01)00224-7
- [21] Damaceno FM, Buligon EL, Restrepo JCPS, Chiarelto M, Niedzialkoski RK, Costa LAM, et al. Semi-continuous anaerobic co-digestion of flotation sludge from broiler chicken slaughter and sweet potato: Nutrients and energy recovery. *Science of the Total Environment*. 2019;**683**:773-781. DOI: 10.1016/j.scitotenv.2019.05.314
- [22] Li C, Strömberg S, Liu G, Nges IA, Liu J. Assessment of regional biomass as co-substrate in the anaerobic digestion of chicken manure: Impact of co-digestion with chicken processing waste, seagrass and *Miscanthus*. *Biochemical Engineering Journal*. 2017;**118**:1-10. DOI: 10.1016/j.bej.2016.11.008
- [23] Begum S, Ahuja S, Anupoj GR, Ahuja DK, Arelli V, Juntupally S. Operational strategy of high rate anaerobic digester with mixed organic wastes: Effect of co-digestion on biogas yield at full scale. *Environmental Technology*. 2020;**41**(9):1151-1159. DOI: 10.1080/09593330.2018.1523232
- [24] Batool N, Qazi JI, Aziz N, Hussain A, Shah SZH. Bio-methane production potential assays of organic waste by anaerobic digestion and co-digestion. *Pakistan Journal of Zoology*. 2020;**52**(3):971-976. DOI: 10.17582/journal.pjz/20190322170334
- [25] Direção-Geral do Território. In: Carta de Ocupação do Solo (COS'2018); 2018
- [26] Instituto da Conservação da Natureza e das Florestas. Nature Conservation Areas Geocatalogue. Available from: <https://geocatalogo.icnf.pt/> [Accessed: 20 April 2020]
- [27] ESRI-PT. Digital Terrain Model 30 m Portugal (ETRS89); 2009
- [28] Gabinete Técnico Florestal da Câmara Municipal de Oliveira de Frades. Forest Roadmap of Oliveira de Frades Municipality. 2020
- [29] Gabinete Técnico Florestal da Câmara Municipal de São Pedro do Sul. Forest Roadmap of Oliveira de Frades Municipality. 2020

[30] Gabinete Técnico Florestal da Câmara Municipal de Vouzela. Forest Roadmap of Oliveira de Frades Municipality. 2020

[31] Caetano M, Marcelino F. Especificações Técnicas da Carta de Uso e Ocupação do Solo (COS) de Portugal Continental para 2018. Technical Report. Direção-Geral do Território; 2019

[32] Fenn ME, Bauer LI, Hernandez-Tejeda T. Urban Air Pollution and Forests: Resources at Risk in the Mexico City Air Basin. Springer Science & Business Media; 2012. p. 394

[33] APHA, AWWA, WEF. Standard Methods for the Examination of Water and Wastewater. 2012

[34] Engineering ToolBox. Fuels—Higher and Lower Calorific Values [Internet]. 2003. Available from: [https://www.engineeringtoolbox.com/fuels-higher-calorific-values-d\\_169.html](https://www.engineeringtoolbox.com/fuels-higher-calorific-values-d_169.html) [Accessed: 20 April 2020]

[35] Rösemann C, Haenel H-D, Dämmgen U. Calculations of gaseous and particulate emissions from German agriculture 1990–2013. 2015. p. 406. DOI: 10.3220/REP\_27\_2015

[36] Oehmichen K, Thrän D. Fostering renewable energy provision from manure in Germany—Where to implement GHG emission reduction incentives. *Energy Policy*. 2017;**110**(August):471–477. DOI: 10.1016/j.enpol.2017.08.014

# Methodology for the Evaluation of the Electrical Energy Potential of Residual Biomass from the Wood Industry: A Case Study in Brazil

*Augusto César de Mendonça Brasil*

## Abstract

This chapter presents in a consolidated manner the step-by-step methodology to estimate the electrical energy potential of industrial wood residues considering the dependency of the efficiency of the power plants with their size. A function of the overall efficiency with power was obtained from a best curve fit of real data both taken from the literature and from Brazilian biomass-fired power plants. The methodology was applied to the determination of the electrical energy potential of wood industry residues in the State of Pará (data collected in 2004). Two cases were analyzed: one where a constant electrical efficiency of 25% was considered (independently of the amount of residues generated) and another where the proposed function of efficiency with power was used. Results show that in the State of Pará, the existent 675 sawmills generated  $2.95 \times 10^6$  t in dry basis. When the dependency of efficiency with plant size is not considered, the electrical energy potential and average installed power (3140.4 GWh and 2 MW<sub>e</sub>) are overestimated in comparison to the herein proposed methodology (1868.8 GWh and 1 MW<sub>e</sub>). The present methodology, considering the efficiency as a function of the power, results in an average efficiency of 12.3% (lower than 25%).

**Keywords:** energy potential methodology, woody biomass, biomass residues, bioelectricity, electrical overall efficiency

## 1. Introduction

A large amount of the Brazilian timber production is concentrated in the northern region of the country, namely in the Amazon region. This can be observed in **Figure 1**, which shows the timber production of the top five timber producer states [1]. Four out of the top five timber producer states in Brazil are within the Amazon region. These states are: Rondônia, Amazonas, Amapá, and Pará. Moreover, the State of Pará is historically the largest producer of timber in the country.

As a result of the timber production in the Amazon region, a large quantity of wood residues is generated. However, only a small amount of these residues is used as a valuable biomass energy source [2, 3]. Other industrial uses of wood residues are also minimal. In 2004, for instance, only 10% of the wood processing factories in the State of Pará used wood residues to produce plywood [4]. Usually, woody

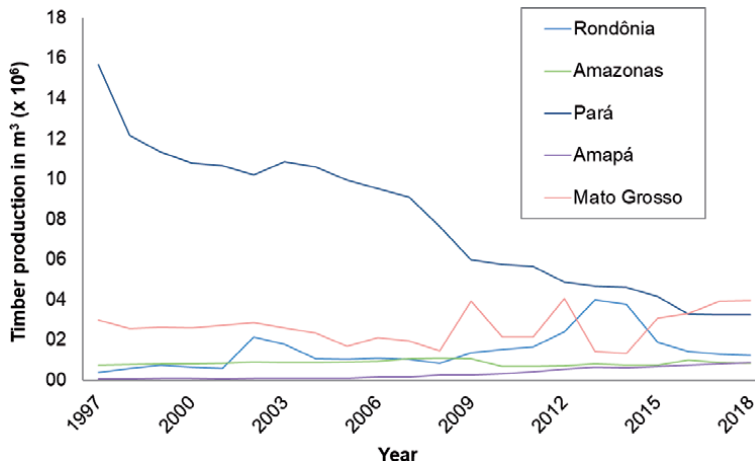


**Figure 1.** Timber production of the top five timber producer states in Brazil from 1997 to 2018.

biomass residues from timber production, which are estimated to be between 58 and 62% of the log volume, become waste [5].

According to the Brazilian Energy Balance [6], in 2019, hydropower in Brazil shared 66.6% of the total 535 TWh of electric generation. At the same time, in the State of Pará, 3.0% of the electric generation is based on fossil fuels and the other 97% is hydropower generation.

The context mentioned above indicates that, in the Amazon region and, more specifically in the State of Pará, the wood residues generated by the industry are not used as an energy source, and that the electric energy resources are mainly based on one single source: hydropower. The strong dependence on hydroelectricity was also identified by da Silva et al. [7] who showed the importance of the diversification of the electricity generation mix to the energy security in Brazil.

That scenario of wood residues availability, with the possibility of using them as an energy source, and the need of diversifying the energy resources in the Amazon region, opens an opportunity for the local lumber mills to install biomass-fired power plants and also to properly valorize the residual woody biomass they generate.

In order to evaluate the viability of using wood residues as an energy resource in the State of Pará, Padilha et al. [4] estimated the electrical energy potential of the residual biomass of the wood industry in that state. The evaluation applied by Padilha et al. [4] used a constant overall efficiency for the steam turbine power plants in the determination of the biomass energy potential. The authors concluded that 70% of the lumber mills in the State of Pará could install biomass-fired power plants with a capacity between 200 and 300 kW<sub>e</sub>.

Brasil et al. [8] revisited part of the data analyzed in 2004 by [4] and estimated an electrical energy potential of 235.5 GWh year<sup>-1</sup> for the wood residues from the 117 sawmills located in a region within a 100-km radius from the main hydropower plant in the State of Pará. In [8], a methodology that takes into account the dependency of the electrical efficiency of the power plants with their capacity was applied, which improved the assessment of the potential of woody biomass wastes for electric energy generation made by Padilha et al. [4]. If the methodology of Padilha et al. [4] was applied to the data analyzed by [8], the electricity potential would be almost twice as large, 429.6 GWh year<sup>-1</sup>. That difference in the energy potential calculated by the two methodologies referred above confirms the importance of considering the influence of the efficiency as

a function of the installed power when estimating the electric energy that can be generated from wood residues.

The approach used to determine the electric energy potential of wood residues followed in work [8] considers not only the dependency of the efficiency on the installed power, but also the geographic location of the lumber mills, the amount of wood residues produced by each mill, and properties, such as the density and lower heating value, of the mixture of the wood residues produced locally.

Following the two works [4, 8], which applied two different approaches, the present study aims to consolidate the step-by-step methodology to estimate the electrical energy potential of residual biomass simultaneously considering the main variables that influence the result of the calculated electric energy generation. Those variables are the geographic location of the timber processing plants where the biomass residues are produced, the amount of residues produced in each of those plants, the density and lower heating value of the mix of the residues, and finally the dependency of the efficiency on the size of the power plants. To illustrate the application of the proposed methodology, a case study determining the potential of implementing biomass power plants fired with wood residues generated by the sawmills in the State of Pará—Brazil—was chosen and investigated. This work highlights the difference in the energy potential obtained when a variable electrical efficiency (dependent on the power) or a constant electrical efficiency is used. That methodological difference can have a great impact on the estimate of the electric energy potential of wood residues in the State of Pará such as the observed in previous works (235.5 GWh year<sup>-1</sup> in [8] and 429.6 GWh year<sup>-1</sup> in [4]).

## **2. Methodology for the evaluation of electric energy potential**

Currently, combustion is the most widely used primary conversion technology of biomass into power and heat (it represents more than 90% of the installed capacity [9]). However, differently from heat, electricity can be integrated into the national grid. In general, steam turbines and the Rankine cycle are used for the conversion of biomass into electricity [10].

In the past, some studies published on the evaluation of the biomass energy potential, such as [4, 11–14], used a constant typical efficiency value. In their study, Brasil, Brasil Jr., and Malico [8] considered the electric efficiency dependence on the size of the power plant when calculating the electric energy potential of wood residues generated by the wood industry. That dependency of the efficiency on the installed power has also been presented, for example, by Bridgwater [15, 16], Dornburg and Faaij [17] and Caputo et al. [18]. Therefore, in order to achieve a more accurate calculation of the electric energy potential of biomass residues combusted in steam cycle power plants located at lumber mills, the efficiency must be a function of the power as proposed in [8]. Hence, the methodology proposed by the present work applies the same function of the efficiency dependency on the power as the suggested by [8].

When considering residues generated by the wood industry, other important variables with great impact on the calculation of the electric energy potential of wood residues are the properties of the mixture of wood species that are processed at the industrial sites and that can be used as fuel in steam cycle power plants of those sites. This is especially important in the Amazon region because the density and lower heating value (LHV) of the wood from the different tree species can vary significantly. It is worth to mention that the appropriate way to determine the residues energy content is multiplying the on-site LHV by the mass of residues.



However, for the evaluation of the electric energy potential of residual biomass, the power generation can only be determined if the power plant efficiency is known, and the efficiency is determined only if the generated power is known; so, the proposed methodology aims to address this circular problem.

## 2.1 Determination of on-site wood residues availability and properties

The first step of the proposed methodology for evaluating the electric energy potential of residual biomass from lumber mills is to gather the coordinates of the location of each mill operating in a study area, and then to store the locations using a geographic information system.

The second step of the methodology is to compute the availability and the properties of the residual biomass generated at each industrial facility. For that, the lumber mills are contacted and asked to provide relevant data. It is important to consider in the methodology what available data are registered and by the wood industries. In general, the available data that are essential to gather are the total trunk volume for each wood species received by the mill yearly, the total volume of processed wood sold yearly, and the total yearly operation hours. The available residues are calculated by the difference of the total trunk volume received and the volume of processed wood sold. Knowing which wood species are processed in the industrial plants, the wood density is determined from a database of wood properties and then the volume of residue for each species is multiplied by its density to obtain the mass. For the Brazilian wood species, the data from [19] and properties measured in laboratory published in [8] can be used.

The annual mass of wood residues on a dry basis of each species  $s$  generated by each lumber mill,  $m_{s,i}$ , is calculated by

$$m_{s,i} = \rho_s V_{s,i} , \quad (1)$$

where  $s$  means the  $s^{th}$  species processed in the  $i^{th}$  lumber mill that is located in the study area,  $\rho_s$  the basic density of each wood species, and  $V_{s,i}$  the volume of wood residues of each species generated yearly by the  $i^{th}$  mill. The total mass of residues generated by each plant in 1 year is the sum of  $m_{s,i}$  for all the species and the total mass of residues generated in a certain region, the sum of the wood residues generated in all the lumber mills located in that region.

## 2.2 Determination of the energy content of residues

For the determination of the energy content of the wood residues, similar to what was mentioned above for the wood density, a database is needed to determine the lower heating value on a dry basis,  $LHV_{db}$ . Values of  $LHV_{db}$  for Brazilian species can be found in [8, 20].

After knowing the  $LHV_{db}$  and the mass of residues for each processed wood species, the next step of the methodology is to compute the energy content of the residues produced annually in the  $i^{th}$  industry located in the study area,  $E_i$ , calculated by

$$E_i = \sum_{s=1}^N m_{s,i} LHV_{db,s} \quad (2)$$

where  $N$  is the number of species processed by the  $i^{th}$  lumber mill and  $LHV_{db,s}$  is the lower heating value on a dry basis of the wood species  $s$  processed by the  $i^{th}$  mill in the study area.

In Eq. (2),  $E_i$  represents the total energy content of the wood residues generated by the  $i^{\text{th}}$  lumber mill in 1 year. If the efficiency of conversion could ideally be 100%, this value would be the total electric energy potential of the  $i^{\text{th}}$  lumber mill. However, because this is not possible,  $E_i$  has to be multiplied by an energy conversion coefficient to determine the electric energy potential of residual woody biomass generated by the industry.

It is important to restate that the main idea of the present work is to propose a methodology focused on the conversion of the energy content of the residues generated by the wood industry into electricity by combustion followed by a steam turbine. Yet, although other final energy use and conversion technologies could be applicable for determining the energy potential of wood residues, the principle of multiplying the energy content of the residues by a conversion overall efficiency maintains. However, for other energy use and conversion technologies, the dependency of the efficiency with the size of the plant would be different from the function observed by [8, 15–18]. This is the case when the end energy use is heat, and that dependency would not occur.

In order to calculate the energy that could be generated from the wood residues and delivered to the electric grid every year,  $E_{\text{out}}$ , the overall efficiency of the energy conversion process,  $\eta_e$ , is defined in Eq. (3).

$$\eta_e = \frac{E_{\text{out}}}{E_i} \quad (3)$$

Typical efficiencies of small power plants with wood combustion and steam turbines are in a range of circa 15%, while larger power plants and those with recent technologies have efficiencies of 30% [21]. Efficiencies as high as 44% are reported by [22], but micro-scale systems operating with steam turbines can have efficiencies as low as 6–8% [23]. The work [4] estimated the electric energy potential of wood residues and considered a typical and constant efficiency value taken from the literature and did not account for the dependency of the efficiency with the installed power. As another example of this approach, Singh [11] considered two different efficiencies of 20 and 25% in converting agricultural residues to electricity, while Vukašinović and Gordić [12] considered an efficiency of 35%, and Weldemichael and Assefa [13] considered an electrical energy efficiency of 33%.

The present methodology proposes the curve for the overall efficiency as a function of the installed power suggested by [8].

### 2.3 Operating time of the power plant

As described in the two previous sections, the amount of wood residues and the energy content of these residues are determined yearly, and the efficiency depends on the installed electric power plant of a wood industry, the latter being defined by Eq. (4).

$$P_{\text{out}} = \frac{E_{\text{out}}}{t} \quad (4)$$

where  $t$  is the total yearly operating time of the power plant. Similarly, an ideal power can be defined by Eq. (5)

$$P_i = \frac{E_i}{t} \quad (5)$$

where  $P_i$  is the total energy content of the wood residues generated by the  $i^{\text{th}}$  lumber mill divided by the total yearly operating time of the power plant installed in that same plant.

Consequently, Eq. (3) can be rewritten as Eq. (6)

$$\eta_e = \frac{P_{out}}{P_i} \quad (6)$$

So, for the methodology proposed, the operating time of the wood industry power plants has an important impact on the calculation of the energy potential of wood residues.

### 2.4 Overall efficiency of residual biomass power plants

Instead of applying a constant value for the conversion efficiency, as already mentioned above, the present methodology recognizes the fact that the overall efficiency of a biomass power plant is expressed as a function of the power plant size, as done in [8]. However, the efficiency can only be determined when the generated power is known, and vice versa; so, a simple mathematical solution is used to overcome this circular reference problem. The procedure is illustrated in **Figure 2** and explained below.

The energy content of the biomass residues, whose calculation was explained in Section 2.2, is determined by Eq. (2). This total energy content of residues divided by the operating time explained in Section 2.3 results in an ideal power  $P_i$  defined by Eq. (5), which is represented by the circle number 1 in **Figure 2**, as if the efficiency of conversion would be ideally 100% (represented by circle number 2 in **Figure 2**). A conversion efficiency equal to 100% is not possible, but the value represented by circle number 2 is fundamental for the mathematical solution, establishing the linear equation crossing the origin and passing through the point of 100% efficiency, represented by the dark dashed line in **Figure 2**.

In the same **Figure 2**, the function of the overall efficiency with the installed power is represented by the solid line. The function represented in this figure is expressed in Eq. (7) and was proposed by [8] from a power law best curve fit to real data from Brazilian biomass-fired power plants and the published works of [15–18].

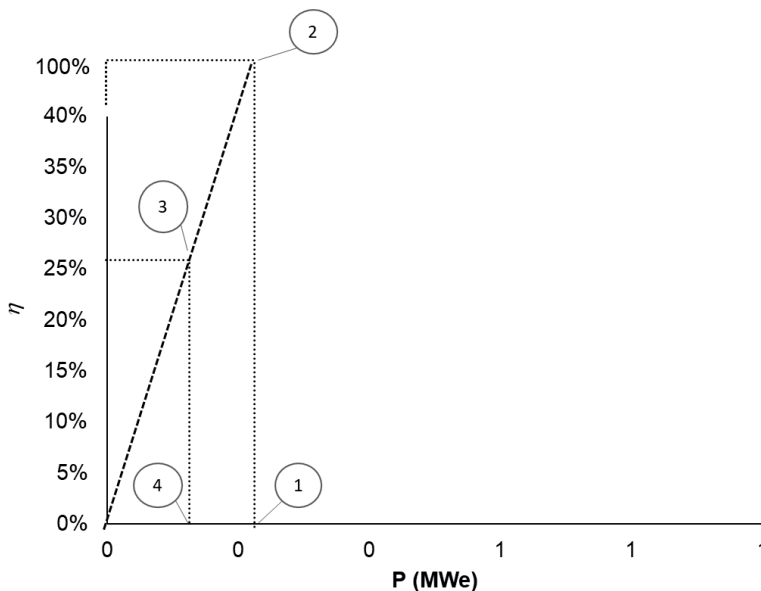


**Figure 2.** Procedure used to calculate the efficiency and installed power of biomass-fired power plants—Solid line is the function of the overall efficiency with the installed power in Eq. (7) and dashed line is the linear equation crossing the origin and passing through the point of 100% efficiency.

$$\begin{cases} \eta_e = 0.0205P^{0.2718} & \text{for } P < 250 \text{ kW}_e \\ \eta_e = 0.0363P^{0.1877} & \text{for } 250 \text{ kW}_e \leq P < 250 \times 10^3 \text{ kW}_e \end{cases} \quad (7)$$

where  $\eta_e$  is the overall efficiency of the biomass power plant and  $P$  the installed power in  $\text{kW}_e$ .

In **Figure 2**, circle number 3 represents the interception of the solid line function defined by Eq. (7), and the dashed line that passes through the origin and the point represented by circle number 2. So, the  $x$ - $y$  values of the intersection represent, respectively, the real overall electric efficiency and the real installed electric power of a biomass power plant with a capacity equal to the value of circle number 4.

### 3. Application of the methodology

A case study was used to demonstrate the application of the proposed methodology detailed in the previous sections. For this purpose, the energy potential of the residual biomass generated by the wood industry in the State of Pará in Brazil was chosen. The present study used the data collected by a massive fieldwork carried out by the Brazilian Federal University of Pará, with results published by Padilha et al. [4] and Rendeiro et al. [24]. That fieldwork [4] collected data from 707 lumber mills in the State of Pará in order to evaluate the quantity of residues available for electric energy conversion. The study of Padilha et al. [4] established that the potential to install electric power plants in the factories processing timber in the State of Pará was 160  $\text{MW}_e$ .

The present work identified that 32 out of the 707 wood processing plants generated virtually zero residues, so wood residues of 675 plants were available for electric energy use.

#### 3.1 Location of residual biomass availability

As proposed by the methodology described above, the locations of the 675 lumber mills in the State of Pará were registered in a geographical information system. This location is shown with blue squares on **Figure 3**. These are all industrial facilities that generate biomass residues that can be valorized for energy. It is noticeable that the lumber mills are concentrated near the roads, because of the need to transport the products.

#### 3.2 Biomass residues availability and properties

The data collected at all the lumber mills of the State of Pará were organized in a database containing the names and addresses of the companies, the geographic coordinates of their location, wood species processed, and the volume of residual biomass produced yearly for each of the wood species handled. Unfortunately, 108 plants only reported the total volume of wood processed and did not report the percentage of each wood species that was processed in that year. In order to overcome that limitation of not knowing the exact amount of wood species processed for these 108 plants and to fill the missing data, it was assumed that in these plants the composition of the processed species was statistically similar to the average of all the other plants in the state. This could be done because of the low variability of the species that are processed by all facilities in that region imposed by the commercial purposes to attend the market.

In accordance to what has been said, the basic density and  $LHV_{db}$  data of all species processed by the timber processing plants in the state was statistically analyzed in two histograms presented in **Figures 4** and **5**. The histogram of **Figure 4** shows the basic density of the species processed by the wood industry in the State of Pará and **Figure 5** shows the histogram of the  $LHV_{db}$  of the species processed by the wood industry in the state.

From the histograms of **Figures 4** and **5**, the statistical percentage of the basic density and  $LHV_{db}$  of species could be extrapolated to the missing data of 108 timber processing plants.

From the data referred before [4], which was gathered from the wood processing plants in the State of Pará in 2004, there were 49 different species processed by the industry. In work [4], samples of wood residues were collected onsite, the species were identified, and some properties measured in the laboratory of the Federal University of Pará. Proximate and elemental analyses were carried out and basic density and  $LHV_{db}$  measured. More details of the analyzed properties can be seen in [8]. The basic density of species was also confirmed by the values published in [19].

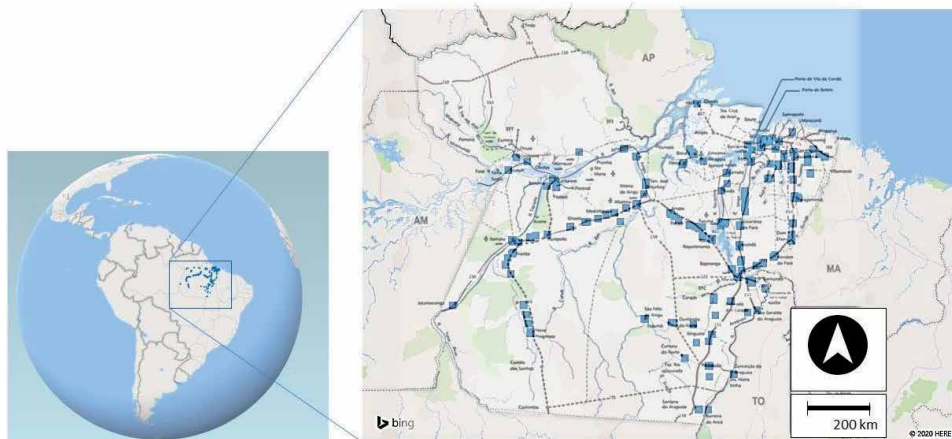


**Figure 3.**  
Location of all lumber mills in the state of Pará—in blue squares.

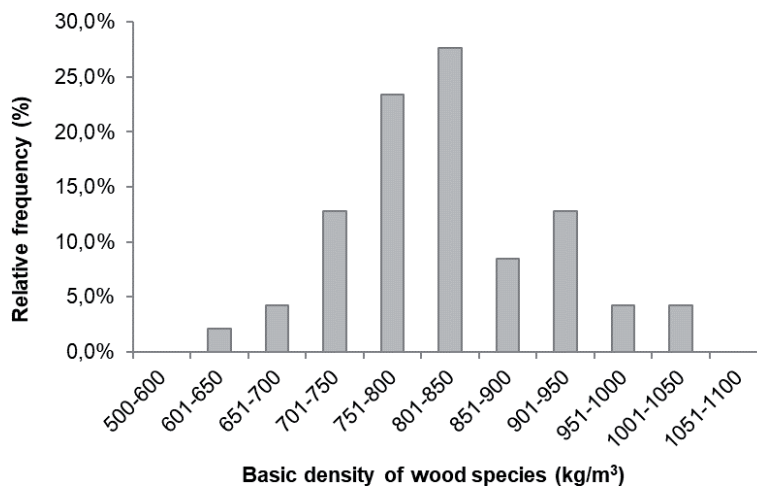


**Figure 4.**  
Histogram of the basic density on a dry basis of wood species processed by the lumber mills in 2004 in the state of Pará.

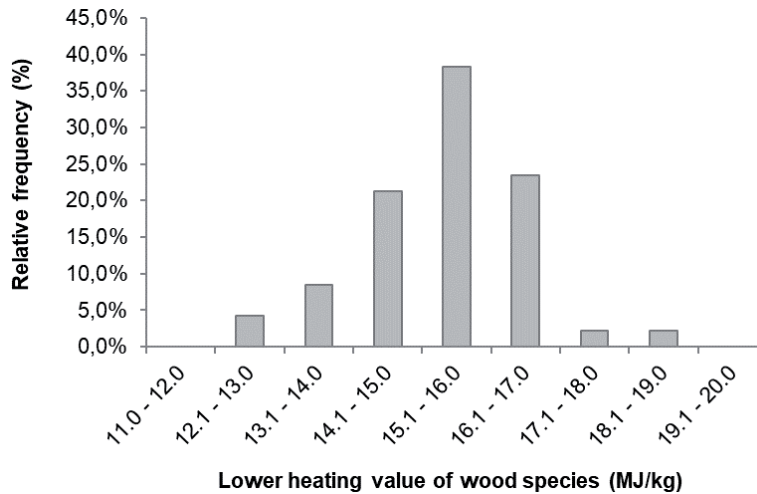


**Figure 5.**  
 Histogram of the lower heating value on a dry basis of wood species processed by the lumber mills in 2004 in the state of Pará.

As seen in Section 2.1, the available residues were calculated by the difference of the total trunk volume received in the plants and the volume of processed wood sold. The annual mass of residual wood of each species processed in each lumber mill was calculated by the sum of all species determined in Eq. (1). As a result, the total wood residues generated by the 675 lumber mills in the State of Pará in 2004 was  $2.95 \times 10^6$  t in dry basis.

### 3.3 Determination of the energy content of residues

After knowing the annual mass of residues of each wood species in each lumber mill, the energy content,  $E_i$ , of the residual biomass in the  $i^{\text{th}}$  mill was calculated by Eq. (2). The total energy content available from the wood residues of the lumber mills in the State of Pará in 2004 was 12,557.5 GWh (this result was obtained by adding the potential for all the plants in the state).

### 3.4 Operating hours of the power plant

In Section 2.3, an ideal power was defined by Eq. (5), and for that, a yearly operating time needs to be established. In the State of Pará two different possibilities can be considered:

- The electricity is needed when the lumber mills are working. Typical working hours of the industry are  $1760 \text{ h year}^{-1}$  ( $10 \text{ months year}^{-1}$ ,  $22 \text{ days month}^{-1}$ ,  $8 \text{ h day}^{-1}$ ). The value of  $10 \text{ months year}^{-1}$  means a  $2 \text{ months year}^{-1}$  period when the lumber mills are not operating during the season of no timber cutting. This is a season when the lumber mills are on scheduled maintenance.
- The case of year-long operating biomass-fired power plants, when  $2112 \text{ h}$  of operating hours can be considered ( $12 \text{ months year}^{-1}$ ,  $22 \text{ days month}^{-1}$ ,  $8 \text{ h day}^{-1}$ ). This is the case for the industries analyzed in data collected by [4].

In this work, the ideal power  $P_i$  was determined considering  $2112 \text{ h}$  in Eq. (5) as the total yearly operating time of the power plants of the wood industry in the State

of Pará. That ideal power defined the value of circle number 1 in **Figure 2** for each timber processing plant.

### 3.5 Overall efficiency of power plant from residues to electricity

Following the procedure described in Section 2.4, after knowing the ideal power represented by circle number 1 for 100% of efficiency, in **Figure 2**, and determining the point of circle number 2, the next step was to calculate point number 3 in order to determine the real overall electric efficiency and the installed electric power represented by circle number 4 in the same **Figure 2**.

The present methodology proposed a correlation function presented in Section 2.4, Eq. (7) and **Figure 2**, and compared the results obtained with the ones obtained using a constant value of 25% applied for the overall efficiency of the power plants,  $\eta_e$  in Eq. (3). In that case, the electrical energy potential would be determined by multiplying the energy content,  $E_i$  (for the residues of each  $i^{th}$  lumber mill) by 25%. This value was used by [4] and was chosen to compare the difference of two methodologies, for the same region and industries.

The present study compares the results of applying a constant value for the overall efficiency and the proposed methodology. **Figure 6** shows the histogram of the electric capacities that could potentially be installed in all lumber mills in the State of Pará. Light gray bars represent the electric power potential in kilowatt ( $kW_e$ ) when a value of 25% is used for the overall efficiency, and dark gray bars, the potential of the electric installed power ( $kW_e$ ) when the steps of proposed methodology are applied, as described in Section 2.4. When an operating time of  $2112 \text{ h year}^{-1}$  is considered, the total energy potential for the residual biomass generated by the wood industry in the State of Pará is  $3140.4 \text{ GWh year}^{-1}$  for the constant efficiency of 25% and  $1868.8 \text{ GWh year}^{-1}$  for the proposed methodology.

The results of the electrical energy potential presented above indicate that the use of the constant value for the efficiency considered overestimates the total predicted available energy, compared to the proposed methodology. Additionally, the modes of the two datasets in the histograms in **Figure 6** indicate that the highest

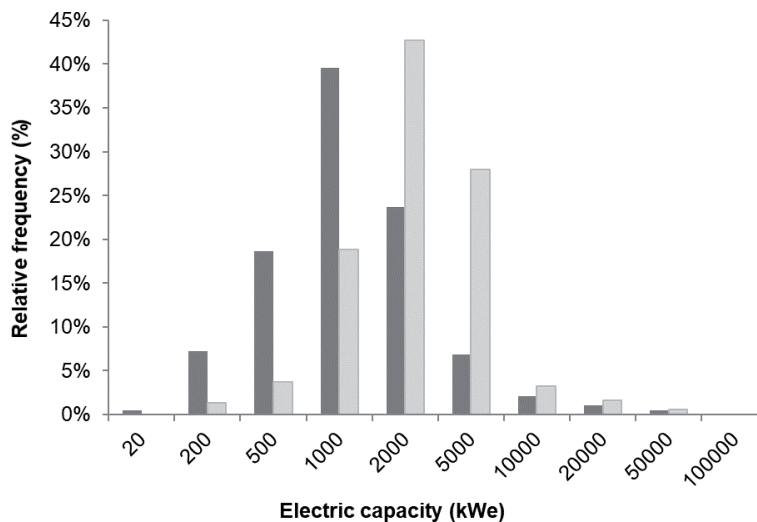


**Figure 6.** Histogram of the electric capacity that can potentially be installed at lumber mills in the State of Pará, considering a constant overall electrical efficiency (light gray) and the dependency of efficiency with power (dark gray).

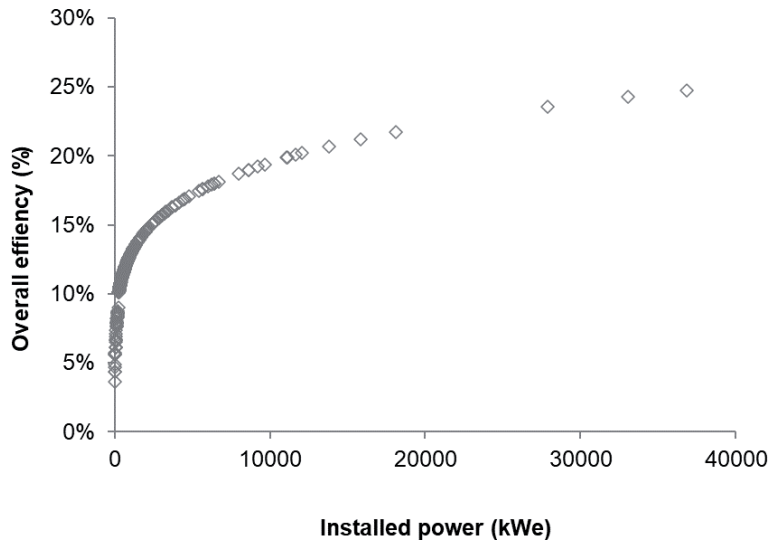


**Figure 7.** Calculated overall efficiency as a function of the power for the 675 lumber mills that existed in 2004 in the state of Pará.

relative frequency is 42.7% at 2000 kWe for a constant efficiency value, and 39.6% at 1000 kWe for the proposed methodology. Also in **Figure 6**, summing the relative frequencies of potential capacities less than the mode value resulted in the conclusion that 66.52% of the lumber mills would have installed power up to 2 MW<sub>e</sub> for a constant value of efficiency, while the proposed methodology indicates that 65.93% of the industrial units would have installed power below 1 MW<sub>e</sub>. That conclusion is significant because one method indicates that most of the industries would have a power plant of 2 MW<sub>e</sub> in comparison to 1 MW<sub>e</sub> from the proposed methodology.

As presented in Section 2.4 and Eq. (7), the overall efficiency is a function of the installed power. Therefore, **Figure 7** shows the results of the efficiencies and potential capacities of the 675 wood industries in the State of Pará, indicating that an efficiency value of 25% is only applicable for power plants with capacities above 40 MW<sub>e</sub>, which is never the case for the scenario in the State of Pará. The results of this case study confirm that a constant efficiency overestimates the electric energy potential when applying a constant value of 25% in Eq. (3) for all biomass plants and based on the total available energy content of residues. Nevertheless, when applying the efficiency as a function of the installed power, the resulting average efficiency is 12.3%, based on the values of efficiencies of all plants in **Figure 7**.

#### 4. Conclusions

The present work systematized a step-by-step methodology to determine the electrical energy potential of residues generated by the wood industry. The application of the proposed methodology was demonstrated through a case study that analyzed the energy potential of the residues generated by the wood industry in the State of Pará in Brazil. In the past, several different studies considered a constant overall efficiency as a conversion factor from residues to electricity. The proposed methodology suggests an overall efficiency as a function of the installed power, with data correlation obtained from a best curve fit of real data both taken from the literature [15–19] and from Brazilian biomass-fired power plants.



The data for the case study was collected in 2004 with results published by Padilha et al. [4] and Rendeiro et al. [24]. The work of Padilha et al. [4] collected data from 675 timber processing plants in the State of Pará, which generated an amount of wood residues equal to  $2.95 \times 10^6$  t on dry basis in that year. In this work, the energy potential of these residues was calculated in two different manners for the sake of comparison: (1) similar to what was done in [4], a constant overall conversion efficiency of 25% was considered; and (2) the methodology presented in this work was used (i.e., the efficiency is a function of the size of the plant).

As a conclusion, the electrical energy potential is overestimated when a constant overall efficiency of 25% is used ( $3140.4 \text{ GWh year}^{-1}$ ) in comparison to the one obtained for the proposed methodology ( $1868.8 \text{ GWh year}^{-1}$ ). Concerning the power that can potentially be installed to valorize the residual biomass, when a constant efficiency was applied; the results indicate that most of the power plants would have a  $2\text{-MW}_e$  capacity, while for the proposed methodology the results indicate that most of the power plants would have a capacity of  $1 \text{ MW}_e$ . Moreover, in agreement with the function presented in this work for the dependency of the efficiency with plant size, a 25% efficiency is only applicable for power plants with a power as high as 40 MW, which is never the case for the wood industry in the State of Pará. The results of the methodology proposed in this work highlight the importance of using the overall electrical efficiency as a function of installed power when determining the residual biomass potential.

## Acknowledgements


The author thanks professor Gonçalo Rendeiro, Cláudio Duarte (in memoriam) and professor Jesse Padilha, from the Federal University of Pará, for the partnership on collecting the wood residues of the sawmills and LHV analysis, and also would like to acknowledge the Brazilian Electricity Regulatory Agency (ANEEL) that funded the project that collected the data, making this work possible.

## Author details

Augusto César de Mendonça Brasil  
Energy Engineering, University of Brasília at Gama, Brasília, DF, Brazil

\*Address all correspondence to: [ambrasil@unb.br](mailto:ambrasil@unb.br)

## IntechOpen

© 2020 The Author(s). Licensee IntechOpen. Distributed under the terms of the Creative Commons Attribution - NonCommercial 4.0 License (<https://creativecommons.org/licenses/by-nc/4.0/>), which permits use, distribution and reproduction for non-commercial purposes, provided the original is properly cited. 

## References

- [1] IBGE. Produção da Extração Vegetal e da Silvicultura 2009 [Harvesting of Forest Products and Silviculture Production 2019 Report]. Rio de Janeiro, Brazil: Instituto Brasileiro de Geologia e Estatística; 2019. [in Portuguese]
- [2] Paixão CPS, Ferreira E, Stachiw R. Produção e destinação dos resíduos gerados em serrarias no município de Rolim de Moura - RO [Production and destiny of the residues generated in the sawmills of the municipality of Rolim de Moura - RO]. *Revista Brasileira de Ciências da Amazônia/Brazilian Journal of Science of the Amazon*. 2015;3:47-56
- [3] Wiecheteck M. Aproveitamento de Resíduos e Subprodutos Florestais, Alternativas Tecnológicas e Propostas de Políticas ao Uso de Resíduos Florestais para Fins Energéticos. [Utilization of Forest Residues and Byproducts, Technological Alternatives and Policy Proposals for the Energetic Use of Forest Residues]. Curitiba, Brazil: Ministério do Meio Ambiente; 2009. [in Portuguese]
- [4] Padilha JL, Rendeiro G, Brasil AM, Santos R, Pinheiro G. Potencial de geração de energia elétrica no estado do Pará, utilizando a biomassa do setor Madeireiro [Potential of Electric Power Generation in the State of Pará Using Lumber Biomass]. *Biomassa & Energia*. 2005;2:267-284. [in Portuguese]
- [5] Verissimo A. Pólos Madeiros Do Estado Do Pará [Wood Industry Clusters in the Pará State]. Belém, Brazil: Imazon; 2002. [in Portuguese]
- [6] EPE. Brazilian Energy Balance 2016: Year 2015. Rio de Janeiro, Brazil: Empresa de Pesquisa Energética; 2016
- [7] da Silva RC, de Marchi Neto I, Seifert SS. Electricity supply security and the future role of renewable energy sources in Brazil. *Renewable and Sustainable Energy Reviews*. 2016;59:328-341
- [8] Brasil ACM, Brasil A Jr, Malico I. Evaluation of the electrical energy potential of Woody biomass in the near region of the hydropower plant Tucuruí-Brazil. *Waste and Biomass Valorization*. 2020;11:2297-2307. DOI: 10.1007/s12649-018-0407-6
- [9] Malico I, Pereira RN, Gonçalves AC, Sousa AM. Current status and future perspectives for energy production from solid biomass in the European industry. *Renewable and Sustainable Energy Reviews*. 2019;112:960-977.0
- [10] Corradetti A, Desideri U. Should biomass be used for power generation or hydrogen production? *Journal of Engineering for Gas Turbines and Power*. 2007;129:629-636
- [11] Singh J. Overview of electrical power potential of surplus agricultural biomass from economic, social, environmental and technical perspective—A case study of Punjab. *Renewable and Sustainable Energy Reviews*. 2015;42:286-297
- [12] Vukašinović V, Gordić D. Optimization and GIS-based combined approach for the determination of the most cost-effective investments in biomass sector. *Applied Energy*. 2016;178:250-259
- [13] Weldemichael Y, Assefa G. Assessing the energy production and GHG (greenhouse gas) emissions mitigation potential of biomass resource for Alberta. *Journal of Cleaner Production*. 2016;112:4257-4264
- [14] Ozcan M, Öztürk S, Oguz Y. Potential evaluation of biomass-based energy sources for Turkey. *Engineering Science and Technology, an International Journal*. 2015;18:178-184

- [15] Bridgwater AV. The technical and economic feasibility of biomass gasification for power generation. *Fuel*. 1995;**74**:631-653
- [16] Bridgwater AV, Toft AJ, Brammer JG. A techno-economic comparison of power production by biomass fast pyrolysis with gasification and combustion. *Renewable and Sustainable Energy Reviews*. 2002;**6**:181-246
- [17] Dornburg V, Faaij APC. Efficiency and economy of wood-fired biomass energy systems in relation to scale regarding heat and power generation using combustion and gasification technologies. *Biomass and Bioenergy*. 2001;**21**:91-108
- [18] Caputo AC, Palumbo M, Pelagagge PM, Scacchia F. Economics of biomass energy utilization in combustion and gasification plants: Effects of logistic variables. *Biomass and Bioenergy*. 2005;**28**:35-51
- [19] de Paula JE, Costa KP. Densidade da Madeira de 932 Espécies Nativas do Brasil [Density of wood of 932 native species from Brazil]. Porto Alegre: Cinco Continentes; 2011. [in Portuguese]
- [20] Quirino WF, do Vale AT, Andrade APA, Abreu VLS, Azevedo ACS. Poder calorífico da madeira e de materiais ligno-celulósicos [Heating value of wood and material ligno-cellulosic]. *Revista da Madeira*. 2005;**89**:100-106. [in Portuguese]
- [21] IEA. Technology Roadmap. Bioenergy for Heat and Power. Paris: IEA Publications; 2012. p. 62
- [22] van den Broek R, Faaij A, van Wijk A. Biomass combustion for power generation. *Biomass and Bioenergy*. 1996;**11**:271-281
- [23] Pritchard D. Biomass Combustion Gas Turbine CHP, ETSU B/U1/00679/00/REP. DTI Pub URN No 02/1346. UK: Talbott's Heating Ltd; 2002
- [24] Rendeiro G, Macedo EN, Pinheiro G, Pinho J. Analysis on the feasibility of biomass power plants adding to the electric power system—Economic, regulatory and market aspects—State of Pará, Brazil. *Renewable Energy*. 2011;**36**(6):1678-1684. DOI: 10.1016/j.renene.2010.11.015

# Opportunities of Circular Economy in a Complex System of Woody Biomass and Municipal Sewage Plants

*Attila Bai and Zoltán Gabnai*

## Abstract

In this chapter, we present the opportunities and general importance of woody biomass production (forests and short-rotation coppices) and waste management in a common system. Wastewater and different forms of sewage sludge, as energy- and nutrient-rich materials, can contribute to reaching resource efficiency, savings in energy, and reduction of CO<sub>2</sub> emissions. Within certain limits, these woody plantations are suitable options for the environmentally sound disposal of wastewater and/or sewage sludge; in addition, they can facilitate the realization of full or partial energy self-sufficiency of the wastewater plant through bioenergy production. Focusing on circular economy, we introduce the aspects of the treatment process and the sizing issues regarding the municipal wastewater treatment and the woody biomass in a complex system. Based on a specific case study, approximately 826 ha of short-rotation coppices (with a 2-year rotation) are required for the disposal of sewage sludge generated by a 250,000 population equivalent wastewater treatment plant. If we look at the self-sufficiency of its energy output, 120–150 ha of short-rotation coppices may be adequate. This complex system can replace the emissions of around 5650 t of CO<sub>2</sub> through electricity generation alone and another 1490 t of CO<sub>2</sub> by utilizing the waste heat.

**Keywords:** circular economy, complex system, sludge management, self-sufficiency, short-rotation coppices

## 1. Introduction

In this chapter, we introduce the possibilities for connecting woody biomass production and municipal-level wastewater management. Both topics are usually examined on their own, but in our opinion, their application in a common system can implement the concept of a circular economy in a very promising way as well as facilitate the implementation of environment protection goals and tasks [e.g., energy efficiency, reduction of greenhouse gas (GHG) emissions, and waste management].

Circular economy is the concept in which products, i.e., materials (or raw materials and feedstock) participate in the economic cycle for as long as possible, and in which waste is used as a secondary raw material that can be recycled and reused.

The focus is on minimizing losses, reusing, and recycling [1]. As a key factor, lack of resources will primarily result in modern forms of waste management [2]. One of the possibilities is to combine wastewater treatment with woody biomass production and to utilize (even for multiple purposes) the resulting outputs.

Wastewater and different forms of sewage sludge (especially sewage sludge compost), as energy- and nutrient-rich materials, can contribute to reaching resource efficiency, energy savings, and CO<sub>2</sub> reductions. Within certain limits, woody plantations are suitable options for the environmentally sound disposal of wastewater and/or sewage sludge; in addition, they can facilitate the realization of full or partial energy self-sufficiency of the wastewater plant through bioenergy production, or sometimes even extra energy can be generated.

We think there is an observable tendency that, all around the world, more and more people are moving to cities and producing an increasing amount of waste, a significant (and difficult to handle) part of which is generated in liquid form. In contrast to smaller settlements, industrial plants operating in urban environments also emit large amounts of organic matter, the treatment of which together with municipal wastewater must be solved, preferably in an automated and cost-effective way. During this process, renewable energy can also be produced by anaerobic digestion. In addition, the utilization of digested material (sludge) with high macro- and microelement content for nutrient management presents a serious problem to be solved, especially in the case of industrial wastewater. In contrast to arable land used for food crops, high levels of inorganic matter and, in some cases, relatively high levels of heavy metals do not pose a food safety threat in the case of short-rotation coppices (SRCs).

It should be noted that the placement of sewage sludge on agricultural land is problematic due to the reluctance of producers, even if the legal environment of the given country allows the use of sewage sludge for agricultural purposes, not to mention the high cost of placing high moisture sludge.

Nowadays, a wide range of technologies for the purification and treatment of generated wastewater are recognized and applied, ranging from extensive drying and the traditional, most widely used (activated sludge) process to innovative, novel, and environmentally sound wastewater treatment solutions.

Here, we first briefly make plain the most important relevant characteristics of SRC and afterward focus on wastewater management issues and the connection between wastewater treatment plants (WWTPs) and SRCs. We continue with introducing a case study to make the sizing problem clear, and finally, we will demonstrate with some international examples that this topic is no longer in the distant future but is now active in the present.

## **2. The significance of forests and short-rotation coppices**

Forests represent an irreplaceable national treasure and a form of land use that provides financial security and intellectual refreshment. Truth be told, they are also fundamental to the protection of our environment. From the cradle to the grave, trees accompany us. Many forms of their benefits cannot be expressed in money, yet they are irreplaceable. The ideological value of forests is incalculable. Long-rotation forests have a wide range of social functions but are no longer able to fully meet the increased need of biomass for energy.

The most important economic characteristics of long-rotation forests can be summarized by the fact that, due to their long production cycle, the significant planting costs are only recovered much later, making market price changes impossible to follow. During their lifetime, only small revenues are expected from clearing and thinning. In average, more than 50% of air-dried wood is carbon, since trees

are able to capture and store significant amounts of carbon [3]. These forests also play an important role in providing protection against winds and floods, in addition to producing oxygen, shade, and a humid microclimate. For example, in Hungary, the utilization of the floodplains for forestry purposes is complicated by the fact that these areas are divided in terms of ownership. Some may be state-owned and managed by the authority of water resources and forestry, as well as national parks, while some of them are privately owned. Game management and hunting offer new land use and income opportunities for foresters and producers leaving agriculture. Wild animal parks and public events can also function as an ancillary activity of agriculture, but they can also be reasonably connected with tourism (e.g., rural and ecotourism) and various rural development programs. However, the role of traditional logging in rural employment cannot be neglected either.

The functions of forests described in the previous section are essential, but their energy role is just as crucial, becoming ever more important. Of the different renewable energy sources, mankind has been using biomass for energy purposes for the longest time, and even today, firewood is the most important energy source for about two billion people [4]. An important aspect of meeting energy needs is that the wood should be of uniform quality, produced in as small an area as possible with relatively high biomass yields at the lowest possible cost—all of which are typical of short-rotation coppices. Another important aspect is to be suitable for use under automated conditions, that is, in large-scale central heating or cogeneration plants. SRCs are probably the best way to relieve the burden on natural forests. SRCs are not suitable for the welfare and social functions of long-rotation forest management, but they are able to produce large amounts of biomass for energy from a much smaller area at a cheaper cost and can be managed in an environmentally friendly way as well [3].

## 2.1 Forest yields and short-rotation coppice yields

In the European Union (EU), the mean annual gross increment achieved by forest tree species is 4.7 m<sup>3</sup>/ha/year [3]. SRCs have both significantly higher annual revenues and expenditures than long-rotation forests as well as higher carbon sequestration (in the produced biomass) and emission values per year. SRCs are more sensitive to production technology than long-rotation forests. In addition, due to more intensive growth at young age and more intensive production technology, their yearly output is approximately three times more than that of long-rotation forests [3].

After the first and second harvests (**Table 1**), no difference is expected regarding the yield, but after the third rotation, it is necessary to calculate the loss of wood yield, due to the weaker growing ability of the SRC, which can be characterized by an estimated practical factor of 0.85–0.90. In the case of the fourth and fifth harvests, the value of the practical factor is 0.80–0.85 [5].

The duration of the production cycle and the number of cutting cycles are influenced not only by the expected yield data but also by the price of biomass, the actual harvesting cost, and the technical feasibility.

**Table 1** shows that if we made our decisions based on the increase in yield, then harvesting after 4 years would be ideal, as opposed to wastewater and sewage sludge disposal, which would be done theoretically every year. All things considered, it seems that there is no solution that is suitable for both the SRC and the wastewater treatment plant. Due to the aspects of the wastewater treatment plant, it is advisable to perform the harvesting earlier, which, in our opinion, may justify harvesting after 2 years, especially in the case of highly productive clones.

Some forest species can be successfully grown in SRC in areas with groundwater inundation, floodplain areas (willow, *Salix* sp.), and even on sandy soils (black locust, *Robinia pseudoacacia*). Under better natural conditions, (hybrid) poplar

| Age (years) | Wood mass (t ha <sup>-1</sup> ) | Average wood yield (t ha <sup>-1</sup> yr. <sup>-1</sup> ) | Yearly increment (t ha <sup>-1</sup> ) |
|-------------|---------------------------------|--|--|
| 1           | 12.8                            | 12.8   | 12.8                                   |
| 2           | 28.7                            | 14.4   | 15.9                                   |
| 3           | 46.9                            | 15.6   | 18.2                                   |
| 4           | 69.3                            | 17.3   | 22.4                                   |
| 5           | 85.7                            | 17.1   | 16.4                                   |
| 6           | 92.0                            | 15.3   | 6.3                                    |

Source: [4].

**Table 1.**  
Yield data of the “Koltay” poplar clone.

| Tree species                                   | Willow   | Poplar   | Black locust |
|--|----------|----------|--------------|
| Yield (t ha <sup>-1</sup> year <sup>-1</sup> ) | 8.4–25.0 | 7.8–24.0 | 5.0–15.0     |

Source: [5–19].

**Table 2.**  
Yield intervals of short rotation energy plantations (different species).

(*Populus* sp.) species are most recommended. By planting SRCs in areas prone to erosion or deflation, an excellent soil protection effect can be achieved due to the almost year-round soil cover, and thus their establishment can be a profitable forest alternative for farmers in addition to preserving the rural population. Based on technical literature data on international SRC, the following yield intervals were reported (**Table 2**) [6–20].

As it can be seen in **Table 2**, the yield of SRC shows an enormous variation, depending on the place of production, climate, tree species, and production technology. Furthermore, the yields could be significantly increased, depending on the intensity and management of fertilization.

## 2.2 The role of woody plants in environmental protection

We consider that biomass has a special place among energy sources in terms of sustainability. It is clearly a renewable resource. However, the balance of GHG emissions moves on a very wide scale compared to the clearly positive balance of other renewable energy sources. This range is mainly influenced by the following factors:

- The amount and nature of the inputs used in the production technology. In this respect, long-rotation forests have lower emissions.
- The biomass yield, which is much higher in SRC than in forests.
- The technology used for energy production: furnaces with medium or large performance (due to the recent legal regulations) have much more favorable environmental characteristics compared to furnaces with smaller performance (e.g., used in family houses, which often have very low-tech combustion units).
- The emission parameters of the substituted energy source; in this respect, the replacements of coal and heating oil are the most favorable.

According to Hungarian regulations, the CO<sub>2</sub> sequestration of 1 ha of average forest area (in the case of natural gas substitution) exceeds the emitted amount of

CO<sub>2</sub> by 3.78 times, and the CO<sub>2</sub> sequestration balance may be 5.3 t/ha/year, based on the authors' previous calculations [3].

CO<sub>2</sub> sequestration in SRC varies widely, depending on tree species, soil quality, and technology intensity [21]. Taking into account these differences and the relevant technical coefficients, the possible amount of CO<sub>2</sub> emissions that can be saved by the different SRCs when replacing natural gas are as follows (t/ha/lifetime): black locust: 23–150, poplar: 35–237, and willow: 35–248 [21, 22].

In accordance with the legal regulations of the given country or production area, we think that the utilization of wastewater and sewage sludge for soil management purposes is possible in the case of both long-rotation forests and SRC. In the case of the latter category, a technology with shorter cutting cycle is preferable than the longer cutting cycle. The harvest is done approximately in every 2–5 years, but some are harvested after 1 year. Accordingly, biomass production and utilization can be realized with this SRC technology in a much shorter and more predictable way compared to long-rotation forests. This fact is compounded by the juvenile growth phase in SRCs, which allows a significant biomass yield to be achieved due to the increased growth rate in the first few years.

Therefore, if not only the waste/by-product utilization function could be achieved, but in addition, the nutrient content of wastewater or sewage sludge could be also utilized for energy production, then the use on SRCs could definitely be recommended.

### **2.3 Sewage sludge as a nutrient source**

Considering our experience, biomass production and the related bioenergy production account for a significant share of the growing energy demand, which is a concomitant phenomenon of economic development and population growth. Due to the—often significant amount of—biomass removed from the soil, in order to preserve the proper condition and productivity of the soils, it is absolutely necessary to perform nutrient replenishment. As a matter of course, the yield of SRC using the wastewater or sewage sludge has a fundamental effect on the amount of energy that can be produced from the biomass removed from SRC. Use of large amounts of wastewater, digested sewage sludge, or sewage sludge compost may result in higher yields, so one can minimize the necessary SRC area to produce enough heat or electricity for the sewage plants' energy self-sufficiency.

Sewage sludge and sewage sludge compost can also be seen as a kind of alternative to chemical fertilizers, especially in areas of nonfood crops [23]. By applying sewage sludge and choosing the suitable SRC, it is also possible to cultivate areas that can be used only to a limited extent or cannot be used at all otherwise [24]. Numerous international examples are known for the use of products containing sewage sludge as raw material in SRC. According to Labrecque-Teodorescu [25], if an adequate amount of sewage sludge is applied on the soil, it has a beneficial effect on the SRC yields. Forest trees are able to absorb significant amounts of nitrogen from the sewage sludge, which helps to achieve higher yields. One of the most critical points in the field use of sewage sludge compost may be the presence of certain heavy metals, which is why the direct application in the case of food and feed production purposes should be avoided. At the same time, in the case of SRC, in addition to the beneficial effects of compost, sewage sludge can also play a direct role in soil remediation: SRC absorbs particularly high concentrations of heavy metals [26]. Moreover, it could be a suitable solution to apply high heavy metal content sewage sludge on the SRC, as it can even significantly reduce the heavy metal content in addition to other nutrients. In this way, it is possible to combine two advantages: on the one hand, the forest trees reduce the harmful heavy metal



content, and on the other hand, the resulting biomass becomes usable for energy purposes, improving the economics of the treatment activity [27].

In the case of long-rotation forests, we consider that flooding technology can be used to dispose of a relatively large amount of treated wastewater in one turn (which, in this case, is not hindered even by the unpleasant odor) or to dispose of sewage sludge or compost between rows. However, in both cases, it is a problem that the total yield and, for this reason, the nutrient requirements of long-rotation forests are much lower than those of intensive SRCs, which allows for the treatment of significantly less organic matter in the case of forests. Altogether, compost is less economical than sewage sludge, but its content parameters are more favorable and the health risk of its use is also lower.

In SRC, chemical or organic fertilizer is best applied after harvest. As a result, the application is both technically and economically more advantageous and allows the placement of large amounts of wastewater or sewage sludge compost on a regular basis at short intervals. For all these reasons, we clearly recommend SRC for sewage sludge disposal, although both methods are technically feasible.

By the end of the treatment process, only some of the macronutrients remain in the sewage sludge that can be used for nutrient management. Treated sludge generally contains about 1–6% nitrogen and 0.8–6.1% phosphorus on a dry weight basis [28]. However, an appropriate aerobic or anaerobic treatment is particularly important for sludge utilization.

The nitrogen content of the sewage sludge compost made from digested sludge is approximately 2.1% of the dry matter content [29], while its phosphorus content is half. Consequently, the composition of treated sludge and the sewage sludge compost is significantly lower in comparison with the N and P content of good quality animal manure (8.5 kg/t and 5.5 kg/t, respectively [30]), which, in addition, is not problematic in terms of its heavy metal content either.

The digested sludge yield is approximately 0.3–0.4 kg sludge dry matter/m<sup>3</sup> wastewater [28, 31–33]. In the calculations of the composting technology, a volume ratio of 1:2 was calculated for the sludge and structural material.

The disposal of sewage sludge as compost is also justified by its beneficial effects in terms of forest tree nutrition, soil improvement, and environmental protection. Compared to liquid and dewatered sewage sludge, the use of compost (1) increases the cation exchange capacity of the soil, (2) forms soil granules that improve soil structure and organic matter content, (3) reduces soil erosion, (4) improves soil water management, (5) slows down the release of nutrients, (6) slows nutrient leaching by buffering, and (7) prevents rapid pH change. From the aspect of forest tree nutrition, the use of sewage sludge has the following advantages: (1) it provides more balanced nutrient uptake (less risk of leaching) and (2) it increases the nutrient storage capacity of the soil due to its high adsorption capacity [34, 35].

Wood chips' properties are quite advantageous when applying as a structural material used in composting [31]. In the developed concept, wood chips from SRC serve as a structural material during composting, a significant part of which can be reused after screening.

### **3. Main characteristics of wastewater management**

Approximately, 330 billion m<sup>3</sup> of wastewater is generated on earth in 1 year [36]. However, the proportion of treated water is favorable (70% on average) in developed, economically prosperous countries, while it is only one third or a quarter of all wastewater generated in average in, developing, as well as underdeveloped, poor

countries [37]. Accordingly, it can be stated that a significant share of the wastewater produced worldwide is released into the environment without proper treatment and purification.

As for the number of wastewater treatment plants in each continent, Europe is the leader with its 60,000 plants [38], while North America is ranked second (with approximately 16,000 plants). In the ranking of countries, the United States has the largest number (14,600) of wastewater treatment plants.

### **3.1 Review on sewage plants and wastewater**

#### *3.1.1 Energy demand and self-sufficiency*

WWTPs are among the largest individual consumers of electricity in municipalities: in some cases, they are responsible for up to 20% of the city's total electricity consumption [39]. For this reason, the treatment of municipal wastewater requires a significant amount of energy, mainly due to the aeration of activated sludge microorganisms—and the operation of the necessary pumps. Its proportion may reach up to 60–70% of the total amount of electricity used [40].

There may be very large differences between different wastewater treatment plants with regard to the electricity used for treatment activities, as this cost group affects operating costs the most. Based on a survey of 369 sewage plants with different technologies examined in the framework of the ENERWATER project [41], it can be concluded that treatment is less efficient in relatively smaller plants (up to 5.50 kWh/m<sup>3</sup>) and very efficient in larger plants (up to 0.13 kWh/m<sup>3</sup>).

Wett et al. [42] say that wastewater contains more energy than what is sufficient for the treatment plant to use electricity, and with the right technology, the purification activity of the plant can even be self-sustaining.

The energy self-sufficiency rate of plants performing state-of-the-art, efficient treatment, digestion sludge treatment, biogas production, and utilization is 60–100% of their electricity need, depending on their size, and more than 100% of the necessary thermal energy [31]. Consequently, if we use wood chips to improve the self-sufficiency in electricity, we need to find the heat utilization capacity for the extra heat, especially in the summer period. Examples include the following:

- fulfilling the on-site cooling demand,
- using the heat not for only heating of buildings on the site, but for other technological purposes, and
- utilization in a district heating system.

As a matter of course, we think that the level of energy demand of a plant can also be influenced by outdated technology or other modifying factors and conditions (e.g., geographical and site-specific conditions, forest area, or industrial plants nearby) related to the given treatment plant.

#### *3.1.2 Energy and nutrient content of wastewater*

From a different viewpoint, nowadays, the approach of wastewater treatment plants is becoming increasingly important, according to which WWTPs can be considered not only as a place of purification activity but also as a source of energy and raw materials. Regarding energy-related characteristics of wastewater, according

to McCarty et al. [43] and Gude [44], three forms of energy may be associated to wastewater. For wastewater with an average composition, in the United States, the specific theoretical energy associated to wastewater can be estimated as follows [43]:

1. Energy of organic pollutants:  $\sim 1.79\text{--}1.93 \text{ kWh/m}^3$
2. Energy to produce fertilizing elements (N and P):  $\sim 0.70\text{--}0.79 \text{ kWh/m}^3$
3. Available thermal energy:  $\sim 7.00 \text{ kWh/m}^3$

The above values were calculated by McCarty et al. [43] based on the chemical oxygen demand (COD) value for the organic constituents present in the wastewater (500 mg/l), assuming a COD theoretical energy production potential of 3.86 kWh/kg.

Similar to the specific energy content of different types of wastewater, their macronutrient contents could also show differences. Municipal wastewater contains mainly water (99.9%) and relatively low concentrations of suspended and dissolved organic and inorganic solids. Organic substances in wastewater include carbohydrates, lignin, fats, soap, synthetic detergents, proteins, and their degradation products as well as various natural and synthetic organic chemicals from the manufacturing industry. **Table 3** shows the levels of the main components of municipal wastewater with high, medium, and low strength, with minor contributions of industrial wastewater. In arid and semiarid countries, water use is often quite low and wastewater has significant nitrogen and phosphorus content. The concentration of raw wastewater also depends on the economic situation of the country and the region as well as its special production activities and consumer habits. Daily wastewater production in developed countries ranges between about 150–300 liters per capita [45].

### 3.2 Aspects of circular economy

In connection with the wastewater treatment activity and in relation to the concept of circular economy, it is a requirement of recycling to strive for the

| Parameter     | Concentration, mg/l |        |     |
|---------------|---------------------|--------|-----|
|               | High                | Medium | Low |
| COD total     | 1200                | 750    | 500 |
| COD soluble   | 480                 | 300    | 200 |
| COD suspended | 720                 | 450    | 300 |
| BOD           | 560                 | 350    | 230 |
| N total       | 100                 | 60     | 30  |
| Ammonia-N     | 75                  | 45     | 20  |
| P total       | 25                  | 15     | 6   |
| Ortho-P       | 15                  | 10     | 4   |

*COD: chemical oxygen demand. The COD analysis measures through chemical oxidation by dichromate the majority of the organic matter present in the sample.*

*BOD: biological oxygen demand. The BOD analysis measures the oxygen used for oxidation of part of the organic matter.*

*Source: [46].*

**Table 3.** Typical composition of raw municipal wastewater with minor contributions of industrial wastewater.

rational use of usable micro- and macroelements in wastewater and composting in order to reduce the volume of wastewater (**Figure 1**).

The utilization of sludge should be considered an integral part of wastewater treatment in order to both reduce the amount of unused wastes and generate valuable products or by-products. Sludge can be used depending on the specific characteristics, circumstances, and regulations of the given country or area. A wide range of solutions and technologies are known, such as landfilling, composting, biogas production, direct utilization on forests, and use in thermal processes [47] (e.g., incineration, pyrolysis, and gasification). Other possible alternatives can be, for example, the utilization in the production of cement [48] or hydrogen [49–51]. In the case of sewage sludge, drying with the help of waste heat and subsequent pelleting is also an option. According to our own previous calculations, primarily, the selling of pellets for heating justify pelleting; the farmer's own use and use for nutrient-related purposes can only be justified in exceptional cases (e.g., if energy and fertilizer prices are very high, or if we cannot utilize the produced heat energy [52]).

In the case of the system established by the sewage plants and the additional technologies organized around them, in order to perform sustainable water management and to preserve and maintain the condition of the natural environment, they must comply with serious international and national regulations, provisions, and directives. The examples presented in Section 5 also illustrate that there are very large differences in the position of each country on the agricultural use of nutrients originating from wastewater.

The topic presented here is primarily influenced by two legal provisions:

1. Regulations on the current emission limit values for plants of different sizes.
2. Legislation governing the disposal of wastewater and sewage sludge compost.

The regulatory environment may differ significantly in each country, but it is important to mention the example of the European Union: the Water Framework

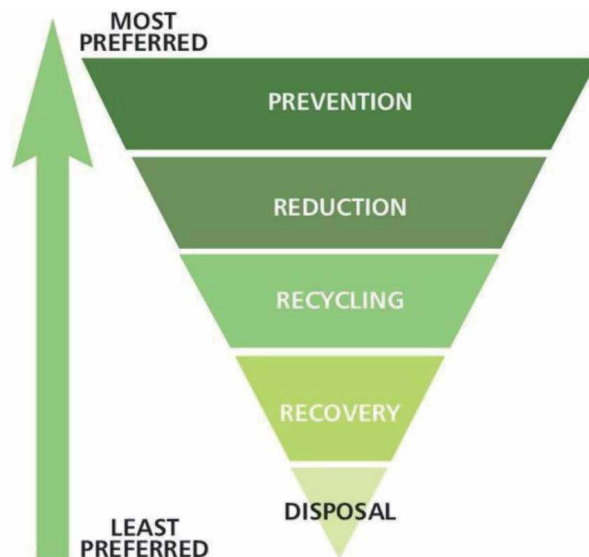


**Figure 1.**  
*The waste management hierarchy. Source: [53].*

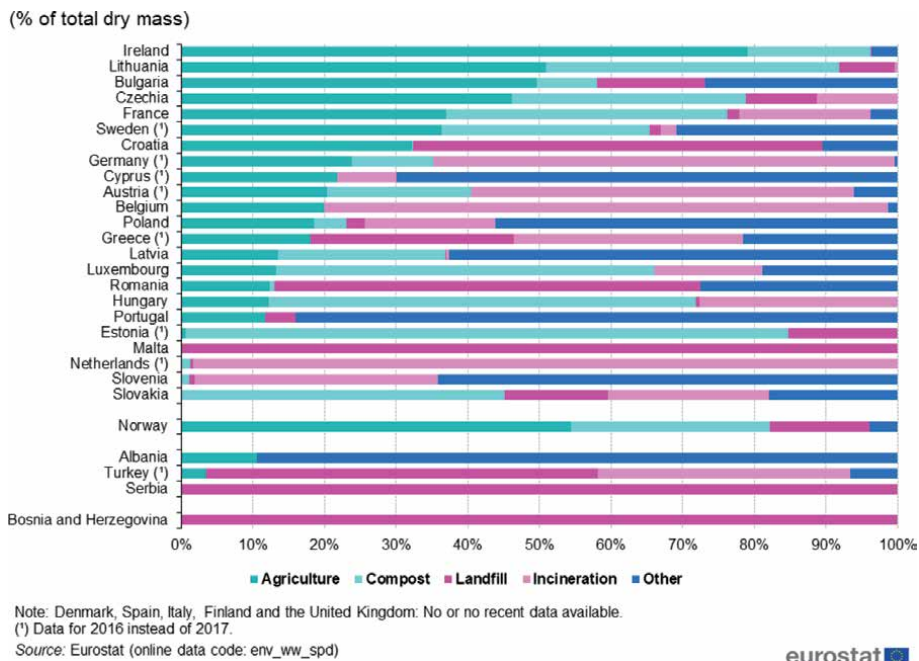


**Figure 2.** Sewage sludge disposal from urban wastewater treatment, by treatment method. Source: [54].

Directive (Directive 2000/60/EC) has a uniform water and aquatic environment policy, which was enforced on December 22, 2000. It is a unique goal in this global respect to bring all surface water and groundwater into good condition throughout the European Union. One of the points of this effort is to improve water quality by reducing pollutant emissions, which also includes emission limits for nitrogen (170 kg N active substance/ha). The importance of this EU-related legislation in our case study is to determine the minimum required size of forest or SRC.

According to the latest EUROSTAT register (as shown in **Figure 2**), there are large differences in the methods of disposal in each EU country, and this usually depends on the prevailing environmental and legal regulations in the given country [54].

The most widely used sludge disposal and sludge utilization/treatment alternatives in the European Union include agricultural utilization (directly or as compost), landfill, soil improvement and soil remediation, and incineration.

#### 4. Case study

Below, we present an estimate of the size of an SRC required to utilize the sewage sludge produced by a 250,000 population equivalent (PE)-sized wastewater treatment plant applying the most commonly used technology (activated sludge technology).

Taking into account the average specific amount of digested sludge (0.35 kg sludge dry matter/m<sup>3</sup>) [28, 31–33], the resulting total amount of digested sludge is slightly more than 13 t sludge dry matter per day (~4790 t sludge dry matter/year). At the end of a 25–30-day composting process, 3346 t of screened compost dry matter per year can be produced. Calculating with a total nitrogen (TN) content of 2.1% and a 2:1 volume ratio of structural material/sewage sludge, the nitrogen-active

ingredient content of the compost is approximately 70 t. According to the relevant EU environmental regulations, the maximum amount that can be disposed of as sewage sludge compost per year is 170 kg/ha of N-active substance. As it is worthwhile or necessary to use sludge in SRC after harvesting, this amount can be applied to 413 ha, calculated with the maximum amount of active nitrogen ingredient that can be applied. This also means that considering SRC with rotation length of 2 years, approximately 826 ha of SRC (twice more) need to be established, as close as possible to the wastewater treatment plant in order to minimize transport costs and alleviate logistical difficulties. One of the reasons for choosing a rotation length of 2 years is that it is a common harvest frequency nowadays in the case of plantations with similar characteristics and purposes, and the amount of both sewage sludge disposal and biomass harvesting is more balanced compared to using a longer rotation length.

According to Gabnai [31], the inclusion of sewage sludge compost utilization—which also results in fertilizer replacement—can reduce the specific cost of wood chips by approximately 10–40%. It is worth mentioning that this value depends on the transport distance, current fertilizer prices, and the market price of wood chips as follows:

- The larger the compost utilization, the price of the substituted fertilizer, and the yield surplus, the lesser the unit cost of wood chip.
- The larger the transport distance and the transport cost, the higher the unit cost of wood chip.
- In case of higher prices of the wood chip or substituted fossil fuel source, the unit cost remains the same, but profit/extra revenue will come in.

In order to ensure the energy self-sufficiency of the wastewater treatment plant, as the amount of electricity from biogas can cover about 70–80% of the plant's energy demand [31], this may be a good opportunity to utilize wood chips produced on SRC for electricity and heat production purposes. In order to achieve full energy self-sufficiency, our calculations were performed on the basis of Patel et al. [55] and Uchman [56] in relation to a gasification plant connected to a cogeneration power plant, taking into account self-produced wood chips at market price.

To determine the required performance of the wood gasifier and the connected combined heat and power technology (CHP) equipment, calculations were performed for the following two approaches:

- Construction and operation of a system with the capacity required to achieve full electricity self-sufficiency.
- Construction and operation of a system with the capacity required to use the total amount of wood chips produced in the areas treated with compost.

Considered specifics and factors in our calculations:

- System useful operation lifetime: 15 years
- Total gas engine efficiency: 94%
  - Gas engine electrical efficiency: 37%

- Gas engine heat generation efficiency: 57%
- Overall system efficiency: 75%
- Electricity self-consumption: 10%

#### **4.1 Construction and operation of a system with the capacity required to achieve full electrical self-sufficiency**

The 2.053 million kWh of electricity needed for self-sufficiency, assuming 8000 operating h per year, can be achieved with a system with a capacity of approximately 260 kW<sub>el</sub>. In the wood gasification unit, taking into account the parameters and efficiency indicated in the study of Uchman [56], this would require 1500 tons of wood chips with 0% water content (atrotens) per year. This quantity, calculated on the basis of the average yield over the entire lifetime of SRC (as detailed in Section 2.1), can be produced on around 120–150 ha of SRC.

When performing system analyses, in addition to the operating parameters, it is important to take into account that, in the initial period, wood chips should be acquired from an external source, as long as the heating energy demand can be covered with self-produced biomass.

#### **4.2 Construction and operation of a power system in order to use all the wood chips produced in compost-treated areas**

Alternatively, the required capacity was determined based on the amount of wood chips produced in all compost-treated areas. In doing so, we took into account the operating parameters of the wood gasification + CHP system, assuming a maximum yearly operating time of 8000 operating h, as well as the varying amounts of wood chips produced each year. Based on our calculations, a nearly 1000 kW<sub>el</sub> system is capable of using up the amount of biomass boasted each year. In our view, sizing based on these considerations can adequately ensure continuous operation.

As Fogarassy and Nábrádi [57] pointed out, in addition to the material and energy saving objectives, significant emissions can be avoided through the above written findings, that is, by eliminating the production and transportation costs of natural gas-based nitrogen fertilizers and by the use of replaced fossil fuel sources (heat energy and electric energy or propellant) by means of avoiding CO<sub>2</sub> emissions.

#### **4.3 Estimated CO<sub>2</sub> emission reductions**

Linking wastewater treatment activities to SRC biomass production at the system level allows for emission reductions in the following areas:

- Fertilizer savings and associated CO<sub>2</sub> emission reduction on the SRC
  - Specific CO<sub>2</sub> emissions from fertilizer production
    - i. Production of N-active substance: 3.47 kg CO<sub>2</sub>/kg active substance [58]
    - ii. Production of P<sub>2</sub>O<sub>5</sub>-active substance: 0.54 kg CO<sub>2</sub>/kg active substance [58]

- CO<sub>2</sub> emissions of fossil fuels replaced by the use of the biomass produced (either through energy self-sufficiency or the sale of surplus energy)
  - Electric energy production output: 0.706 kg/kWh [59]
  - Heat energy production output: 0.273 kg/kWh [59]

These specific units can be used to estimate the CO<sub>2</sub> emission savings if we use sewage sludge instead of N- or P-fertilizers as well as if we use renewable electricity instead of fossil-based ones. Each of them includes uncertainties. Since there are many differential N- and P-fertilizers, with differential N- and P-content and with differential production technologies, we did not make any calculations for estimating their CO<sub>2</sub> savings. Considering the substituted energy sources, we considered the renewable heat instead of natural gas (which is the typical fossil fuel in wastewater treatment plants) and renewable electricity instead of the typical electricity mix in Hungary. Taking into consideration the abovementioned assumptions, the use of an SRC connected to a wastewater treatment plant with 250,000 population equivalents using cogeneration technology, the following amount of yearly CO<sub>2</sub> savings can be estimated:

1. Construction and operation of a system with the capacity required to achieve full electricity self-sufficiency
  - 1450 t of CO<sub>2</sub> connected to eliciting of electricity
  - 380 t of CO<sub>2</sub>, if the surplus heat energy can be utilized
2. Construction and operation of a power system for the use of the total amount of wood chips produced in the areas treated with compost
  - 5650 t of CO<sub>2</sub> connected to the electricity savings
  - 1490 t of CO<sub>2</sub> connected to the heat energy savings

The achievable environmental impacts are also significantly influenced by the country's energy mix and the specific CO<sub>2</sub> emissions of the energy sources used to ensure the operation of the system.

## **5. International examples**

Irrigation with wastewater dates back thousands of years and can be traced back to water scarcity and the need to utilize the valuable nutrients it contains. As technological efficiency improves, so does the rate and quality of treatment, which creates even more favorable conditions for wastewater irrigation, reducing environmental and social risks. Examples are known for the disposal of both wastewater and sewage sludge as well as for the implementation of nutrient replenishment in field crop production, in the different horticultural sectors and forestry as well as in biomass production for energy purposes. According to Zhang and Shen [60], while complying with relevant regulations, the rate of direct recycling of treated wastewater increases by approximately 10–29% every year in the EU, the United States, and China, while in Australia it is 41%. The situation is significantly worse in developing and lagging countries.



Although in many parts of the world, the disposal of wastewater or sewage sludge on arable crops is only minimally or not at all restricted, it may be favorable to apply it in long-rotation forests or SRC in order to avoid social risks.

In the next section, examples of use of wastewater, sewage sludge, and sewage sludge compost in forests in different countries are presented.

### 5.1 Egypt

Due to the dry climate and minimal water resources, 95% of Egypt consists of deserts and marginal areas unsuitable for crop production. Accordingly, most of the arable land is located in and around the Nile Valley. The River Nile has been the main source of water for agriculture and households since ancient times, but recycled wastewater has also emerged as another significant source. Due to the relatively low nutrient content, high treatment costs, as well as environmental and health problems, wastewater appears unsuitable for irrigating food-producing areas. At the same time, there is great potential for irrigating high-value industrial forests in desert areas. To this end, afforestation projects were started around the turn of the millennium based on raw and primarily treated wastewater. In this way, it is possible to contribute to the rehabilitation of dry, desert areas using wastewater. Successful attempts have been made to implement both short- and long-rotation coppices with trees of different species such as *Sesbania* (*Sesbania bispinosa*), *Casuarina* (*Casuarina equisetifolia*), *Eucalypt* (*Eucalyptus regnans*), *Khaya* (*Khaya anthotheca*), and *Jatropha* (*Jatropha curcas*). In addition to the involvement of land in production, this activity can also be of great importance for the implementation of a sustainable supply of feedstock as well as the production of industrial or energy wood and other high value-added downstream products [61].

### 5.2 South Africa

As a result of gradual economic development and population growth, the amount of wastewater generated is also increasing significantly, especially in developing countries and regions. In Durban, fecal sludge from pit latrines was buried using deep row entrenchment. Then forest trees were planted over the area, leaving about a meter of soil between the sludge and the surface. In the first small plot experiments, trees were planted on the buried sludge. As a result of the experiment, the sludge also had a beneficial effect on the growth and health of the trees. In addition, monitoring in the area showed that 3–4 years later the groundwater was not polluted and pathogenic organisms were not present either. As a result of this research, it can be concluded that, although there is a risk of soil contamination, the above example can be mentioned as a promising, simple, cost-effective, and safe sludge management option with controlled application, which also results in significant fertilizer replacement [62].

### 5.3 Estonia and Latvia

In both countries, sewage sludge from wastewater treatment plants and sewage sludge compost were delivered to SRC established with willow species. In addition to increasing biomass yields, the goal was to properly dispose of sewage sludge and replenish soil nutrients. In addition to complying with environmental and soil protection regulations, a significant increase in biomass yield was observed in each experiment, starting from the second harvest [63, 64].

## 5.4 Sweden

An example of the use of treated wastewater and sewage sludge in an SRC is Enköping (Sweden), where a phytoremediation-bioenergy project involves the application of 200,000 m<sup>3</sup> treated wastewater and sludge on a 75-ha SRC willow (*Salix* sp.) plantation. As a result, by utilizing the N and P content of wastewater, fertilizer costs can be significantly reduced and an increase in biomass yield of more than 50% can be observed.

An excellent example of the link between circular economy and wastewater management is the Swedish Hammarby Sjöstad project (Stockholm), which implemented an integrated closed wastewater energy system based on municipal wastewater. Until 1998, the site was an industrial area where significant amounts of oil, heavy metals, and other contaminants had accumulated earlier. Accordingly, the development of the area had to begin with purification. The aim of the designers was to reduce the environmental impact by half by environmentally conscious and modern planning of land use, public transport, construction, energy, as well as water and waste management, and by maximizing circular processes, thus moving toward environmental and economic sustainability [65].

## 5.5 Poland

Fijałkowska et al. [66] carried out a field experiment with three willow (*Salix viminalis*) clones, applying compost from the municipal sewage sludge, where different treatments with fertilizer were used in order to assess the remaining amounts of alkaline elements and heavy metals in the soil up to 90 cm of depth. The compost from the municipal sewage sludge proved to be a useful amendment in the production of willow biomass due to a considerable content of biogenous substances and alkaline metals, together with a low content of heavy metals, as well as little odorous noxiousness for the environment.

## 5.6 China

China produces an enormous amount (more than 30 million t) of municipal sewage sludge annually, with a yearly increase of 10% [67], thus sewage sludge disposal has become a significant challenge in China as well. Chu et al. [68] applied sewage sludge compost as a fertilizer and conducted an experiment to investigate the effects of compost on *Mangifera persiciforma* growth and quantified its uptake of heavy metals. As a conclusion, consistent with other studies (with species such as *Larix decidua* [69] and *Pinus radiata* [70]) focusing on sewage sludge compost's effect on different species, Chu et al.'s experiment clearly indicated that the application of sludge compost is an effective way for improvement of *M. persiciforma* growth. As a result, plant height, ground diameter, and biomass yield have significantly increased by the application of sludge compost. Their findings suggest that sewage sludge compost at reasonably low application rates can promote the growth of the landscape tree with minimal risk of contaminating landscaping soil with heavy metals [68]. It can be added that health risks can be minimized if the material generated at the sewage plant is disposed on the areas planted with only forestry tree species.

## 6. Conclusion

Wastewater and sewage sludge, as energy- and nutrient-rich materials, can contribute to increasing the yield of woody biomass (forests, SRCs). This woody

biomass is suitable for the environmentally sound disposal of sewage sludge or treated wastewater, and it can contribute to increasing the energy self-subsistence of the wastewater plant or even extra energy generation.

The utilization of sewage sludge for nutrient management is a serious problem to be solved, especially in the case of industrial wastewater. In contrast to arable land used for food crops, high levels of inorganic matter and, in some cases, relatively high levels of heavy metals do not pose a food safety threat in the case of forest biomass.

Using large amounts of wastewater, sewage sludge, or sludge compost—complying with environmental regulations of the specific area or region—may result in higher yields, so one can minimize the necessary SRC area to produce enough heat or electricity for sewage plants' energy self-sufficiency. In this way, it is possible to combine two advantages: on the one hand, the tree reduces the harmful heavy metal content of soil, and on the other hand, the produced biomass becomes usable for energy purposes, improving the economic characteristics of the wastewater treatment activity. Due to the aspects of the operation and sludge production of the wastewater treatment plant, it is advisable to perform the harvesting earlier, which, in our opinion, may justify harvesting after 2 years, especially in the case of intensive management.

Based on our case study, approximately 826 ha of SRC (with a 2-year rotation) are required for the disposal of sewage sludge generated by a 250,000 population equivalent wastewater treatment plant. Considering the wastewater treatment plant's electricity self-sufficiency, 120–150 ha of short-rotation coppice would be well enough. This complex system can avoid the emissions of 5650 t of CO<sub>2</sub> via electricity generation and another 1490 t of CO<sub>2</sub> through utilization of waste heat.

It should be highlighted that the achievable environmental impacts are also significantly influenced by the country's energy mix and by the specific CO<sub>2</sub> emissions of the energy sources used to ensure the operation of the system.

It can be concluded that the bottleneck of this two-sided sizing technique is the waste disposal. Thus, there is a need for much higher SRC area compared to the area demand of electricity self-sufficiency in the WWTP. Joint design of WWTP and SRC may be a potential reserve in economic and environmental operation.

## **Acknowledgements**


This publication was financed by the EFOP-3.6.2-16-2017-00001 project (research of complex rural economic and sustainable development, elaboration of its service networks in the Carpathian Basin). The research has also been supported by the (1) Higher Education Institutional Excellence Programme (NKFIH-1150-6/2019) of the Ministry of Innovation and Technology in Hungary, within the framework of the 4th thematic programme of the University of Debrecen; (2) National Research, Development and Innovation Office through the Project No. 2019-1.3.1-KK-2019-00015, titled “Establishment of a circular economy-based sustainability competence center at the University of Pannonia”; and (3) ÚNKP-20-4-II-DE-466 New National Excellence Program of the Ministry of Human Capacities.

## Author details

Attila Bai\* and Zoltán Gabnai  
Department of Business Economics, Faculty of Economics and Business, Institute  
of Applied Economics, University of Debrecen, Debrecen, Hungary

\*Address all correspondence to: [bai.attila@econ.unideb.hu](mailto:bai.attila@econ.unideb.hu)

## IntechOpen

© 2020 The Author(s). Licensee IntechOpen. Distributed under the terms of the Creative Commons Attribution - NonCommercial 4.0 License (<https://creativecommons.org/licenses/by-nc/4.0/>), which permits use, distribution and reproduction for non-commercial purposes, provided the original is properly cited. 

## References

- [1] Geissdoerfer M, Savaget P, Bocken N, Hultink E. The circular economy—A new sustainability paradigm? *Journal of Cleaner Production*. 2017;**143**(1):757-768
- [2] Kiss T, Hetesi ZS. *Man and Nature. Way out of the Impasse*. Budapest, Hungary: University of Public Service; 2018. p. 78
- [3] Bai A, Popp J, Pető K, Szőke I, Harangi-Rákos M, Gabnai Z. The significance of forests and algae in CO<sub>2</sub> balance: A Hungarian case study. *Sustainability*. 2017;**9**(5):857
- [4] Blazev AS. *Global energy market trends*. The Fairmont Press, Inc; 2016. ISBN: 9781498786577
- [5] Ivelics R. *Development of the production technology and utilisation of mini-rotation coppices* [PhD thesis]. Kitaibel Pál Doctoral School of Environmental Sciences. Sopron, Hungary: University of West Hungary, Faculty of Forestry; 2006
- [6] Kauter D, Lewandowski I, Claupein W. Quantity and quality of harvestable biomass from *Populus* short rotation coppice for solid fuel use—A review of the physiological basis and management influences. *Biomass and Bioenergy*. 2003;**24**(6):411-427
- [7] Rae AM, Robinson KM, Street NR, Taylor G. Morphological and physiological traits influencing biomass productivity in short-rotation coppice poplar. *Canadian Journal of Forest Research*. 2004;**34**(7):1488-1498
- [8] Laureysens I, Bogaert J, Blust R, Ceulemans R. Biomass production of 17 poplar clones in a short-rotation coppice culture on a waste disposal site and its relation to soil characteristics. *Forest Ecology and Management*. 2004;**187**(2-3):295-309
- [9] Bungart R, Hüttl RF. Growth dynamics and biomass accumulation of 8-year-old hybrid poplar clones in a short-rotation plantation on a clayey-sandy mining substrate with respect to plant nutrition and water budget. *European Journal of Forest Research*. 2004;**123**(2):105-115
- [10] Labrecque M, Teodorescu TI. Field performance and biomass production of 12 willow and poplar clones in short-rotation coppice in southern Quebec (Canada). *Biomass and Bioenergy*. 2005;**29**(1):1-9
- [11] Linderson ML, Iritz Z, Lindroth A. The effect of water availability on stand-level productivity, transpiration, water use efficiency and radiation use efficiency of field-grown willow clones. *Biomass and Bioenergy*. 2007;**31**(7):460-468
- [12] Rédei K, Veperdi I. The role of black locust (*Robinia pseudoacacia* L.) in establishment of short-rotation energy plantations in Hungary. *International Journal of Horticultural Science*. 2009;**15**(3):41-44
- [13] Grünewald H, Böhm C, Quinkenstein A, Grundmann P, Eberts J, von Wühlisch G. *Robinia pseudoacacia* L.: A lesser known tree species for biomass production. *Bioenergy Research*. 2009;**2**(3):123-133
- [14] Guidi W, Tozzini C, Bonari E. Estimation of chemical traits in poplar short-rotation coppice at stand level. *Biomass and Bioenergy*. 2009;**33**(12):1703-1709
- [15] Christersson L. Wood production potential in poplar plantations in Sweden. *Biomass and Bioenergy*. 2010;**34**(9):1289-1299
- [16] Bergante S, Facciotto G. Nine years measurements in Italian SRC trial in

- 14 poplar and 6 willow clones. In: 19th European Biomass Conference and Exhibition, Berlin, Germany. 2011. pp. 6-10
- [17] Stolarski MJ, Szczukowski S, Tworkowski J, Klasa A. Yield, energy parameters and chemical composition of short-rotation willow biomass. *Industrial Crops and Products*. 2013;**46**:60-65
- [18] Searle SY, Malins CJ. Will energy crop yields meet expectations? *Biomass and Bioenergy*. 2014;**65**:3-12
- [19] Aronsson P, Rosenqvist H, Dimitriou I. Impact of nitrogen fertilization to short-rotation willow coppice plantations grown in Sweden on yield and economy. *Bioenergy Research*. 2014;**7**(3):993-1001
- [20] Stolarski MJ, Krzyżaniak M, Szczukowski S, Tworkowski J, Załuski D, Bieniek A, et al. Effect of increased soil fertility on the yield and energy value of short-rotation woody crops. *Bioenergy Research*. 2015;**8**(3):1136-1147
- [21] Kohlheb N, Gergely S, Laki G, Podmaniczky L, Skutai J, Szakál F. Proposals for the Development of Agricultural Support System Enabling the Faster Spreading of Renewable Energy Sources. Final Report. Gödöllő, Hungary, 2004; Project ID: K-36-02-00114H. p. 148
- [22] Covenant of Mayors. Technical Annex to the SEAP Template Instructions Document: The Emission Factors. Available online: [http://www.eumayors.eu/IMG/pdf/technical\\_annex\\_en.pdf](http://www.eumayors.eu/IMG/pdf/technical_annex_en.pdf) [Accessed: 12 May 2017]
- [23] Nabel M, Barbosa DBP, Horsch D, Jablonowski ND. Energy crop (*Sida hermaphrodita*) fertilization using digestate under marginal soil conditions: A dose-response experiment. European Geosciences Union General Assembly 2014, EGU 2014. *Energy Procedia*. 2014;**59**:127-133
- [24] Pszczółkowska A, Romanowska-Duda Z, Pszczółkowski W, Grzesik M, Wysokińska Z. Biomass production of selected energy plants: Economic analysis and logistic strategies. *Comparative Economic Research*. 2012;**15**(3):77-103
- [25] Labrecque M, Teodorescu TI. High biomass production by *Salix* clones on SRC following two 3-year coppice rotation on abandoned farmland in southern Quebec, Canada. *Biomass and Bioenergy*. 2003;**25**:135-146
- [26] Gyuricza C. Cultivating woody energy crops for energetic purposes. *Biowaste*. 2007;**2**(4):25-32
- [27] Kurucz E, Fári MG, Antal G, Gabnai Z, Popp J, Bai A. Opportunities for the production and economics of Virginia fanpetals (*Sida hermaphrodita*). *Renewable and Sustainable Energy Reviews*. 2018;**90**:824-834
- [28] Metcalf L, Eddy HP, Tchobanoglous G. *Wastewater Engineering: Treatment, Disposal, and Reuse*. 3rd ed. New York: McGraw-Hill. 1334p; 1991. ISBN 0-07-041690-7
- [29] Bousselhaj K, Fars S, Laghmari A, Nejmeddine A, Ouazzani N, Ciavatta C. Nitrogen fertilizer value of sewage sludge co-composts. *Agronomie*. 2004;**24**(8):487-492
- [30] Ladányi K, Szűcs I. Economic analysis of organic manure application in Hungary. *Annals of the Polish Association of Agricultural and Agribusiness Economists*. 2016;**18**(4):157-162
- [31] Gabnai Z. Economic evaluation of wastewater plant technologies and their role in energy, nutrient and carbon dioxide management. Doctoral

[PhD thesis]. Faculty of Economics and Business, Károly Ihrig PhD School of Management and Business Administration. Debrecen, Hungary: University of Debrecen; 2019

[32] Kárpáti Á. Modern methods of wastewater treatment. In: Domokos E, editor. Environmental Engineering Knowledge Base. Vol. XXXII. Institute of Environmental Engineering. Veszprém, Hungary: University of Pannonia; 2014. p. 280

[33] Thury P. The quality of sludge water generated after anaerobic sludge digestion and its effect on the main branch of treatment [PhD thesis]. Doctoral School of Chemical Engineering and Materials Science. Veszprém, Hungary: University of Pannonia; 2009

[34] Usman K, Khan S, Ghulam S, Khan MU, Khan N, Khan MA, et al. Sewage sludge: An important biological resource for sustainable agriculture and its environmental implications. *American Journal of Plant Sciences*. 2012;**3**(12):1708-1721

[35] Alvarenga P, Palma P, Mourinha C, Farto M, Dôres J, Patanita M, et al. Recycling organic wastes to agricultural land as a way to improve its quality: A field study to evaluate benefits and risks. *Waste Management*. 2017;**61**:582-592

[36] Mateo-Sagasta J, Raschid-Sally L, Thebo A. Global wastewater and sludge production, treatment and use. In: *Wastewater*. Dordrecht: Springer; 2015. pp. 15-38

[37] Sato T, Qadir M, Yamamoto S, Endo T, Zahoor A. Global, regional, and country level need for data on wastewater generation, treatment, and use. *Agricultural Water Management*. 2013;**130**:1-13

[38] FAO. Number of Municipal Wastewater Treatment Facilities.

Rome, Italy: AQUASTAT - Food and Agriculture Organization of the United Nations; 2020. Available from: [http://www.fao.org/nr/water/aquastat/data/query/results.html?regionQuery=true&yearGrouping=SURVEY&yearRange.fromYear=1960&yearRange.toYear=2015&varGrpIds=4515&regIds=9805,9806,9807,9808,9809&includeRegions=true&showValueYears=true&categoryIds=-1&XAxis=YEAR&showSymbols=true&showUnits=true&hideEmptyRowsColumns=true&\\_hideEmptyRowsColumns=on&lang=en&query\\_type=glossary](http://www.fao.org/nr/water/aquastat/data/query/results.html?regionQuery=true&yearGrouping=SURVEY&yearRange.fromYear=1960&yearRange.toYear=2015&varGrpIds=4515&regIds=9805,9806,9807,9808,9809&includeRegions=true&showValueYears=true&categoryIds=-1&XAxis=YEAR&showSymbols=true&showUnits=true&hideEmptyRowsColumns=true&_hideEmptyRowsColumns=on&lang=en&query_type=glossary)

[39] Weigert B. From a treatment plant to a power plant. *Waterworks Panorama*. 2015;**23**(1):28-29

[40] Gu Y, Li Y, Li X, Luo P, Wang H, Wang X, et al. Energy self-sufficient wastewater treatment plants: Feasibilities and challenges. *Energy Procedia*. 2017;**105**:3741-3751

[41] ENERWATER. ENERWATER Project H2020 Framework Programme for Research and Innovation. Grant agreement number 644771. 2017. Available from: <http://www.enerwater.eu/>

[42] Wett B, Buchauer K, Fimml C. Energy self-sufficiency as a feasible concept for wastewater treatment systems. In: *IWA Leading Edge Technology Conference*. Singapore: Asian Water; 2007. pp. 21-24

[43] McCarty L, Bae J, Kim J. Domestic wastewater treatment as a net energy producer—Can this be achieved? *Environmental Science & Technology*. 2011;**45**:7100-7106

[44] Gude VG. Energy and water autarky of wastewater treatment and power generation systems. *Renewable and Sustainable Energy Reviews*. 2015;**45**:52-68

[45] van der Beken A. Water Related Education, Training and Technology Transfer. *Encyclopedia of Life Support Systems*. Oxford, United Kingdom:

UNESCO/Eolss Publishers Co. Ltd;  
2009. ISBN-978-1-84826-465-6

[46] Henze M, van Loosdrecht MC, Ekama GA, Brdjanovic D. Biological Wastewater Treatment. London, United Kingdom: IWA Publishing; 2008

[47] Samolada MC, Zabaniotou AA. Comparative assessment of municipal sewage sludge incineration, gasification and pyrolysis for a sustainable sludge-to-energy management in Greece. *Waste Management*. 2014;**34**:411-420

[48] Lin Y, Zhou S, Li F, Lin Y. Utilization of municipal sewage sludge as additives for the production of eco-cement. *Journal of Hazardous Materials*. 2012;**213-214**:457-465

[49] Fytily D, Zabaniotou A. Utilization of sewage sludge in EU application of old and new methods—A review. *Renewable and Sustainable Energy Reviews*. 2008;**12**:116-140

[50] Kim S-H, Han S-K, Shin H-S. Feasibility of biohydrogen production by anaerobic co-digestion of food waste and sewage sludge. *International Journal of Hydrogen Energy*. 2004;**29**:1607-1616

[51] Iacovidou E, Ohandja D-G, Voulvoulis N. Food waste co-digestion with sewage sludge—Realising its potential in the UK. *Journal of Environmental Management*. 2012;**112**:267-274

[52] Nagy D, Balogh P, Gabnai Z, Popp J, Oláh J, Bai A. Economic analysis of pellet production in co-digestion biogas plants. *Energies*. 2018;**11**(5):1135

[53] Komen K. Framework for a Green Economy Transition: Towards a Low-Carbon, Climate-Resilient and Resource Efficient City. Technical Report; 2013. p. 38

[54] EUROSTAT. Sewage Sludge Disposal from Urban Wastewater Treatment, by Treatment Method,

2017 (% of Total Dry Mass). 2019. Available from: [https://ec.europa.eu/eurostat/statistics-explained/index.php?title=File:Sewage\\_sludge\\_disposal\\_from\\_urban\\_wastewater\\_treatment,\\_by\\_treatment\\_method,\\_2017\\_\(%25\\_of\\_total\\_dry\\_mass\).png](https://ec.europa.eu/eurostat/statistics-explained/index.php?title=File:Sewage_sludge_disposal_from_urban_wastewater_treatment,_by_treatment_method,_2017_(%25_of_total_dry_mass).png)

[55] Patel M, Zhang X, Kumar A. Techno-economic and life cycle assessment on lignocellulosic biomass thermochemical conversion technologies: A review. *Renewable and Sustainable Energy Reviews*. 2016;**53**:1486-1499

[56] Uchman W. Evaluation of the potential of the production of electricity and heat using energy crops with phytoremediation features. *Applied Thermal Engineering*. 2017;**126**:194-203

[57] Fogarassy CS, Nábrádi A. Proposals for low-carbon agriculture production strategies between 2020 and 2030 in Hungary. *APSTRACT: Applied Studies in Agribusiness and Commerce*. 2015;**9**(4):5-16

[58] Fertilizers Europe. Carbon Footprint Reference Values. Energy Efficiency and Greenhouse Gas emissions in European Mineral Fertilizer Production and Use. 2008. Available from: [https://issuu.com/efma2/docs/carbon\\_footprint\\_web\\_v4](https://issuu.com/efma2/docs/carbon_footprint_web_v4)

[59] KVVVM. Climate Policy. Energy Aspects of Reducing Greenhouse Gas Emissions. Climate Policy Background Study. 2014. Available from: [http://klima.kvvm.hu/documents/14/NES\\_energetika.pdf](http://klima.kvvm.hu/documents/14/NES_energetika.pdf)

[60] Zhang Y, Shen Y. Wastewater irrigation: Past, present, and future. *Wiley Interdisciplinary Reviews Water*. 2019;**6**(3):e1234

[61] Hashim MN, Razak OA, Rosdi K, Soliman MK. Wastewater-irrigated industrial woody plantations for



- rehabilitation of arid areas in Egypt. In: Conference Proceedings of the International Symposium on Forestry and Forest Products, Kuala Lumpur, Malaysia. 2010
- [62] Mwale J. Fecal sludge management in Africa. Developments, Research & Innovations. 2013;**2013**(4):1-28
- [63] Holm B, Heinsoo K. Influence of composted sewage sludge on the wood yield of willow short rotation coppice. An Estonian case study. Environment Protection Engineering. 2013;**39**(1):17-32
- [64] Lazdina D, Lazdinš A, Karinš Z, Kāposts V. Effect of sewage sludge fertilisation in short-rotation willow plantations. Journal of Environmental Engineering and Landscape Management. 2007;**15**(2):105-111
- [65] Fränne L. Hammarby Sjöstad—A Unique Environmental Project in Stockholm. Stockholm, Sweden: GlashusEtt; 2007. p. 40
- [66] Fijałkowska D, Janowska B, Styszko L. Influence of amendment of short-rotation willow plantation in the vicinity of Koszalin with sewage sludge compost on modifications of content of some metals in the soil. Fresenius Environmental Bulletin. 2010;**19**(2a):327-329
- [67] Yue Y, Yao Y, Lin Q, Li G, Zhao X. The change of heavy metals fractions during hydrochar decomposition in soils amended with different municipal sewage sludge hydrochars. Journal of Soils and Sediments. 2017;**17**(3):763-770
- [68] Chu S, Wu D, Liang LL, Zhong F, Hu Y, Hu X, et al. Municipal sewage sludge compost promotes *Mangifera persiciforma* tree growth with no risk of heavy metal contamination of soil. Scientific Reports. 2017;**7**(1):1-11
- [69] Bouriou M, Alaoui-Sehmer L, Laffray X, Benbrahim M, Aleya L, Alaoui-Sossé B. Sewage sludge fertilization in larch seedlings: Effects on trace metal accumulation and growth performance. Ecological Engineering. 2015;**77**:216-224
- [70] Ferreiro-Domínguez N, Rigueiro-Rodríguez A, Mosquera-Losada MR. Sewage sludge fertiliser use: Implications for soil and plant copper evolution in forest and agronomic soils. Science of The Total Environment. 2012;**424**:39-47



*Edited by Ana Cristina Gonçalves,  
Adélia Sousa and Isabel Malico*

Forests are responsible for the largest net biomass carbon production. They store the most standing biomass and carbon and thus they are an important source of bioenergy. Their importance is linked to their relative abundance and uniformity worldwide and the neutrality of CO<sub>2</sub> emissions from biomass conversion to energy. Yet, the use of biomass for energy presents risks related to forest system sustainability and demands for new environmentally sustainable strategies for its use. This book provides a comprehensive overview of the current state of the art in a multitude of subjects related to forest bioenergy, ranging from trees, forest stand management, and biomass assessment to waste management, conversion technologies, and routes and energy applications.

Published in London, UK

© 2021 IntechOpen  
© rdonar / iStock

**IntechOpen**

